

Fiscal Year 2015 Second Quarter Progress Report for the Advanced Battery Materials Research (BMR) Program

June 2015

Approved by

Tien Q. Duong, Advanced Battery Materials Research Manager
Vehicle Technologies Office, Energy Efficiency and Renewable Energy

TABLE OF CONTENTS

A Message from the Advanced Battery Materials Research Manager	1
Task 1 – Advanced Electrode Architectures	3
Task 1.1 – Physical, Chemical, and Electrochemical Failure Analysis of Electrodes and Cells (Vincent Battaglia, Lawrence Berkeley National Laboratory)	4
Task 1.2 – Electrode Architecture-Assembly of Battery Materials and Electrodes (Karim Zaghib, HydroQuebec).....	6
Task 1.3 – Design and Scalable Assembly of High-Density, Low-Tortuosity Electrodes (Yet-Ming Chiang, Massachusetts Institute of Technology).....	8
Task 1.4 – Hierarchical Assembly of Inorganic/Organic Hybrid Si Negative Electrodes (Gao Liu, Lawrence Berkeley National Laboratory)	11
Task 1.5 – Studies in Advanced Electrode Fabrication (Vincent Battaglia, Lawrence Berkeley National Laboratory)	14
Task 2 – Silicon Anode Research.....	16
Task 2.1 – Development of Silicon-Based High Capacity Anodes (Ji-Guang Zhang/Jun Liu, PNNL; Prashant Kumta, University of Pittsburgh; Jim Zheng, PSU)	17
Task 2.2 – Pre-Lithiation of Silicon Anode for High Energy Li Ion Batteries (Yi Cui, Stanford University)	20
Task 3 – High Energy Density Cathodes for Advanced Lithium-ion BATTERIES.....	23
Task 3.1 – Studies of High Capacity Cathodes for Advanced Lithium-ion Systems (Jagjit Nanda, Oak Ridge National Laboratory).....	24
Task 3.2 – High Energy Density Lithium Battery (Stanley Whittingham, SUNY Binghamton)	27
Task 3.3 – Development of High-Energy Cathode Materials (Ji-Guang Zhang and Jie Xiao, Pacific Northwest National Laboratory)	30
Task 3.4 – <i>In situ</i> Solvothermal Synthesis of Novel High Capacity Cathodes (Patrick Looney, Feng Wang, Brookhaven National Laboratory)	32
Task 3.5 – Novel Cathode Materials and Processing Methods (Michael M. Thackeray and Jason R. Croy, Argonne National Laboratory).....	35
Task 3.6 – High-capacity, High-voltage Cathode Materials for Lithium-ion Batteries (Arumugam Manthiram, University of Texas, Austin)	38
Task 3.7 – Lithium-bearing Mixed Polyanion (LBMP) Glasses as Cathode Materials (Jim Kiggans and Andrew Kercher, Oak Ridge National Laboratory).....	41
Task 3.8 – Design of High Performance, High Energy Cathode Materials (Marca Doeff, Lawrence Berkeley National Laboratory)	43
Task 3.9 – Lithium Batteries with Higher Capacity and Voltage (John B. Goodenough, UT Austin).....	46
Task 3.10 – Exploiting Co and Ni Spinel in Structurally-Integrated Composite Electrodes (Michael M. Thackeray and Jason R. Croy, Argonne National Laboratory)	48

Task 4 – Electrolytes for High Voltage High Energy Lithium-ion Batteries	51
Task 4.1 – Fluorinated Electrolyte for 5-V Li-ion Chemistry (Zhengcheng Zhang, Argonne National Laboratory)	52
Task 5 – Diagnostics.....	54
Task 5.1 – Design and Synthesis of Advanced High-Energy Cathode Materials (Guoying Chen, Lawrence Berkeley National Laboratory)	55
Task 5.2 – Interfacial Processes – Diagnostics (Robert Kostecki, Lawrence Berkeley National Laboratory)	58
Task 5.3 – Advanced <i>in situ</i> Diagnostic Techniques for Battery Materials (Xiao-Qing Yang and Xiqian Yu, Brookhaven National Laboratory)	61
Task 5.4 – NMR and Pulse Field Gradient Studies of SEI and Electrode Structure (Clare Grey, Cambridge University)	64
Task 5.5 – Optimization of Ion Transport in High-Energy Composite Cathodes (Shirley Meng, UC San Diego)	66
Task 5.6 – Analysis of Film Formation Chemistry on Silicon Anodes by Advanced <i>In situ</i> and <i>Operando</i> Vibrational Spectroscopy (Gabor Somorjai, UC Berkeley and Phil Ross, Lawrence Berkeley National Laboratory)	69
Task 5.7 – Microscopy Investigation on the Fading Mechanism of Electrode Materials (Chongmin Wang, Pacific Northwest National Laboratory)	71
Task 5.8 – Energy Storage Materials Research using DOE's User Facilities and Beyond (Michael M. Thackeray and Jason R. Croy, Argonne National Laboratory)	74
Task 6 – Modeling Advanced Electrode Materials	77
Task 6.1 – Electrode Materials Design and Failure Prediction (Venkat Srinivasan, Lawrence Berkeley National Laboratory)	78
Task 6.2 – Predicting and Understanding Novel Electrode Materials from First-Principles (Kristin Persson, Lawrence Berkeley National Laboratory)	80
Task 6.3 – First Principles Calculations of Existing and Novel Electrode Materials (Gerbrand Ceder, MIT)	82
Task 6.4 – First Principles Modeling of SEI Formation on Bare and Surface/Additive Modified Silicon Anode (Perla Balbuena, Texas A&M University)	84
Task 6.5 – A Combined Experimental and Modeling Approach for the Design of High Current Efficiency Si Electrodes (Xingcheng Xiao, General Motors and Yue Qi, Michigan State University)	87
Task 6.6 – Predicting Microstructure and Performance for Optimal Cell Fabrication (Dean Wheeler and Brian Mazzeo, Brigham Young University)	90
Task 7 – Metallic Lithium and Solid Electrolytes	93
Task 7.1 – Mechanical Properties at the Protected Lithium Interface (Nancy Dudney, ORNL; Erik Herbert, UTK; Jeff Sakamoto UM)	94
Task 7.2 – Solid Electrolytes for Solid-State and Lithium-Sulfur Batteries (Jeff Sakamoto, University of Michigan)	96
Task 7.3 – Composite Electrolytes to Stabilize Metallic Lithium Anodes (Nancy Dudney and Sergiy Kalnaus, Oak Ridge National Laboratory)	98
Task 7.4 – Overcoming Interfacial Impedance in Solid-State Batteries (Eric Wachsman, University of Maryland, College Park)	100

Task 7.5 – Nanoscale Interfacial Engineering for Stable Lithium Metal Anodes (Yi Cui, Stanford University)	103
Task 7.6 – Lithium Dendrite Suppression for Lithium-Ion Batteries (Wu Xu and Ji-Guang Zhang, Pacific Northwest National Laboratory)	105
Task 8 – Lithium Sulfur Batteries	107
Task 8.1 – New Lamination and Doping Concepts for Enhanced Li – S Battery Performance (Prashant N. Kumta, University of Pittsburgh)	108
Task 8.2 – Simulations and X-ray Spectroscopy of Li-S Chemistry (Nitash Balsara, Lawrence Berkeley National Laboratory)	111
Task 8.3 – Novel Chemistry: Lithium Selenium and Selenium Sulfur Couple (Khalil Amine, Argonne National Laboratory)	114
Task 8.4 – Multi-Functional Cathode Additives (MFCA) for Li-S Battery Technology (Hong Gan, Brookhaven National Laboratory and Co-PI Esther Takeuchi, Brookhaven National Laboratory and Stony Brook University)	117
Task 8.5 – Development of High-Energy Lithium-Sulfur Batteries (Jie Xiao and Jun Liu, Pacific Northwest National Laboratory)	120
Task 8.6 – Nanostructured Design of Sulfur Cathodes for High Energy Lithium-Sulfur Batteries (Yi Cui, Stanford University)	123
Task 8.7 – Addressing Internal “Shuttle” Effect: Electrolyte Design and Cathode Morphology Evolution in Li-S Batteries (Perla Balbuena, Texas A&M University)	125
Task 9 – Li-Air Batteries	128
Task 9.1 – Rechargeable Lithium-Air Batteries (Ji-Guang Zhang and Wu Xu, PNNL)	129
Task 9.2 – Efficient Rechargeable Li/O ₂ Batteries Utilizing Stable Inorganic Molten Salt Electrolytes (Vincent Giordani, Liox)	132
Task 9.3 – Li-Air Batteries (Khalil Amine, ANL)	135
Task 9.4 – Overcome the Obstacles for the Rechargeable Li-air Batteries (Deyang Qu, University of Massachusetts, Boston and Xiao-Qing Yang, Brookhaven National Laboratory)	138
Task 10 – Na-ion Batteries	141
Task 10.1 – Exploratory Studies of Novel Sodium-Ion Battery Systems (Xiao-Qing Yang and Xiqian Yu, Brookhaven National Laboratory)	142

LIST OF FIGURES

Figure 1: The cycling performance of LCO and HV-LCO in half cells with 4.1 V upper cut-off.....	5
Figure 2: The average cell voltage of LCO and HV-LCO in half cells with 4.1 V upper cut-off.....	5
Figure 3: Photos of anode slurries obtained from (a) nano-Si, (b) PAA surface coated nano-Si powder.....	7
Figure 4: Cycle life of Li/Si cells at 40% DoD with different loading levels (a) 0.45 mg/cm ² , (b) 0.75 mg/cm ² , (c) 0.99 mg/cm ² , (d) 1.26 mg/cm ² and (e) 1.96 mg/cm ²	7
Figure 5: Cross sections of graphite anodes formulated with CMC binder and freeze-cast at the cooling rates indicated. Electrodes were lyophilized to retain structure. Total porosity is 58-60 vol%.....	9

Figure 6: Galvanostatic discharge voltage vs. capacity for 800 μm thick electrode sectioned from sample directionally freeze-cast at 7.5°C/min. Left: Multiple cycles at C/5 rate. Right: Comparison of result at C/10, C/5 and 1C discharge rate.	9
Figure 7: Voltage-area capacity results from HPPC test of 800 μm thick electrode (see Figure 6).	9
Figure 8: (a) Structure of poly(1-pyrenemethyl methacrylate) (PPy) and poly(1-pyrenemethyl methacrylate-co-triethylene oxide methyl ether methacrylate) (PPyE). High-resolution TEM (HRTEM) images of (b) PPy and (c) PPyE.	12
Figure 9: (a) Charge (delithiation) capacities of PPy and PPyE-based Si electrodes at C/10. (b) First-cycle voltage curves. (c) Rate performance. (d) Charge (delithiation) capacities of PPy and PPyE-based Si electrodes at 2C rate. The mass loadings of Si for each cell are labelled in the plot.	12
Figure 10: Cycling stability of thermite porous Si after heat treatment	18
Figure 11: Specific charge/discharge capacity/Coulombic efficiency vs cycles of nc-Si and nc-Si/carbon in Li/Li+ system.	18
Figure 12: Representative first cycle voltage profile of SiNPs-CNTs anodes (a) with and (b) without SLMP.	18
Figure 13: (a) Schematic diagrams showing Si NPs react with melted Li to form Li_xSi NPs. A dense passivation layer is formed on the Li_xSi NPs after exposure to trace amounts of oxygen, preventing the Li_xSi alloy from further oxidation in dry air. (b) First cycle delithiation capacity of Li_xSi - Li_2O NPs, using different solvents to form the slurry.	21
Figure 14: First cycle voltage profiles of graphite flakes/ Li_xSi - Li_2O (83:7 by weight) and graphite flakes control cell. (b) Cycling performance of graphite flakes/ Li_xSi - Li_2O and graphite flakes control cell. The purple line is the Coulombic efficiency of graphite flakes/ Li_xSi - Li_2O composite. (c) First cycle voltage profiles of graphite/ LiFePO_4 full cell with and without Li_xSi - Li_2O nanoparticles. (d) Cycling performance of full cell with and without Li_xSi - Li_2O nanoparticles. The purple line is the Coulombic efficiency of full cell with Li_xSi - Li_2O nanoparticles.	21
Figure 15: Top left: SEM micrograph of $\text{Li}_2\text{Cu}_{0.5}\text{Ni}_{0.5}\text{O}_2$; Top right: XANES showing Cu K edge of Li_2CuO_2 and $\text{Li}_2\text{Cu}_{0.5}\text{Ni}_{0.5}\text{O}_2$; Bottom left: Charge-discharge voltage profile of $\text{Li}_2\text{Cu}_{0.5}\text{Ni}_{0.5}\text{O}_2$; Bottom right: Capacity versus no. of cycles for $\text{Li}_2\text{Cu}_{0.5}\text{Ni}_{0.5}\text{O}_2$	25
Figure 16: XRD pattern of CuF_2 and Fe substituted CuF_2	28
Figure 17: The powder XRD pattern of different discharge states of CuF_2 and $\text{Cu}_{0.5}\text{Fe}_{0.5}\text{F}_2$. The tick marks are the standard patterns of the different phases. The top shows electrochemistry discharge curves of the two compounds.	28
Figure 18: (a) Specific energy density of LMR cathode prepared by HA method as a function of cycle number. (b) Mn 2p XPS spectra; (c) charge/discharge profiles at C/10; and (d) cycling performance of $\text{Li}[\text{Li}_{0.2}\text{Ni}_{0.2}\text{Mn}_{0.6}]\text{O}_{2-5}$ materials prepared by co-precipitation method.	31
Figure 19: Structure and electrochemical properties of the $\text{Li}_x\text{Na}_{(1-x)}\text{VPO}_5\text{F}_{0.5}$ (LVPOF) electrode. (a) typical transmission electron microscopy (bright field) image (inset: electron diffraction recorded from the particle along the zone axis [001]), (b) voltage profiles (at C/10 rate) of the LVPOF electrode ($x=1.34$) for the 1st and 2nd cycles, (c) voltage profile (at C/10 rate) and cycling stability of the LVPOF electrode ($x=1.02$).	33
Figure 20: (a) First-cycle charge and discharge profiles (4.6 – 2.0 V, 15 mA/g, half-cells at RT) for $0.1\text{Li}_2\text{MnO}_3 \cdot 0.9\text{LiMn}_{0.4}\text{Ni}_{0.55}\text{Co}_{0.5}\text{O}_2$ (black) and after acid treatment in the presence of Co, followed by annealing at 450°C (red) and 750°C (blue), in order to integrate a Co-based spinel component. (b) First charge (black) and discharge (red) capacities along with FCE's (blue) of the LL and LLS samples shown in (a)	36
Figure 21: Powder XRD patterns of as-synthesized and post-heated LFTP samples.	39
Figure 22: Molybdate substitution can be used as an environmentally friendlier alternative to vanadate substitution for MP glass cathodes.	42
Figure 23: Borate substitution had no significant effect on copper-bearing MP glass cathodes (CuMP = copper metaphosphate, %B = borate substitution, %V = vanadate substitution).	42
Figure 24: STEM-EELS characterization of a region in the vicinity of a particle-particle interface from spray pyrolysis. (a) STEM image and the corresponding FFT results in the upper left and lower right regions, (b) EELS line	

scale profile along the marked region in (a), and overlapped curves on the top of the figure demonstrate the nearly identical EELS characteristics at different locations.	44
Figure 25: FTIR spectra of the crosslinked polymer membranes made of the tetrathiol crosslinkers and (a) ethylene oxide groups or (b) ester groups.	47
Figure 26: Mn arrangements in (a) (111) plane of LiMn_2O_4 and (b) (001) plane of Li_2MnO_3	49
Figure 27: (a) XRD patterns of LT- LiCoO_2 and LT- $\text{LiCo}_{0.9-y}\text{Ni}_{0.1}\text{Mn}_y\text{O}_2$ samples ($y = 0, 0.1$, and 0.2). Initial voltage profiles of Li/LT- $\text{LiCo}_{0.9-y}\text{Ni}_{0.1}\text{Mn}_y\text{O}_2$ ($y = 0, 0.1$, and 0.2) cells charged to upper cut-off voltages of (b) 3.9 V and (c) 4.2 V at a rate of 15 mA/g. Capacity vs. cycle number plots are provided as insets in (b) and (c).	49
Figure 28: (a) Thermal decomposition of FEC-LiPF ₆ ; (b) ¹ H-NMR of 0.5 M LiPF ₆ in FEC (top), 0.5 M LiTFSI in FEC (center) and FEC (bottom) after 5-day thermal treatment at 50°C; (c) ¹⁹ F-NMR of 0.5 M LiPF ₆ in FEC after 5-day thermal treatment at 50°C; (d) proposed pathway of FEC thermal decomposition catalyzed by Lewis base PF ₅	53
Figure 29: (a) 1 st cycle voltage profiles and (b) cycling data of LNMO/Li cell with 1.0 M LiPF ₆ TFPC-FEMC (5/5) electrolyte; (c) 1 st lithiation and delithiation profiles of graphite/Li cell with 1.0 M LiPF ₆ TFPC-FEMC (5/5) electrolyte; (d) cycling performance of LNMO/graphite full cell with 1.0 M LiPF ₆ TFPC-FEMC (5/5) electrolyte.	53
Figure 30: SEM images of $\text{Li}_{1.2}\text{Ni}_{0.13}\text{Mn}_{0.54}\text{Co}_{0.13}\text{O}_2$ crystals.	56
Figure 31: Soft XAS spectra of Mn, Co and Ni L- edges collected in AEY, TEY and FY modes on pristine $\text{Li}_{1.2}\text{Ni}_{0.13}\text{Mn}_{0.54}\text{Co}_{0.13}\text{O}_2$ crystals.	56
Figure 32: Soft XAS spectra of Co L- edge collected in AEY (a and d), TEY (b and e) and FY (c and f) modes on pristine (bottom) and cycled (top) $\text{Li}_{1.2}\text{Ni}_{0.13}\text{Mn}_{0.54}\text{Co}_{0.13}\text{O}_2$ composite electrodes.	56
Figure 33: SEI layer forms after 50 cycles on 100 nm Si thin film (coated 8 nm Alucone/non coated) in 1M LiPF ₆ EC:DEC [1:2] and corresponding impedance spectra.	59
Figure 34: (a) Near-field IR (top) spectrum of particle in Si surface film compared to ATR-FTIR spectrum of $\text{Li}_2\text{C}_2\text{O}_4$. Inset: AFM topography with particle marked.	59
Figure 35: <i>In situ</i> X-ray diffraction (XRD) of Li_2MoO_3 during the first charge. (a) The XRD pattern of the Li_2MoO_3 electrode right after charging to 4.8 V. (b) Contour plot of diffraction peak evolution of (003), (101), (104), (107), (108) and (110) during delithiation. (c) The XRD pattern of the Li_2MoO_3 electrode before charge. (d) Charge curve at a current density of 10 mA g ⁻¹ from open circuit voltage (OCV) to 4.8 V during XRD data collection.	62
Figure 36: ¹ H, ⁷ Li and ¹⁹ F MAS NMR spectra of reduced protonated (H-FEC) and deuterated (D-FEC).	65
Figure 37: Two proposed reduction products of FEC/VC, LiVD (top) and the carbonate polymer (bottom). ¹	65
Figure 38: (a) cation ordering in transition metal layer: $0.5\text{Li}_{4/3}\text{Mn}_{2/3}\text{O}_2 \cdot 0.5\text{LiNi}_{1/2}\text{Mn}_{1/2}\text{O}_2$. (b) oxygen vacancy formation energy of $\text{Li}_{8/12}\text{Ni}_{3/12}\text{Mn}_{6/12}\text{M}_{1/12}\text{O}_2$ at different configurations. #1 is the model without substitution.	67
Figure 39: A relative composition of the 10nm outer SEI after 100 cycles. The layer is adjacent to and in contact with the electrolyte 1:1 EC:DEC and 45:45:10 EC:DEC:FEC when cycled.	67
Figure 40: first negative scan segment and <i>in situ</i> ATR-FTIR spectra of Si electrode obtained after applying a potential from open circuit potential (OCP) to 0.4 V. <i>In situ</i> CV scan speed is 1mV/s, ATR-FTIR incident angle is 60 degree, electrolyte is EC/DEC/LiPF ₆ (1:2 v/v)	70
Figure 41: A) and B) Time-resolved TEM images show the development of lithiation profiles of the alucone and Al_2O_3 coated SiNWs and schematics of the Li diffusion paths through the SiNWs that dictate the lithiation behavior; C) Average lithiation thickness vs. time for the alucone (black square) and Al_2O_3 (red dot) coated SiNWs.	72
Figure 42: (a) Model of pure C2/m stacking in Li_2MnO_3 (grey=Li, pink=Mn). (b) HRXRD data of Li_2MnO_3 made at 850°C (black) along with standard Rietveld analysis (red). (c) HRXRD data of the 850°C Li_2MnO_3 (blue) and the DIFFaX model including stacking faults (brown).	75
Figure 43: Trial cycling data from Li-S cell.	79
Figure 44: Lithium-ion migration in delithiated Li-layer, showing the interaction of the nearest Li neighbor distortions as the migrating Li moves.	81
Figure 45: All Na-vacancy orderings that occur in the Na_xMO_2 systems with seven different choices of M.	83

Figure 46: Convex energy hull of the ground states of the Na_xCrO_2 systems showing that a large number of ordered structures can occur, explaining the stepped voltage curve of this material.	83
Figure 47: Shell failure mechanisms. (a) Shell thickness with time (b) exampled mechanically intact shell: 7.5\AA Al_2O_3 (c) exampled cracked shell: 4.5\AA Al_2O_3 , 7.5\AA SiO_2 (d) exampled broken shell: 2.5\AA Al_2O_3 , 2.5\AA SiO_2 , and 4.5\AA SiO_2 (Si: yellow, O: red, Al: green).	88
Figure 48: Schematic picture of the 1-D model for LiF (001) plane. Mechanical stability of yolk-shell structure.	88
Figure 49: Critical shell thickness from the finite element simulations of lithiation in a Si-C yolk-shell structure.	88
Figure 50: (left) Micro-four-line-probe with electrode film sample on top. Sampling area for ionic conductivity is $70 \times 500 \mu\text{m}$	91
Figure 51: (right) The DPP model uses super-positions of spheres to represent active material (blue) and carbon/binder/solvent domains (green).	91
Figure 52: Simulated cross section of cathode (left) compared to experimental results. The SEM/FIB image (center) is segmented (right) using computer tools developed at BYU.	91
Figure 53: Elastic modulus for the glass ceramic (black) and sintered (red) LATP electrolytes.	95
Figure 54: Plots of testing LLZO with Ta doping of 0.25 to 1.5 mol%.	95
Figure 55: Change in mechanical properties with Li cycling.	95
Figure 56: Secondary electron SEM images of LLZO fracture surfaces RIHP'ed between 900 and 1100 C (10,000 X).	97
Figure 57: Effect of solvents on conductivity of composite electrolyte.	99
Figure 58: Effect of DMC on ceramics/polymer interface resistance.	99
Figure 59: EIS of laminated LLCZN/LFMO.	101
Figure 60: Synthesis method for PFPE-DMC.	101
Figure 61: $\text{Li} \text{LiAlO}_2$ and $\text{Li} \text{Li}_2\text{CO}_3$ interface configurations.	101
Figure 62: Conceptual Demonstration of a full cell with empty anode. The copper foil with h-BN protection exhibited better capacity retention at full cell condition.	104
Figure 63: Stimulated lithium metal cycling test on h-BN synthesized at different temperatures. Tests were carried out with fixed lithium metal capacity of 1.0 mAh/cm^2 at 2.0 mA/cm^2 . The sample synthesized at 600°C on preannealed copper foil demonstrated best performance.	104
Figure 64: h-BN as interfacial layer for lithium metal cycled in ether electrolyte with LiNO_3 as additive. Stable cycling with Coulombic efficiency above 98% was achieved for more than 100 cycles, with the voltage hysteresis stable at minimum level.	104
Figure 65: SEM (a, b) and TEM (c, d) images of graphite anodes from the graphite NCA full cells with E1Cs (a,c) or E1FEC (b, d).	106
Figure 66: (A) ^{17}O NMR spectra of various solvents and electrolytes. (B) ESI-MS results of electrolyte E1Cs.	106
Figure 67: Comparison of cycling behavior of various FSW materials and LIC coated materials.	109
Figure 68: Activation barriers for different migration paths of Li-ions in Li_4SiO_4 . Inset: pink 0 - Li-ion site; red (1)-(5) - Li vacancy sites for different migration pathways.	109
Figure 69: Comparison of the best fit spectra from theory (dashed lines) compared to experiments (solid lines) for each of the three voltages (spectrum I – 2.25V , spectrum II – 2.02V , spectrum III – 1.50V). The isolated species used to obtain the best fit are also indicated: the major components are in red, while the minor components are in black. <i>Right insets:</i> Relative ratios types of sulfur species (S_8 (red), Li_2S (orange), neutrals: S_3 (grey), radicals (yellow) and dianions) that constitute each best fit spectra from theory. We separately consider short (S_2^{2-} to S_2^{5-} , blue) and long ($\text{S}_6^{2-}/\text{S}_7^{2-}/\text{S}_8^{2-}$, green) polysulfide dianions.	112
Figure 70: <i>In situ</i> high-energy XRD characterization of Li-Se cell in GenII electrolyte cycled between 0.8 and 3.5 V with a charging rate of 30 mA/g : (a) XRD pattern of the cell during cycling and the reference material Se and Li_2Se and (b) voltage profile.	115
Figure 71: <i>In situ</i> XANES measurement for Li-Se pouch cell in GenII electrolyte: (a) normalized XANES spectra of the cycling cell, (b) voltage profile, (c) derivative of normalized XANES spectra, and (d) linear combination fitting of residue values and corresponding phase compositions in different state of charge/discharge.	116
Figure 72: <i>In situ</i> XANES measurement for Li-Se cell using an ether-based electrolyte.	116
Figure 73: Li/Sulfur Cycling Voltage Profiles.	118

Figure 74: Li/Sulfur Cell Cycling Test.....	118
Figure 75: Li/Li ₂ S Cycling Voltage Profiles	118
Figure 76: Li/Li ₂ S Cell Cycling Test	118
Figure 77: a) <i>In situ</i> EPR cell for Li-S batteries. b) 3D plot of EPR spectra in a functioning Li-S cell vs. time during cyclic voltammetry (CV) scan at 0.2 mV/s between 1-3 V. c) Proposed discharge-charge reaction mechanisms for Li-S batteries.	121
Figure 78: (a,b) SEM images of (a) Li ₂ S@ZrS ₂ and (b) Li ₂ S@VS ₂ structures. (c,d) <i>Ab initio</i> simulations showing the most stable binding configuration of Li ₂ S with a single layer of (c) ZrS ₂ and (d) VS ₂ with calculated binding energies of 2.70 and 2.94 eV respectively. (e) Specific capacity of Li ₂ S@ZrS ₂ and Li ₂ S@VS ₂ cathodes cycled at 0.2C (1C = 1,166 mA g ⁻¹ Li ₂ S). (f) Areal capacity of Li ₂ S@ZrS ₂ and Li ₂ S@VS ₂ cathodes with high mass loading cycled from 0.1 to 0.6 mA cm ⁻²	124
Figure 79: Time evolution of the Li (100) surface in contact with an electrolyte solution containing 1M solution of Li ₂ S ₈ . Color code: Li is purple, S yellow, O red, C gray, H white.....	126
Figure 80: (a) XRD pattern of ZCO/SWCNTs composite powders. (b-d) Typical SEM images of ZCO/SWCNTs composite powders. (e,f) SEM images of the as-prepared ZCO-based electrodes by coating ZCO/SWCNTs/PVDF on carbon paper. (g,h) Schematic illustration of the synthesized ZCO/SWCNTs composites and the fabricated ZCO/SWCNT/PVDF/carbon paper air-electrodes.	130
Figure 81: (a-c) Voltage profiles of selected cycles for ZCO/SWCNTs (a), SWCNTs (b) electrodes at a current density of 0.1 mA cm ⁻² . (c-d) 1 st cycle voltage profile and cycling performance.	130
Figure 82: a) Electrochemistry of Li ₂ O in LiNO ₃ -KNO ₃ eutectic at 150 °C, at a Pt RDE (CE: Pt wire, RE: Li rod): Linear sweep voltammograms recorded at 5 mV/s at various electrode rotation rates, with Levich plot inset. b) Synthesis of oxidation-resistant carbons: TGA analysis of newly synthesized MWCNT and B-doped CNT (under O ₂ , 20 °C/min).....	133
Figure 83: Galvanostatic discharge/charge curves of cells under the six different conditions. The discharged capacity is 1000 mAh/g, and the discharge/charge current density is 0.2 and 0.1 mA/cm ² , respectively.....	136
Figure 84: Raman spectra of the toroids on the surface of the discharged AC cathode for the six different conditions described in the text. The values of the peaks (in cm ⁻¹) are: 1123 (S1), 1505 (S2), 1340 (D), 1600 (G).	136
Figure 85: Charge transfer (light blue) at the LiO ₂ slab/electrolyte interface from a charge density plot during a particular snapshot of a AIMD trajectory. This may be the reason for suppression of the disproportionation.	136
Figure 86: Distribution of DMSO in the Li ⁺ solvation adducts obtained from ESI-MS spectra of 5mM LiBF ₄ DMSO and other solvents (1:1) mixture (left); The CID spectra of [DMSO+Li+DMSO ^{de6}] ⁺ obtained at collision voltage= 20V, and the scheme of CID procedure (right).....	139
Figure 87: Cyclic voltammetry oxygen reduction in acetonitrile with various concentration of borate.	139
Figure 88: <i>In situ</i> XRD patterns of NaFe(1.63) electrode collected during first charge and discharge. The major diffraction peaks selected from the full XRD patterns are plotted to clearly show the phase transitions between the pristine rhombohedral and cubic phases. The charge and discharge curves are shown on the right column respectively.	143

LIST OF TABLES

Table 1: ICP-OES results for LFTP.....	39
Table 2: Results of testing LLZO with Ta doping of 0.25 to 1.5 mol%	95
Table 3: Concentrations and Diffusion coefficients for Li ₂ O ₂ , Li ₂ O in LiNO ₃ -KNO ₃ eutectic, obtained by Levich/Cottrell method; and O ₂ in NaNO ₃ -KNO ₃ eutectic at 150 °C.	133
Table 4: Reaction rate constants calculated from table 3. Initial concentration for O ₂ ^{•-} was 0.01 M.....	139

A MESSAGE FROM THE ADVANCED BATTERY MATERIALS RESEARCH MANAGER

The newly devised Advanced Battery Materials Research (BMR) Program is off to a productive start. Among recent developments, the 2015 Annual Merit Review and Peer Evaluation Meetings (AMR) event for the Vehicle Technologies Office was held June 8–12, 2015, in Arlington, Virginia. It allowed BMR Investigators review their project accomplishments and plans for the upcoming year. This year, nearly 35 BMR projects were presented and reviewed for merit. The projects were assessed in terms of their advancement of DOE's mission and goals as well as their technical approach and accomplishments over the past fiscal year. AMR proceedings are available online at <http://www.annualmeritreview.energy.gov/>.

More recent BMR accomplishments are reported here. A few selected highlights for the BMR projects are as follows:

- Stanford University (Cui's Group) used $\text{Li}_x\text{Si-Li}_2\text{O}$ core-shell nanoparticles as an excellent prelithiation reagent with high specific capacity to compensate for the first cycle capacity loss in Si-based anodes.
- Argonne National Laboratory (Amine's Group) found that interfacial effects involving the electrolyte can suppress disproportionation of a LiO_2 component in the discharge product. The LiO_2 component can possibly remain stable for days when an electrolyte is left on the surface of the discharged cathode.
- Argonne National Laboratory (Zhang's Group) developed a fluorinated PC-based high voltage electrolyte for 5-volt $\text{LiNi}_{0.5}\text{Ni}_{1.5}\text{O}_4$ spinel cathode with high compatibility with graphite and enhanced thermal stability.
- Lawrence Berkeley National Laboratory (Chen's Group) reported on transition metal reduction on the surface of pristine Li- and Mn-rich layered oxides and demonstrated its dependence on particle morphology.
- Pacific Northwest National Laboratory (Wang's Group) visualized the effect of thin coating on the lithiation kinetics of Si anode using in situ transmission electron microscopy on alucon and Al_2O_3 coated Si nanowires.
- Lawrence Berkeley National Laboratory (Kostecki's Group) validated the positive effect of alucone coating on Si anode with improved cycling performance and reduced interfacial resistance.

The next BMR quarterly report will cover the progress made during April through June and will be available September 2015.

Sincerely,

Tien Q. Duong

Manager, Advanced Battery Materials Research (BMR) Program
Energy Storage R&D
Office of Vehicle Technologies
Energy Efficiency and Renewable Energy
U.S. Department of Energy

TASK 1 – ADVANCED ELECTRODE ARCHITECTURES

Summary and Highlights

Energy density is a critical characterization parameter for batteries for electric vehicles as there is only so much available space for the battery and the vehicle needs to travel over 200 miles. The DOE targets are 500 Wh/L on a system basis and 750 Wh/L on a cell basis. Not only do the batteries have to have a high energy density, they need to do so and still deliver 1,000 Wh/L for 30 seconds on the system level. To meet these requirements entails not only finding new, high energy density electrochemical couples, but also highly efficient electrode structures that minimize inactive material content, allow for expansion and contraction from one to several thousand cycles, and allow full access to the active materials by the electrolyte during pulse discharges. In that vein, the DOE VTO supports five projects in the BMR Program under electrode architectures: (1) electrode fabrication and materials benchmarking (LBNL), (2) assembly of battery materials and electrodes (HydroQuebec), (3) design and scalable assembly of high-density, low-tortuosity electrodes (MIT), (4) hierarchical assembly of inorganic/organic hybrid Si negative electrodes (LBNL), and (5) electrode failure analysis (LBNL).

One of the more promising approaches for higher energy-density Li-ion batteries involves the use of Si as the anode. It has a specific capacity above 3,500 mAh/g and an average voltage during delithiation of 0.4 V vs. the Li/Li⁺ electrode. However, this material suffers from two major problems – both associated with the 300% volume change it experiences as it goes from a fully-delithiated state to a fully-lithiated state: (1) the volume change results in a change in the exposed surface area to electrolyte during cycling that consumes electrolyte and results in a lithium imbalance between the two electrodes, and (2) the volume change causes the particles to become electrically disconnected (which is further enhanced if particle fracturing also occurs) during cycling. Tasks 2, 4, and 5 are focused on Si to make it a more robust electrode by finding better binders.

Another approach to obtaining a higher energy density is to make the electrodes thicker. The problem with thicker electrodes is that the salt in the electrolyte has to travel farther to meet the current needs of the entire electrode throughout the discharge. If the salt cannot reach the back of the electrode at discharge rates required of batteries for automobiles, the battery is said to be running at its limiting current. If the diffusional path through the electrode is tortuous or the volume for electrolyte is too low, the limiting current gets reduced. The other problem with thicker electrodes is that they tend to cycle less well than the thinner electrodes and thus they reach the end-of-life condition sooner, delivering fewer cycles. Tasks 1, 3, and 5 are focused on increasing the limiting current of thick electrodes while maintaining cycleability through the fabrication of less tortuous electrodes or of electrodes with less binder and more room for electrolyte.

If these projects are successful, they will result in a 25% increase in energy density as a result of replacing graphite with Si, and another 20% increase in energy density by moving from 2 mAh/cm² electrodes to 4 mAh/cm² electrodes. This would result in a net increase of 50% in energy density for the cell, and enable a battery previously allowing a vehicle to travel only 200 miles to now travel 300 miles.

Task 1.1 – Physical, Chemical, and Electrochemical Failure Analysis of Electrodes and Cells (Vincent Battaglia, Lawrence Berkeley National Laboratory)

PROJECT OBJECTIVE: This project investigates failure modes of targeted chemistries as defined by the BMR Program and its Focus Groups. The emphasis of the effort for 2015 is on the High-Voltage and Si Anode Focus Groups. The objectives are to identify and quantify the chemical and physical aspects of cell cycling and aging that lead to reduced electrochemical performance. Specifically, research will focus on the effects on material stability as a result of increasing the cell voltage of Graphite/NCM cells from 4.2 V to 4.7 V. In addition, differences in performance between Graphite/NCM and Si/NCM will be investigated. Specifically, investigations into the differences in cell performance as a result of coulombic inefficiencies and the effects of increased electrode loadings on cycleability will be carried out.

PROJECT IMPACT: Success with understanding and improving the stability of NCM in the presence of electrolyte at voltages greater than 4.3 V vs. Li/Li⁺ will translate to an increase in capacity and voltage and hence a compounding improvement in energy density by as much as 45%. Improvement in the loading of anodes and cathodes from 2 to 5 mAh/cm² could result in larger fractions of active materials in cells and a projected increase in energy density by an additional 20 %.

OUT-YEAR GOALS: Provide a prescription of the physical and structural properties required to increase the accessible capacity of layered oxide materials. Demonstrate high loading cells with an increased energy density of 20% with no change in chemistry or operating parameters.

COLLABORATIONS: Several BMR PIs

Milestones

1. Measure and report the difference in capacity fade in mAh/h between LCO and HV-LCO at 4.3 V in mAh/h. (12/31/14) **Complete**
2. Identify and report the electrochemical phenomena responsible for the capacity fade of the LCO and HV-LCO cells at 4.3 V. (3/31/15) **Complete**
3. Measure and report the phenomena responsible for the capacity fade of a 3 mAh/cm² cell in mAh/h (6/30/15) **Ongoing**
4. Measure and report the self-discharge rate of the baseline Li/S cell in mA/(g of S) and decide if this is an appropriate baseline design. (9/30/15) **Ongoing**

Progress Report

Milestone 1. Measure and report the difference in capacity fade (in mAh/h) between LCO and HV-LCO at 4.3 V in mAh/h. Completed, see Quarterly Report 1.

Milestone 2. Identify and report the electrochemical phenomena that is responsible for the capacity fade of the LCO and HV-LCO cells at 4.3 V.

In the previous quarter, the cycling performance of LCO and HV-LCO in half cells with 4.1 V upper cutoff was provided (see Figure 1). Both cells showed good cycling stability for 80 cycles or more. The cycling performance of the same cathode materials was also provided, and again here, for cells cycled to 4.3 V upper cutoff. Charging was performed at C/10 and discharge at C/2.

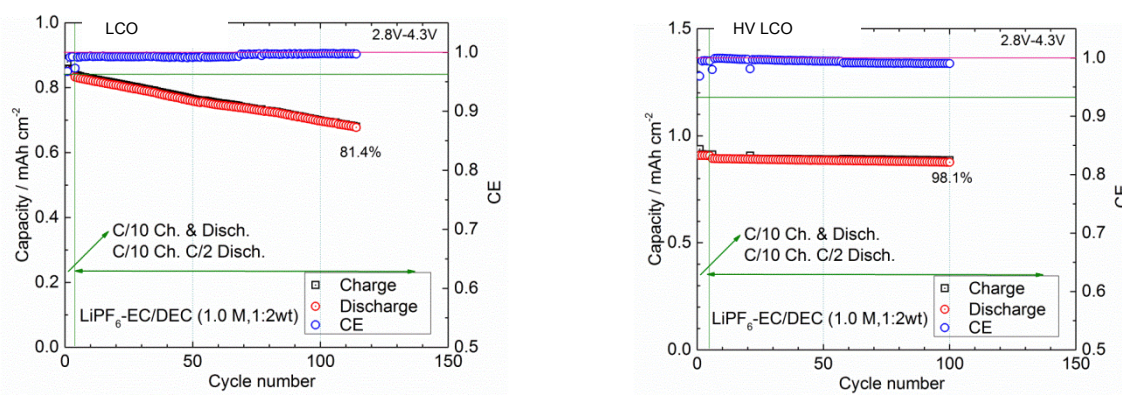


Figure 1: The cycling performance of LCO and HV-LCO in half cells with 4.1 V upper cut-off

Typically, cells die as a function of three factors, Li-ion cell imbalance from side reactions, impedance rise, or loss of Li sites (the sites become inaccessible.) In half cells, the side reactions do not result in capacity fade. Thus, the fade in the cells we are examining is a result of either a loss of Li sites or an impedance rise. If the cells fail from resistance rise then the average discharge voltage of a half-cell will decrease with the cycle number. Below (see Figure 2) is the corresponding average cell voltage of the LCO and HV-LCO cells cycled to a 4.3 V upper cutoff.

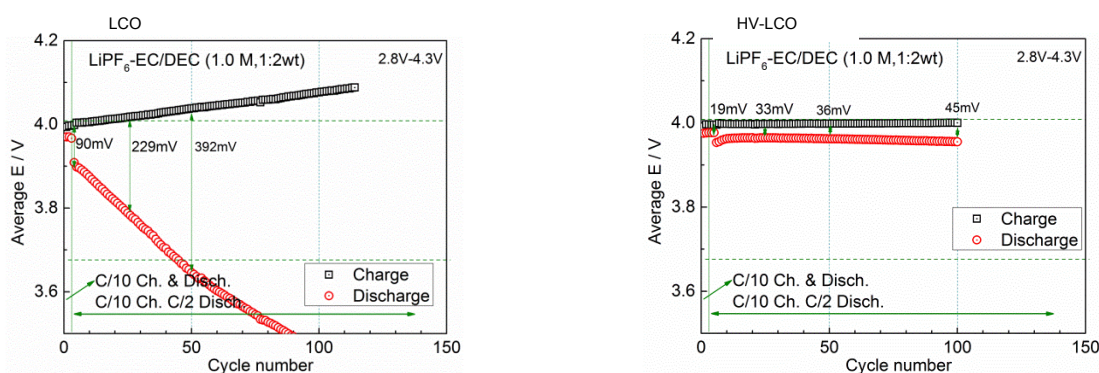


Figure 2: The average cell voltage of LCO and HV-LCO in half cells with 4.1 V upper cut-off

As can be seen, the average voltage drop with cycling is significant for the LCO cell. One cannot determine the effect of Li-site loss on capacity fade but there is clearly resistance rise in the LCO cell.

Task 1.2 – Electrode Architecture-Assembly of Battery Materials and Electrodes (Karim Zaghib, HydroQuebec)

PROJECT OBJECTIVE: To develop high-capacity, low-cost electrodes with good cycle stability and rate capability to replace graphite in Li-ion batteries, the aim of this project is to overcome the limit of electrochemical capacity (both gravimetric and volumetric) of conventional carbon anodes. This is achieved by developing low-cost electrodes that utilize a high-capacity material such as silicon. Controlling the composition (i.e., loading of the active material, ratio of binder and carbon additive) of the electrode will yield a more tolerant anode with acceptable volume change, useful cycle life and low capacity fade. A high-energy large-format Li-ion cell will be produced using optimized Si-based anode and high-energy cathode electrodes.

PROJECT IMPACT: Production of Si nano-powder using commercially scalable and affordable methods will justify replacing the graphite anode without jeopardizing the cost structure of conventional batteries. In addition, the energy density of cells gets increased to > 250 Wh/kg by using a high content of Si ($> 50\%$) with reasonable loading (2 mAh/cm^2). The results obtained in large-format cells ($> 20\text{Ah}$) will enable us to study the wide spectrum of electrochemical performance under actual vehicle operation conditions.

OUT-YEAR GOALS: Complete the optimization of the electrode composition by varying the carbon additive ratio and the type of carbon. In addition to *in situ* SEM analyses, *in situ* impedance spectroscopy will be employed to enhance the understanding of capacity fade of the Si-material. These analyses will clarify the mechanism leading to electrode failure and guide further improvement and design of the electrode architecture. Complete optimization of the method to synthesize Si-nano powder developed at HQ. As a final goal, the optimized Si-anode and high-energy cathode will be coated in the pilot line and then assembled in large-format cells ($> 20\text{Ah}$) using the new automatic stacking machine at HQ.

COLLABORATIONS: Collaborations with BMR members: V. Battaglia and G. Liu from LBNL, C. Wong and Z. Jiguang from PNNL and J. Goodenough from the University of Texas.

Milestones

1. Complete the optimization of the nano-Si-anode formulation. (12/31/14), **Complete**
2. Complete the optimization of the synthesis of nano-size Si developed at HQ. Go/No-Go decision: Terminate the Si synthesis effort if the capacity is less than 1200 mAh/g (3/31/15), **Complete**
3. Produce and supply laminate films of Si-anode and LMNO-cathode (10 m) to BMR PIs (6/30/15), **Ongoing**
4. Produce and supply large-format 20 Ah high-energy stacking cells (4) to BMR PIs (9/30/15), **Ongoing**

Progress Report

In our previous work, we observed that a large volume of gas was generated during the mixing and coating processes. This gas causes many process problems; unstable slurry, difficult control of the loading level and inhomogeneous surface. In this quarter, we addressed solutions to eliminate gas generation. PAA (poly acrylic acid) was used to treat the surfaces of the Si-nano particles by spray drying. Figure 3 shows the photos of the slurries during the mixing process. In the case of bare Si-nano powder (a), a strong release of gas in the suspension was observed, even after aging overnight. However, the Si nano-powder that was surface-treated with PAA showed no gas evolution during the slurry mixing (b) or coating process.

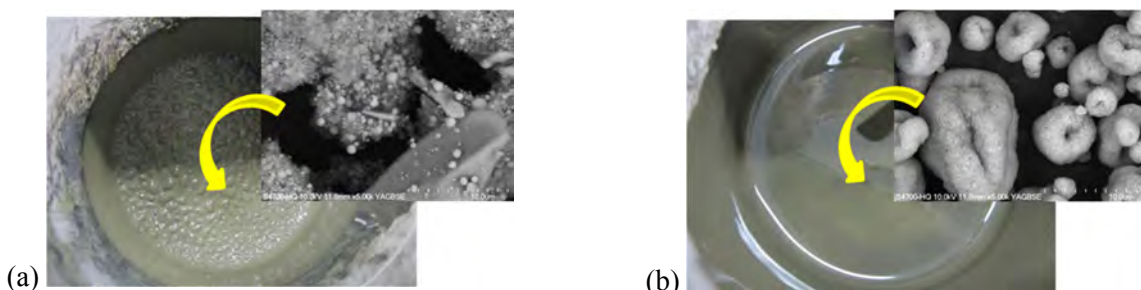


Figure 3: Photos of anode slurries obtained from (a) nano-Si, (b) PAA surface coated nano-Si powder

The morphology of nano-Si powder, treated with PAA, was completely changed. With untreated nano-Si powder, the primary particles agglomerated to form larger secondary particles without any specific shape. However, the PAA-coated nano-Si powder shows some hollow spherical secondary particles with a size distribution of 1-5 μm . The electrochemical evaluation of this powder is ongoing. To achieve a high-energy battery with the Si-anode and NMC or LMNO cathodes, our calculations indicate the anode loading must be $\geq 2\text{mg}/\text{cm}^2$. Then, the effect of loading on the architecture and performance of the anode is a key parameter which should be studied.

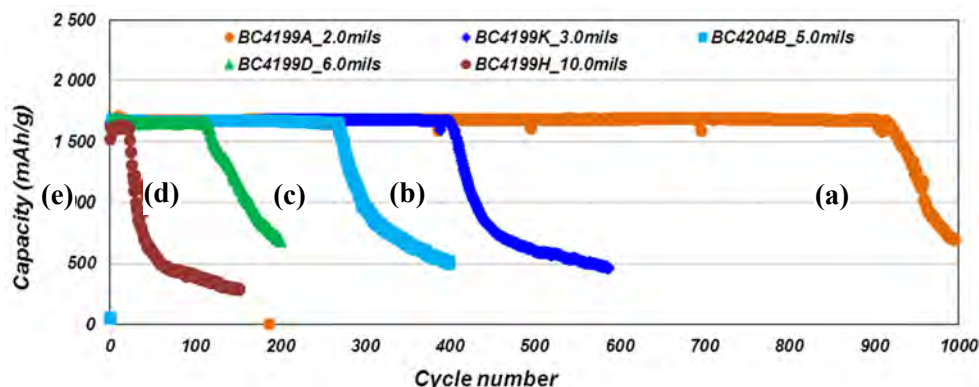


Figure 4: Cycle life of Li/Si cells at 40% DoD with different loading levels (a) $0.45\text{ mg}/\text{cm}^2$, (b) $0.75\text{ mg}/\text{cm}^2$, (c) $0.99\text{ mg}/\text{cm}^2$, (d) $1.26\text{ mg}/\text{cm}^2$ and (e) $1.96\text{ mg}/\text{cm}^2$

Figure 4 shows the cycle life performance of the Li/Si cells with different total loading level of $0.45 \sim 1.96\text{ mg}/\text{cm}^2$. Charge and discharge was controlled with %DoD and was fixed at 40% of the theoretical capacity of Si material based on our previous data. The cycle life reached more than 900 cycles with 1,670 mAh/g capacity in a cell with a low loading of $0.45\text{ mg}/\text{cm}^2$. This cycle number is very close to that of current Li-ion batteries with graphite anodes. However, with this loading level, the battery delivers a low gravimetric energy density of $\sim 120\text{ Wh}/\text{kg}$. To obtain a higher gravimetric energy density $\geq 250\text{ Wh}/\text{kg}$, the anode loading should be $\geq 2.0\text{ mg}/\text{cm}^2$, and HQ will focus more effort to increase the anode loading to achieve better performance.

Task 1.3 – Design and Scalable Assembly of High-Density, Low-Tortuosity Electrodes (Yet-Ming Chiang, Massachusetts Institute of Technology)

PROJECT OBJECTIVE: The objective is to develop scalable high density low-tortuosity electrode designs and fabrication processes enabling increased cell-level energy density compared to conventional Li-ion technology, characterize and optimize the electronic and ionic transport properties of controlled porosity and tortuosity cathodes as well as densely- sintered reference samples. Success is measured by the area capacity (mAh/cm^2) that is realized at defined C-rates or current densities.

PROJECT IMPACT: The high cost (i.e., a high $\$/\text{kWh}$ value) and low energy density of current automotive lithium-ion technology is in part due to the need for thin electrodes and associated high inactive materials content. If successful, this project will enable the use of electrodes based on known families of cathode and anode actives but with at least 3 times the areal capacity (mAh/cm^2) of current technology while satisfying the duty cycles required for vehicle applications. This will be accomplished via new electrode architectures fabricated by scalable methods with higher active materials density and reduced inactive content, and will in turn enable higher energy density and lower-cost EV cells and packs.

APPROACH: Two techniques are used to fabricate thick, high density electrodes with low tortuosity porosity oriented normal to the electrode plane: 1) Directional freezing of aqueous suspensions; and 2) Magnetic alignment. Characterization includes measurement of single-phase material electronic and ionic transport using blocking and non-blocking electrodes with AC and DC techniques, electro-kinetic measurements, and drive-cycle tests of electrodes using appropriate battery scaling factors for EVs.

OUT-YEAR GOALS: Identify anodes and fabrication approaches that enable full cells in which both electrodes have high areal capacity under EV operating conditions. Anode approach will include identifying compounds amenable to same fabrication approach as cathode, or use of very high capacity anodes such as stabilized lithium or Si-alloys that in conventional form can capacity-match the cathodes. Use data from best performing electrochemical couple in techno-economic modeling of EV cell and pack performance parameters.

COLLABORATIONS: Within BMR, this project collaborates with Antoni P. Tomsia (LBNL) in fabrication of low-tortuosity high density electrodes by directional freeze-casting and with Gao Liu (LBNL) in evaluating Si anodes. Outside of BMR, the project collaborates with Randall Erb (Northeastern University) on alternative fabrication methods for low tortuosity electrodes.

Milestones

1. Fabricate and test at least one anode compound in an electrode structure having at least a $10 \text{ mAh}/\text{cm}^2$ theoretical capacity. (12/31/14). **Complete**
2. Demonstrate at least $5 \text{ mAh}/\text{cm}^2$ capacity per unit area at 1C continuous cycling rate for at least one candidate anode. (3/31/15). **Complete**
3. Down-select at least one anode composition for follow-on work. *Go/No-Go milestone:* Down-select based on demonstrated area capacity of at least $7.5 \text{ mAh}/\text{cm}^2$ at 1C continuous rate. (6/30/15). **Initiated**
4. Demonstrate an anode with at least $10 \text{ mAh}/\text{cm}^2$ capacity per unit area for a 2C 30 sec pulse. (9/30/15).

Progress Report

Milestone 2. Demonstrate at least 5 mAh/cm² capacity per unit area at 1C continuous cycling rate for at least one candidate anode. (3/31/15).

As reported last quarter, the

Milestone 2 was completed by fabricating graphite anodes using directional freezing and lyophilization of suspensions with formulations similar to suspensions for aqueous electrode coating processes for Li-ion (see Figure 5). When sectioned to 800 μm thickness, the anodes have a theoretical area capacity of about 25 mAh/cm². When tested at C/5 rate, stable cycling was observed over 10 cycles, as shown in Figure 6 (left) with area capacity of 15 mAh/cm². At C/10 rate, it reaches approximately 18 mAh/cm², see Figure 6 (right).

At 1C rate, the area capacity is 6 mAh/cm², meeting Milestone 2.

During the present quarter, evaluations of the capability of such electrodes to perform under pulse conditions appropriate to EV use were initiated. HPPC characterization of the above described graphite anodes was conducted in which half-cells charged at C/5 rate were sequentially discharged at 1C rate for 10% of SOC, followed by 2C pulse discharge for 30s. The sequence was repeated after 1h rest until 0% SOC was reached. Results are plotted in Figure 7 as voltage vs. area capacity. It is notable that whereas the same electrode at continuous 1C discharge only yields 6 mAh/cm², the HPPC sequence allows the electrode to deliver 14 mAh/cm². It is believed that for the thick, high area capacity, low tortuosity electrodes being fabricated in this project, continuous discharge tests underestimate to a large extent the energy that can be delivered in EV-type duty cycles. Accordingly, a modification to Milestones 3 and 4 to reflect more meaningful demonstrations of EV performance capability is proposed. It is proposed that the Q3 Go/No-go Milestone be modified to: “Demonstrate an electrode with at least 7.5 mAh/cm² that passes the USABC dynamic stress test (DST) with peak discharge C-rate of 2C.”

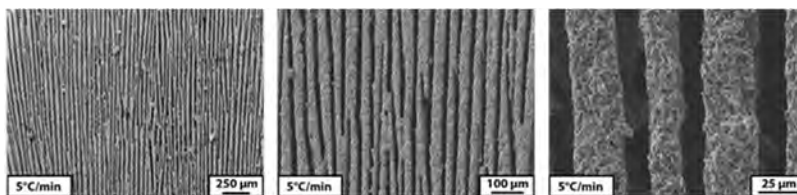


Figure 5: Cross sections of graphite anodes formulated with CMC binder and freeze-cast at the cooling rates indicated. Electrodes were lyophilized to retain structure. Total porosity is 58-60 vol%

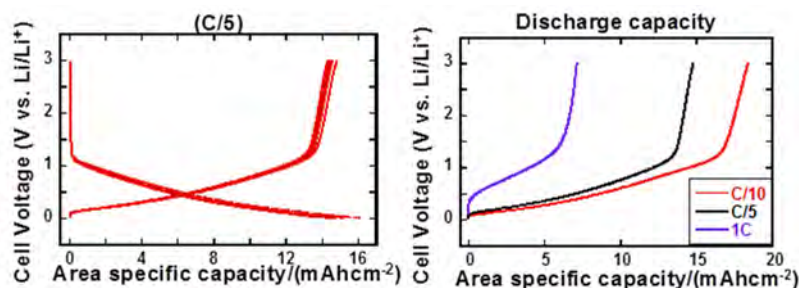


Figure 6: Galvanostatic discharge voltage vs. capacity for 800 μm thick electrode sectioned from sample directionally freeze-cast at 7.5°C/min. Left: Multiple cycles at C/5 rate. Right: Comparison of result at C/10, C/5 and 1C discharge rate.

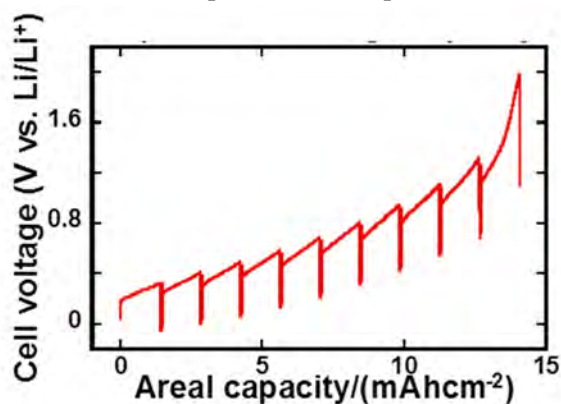


Figure 7: Voltage-area capacity results from HPPC test of 800 μm thick electrode (see Figure 6).

Patents/Publications/Presentations

1. Characterization of Electronic and Ionic Transport in $\text{Li}_{1-x}\text{Ni}_{0.8}\text{Co}_{0.15}\text{Al}_{0.05}\text{O}_2$ (NCA)", R. Amin, D. B. Ravnsbæk, and Y.-M. Chiang, *J. Electrochem. Soc.*, **162** (7) A1163-A1169 (2015).
2. "Highly-Structured, Additive-Free Lithium-Ion Cathodes by Freeze-Casting Technology" S. Behr, R. Amin, Y.-M. Chiang and A. P. Tomsia, *Process engineering*, **DKG 92, No 4**, E39-E43 (2015).

Task 1.4 – Hierarchical Assembly of Inorganic/Organic Hybrid Si Negative Electrodes (Gao Liu, Lawrence Berkeley National Laboratory)

PROJECT OBJECTIVE: The proposed work aims to enable Si as a high capacity and long cycle-life material for negative electrode to address two of the barriers of lithium-ion chemistry for EV/PHEV application, insufficient energy density and poor cycle life performance. The proposed work will combine material synthesis and composite particle formation with electrode design and engineering to develop high capacity, long life and low cost hierarchical Si based electrode. State of the art Li-ion negative electrodes employ graphitic active materials with theoretical capacities of 372 mAh/g. Si, a naturally abundant material, possesses the highest capacity of all Li-ion anode materials. It has a theoretical capacity of 4,200 mAh/g for full lithiation to the $\text{Li}_{22}\text{Si}_5$ phase. However, Si volume change disrupts the integrity of electrode and induces excessive side reactions, leading to a fast capacity fade.

PROJECT IMPACT: This work addresses the adverse effects of Si volume change and minimizes the side reactions to significantly improve capacity and lifetime to develop negative electrode with Li-ion storage capacity over 2,000 mAh/g (electrode level capacity) and significantly improve the coulombic efficiency. The research and development activity will provide an in-depth understanding of the challenges associated with assembling large volume change materials into electrodes, and will develop a practical hierarchical assembly approach to enable Si materials as negative electrodes in Li-ion batteries.

OUT-YEAR GOALS: There are three aspects of this proposed work - bulk assembly, surface stabilization and lithium enrichment – which are formulated into 10 tasks in a four-year period. 1) Develop hierarchical electrode structure to maintain electrode mechanical stability and electrical conductivity. (Bulk assembly) 2) Form *in situ* compliant coating on Si and electrode surface to minimize Si surface reaction. (Surface stabilization) 3) Use prelithiation to compensate first cycle loss of the Si electrode. (Li enrichment) In the end of the 4th year, the goal is to achieve a Si based electrode at higher mass loading of Si, and can be extensively cycled with minimum capacity loss at high coulombic efficiency to qualified for vehicle application.

COLLABORATIONS: Vince Battaglia and Venkat Srinivasan (LBNL), Xingcheng Xiao (GM), Jason Zhang (PNNL), Tong Wei, Wanli Yang, Chongming Wang (PNNL), and the Si-Anode Focus Group.

Milestones

1. Design and synthesis of at least two functional conductive polymers for Si based electrode. (Dec. 31) **Complete**
2. Develop methodologies to improve the Si electrode first cycle efficiency to 90%. (Mar. 31) **Complete**
3. Design and synthesize new surface stabilizing additive, and test it with Si based electrode. (Jun. 30) **Ongoing**
4. Go/No-Go Apply hierarchical electrode design to achieve a 3 mAh/cm² loading. (Sep. 31) **Ongoing**

Progress Report

Here we describe a class of electric-conducting polymers that conduct electron via the side chain π - π stacking. These polymers can be designed and synthesized with different chemical moieties to perform different functions, extremely suitable as conductive polymer binder for lithium battery electrode. A class of methacrylate polymers based on a polycyclic aromatic hydrocarbon side moiety, pyrene, was synthesized and applied as an electrode binder to fabricate a silicon (Si) electrode (see Figure 8). The electron mobilities for PPy and PPyE are characterized as $1.9 \times 10^{-4} \text{ cm}^2 \text{ V}^{-1} \text{ s}^{-1}$ and $8.5 \times 10^{-4} \text{ cm}^2 \text{ V}^{-1} \text{ s}^{-1}$, respectively. These electric conductive polymeric binders can maintain the electrode mechanical integrity and Si interface stability over a thousand cycles of charge and discharge.

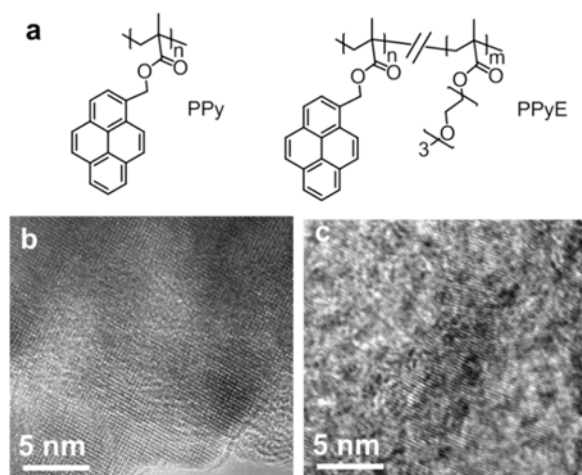


Figure 8: (a) Structure of poly(1-pyrenemethyl methacrylate) (PPy) and poly(1-pyrenemethyl methacrylate-co-triethylene oxide methyl ether methacrylate) (PPyE). High-resolution TEM (HRTEM) images of (b) PPy and (c) PPyE.

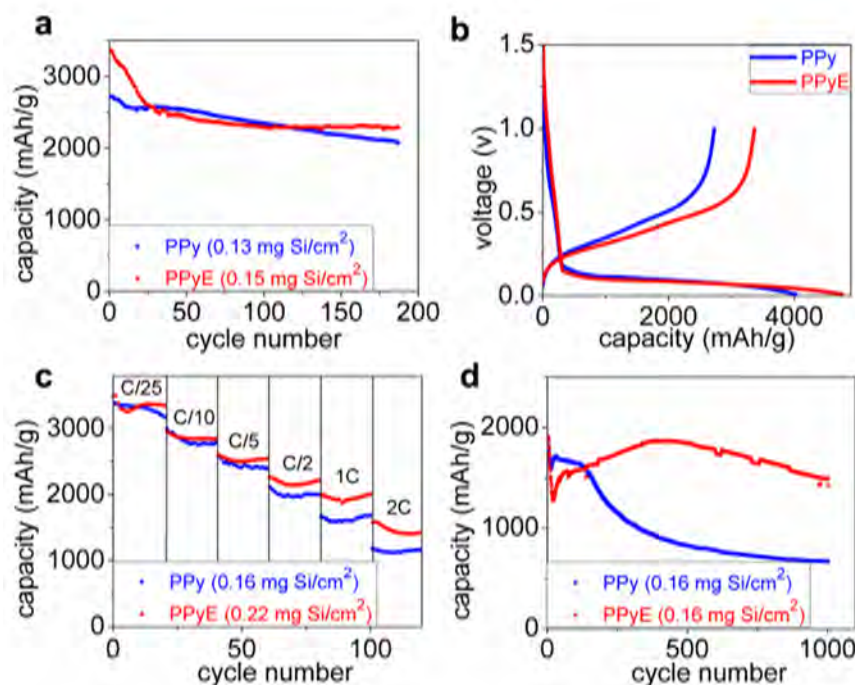


Figure 9: (a) Charge (delithiation) capacities of PPy and PPyE-based Si electrodes at C/10. (b) First-cycle voltage curves. (c) Rate performance. (d) Charge (delithiation) capacities of PPy and PPyE-based Si electrodes at 2C rate. The mass loadings of Si for each cell are labelled in the plot.

The as-assembled batteries exhibit a high capacity and excellent rate performance due to the self-assembled solid-state nanostructures of the conductive polymer binders (see Figure 9). The physical properties of this polymer are further tailored by incorporating ethylene oxide moieties at the side chains to enhance the adhesion and adjust swelling to improve the stability of the high loading Si electrode.

Q2 Patents/Publications/Presentations

1. Sangjae Park, Hui Zhao (**co-first author**), Guo Ai, Cheng Wang, Xiangyun Song, Neslihan Yuca, Vincent S. Battaglia, Wanli Yang, and Gao Liu, Side-chain conducting and phase-separated polymeric binders for high performance silicon anodes in lithium-ion batteries. *J. Am. Chem. Soc.*, **2015**, 137, 2565-2571.
2. Ying Bai, Yang Tang, Zhihui Wang, Zhe Jia, Feng Wu, Chuan Wu, Gao Liu. Electrochemical performance of Si/CeO₂/Polyaniline composites as anode materials for lithium ion battery. *Solid State Ionics*, **2015**, 272, 24-29.
3. Hui Zhao, Wen Yuan, Gao Liu. Hierarchical electrode design of high-capacity alloy nanomaterials for lithium-ion batteries. *Nano Today*, **2015**, Accepted.
4. Feifei Shi, Phillip N. Ross, Hui Zhao, Gao Liu, Gabor A. Somorjai, and Kyriakos Komvopoulos. A catalytic path for electrolyte reduction in lithium-ion cells revealed by *in situ* attenuated total reflection-fourier transform infrared spectroscopy. *J. Am. Chem. Soc.* **2015**, 137(9), 3181-3184.
5. Wen Yuan, Mingyan Wu (**co-first author**), Hui Zhao, Xiangyun Song, Vincent Battaglia, and Gao Liu. “Baseline Si electrode fabrication and performance for the Battery for Advanced Transportation Technologies program.” *J. Power Sources*, **2015**, 282, 223-227.
6. Kehua Dai, Jing Mao, Xiangyun Song, Vincent Battaglia, Gao Liu, Na_{0.44}MnO₂ with very fast sodium diffusion and stable cycling synthesized via polyvinylpyrrolidone-combustion method. *Journal of Power Sources*, **2015**, 285, 161-168.

Presentations at the Materials Research Society meeting, 2015 Spring, San Francisco (April 6th to 10th, 2015)

1. Toward a Better Understanding of the Surface Effect through the Design of Binders in Lithium Sulfur Battery, Oral presentation, Presenter (Guo Ai)
2. Side-Chain Conducting and Phase-Separated Polymeric Binders for High-Performance Silicon Anodes in Lithium-Ion Batteries. Oral presentation, Presenter (Hui Zhao)
3. Toward Practical Application of Functional Conductive Polymer Binder for a High-Energy Lithium-Ion Battery Design. Oral presentation, Presenter (Hui Zhao)

Task 1.5 – Studies in Advanced Electrode Fabrication (Vincent Battaglia, Lawrence Berkeley National Laboratory)

PROJECT OBJECTIVE: This project supports BMR PIs through the supply of electrode materials, laminates, and cells as defined by the BMR Focus Groups. The emphasis of the 2015 effort will be on the High-Voltage Focus Group, the Si-Anode Focus Group, and a nascent Li/S effort. The objectives are to screen sources of materials, define baseline chemistries, and benchmark performance of materials targeted to specific Focus Group topics. This provides common chemistry and performance metrics that other BMR institutions can use as a benchmark for their own efforts on the subject. In addition, test configurations are designed and built to identify and isolate problems associated with poor performance. Also, Li/S cells is to be designed and tested.

PROJECT IMPACT: Identification of baseline chemistries and availability of baseline laminates will allow a group of BMR PIs to work as a team. Such team work is considered crucial in the acceleration of the advancement of today's Li-ion and Li/S systems. Since all of the focus groups are dedicated on some aspect of increased energy density, the cumulative work will have a significant impact on this area.

OUT-YEAR GOALS: This framework of a common chemistry will accelerate advancements in energy density and should lead to baseline systems with an increased energy density of at least 40%. It should also provide a recipe for making electrodes of experimental materials that are of high enough performance to allow for critical down select – an important part of the process in advancing any technology.

COLLABORATIONS: Several BMR PIs

Milestones

1. Identify and report the source of additional impedance of a symmetric cell. (12/31/14) **Complete**
2. Measure and report the gas composition of a symmetric cathode/cathode cell and an anode/anode cell. (3/31/15) **Complete**
3. Identify the first iteration of the baseline Li/S cell. (6/30/15) **Ongoing**
4. Measure and report gas volume *versus* rate of side reaction at several upper voltage cut-off points. (9/30/15) **Ongoing**

Progress Report

Milestone 1. Identify and report the source of additional impedance of a symmetric cell.

Milestone 2. Measure and report the gas composition of a symmetric cathode/cathode cell and an anode/anode cell.

We are presently studying the difference in cycleability of three cathode materials, LCO, high-voltage LCO, and NCM. Of the three materials, LCO shows the greatest impedance rise. Therefore, a pouch cell of LCO and Li metal was fabricated. To form gas, the cell was taken to various upper cut-off voltages and held there for 24 hours to see if a gas was generated. At reasonable working voltages (voltages below 4.6 V), no gas generation was evident as the cells did not puff up. The cells were then hooked to a mass spectrometer to measure the composition of any gas that may have been formed, but the device was not of sufficient accuracy to detect a significant change in gas composition. One cell was pushed to ever increasing cut-off voltages in an effort to generate gas. It finally occurred at around 5.2 V. It is fairly well known that the electrolyte loses all stability at this voltage and finally breaks down. This is most familiar to researchers that perform abuse tolerance experiments. This situation was considered too dangerous to continue and we halted the experiment. We still believe there is value in measuring the rate of gas generation in a cell and its composition but we need to find a chemistry that does this under slightly more stable conditions. We also acquired another mass spec and will try our experiment again without going to high voltages to see if the gas is detectable.

Milestone 3. Identify the first iteration of the baseline Li/S cell.

Cell hardware for testing Li/S cells was identified and purchased. The cell is due to arrive early January. There are only a handful of investigators at LBNL developing technologies for this chemistry including Elton Cairns, Gao Liu, Venkat Srinivasan, and Nitash Balsara. We intend to work closely with them investigators and incorporate their technologies into the selected cell hardware.

Milestone 4. Measure and report gas volume *versus* rate of side reaction at several upper voltage cut-off points.

See reports under Milestones 1 and 2.

TASK 2 – SILICON ANODE RESEARCH

Summary and Highlights

Most Li-ion batteries used in the state of the art electric vehicles (EVs) use graphite as the anode material. The limited capacity of graphite (LiC_6 , 372 mAh/g) is one of the barriers that prevent long range operation of EVs required to meet the *EV Everywhere* Grand Challenge from DOE/EERE. In this regard, Silicon (Si) is one of the most promising candidates as an alternative anode for Li-ion battery applications. Si is environmentally benign and available everywhere. The theoretical specific capacity of silicon is 4,212 mAh/g ($\text{Li}_{21}\text{Si}_5$), which is 10 times greater than the specific capacity of graphite. However, the high specific capacity of silicon is also associated with large volume changes (of more than 300 percent) when alloyed with lithium. These extreme volume changes can cause severe cracking and disintegration of the electrode and lead to a significant capacity loss.

Significant scientific research has been conducted to circumvent the deterioration of silicon-based anode materials during cycling. Various strategies, such as the reduction of particle size, generation of active/inactive composites, fabrication of silicon-based thin films, use of alternative binders, and the synthesis of one-dimensional silicon nanostructures have been implemented by a number of research groups. Fundamental mechanistic research also has been performed to better understand the electrochemical lithiation and delithiation processes during cycling in terms of crystal structure, phase transitions, morphological changes, and reaction kinetics. Although significant progress has been made on the development of the silicon-based anodes, there are still many obstacles that prevent their practical application. Long-term cycling stability remains the foremost challenge for Si based anode, especially for high loading electrode ($> 3\text{mAh/cm}^2$) required in many practical applications. The cyclability of full cells using silicon-based anodes is also complicated by multiple factors, such as diffusion-induced stress and fracture, loss of electrical contact among silicon particles and between silicon and current collector, and the breakdown of SEI layers during volume expansion/contraction processes. The design and engineering of a full cell with a silicon-based anode still needs to be optimized. Critical research remaining in this area includes, but is not limited to, the following:

- The effects of SEI formation and stability on the cyclability of silicon-based anodes need to be further investigated. Electrolytes and additives that can produce a stable SEI layer need to be developed.
- Low-cost manufacturing processes have to be found to produce nano-structured silicon with desired properties.
- Better binder and conductive matrices need to be developed. They should provide flexible but stable electrical contacts among silicon particles and between particles and the current collector under repeated volume changes during charge/ discharge processes.
- The performances of full cells using silicon-based anode need to be investigated and optimized.

The main goal of the BMR Task 2 is to have a fundamental understanding of the failure mechanism of Si based anode and improve its long term stability, especially for a thick electrode operated at full cell conditions. The Stanford group will address the problem of large first cycle loss in Si based anode by novel prelithiation approaches. Two approaches will be investigated in this study: 1) developing facile and practical methods to increase the first-cycle Coulombic efficiency of Si anodes, and 2) synthesizing fully lithiated Si to pair with high capacity lithium-free cathode materials. PNNL/UP/FSU team will explore new electrode structures using nano Si and SiO_x to enable high-capacity and low-cost Si-based anodes with good cycle stability and rate capability. Nanocomposites of silicon lithium oxide will be prepared by novel *in situ* chemical reduction methods to reduce the first cycle loss. Mechanical and electrochemical stability of the SEI layer formed on the surface of Si particles will be investigated by electrochemical evaluation and *in situ/ex situ* microscopic analysis. Success of this project will accelerate large scale application of Si-based anodes and improve the energy density of Li-ion batteries to meet *EV everywhere* goals.

Task 2.1 – Development of Silicon-Based High Capacity Anodes (Ji-Guang Zhang/Jun Liu, PNNL; Prashant Kumta, University of Pittsburgh; Jim Zheng, PSU)

PROJECT OBJECTIVE: The objective of this project is to develop high-capacity and low-cost Si-based anodes with good cycle stability and rate capability to replace graphite in Li-ion batteries. Nanocomposites of silicon and Li-ion conducting lithium oxide will be prepared by novel *in situ* chemical reduction methods to solve the problems associated with large first cycle irreversible capacity loss, while achieving acceptable Coulombic efficiencies. Large irreversible capacity loss in the first cycle will also be minimized by pre-doping Li into the anode using stabilized lithium metal powder or additional sacrificial Li electrode. The optimized materials will be used as the baseline for both thick electrode fabrication and studies to advance our fundamental understanding of the degradation mechanism of Si-based anodes. The electrode structures will be modified to enable high utilization of thick electrode. Mechanical and the electrochemical stability of the SEI layer will be investigated by electrochemical method, simulation and *in situ* microscopic analysis to guide their further improvement.

PROJECT IMPACT: Si-based anodes have much larger specific capacities compared with the conventional graphite anodes. However, the cyclability of Si-based anodes is limited because of the large volume expansion that is characteristic of these anodes. This work will develop a low-cost approach to extend the cycle life of high-capacity, Si-based anodes. The success of this work will further increase the energy density of Li-ion batteries and accelerate market acceptance of electrical vehicles (EV), especially for plug-in hybrid electrical vehicles (PHEV) required to meet the *EV Everywhere* Grand Challenge proposed by DOE/EERE.

OUT-YEAR-GOALS: The main goal of the proposed work is to enable Li-ion batteries with a specific energy of >200 Wh/kg (in cell level for PHEVs), 5,000 deep-discharge cycles, 15-year calendar life, improved abuse tolerance, and less than 20% capacity fade over a 10-year period.

COLLABORATIONS: We will continue to collaborate with following battery groups on anode development:

- Dr. Karim Zaghib, Hydro Quebec – Preparation of nano-Si
- Prof. Michael Sailor, UCSD – Preparation of porous Si.
- Prof. David Ji, Oregon State University – Preparation of porous Si by thermite reactions.

Milestones

1. Identify the stability window of SEI formed on Si based anode (12/31/2014) **Completed**
2. Optimize the synthesis conditions of the rigid-skeleton supported Si composite (3/31/2015) **Completed.**
3. Demonstrate the operation of full cell using Si anode and selected cathode with >80% capacity retention over 100 cycles. (6/30/2015)
4. Achieve >80% capacity retention over 200 cycles of thick electrodes (~3 mAh/cm²) through optimization of the Si electrode structure and binder. (9/30/2015)

Progress Report

In this quarter, porous Si prepared by thermite reaction was treated by calcination. The treated samples demonstrated a capacity of $\sim 3 \text{ mAh/cm}^2$ and a capacity- retention of $\sim 78\%$ over 150 cycles as shown in Figure 10.

A new binder for Si based anode has been investigated. The optimized SBG composite with the new binder exhibits good cycle stability but the capacity is lower than that for the CMC binder. The structure of the binder will be further modified to improve its performance. A new type of multi-layer core-shell structured Si composite has been investigated. The main purpose of this design is to coat Si on the outside of spherical graphite particles. The outside of Si will be covered by another layer of carbon as a barrier between Si and electrolyte. It is expected that by adjusting the ratio of Si:graphite:carbon, cycling stability of high loading Si anodes can be obtained while still maintaining a reasonable anode capacity.

Direct mechanochemical reduction of SiO with the metallic Li has been used to generate $\alpha\text{-Si}+\text{Li}_2\text{O}$ nanocomposite as follows:

$\text{SiO}+2\text{Li}\rightarrow\text{Si}+\text{Li}_2\text{O}$. The system shows an initial capacity of $\sim 1,620 \text{ mAh/g}$ indicating presence of unreacted SiO . In a separate effort, SiO was reduced with Mg_2Si using mechanochemical reduction to obtain Si and MgO .

Subsequently, the material was washed and etched with acids to yield nanocrystalline Si (nc-Si). The resulting nc-Si was then coated with carbon. The nc-Si/C composite material shows better cycling stability (10cycles @50mA/g + 90cycles @100mA/g, 0.12% per cycle fade rate, $\sim 495 \text{ mAh/g}$ at the end of 100 cycles) compared to pure nc-Si material which shows a very rapid fade rate within the first 20 cycles (see Figure 11). The high surface area of nc-Si and unreacted SiO are the major contributors to the FIR loss ($\sim 55\text{-}65\%$) which will be improved by increasing the kinetics of the reduction reaction by a combination of milling and thermal activation.

Freestanding flexible light-weight silicon nanoparticles-carbon nanotubes (SiNPs-CNTs) composite paper anodes for lithium (Li) ion batteries (LIBs) have been prepared by ultrasonication and pressure filtration without using conductive additive, binder or current collector. Electrochemical testing has shown that the SiNPs-CNTs composite electrode material achieves first cycle specific discharge and charge capacities of 2,298 and 1,492 mAh/g, respectively (see Figure 12). To address the first cycle irreversibility, stabilized Li metal powder (SLMP) has been utilized to pre-lithiate composite anodes. Compared to cell without SLMP, the cell with an SLMP loading of SLMP/anode mass ratio of 0.26 has the first cycle irreversible capacity loss reduced from 806 to 28 mAh/g and the first cycle Coulombic efficiency increased from 65 to 98%. Use of the SiNPs-CNTs anodes containing SLMP as Li source opens the door to a broad range of non-Li-containing cathode materials and enables the creation of future high capacity and high energy LIBs.

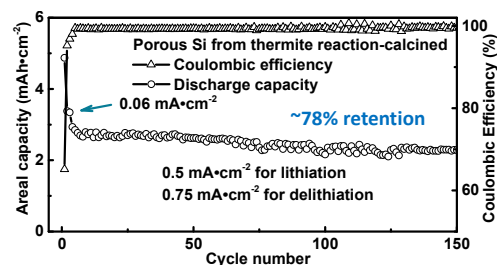


Figure 10: Cycling stability of thermite porous Si after heat treatment

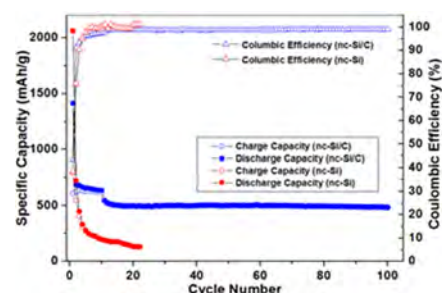


Figure 11: Specific charge/discharge capacity/Coulombic efficiency vs cycles of nc-Si and nc-Si/carbon in Li/Li^+ system.

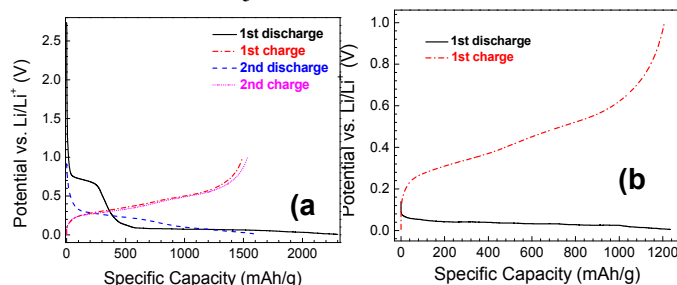


Figure 12: Representative first cycle voltage profile of SiNPs-CNTs anodes (a) with and (b) without SLMP

Patents/Publications/Presentations

1. Rigved Epur, Luke Minardi, Moni K. Datta, Sung Jae Chung, Prashant N. Kumta, “A simple facile approach to large scale synthesis of high specific surface area silicon nanoparticles”, Journal of Solid State Chemistry 208 (2013) 93-98.

Task 2.2 – Pre-Lithiation of Silicon Anode for High Energy Li Ion Batteries (Yi Cui, Stanford University)

PROJECT OBJECTIVE: Prelithiation of high capacity electrode materials such as Si is an important means to enable those materials in high-energy batteries. This study pursues two main directions: 1) developing facile and practical methods to increase first-cycle Coulombic efficiency of Si anodes, and 2) synthesizing fully lithiated Si to pair with high capacity lithium-free cathode materials.

PROJECT IMPACT: The first-cycle Coulombic efficiency of anode materials will be increased dramatically via prelithiation. Prelithiation of high capacity electrode materials will enable the use of those materials in next generation high-energy-density lithium ion batteries. This project's success will make high-energy-density lithium ion batteries for electric vehicles.

OUT-YEAR GOALS: Compounds containing large quantity of Li will be synthesized for pre-storing Li ions inside batteries. First-cycle Coulombic efficiency (1st CE) will be improved and optimized (over 95%) by prelithiating anode materials with the synthesized Li-rich compounds.

COLLABORATIONS:

- BMR program PI's
- SLAC: *In situ* X-ray, Dr. Michael Toney.
- Stanford: Prof. Nix, mechanics.

Milestones

1. Prelithiate anode materials by direct contact of Li metal foil to anodes (Jan-14) **Completed**
2. Synthesize Li_xSi nanoparticles with high capacity ($>1000\text{mAh/g Si}$) (July-14) **Completed**
3. Prelithiate anode materials with dry-air-stable $\text{Li}_x\text{Si-Li}_2\text{O}$ core-shell nanoparticles (April-15). **Completed**

Progress Report

$\text{Li}_x\text{Si-Li}_2\text{O}$ core-shell nanoparticles (NPs) were used as excellent prelithiation reagents with high specific capacity to compensate the first cycle capacity loss. These NPs were produced with a facile and scalable synthesis approach by direct alloying of Si NPs with Li metal foil as shown in Figure 13a. A dense passivation layer was formed on the Li_xSi NPs after exposure to trace amounts of oxygen. Due to the high chemical reactivity, $\text{Li}_x\text{Si-Li}_2\text{O}$ NPs are not compatible with the commercial slurry solvent, N-Methyl-2-pyrrolidone (NMP). Figure 13b shows that the $\text{Li}_x\text{Si-Li}_2\text{O}$ NPs show a small Li extraction capacity of $\sim 300 \text{ mAh g}^{-1}$. Excitingly, $\text{Li}_x\text{Si-Li}_2\text{O}$ NPs are compatible with 1,3-dioxolane (DOL) and toluene, showing high extraction capacities of 1,200-1,400 mAh g^{-1} , which is sufficient to qualify it as a prelithiation reagent. Since PVDF binder does not dissolve in toluene to form a uniform slurry, DOL is selected as the slurry solvent.

Prelithiation of graphite flakes by $\text{Li}_x\text{Si-Li}_2\text{O}$ NPs (mass ratio 83:7) increased 1st cycle Coulombic efficiency (CE) from 87% to 99% (Figure 14a). Graphite/ LiFePO_4 full cells are used to investigate the effect of $\text{Li}_x\text{Si-Li}_2\text{O}$ particles on full cell performance. One full cell consists of graphite flake anode prelithiated with $\text{Li}_x\text{Si-Li}_2\text{O}$ particles (graphite flakes: $\text{Li}_x\text{Si-Li}_2\text{O}$:PVDF= 83:7:10), whereas another one consists of a anode with regular graphite flakes (graphite flakes: PVDF=90:10). The cells are measured in the voltage window from 2.5 V to 3.8 V at C/10 (Figure 14c). The blue voltage profile reveals a plateau between 2.6 and 3.2 V, corresponding to the SEI formation in the anode during charging. As shown by the red voltage profile, the incorporation of $\text{Li}_x\text{Si-Li}_2\text{O}$ NPs compensates the irreversible Li consumption resulting from SEI formation. Accordingly, the 1st CE increases from 77.6% to 90.8%. In the following cycles, the cell with $\text{Li}_x\text{Si-Li}_2\text{O}$ NPs consistently shows a higher capacity than the regular cell (Figure 14d). Therefore, $\text{Li}_x\text{Si-Li}_2\text{O}$ NPs can effectively increase the 1st CE of both half cells and full cells.

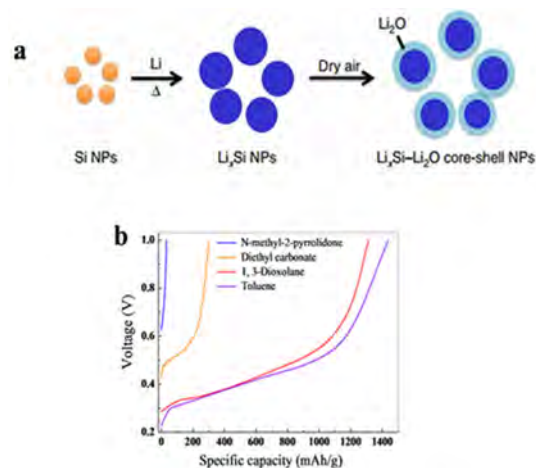


Figure 13: (a) Schematic diagrams showing Si NPs react with melted Li to form Li_xSi NPs. A dense passivation layer is formed on the Li_xSi NPs after exposure to trace amounts of oxygen, preventing the Li_xSi alloy from further oxidation in dry air. (b) First cycle delithiation capacity of $\text{Li}_x\text{Si-Li}_2\text{O}$ NPs, using different solvents to form the slurry

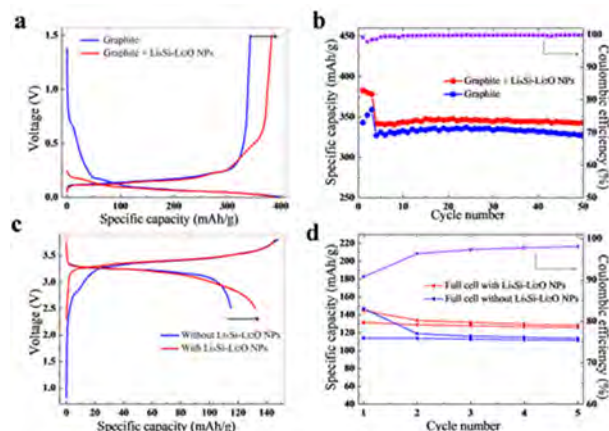


Figure 14: First cycle voltage profiles of graphite flakes/ $\text{Li}_x\text{Si-Li}_2\text{O}$ (83:7 by weight) and graphite flakes control cell. (b) Cycling performance of graphite flakes/ $\text{Li}_x\text{Si-Li}_2\text{O}$ and graphite flakes control cell. The purple line is the Coulombic efficiency of graphite flakes/ $\text{Li}_x\text{Si-Li}_2\text{O}$ composite. (c) First cycle voltage profiles of graphite/ LiFePO_4 full cell with and without $\text{Li}_x\text{Si-Li}_2\text{O}$ nanoparticles. (d) Cycling performance of full cell with and without $\text{Li}_x\text{Si-Li}_2\text{O}$ nanoparticles. The purple line is the Coulombic efficiency of full cell with $\text{Li}_x\text{Si-Li}_2\text{O}$ nanoparticles.

Patents/Publications/Presentations

1. Patent: S14-109| Dry-air-stable Li_xSi – Li_2O core–shell nanoparticles as high-capacity prelithiation reagents.
2. Publication: Zhao, J. et al. Dry-air-stable lithium silicide–lithium oxide core–shell nanoparticles as high-capacity prelithiation reagents. Nat. Commun. 5: 5088 (2014).

TASK 3 – HIGH ENERGY DENSITY CATHODES FOR ADVANCED LITHIUM-ION BATTERIES

Summary and Highlights

High energy density, low-cost, thermally stable, and environmentally safe electrode materials can be one of the key enablers of advanced batteries for transportation. High energy density is synonymous with reducing cost per unit weight or volume. Currently, one major technical barrier towards development of high energy density lithium-ion batteries (LiBs) is the lack of robust, high-capacity cathodes. For example, the most commonly used anode material for LiBs is graphitic carbon, which has a specific capacity of 372 mAh/g, while even the most advanced cathodes like lithium nickel manganese cobalt oxide (NMC) have a maximum capacity of ~180 mAh/g. This calls for an immediate need to develop high capacity (and voltage) intercalation type cathodes that have stable reversible capacities of 300 mAh/g or more. High volumetric density is also critical for transportation applications. Alternative high capacity cathode chemistries such as those based on conversion mechanisms, Li-S, or metal air chemistries still have fundamental issues that need to be addressed before integration into cells for automotive use. Successful demonstration of high energy cathodes will enable high energy cells that meet or exceed the DOE cell level targets of 400 Wh/kg and 600 Wh/L with a system level cost target of \$125/kWh.

Over the last decade, many high voltage cathode chemistries have been developed under the BATT (predecessor to BMR) program including Li-rich NMC and Ni-Mn spinels. Current efforts are directed towards new syntheses and modifications to improve stability (both bulk and interfacial) under high voltage cycling condition (> 4.6 V) for Li-rich NMC [Nanda, ORNL, Zhang & Jie, PNNL, Thackeray and Croy, ANL, Marca Doeff, LBNL]. Three other subtasks are directed towards synthesis and structural stabilization of high capacity, multivalent, polyanionic cathodes both in crystalline and amorphous phases [Manthiram, UT-Austin, Looney and Wang, BNL, Whittingham, SUNY-Binghamton and Kercher-Kiggans, ORNL]. Approaches also include aliovalent or isovalent doping to stabilize cathode structures during delithiation as well as surface coatings to improve interfacial stability. John Goodenough's group at UT-Austin is developing novel separators to enable lithium metal anodes and high capacity cathodes in a flow cell.

The highlights for this quarter are as follows:

Task 3.1: $\text{Li}_2\text{Cu}_{1-x}\text{Ni}_x\text{O}_2$ solid solution cathodes with capacities > 200 mAh/g for 30 cycles

Task 3.2: Fe substitution of CuF_2 shows evidence of single phase formation upto 50% Fe

Task 3.3: Hydrothermal synthesis of LMR-NMC showed 90% capacity retention for 200 cycles

Task 3.4: $\text{Li}_x\text{Na}_{1-x}\text{VOPO}_4\text{F}_{0.5}$ was synthesized *via* ion exchange from $\text{Na}_{1.5}\text{VOPO}_4\text{F}_{0.5}$

Task 3.5: Stabilizing Li-rich NMC with a Co based spinel component with capacity ~200 mAh/g

Task 3.6: Aliovalent substitution of Ti^{4+} for Fe^{2+} in $\text{LiFe}_{1-2x}\text{Ti}_x\text{PO}_4$ improved stability

Task 3.7: Glass cathodes with molybdate substitution provide a high capacity (500 mA/g), and environmentally friendly alternative to vanadate substitution.

Task 3.8: STEM-EELS study of spray pyrolyzed Ni-rich NMC cathodes shed light on their electronic structure and homogeneity.

Task 3.9: Modified the membrane functional group from divinyl ether to divinyl adipate that has ester groups to enable higher electronic interactions with cathode molecules in electrolyte

Task 3.10: Synthesis and structural characterization of $\text{LT-LiCo}_{1-y}\text{Ni}_{0.1}\text{Mn}_y\text{O}_2$ ($y=0, 0.1, 0.2$) to stabilize spinel in layered TM oxides

Task 3.1 – Studies of High Capacity Cathodes for Advanced Lithium-ion Systems (Jagjit Nanda, Oak Ridge National Laboratory)

PROJECT OBJECTIVE: The overall project goal is the development of high energy density lithium-ion electrodes for EV and PHEV applications that meet or exceed DOE energy density and life cycle targets included in the USDRIVE/USABC roadmap. Specifically, this project aims to address and mitigate technical barriers associated with high voltage cathode compositions such as lithium-manganese rich NMC (LMR-NMC) and $\text{Li}_2\text{MIMiIO}_2$, where MI and MII are transition metals that do not include Mn or Co. Major emphasis is placed on developing new materials modifications (including synthetic approaches) for high voltage cathodes that will mitigate issues such as: (i) voltage fade associated with LMR-NMC composition that leads to a loss of energy over the cycle life; (ii) transition metal dissolution that leads to capacity and power fades; (iii) thermal and structural stability under the operating SOC range; and (iv) voltage hysteresis associated with multivalent transition metal compositions. Another enabling feature of the project is utilizing (and developing) various advanced characterization and diagnostic methods at the electrode and/or cell level for studying cell and/or electrode degradation under abuse conditions. The techniques include electrochemical impedance spectroscopy, Micro-Raman, aberration corrected electron microscopy combined with EELS, X-ray photoelectron spectroscopy, ICP-AES, Fluorescence, and X-ray and Neutron diffraction.

PROJECT IMPACT: The project has both short term and long term deliverables directed towards VTO 2015 and 2022 Energy Storage goals. Specifically, we are working on advanced electrode couples that have cell-level energy density targets of 400 Wh/kg and 600 Wh/l for 5,000 cycles. Increasing the energy density per unit mass or volume ultimately reduces the cost of battery packs consistent with DOE 2022 *EV everywhere* goal of \$125/kWh.

OUT-YEAR GOALS: The project is directed towards developing high capacity cathodes for advanced lithium-ion batteries. The goal is to develop new cathode materials that have a high capacity, are based on low cost materials and meet the DOE road map in terms of safety and cycle life. Under this project, two kinds of high-energy cathode materials are studied. Over the last few years, the PI has worked on improving cycle life and mitigating energy losses of high voltage Li-rich composite cathodes (referred to as LMR-NMC) in collaboration with the voltage fade team at Argonne National Laboratory. Efforts also include surface modification of LMR-NMC cathode materials to improve their electrochemical performance under high voltage cycling ($> 4.5\text{V}$). The task also includes working in collaboration with researchers at Stanford Synchrotron Research Laboratory (SSRL) and APS (LBNL) to understand local changes in morphology and microstructure under *in situ* and *ex situ* conditions.

COLLABORATIONS:

Johanna Nelson, SSRL, SLAC: X-ray imaging and XANES; Guoying Chen, LBNL: *in situ* XAS and XRD; Feng Wang, Brookhaven National Lab: X-ray synchrotron spectroscopy and microscopy; Bryant Polzin, Argonne Research Laboratory: CAMP Facility for electrode fabrication

Milestones

1. Q1: Investigation of the surface reactivity, vacancy disorder and interfacial kinetics of LMR-NMC composite cathodes to mitigate voltage fade and TM dissolution to achieve DOE cell level EV goals of 400 Wh/Kg and 600 Wh/L for 5,000 cycles.
2. Q2: Undertake temperature dependent EIS measurements to separate the charge transfer and passive film resistance for LMR-NMC full cells as a function of SOC and cycle life (using baseline graphite anode).

3. Q3: Undertake *in situ* and *ex situ* X-ray synchrotron and spectroscopic studies to correlate changes in local structure, surface chemistry and morphology of cycled high energy density electrodes (LMR-NMC and 5V Mn-Ni spinel) and compare the changes with pristine or uncycled electrodes.
4. Q4: Stabilize the structure and electrochemical performance of high capacity $\text{Li}_2\text{Cu}_x\text{Ni}_{1-x}\text{O}_2$ cathodes to achieve capacity between 250-300 mAh/g for > 50 charge-discharge cycles at C/3 rate.

Progress Report

During this quarter, we synthesized two cathode compositions, Li_2CuO_2 (LCuO) and $\text{Li}_2\text{Cu}_{0.5}\text{Ni}_{0.5}\text{O}_2$ (LCuNiO), characterized the structures, and measured their initial electrochemical performance. The LCuO and LCuNiO were synthesized following a modified version of the procedure reported by Takeda, et al. [Solid State Ionics 2006, 177, 1341-1346]. Nickel oxide is a common impurity in most standard solid state syntheses. To reduce this impurity, the mixed transition metal hydroxides were first synthesized via co-precipitation, followed by solid state reaction with lithium. We carried out X-ray and neutron refinement to determine the structure and phase purity. Refinement results (not shown here) confirm the formation of the desired Li_2CuO_2 and $\text{Li}_2\text{Cu}_{0.5}\text{Ni}_{0.5}\text{O}_2$ phases with about 90% phase purity.

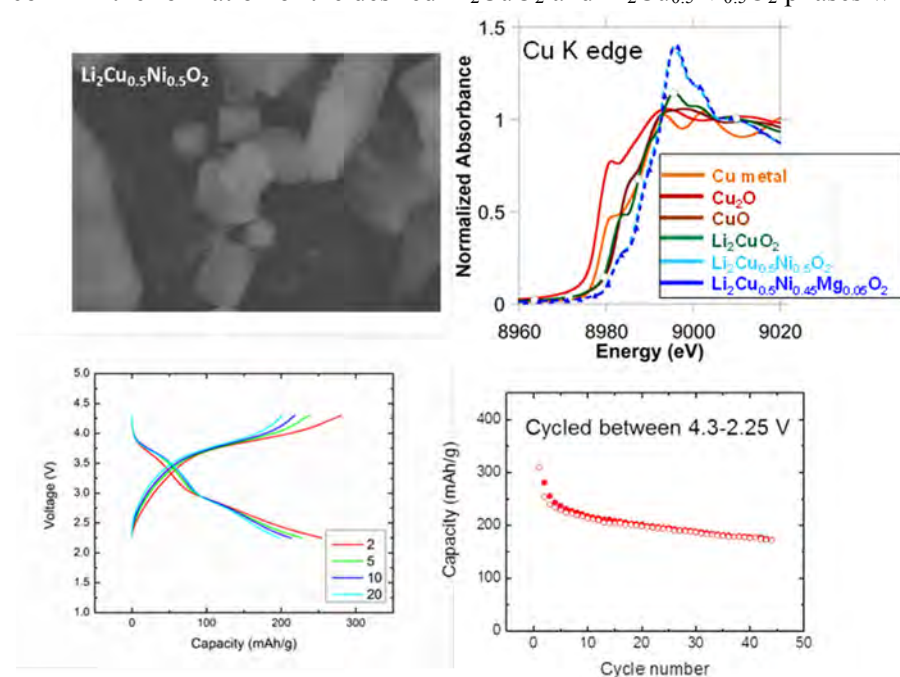


Figure 15: Top left: SEM micrograph of $\text{Li}_2\text{Cu}_{0.5}\text{Ni}_{0.5}\text{O}_2$; Top right: XANES showing Cu K edge of Li_2CuO_2 and $\text{Li}_2\text{Cu}_{0.5}\text{Ni}_{0.5}\text{O}_2$; Bottom left: Charge-discharge voltage profile of $\text{Li}_2\text{Cu}_{0.5}\text{Ni}_{0.5}\text{O}_2$; Bottom right: Capacity versus no. of cycles for $\text{Li}_2\text{Cu}_{0.5}\text{Ni}_{0.5}\text{O}_2$

several microns. By using oxalates as precursors (instead of hydroxides) we hope to form smaller particles with some porosity, thereby increasing capacity utilization within the measured voltage window. Alternative binder materials are being explored since PVDF reacts with the copper oxide material and forms a gel which is difficult to process. Changing the binder chemistry should enable us to fabricate higher quality electrodes with fewer agglomerates. We are also working to optimize the voltage window for electrochemical cycling. Recent experiments indicate (data not shown) the electrochemical stability can be significantly improved by carefully controlling the upper and lower cut-off voltage to avoid Cu^+ formation at lower voltage and gas evolution at higher voltage.

Li_2CO_3 , $\text{Li}_x\text{Ni}_{1-x}\text{O}$, and Li_2O are the primary impurities. Synchrotron X-ray absorption near edge spectroscopy (XANES) confirm both Cu and Ni are in +2 oxidation state (see Figure 15). Initial capacity estimates are in the range of 200 mAh/g when cycled between 4.3 - 2.25 V, but the capacity seems to be falling off after 25 cycles. Several parallel efforts are in progress to improve the electrochemical performance and cycle stability. New synthetic routes are under development to reduce impurities and decrease the primary particle size currently in the range of

Patents/Publications/Presentations

Presentation (this quarter)

1. High Voltage (Capacity) Cathodes for Advanced Lithium-Ion Batteries, J. Nanda and R. Ruther *et al.*, ACS Spring Meeting, March 22nd- 26th 2015 Denver (Invited).
2. Quantifying the Chemical and Morphological Heterogeneities in High Capacity Battery Materials Under Electrochemical Cycling, 2015 TMS Meeting, March 15-22nd, Orlando (Invited).

Task 3.2 – High Energy Density Lithium Battery (Stanley Whittingham, SUNY Binghamton)

PROJECT OBJECTIVE: To develop the anode and cathode materials for high-energy density cells for use in plug-in hybrid electric vehicles (PHEVs) and in electric vehicles (EV) that offer substantially enhanced performance over current batteries used in PHEVs and with reduced cost.

Specifically, the primary objectives are to:

- Increase the volumetric capacity of the anode by a factor of 1.5 over today's carbons
 - Using a SnFeC composite conversion reaction anode
- Increase the capacity of the cathode
 - Using a high capacity conversion reaction cathode, CuF_2 , and/or
 - Using a high capacity 2 Li intercalation reaction cathode, VOPO_4
- Enable cells with an energy density exceeding 1 kWh/liter

PROJECT IMPACT: The volumetric energy density of today's lithium-ion batteries is limited primarily by the low volumetric capacity of the carbon anode. If the volume of the anode could be cut in half, and the capacity of the cathode raised to over 200 Ah/kg, the cell energy density can be increased by over 50% to approach 1 kWh/liter (actual cell). This will increase the driving range of vehicles. Moreover, smaller cells using lower cost manufacturing will lower the cost of tomorrow's batteries.

OUT-YEAR GOALS:

The long-term stretch goal of this project is to enable cells with an energy density of 1 kWh/liter. This will be accomplished by replacing both the present carbon used in Li-ion batteries with anodes that approach double the volumetric capacity of carbon, and the present intercalation cathodes with materials that significantly exceed 200 Ah/kg. By the end of this project it is anticipated that cells will be available that can exceed the volumetric energy density of today's Li-ion batteries by 50%.

COLLABORATIONS:

The Advanced Photon Source (Argonne National Laboratory) and (when available) the National Synchrotron Light Source II (Brookhaven National Laboratory) will be used to determine the phases formed in both *ex situ* and *operando* electrochemical cells. University of Colorado, Boulder will provide some of the electrolytes to be used

Milestones

1. Demonstrate synthesis and complete characterization of CuF_2 . (Dec-14) **Completed**
2. Determine discharge product of CuF_2 . (Mar-15) **Completed**
3. Begin cyclability testing of CuF_2 (Jun-15) **Ongoing**
4. Demonstrate more than 100 cycles on Sn_2Fe at 1.5 times the volumetric energy density of carbon. (Sep-15) **Ongoing**
5. Go/No-Go: Demonstrate cyclability of CuF_2 . Criteria: Capacity of 200 mAh/g over 10 cycles. (Sep-15)

Progress Report

The goal of this project is to synthesize tin-based anodes that have 1.5 times the volumetric capacity of the present carbons, and work on conversion and intercalation cathodes with capacities over 200 Ah/kg. The major effort in this second quarter was to study the discharge products of CuF_2 and its Fe derivatives.

Milestone (1): $\text{Cu}_{1-y}\text{Fe}_y\text{F}_2$, $y = 0, 0.2$ and 0.5 are single-phases as observed in XRD. Figure 16 shows the structural evolution with increase of Fe in the CuF_2 structure. The formation of single-phase is further supported by changes in the lattice parameters and the lower distortion of the rutile structure.

Milestone (2): The discharge products of $\text{Cu}_{1-y}\text{Fe}_y\text{F}_2$, $y = 0$ and 0.5 , were characterized by *ex situ* XRD at different states of discharge. CuF_2 is converted to Cu and LiF as the only discharge products as observed in powder XRD pattern (Figure 17). No CuF_2 remains at the end of discharge. Similarly, in the case of $\text{Cu}_{0.5}\text{Fe}_{0.5}\text{F}_2$, we observe the formation of Cu and LiF. The peaks of Fe phase overlaps with the LiF phase, therefore may not be observed. The reaction however, is observed to continue below 2.4 V where all Cu^{2+} ought to have Cu^0 . The $\text{Cu}_{0.5}\text{Fe}_{0.5}\text{F}_2$ phase continues to decrease while the LiF phase increases. In addition there is no observable change in the relative intensity of the Cu peaks below this voltage. The reaction of $\text{Cu}_{0.5}\text{Fe}_{0.5}\text{F}_2$ is not complete even at 1.8 V as evident by the remnant phase of the rutile structure.

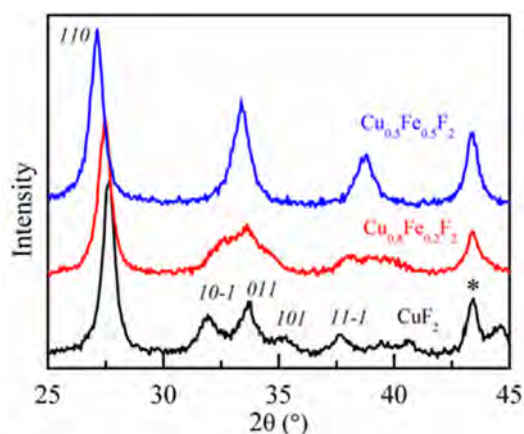


Figure 16: XRD pattern of CuF_2 and Fe substituted CuF_2 .

The cyclability of $\text{Cu}_{1-y}\text{Fe}_y\text{F}_2$ is being evaluated in LiPF_6 and will be presented next quarter when data for more cycles is obtained.

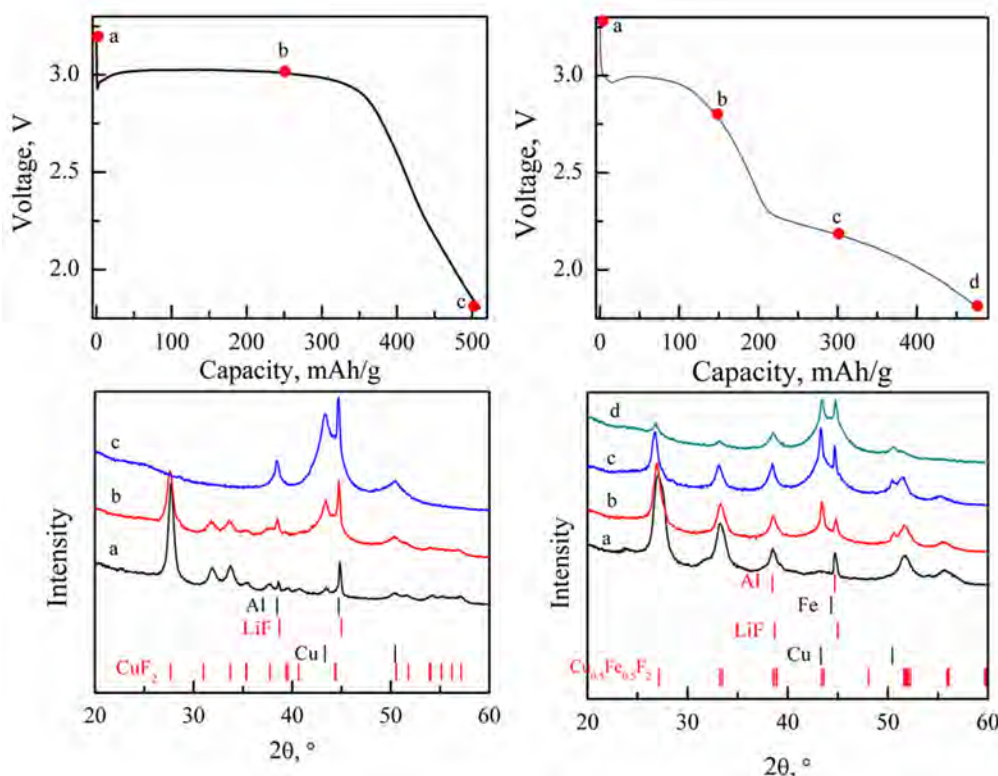


Figure 17: The powder XRD pattern of different discharge states of CuF_2 and $\text{Cu}_{0.5}\text{Fe}_{0.5}\text{F}_2$. The tick marks are the standard patterns of the different phases. The top shows electrochemistry discharge curves of the two compounds.

Q2 Patents/Publications/Presentations

Presentation:

1. M. Stanley Whittingham, “Cathode: Pushing the limits of Intercalation Electrodes: What is next”, 10th China-US Electric Vehicle and Battery Workshop (China-US EVI Meeting), Beijing, China, March 29-30, 2015. Sponsored by US DOE EERE.

Task 3.3 – Development of High-Energy Cathode Materials (Ji-Guang Zhang and Jie Xiao, Pacific Northwest National Laboratory)

PROJECT OBJECTIVE:

The objective of this project is to develop high-energy, low-cost, cathode materials with long cycle-life. Based on the knowledge gathered in FY14 on the failure mechanism of Li-Mn-rich (LMR) cathode, synthesis modification will be pursued to improve the distribution of different transition metal cations at the atomic level. Leveraging PNNL's advanced characterization capabilities, the effects from synthesis alteration and the surface treatment will be monitored and correlated to the electrochemical properties of LMR to guide the rational design of LMR. Extension of the cutoff voltage on traditional layered $\text{LiNi}_{1/3}\text{Mn}_{1/3}\text{Co}_{1/3}\text{O}_2$ (NMC) will be also investigated to increase the usable energy density from NMC while still maintaining the structural integrity and long lifespan.

PROJECT IMPACT:

Although state-of-the-art cathode materials such as LMR layered composites have very high energy densities, their voltage fade and long-term cycling stability characteristics still need to be further improved. In this work, we will investigate the fundamental fading mechanism of LMR cathodes and develop new approaches to reduce the energy loss of these high-energy cathode materials. The success of this work will increase the energy density of Li-ion batteries and accelerate market acceptance of electrical vehicles (EV), especially for plug-in hybrid electrical vehicles (PHEV) required by the *EV Everywhere* Grand Challenge proposed by DOE/EERE.

OUT-YEAR-GOALS:

- The long-term goal of the proposed work is to enable Li-ion batteries with a specific energy of >96 Wh/kg (for PHEVs), 5,000 deep-discharge cycles, 15-year calendar life, improved abuse tolerance, and less than 20% capacity fade over a 10-year period.

COLLABORATIONS:

- Dr. Bryant Polzin (ANL)- LMR electrode supply
- Dr. X.Q. Yang (BNL) – *in situ* XRD characterization during cycling
- Dr. Karim Zaghib (Hydro-Quebec) – material synthesis
- Dr. Kang Xu (ARL) – new electrolyte

Milestones

1. Investigate the transition metal migration pathway in LMR during cycling. (12/31/14) **Complete**
2. Identify appropriate synthesis step to enhance the homogenous cation distribution in the lattice and demonstrate 200 stable cycling with less than 10% energy loss. (3/31/15) **Complete**
3. Develop the surface treatment approaches to improve the stability of high energy cathode at high voltage conditions. (6/30/2015) **On going**
4. Demonstrate high voltage operation of modified NCM with 180 mAh/g capacity and less than 20% capacity fade for 100 cycling. (9/30/2015) **On going**

Progress Report

The Q2 milestone has been completed. The energy (in Wh kg^{-1}) retention of LMR cathode prepared by HA method was more than 90% over 200 cycles as shown in Figure 18a. Different synthesis methods were used to prepare Li-Mn-rich (LMR) cathode materials with the same composition of $\text{Li}[\text{Li}_{0.2}\text{Ni}_{0.2}\text{Mn}_{0.6}]\text{O}_{2-\delta}$. It was found that hydrothermal-assisted (HA) synthesis largely improved the homogeneous distribution of transition metal cations within the lattice at the atomic level.

LMR cathode $\text{Li}[\text{Li}_{0.2}\text{Ni}_{0.2}\text{Mn}_{0.6}]\text{O}_{2-\delta}$ with different oxygen non-stoichiometry / Mn^{3+} have also been prepared by different heat treatment processes. X-ray photoelectron spectroscopy (XPS) analysis demonstrated that the re-quenched material showed the highest amount of Mn^{3+} (28.7%), followed by the quenched (25.9%) and annealed (21.8%) counterparts (Figure 18b). It was found that the elevated oxygen non-stoichiometry / Mn^{3+} facilitated the activation of Li_2MnO_3 component and thus significantly improved the discharge capacity of LMR cathode. The LMR material with higher amount of Mn^{3+} exhibited considerably prolonged voltage plateau at ~ 4.5 V that is associated with the removal of lithium ions concomitant with an irreversible loss of oxygen from the Li_2MnO_3 component (Figure 18c). During discharge process, the re-quenched material exhibited the least electrode polarization and the highest discharge capacity of 270 mAh g^{-1} , as compared to quenched material (249 mAh g^{-1}) and annealed material (218 mAh g^{-1}) (Figure 18c). The initial Coulombic efficiency increased in the order of annealed (77.3%) < quenched (80.5%) < re-quenched material (81.9%). The enhanced performance was ascribed to the increase of oxygen non-stoichiometry / Mn^{3+} that provided additional electron hopping pathways and thus enabled the reversible lithium ion de/intercalation. However, increased activation of Li_2MnO_3 resulted in accelerated structural transformation from layered to spinel-like/disordered rock-salt phases, leading to rapid capacity degradation (Figure 18d). In this regard, the amount of oxygen non-stoichiometry / Mn^{3+} needs to be well controlled during synthesis of LMR cathode materials in order to reach a reasonable compromise between the initial activity and long-term cycling stability. The fundamental findings of this work could be widely applied to explain the effects of oxygen non-stoichiometry / Mn^{3+} on different kinds of LMR cathodes and provide useful guide for the synthesis of high performance LMR cathodes.

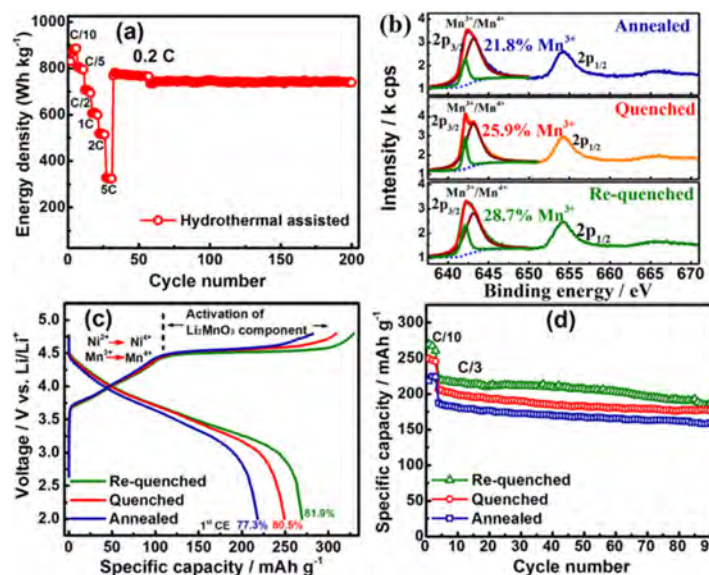


Figure 18: (a) Specific energy density of LMR cathode prepared by HA method as a function of cycle number. (b) Mn 2p XPS spectra; (c) charge/discharge profiles at C/10; and (d) cycling performance of $\text{Li}[\text{Li}_{0.2}\text{Ni}_{0.2}\text{Mn}_{0.6}]\text{O}_{2-\delta}$ materials prepared by co-precipitation method.

Q2 Patents/Publications/Presentations

1. Structural and Chemical Evolution of Li- and Mn-rich Layered Cathode Material, Jianming Zheng, Pinghong Xu, Meng Gu, Jie Xiao, Nigel Browning, Pengfei Yan, Chongmin Wang, and Ji-Guang Zhang, *Chemistry of Materials*, 2015, 27 (4), pp 1381–1390.
2. Structural and Chemical Evolution of Li- and Mn-rich Layered Cathode Material, J. Zheng, P. Yan, M. Gu, J. Xiao, C. Wang, J.-G. Zhang, presented in Materials Challenges in Alternative & Renewable Energy, Jeju, S. Korea, Feb. 25, 2015.

Task 3.4 – *In situ* Solvothermal Synthesis of Novel High Capacity Cathodes (Patrick Looney, Feng Wang, Brookhaven National Laboratory)

PROJECT OBJECTIVE: Develop low-cost cathode materials that offer high energy density (≥ 660 Wh/kg) and electrochemical properties (cycle life, power density, safety) consistent with USABC goals.

PROJECT IMPACT: Present-day Li-ion batteries are incapable of meeting the 40-mile all-electric-range within the weight and volume constraints established for PHEVs by DOE/USABC. Higher energy density cathodes are needed for Li-ion batteries to be widely commercialized for PHEV applications. This effort will focus on increasing the energy density (while maintaining the other performance characteristics of current cathodes) using synthesis methods that have the potential to lower the cost. The primary deliverable for this project is a reversible cathode with an energy density of about 660 Wh/kg or higher.

OUT-YEAR GOALS: In FY15, we will continue our work on *in situ* solvothermal synthesis, structural and electrochemical characterization of V-based (fluoro)phosphates and other high-capacity cathodes. We will also put efforts on technique development for *in situ* synthesis. The out-year-goals we aim to achieve include:

- Determining the reaction pathway during ion-exchange of $\text{Li}(\text{Na})\text{VPO}_5\text{F}_x$
- Optimizing the ion-exchange procedures to maximize the Li-exchange content in $\text{Li}(\text{Na})\text{VPO}_5\text{F}_x$
- Characterizing the structure of the intermediate and final exchanged products of $\text{Li}(\text{Na})\text{VPO}_5\text{F}_x$ and their electrochemical properties
- Identifying at least one cathode material, with reversible specific capacity higher than 200 mAh/g under moderate cycling conditions
- Developing new *in situ* reactors that may be applied for different types of synthesis methods (beyond solvothermal) in making phase-pure cathodes
- Building new capabilities for simultaneous *in situ* measurements of multiple synthesis reactions in the newly built beam lines at NSLS II.

COLLABORATIONS: Jianming Bai, Lijun Wu, Yimei Zhu (Brookhaven Nat. Lab), Peter Khalifah (Stony Brook U.), Kirsuk Kang (Seoul Nat. U.), Nitash Balsara, Wei Tong (Lawrence Berkeley Nat. Lab), Jagjit Nanda (Oak Ridge Nat. Lab), Arumugam Manthiram (U. Texas at Austin), Brett Lucht (U. Rhode Island), Zaghbir Karim (Hydro-Quebec), Jason Graetz (HRL).

Milestones

1. Determine the reaction pathways and phase evolution during hydrothermal ion exchange synthesis of $\text{Li}(\text{Na})\text{VPO}_5\text{F}_x$ cathodes *via in situ* studies. (12/01/14) **Complete**
2. Optimize ion exchange synthesis for preparing $\text{Li}(\text{Na})\text{VPO}_5\text{F}_x$ with maximized Li content, and characterize its structural and electrochemical properties. (03/01/15) **Complete**
3. Develop new reactor design to enable high-throughput synthesis of phase-pure cathode materials. (06/01/15) *On schedule*
4. Obtain good cycling stability of one high-capacity cathode in a prototype cell with specific capacity higher than 200 mAh/g. *No-Go* if 80% capacity retention after 50 cycles cannot be achieved. (09/01/15) *On schedule*

Progress Report

In the previous quarters, we showed that $\text{Li}_x\text{Na}_{(1-x)}\text{VOPO}_4\text{F}_{0.5}$ (LVOPF) may be obtained *via* hydrothermal ion-exchange from the Na counterpart ($\text{Na}_{1.5}\text{VOPO}_4\text{F}_{0.5}$). Through *in situ* investigation the dependence of exchange process on the synthesis parameters (temperature, concentration of LiBr solution, Li/Na ratio and heating rate) was determined and utilized to obtain a series of LVOPF with varying lithium content. In this quarter, some of the results from structural and electrochemical characterization on the LVOPF series are reported.

The LVOPF particles are typically micron-sized, and single crystalline as shown by transmission electron microscopy imaging and electron diffraction of individual particle (Figure 19(a)). The morphology is preserved during the ion-exchange process without particle pulverization. The subtle structural change in the $\text{Li}_x\text{Na}_{1.5-x}\text{VOPO}_4\text{F}_{0.5}$ as a function of x was determined by high-resolution synchrotron X-ray diffraction (XRD) combined with Rietveld refinements, indicating a phase transformation from tetragonal ($P4_2/mnm$) to orthorhombic ($Pnmm$) at about $x = 0.5$, with a small volume shrinkage (only about 1% being measured). A maximum of lithium content of $x=1.34$ was obtained by further lithium substitution at a temperature of 160°C *via* a slow solid solution process, with enough exchange time and lithium source.

The electrochemical properties of $\text{Li}_x\text{Na}_{1.5-x}\text{VOPO}_4\text{F}_{0.5}$ electrodes for different stoichiometries (x) were investigated with Li metal as counter electrode. Some of the results were given in (Figure 19(b), (c)), for high lithium contents ($x = 1.34$ and 1.02 respectively). For $x = 1.34$ (maximum Li content), the reversible capacity at a C/10 rate reached 145 mAh g^{-1} . Moreover, a high voltage of $\sim 4 \text{ V}$ (vs. Li^+/Li) was observed, leading to a high energy density of 580 Wh kg^{-1} . Excellent rate capability and cyclability of the electrode were also found, suggesting a high structural stability upon cycling (to be reported in the future). This makes it a promising candidate as a high-power cathode for Li-ion batteries. In contrast, the electrochemical properties of the $x = 1.02$ electrode were significantly inferior to that for $x = 1.34$, in terms of capacity (of only 80 mAh/g for the 1st charge) and cycling stability (inset in (Figure 19(c))). The electrochemical tests indicate a strong dependence of electrochemical property on the extent of Li^+ exchange, and maximizing lithium ion exchange appears to be essential to the achieving high capacity as well as the long-term cyclability. This is likely due to the enhancement of structural stability with a close-to-complete replacement of Na^+ by Li^+ according to the structural analysis.

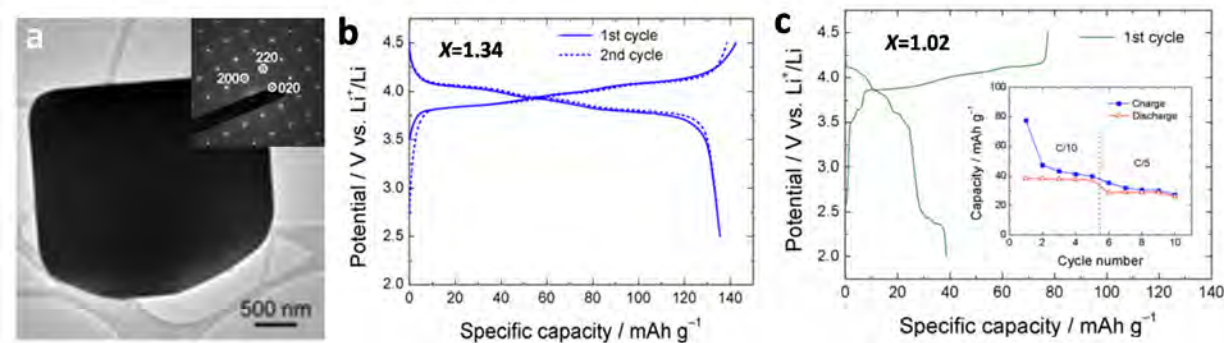


Figure 19: Structure and electrochemical properties of the $\text{Li}_x\text{Na}_{(1-x)}\text{VOPO}_4\text{F}_{0.5}$ (LVPOF) electrode. (a) typical transmission electron microscopy (bright field) image (inset: electron diffraction recorded from the particle along the zone axis [001]), (b) voltage profiles (at C/10 rate) of the LVPOF electrode ($x=1.34$) for the 1st and 2nd cycles, (c) voltage profile (at C/10 rate) and cycling stability of the LVPOF electrode ($x=1.02$).

Patents/Publications/Presentations

Publication

1. Z. Wei, W. Zhang, F. Wang, Q. Zhang, B. Qiu, S. Han, Y. Xia, Y. Zhu, and Z. Liu “Eliminating Voltage Decay of Lithium-Rich $\text{Li}_{1.14}\text{Mn}_{0.54}\text{Ni}_{0.14}\text{Co}_{0.14}\text{O}_2$ Cathodes by Controlling the Electrochemical Process”. **Chem. Eur. J.** (accepted).

Presentation

1. *F. Wang* et al., “High-Energy Conversion Cathodes for Rechargeable Lithium Batteries”, TMS 2015 144th Meeting, March 15-19, Orland, FL.

Task 3.5 – Novel Cathode Materials and Processing Methods (Michael M. Thackeray and Jason R. Croy, Argonne National Laboratory)

PROJECT OBJECTIVE: The goal of this project is to develop low-cost, high-energy and high-power Mn-oxide-based cathodes for lithium-ion batteries that will meet the performance requirements of PHEV and EV vehicles. Improving the design, composition and performance of advanced electrodes with stable architectures and surfaces, facilitated by an atomic-scale understanding of electrochemical and degradation processes, is a key objective of this work.

PROJECT IMPACT: Standard lithium-ion battery technologies are currently unable to meet the demands of next-generation PHEV and EV vehicles. Battery developers and scientists alike will take advantage of the knowledge generated from this project, both applied and fundamental, to further advance the field. In particular, it is expected that this knowledge will enable progress towards meeting the DOE goals for 40-mile, all-electric range, PHEVs.

APPROACH: Exploit the concept and optimize the performance of structurally-integrated “composite” electrode structures with a prime focus on “layered-layered-spinel” materials. Alternative processing routes will be investigated; Argonne National Laboratory’s comprehensive characterization facilities will be used to explore novel surface and bulk structures by both *in situ* and *ex situ* techniques in the pursuit of advancing the properties of state-of-the-art cathode materials. A theoretical component will complement the experimental work of this project.

OUT-YEAR-GOALS:

- Identify high capacity (‘layered-layered’ and ‘layered-spinel’) composite electrode structures and compositions that are stable to electrochemical cycling at high potentials (~4.5 V).
- Identify and characterize surface chemistries and architectures that allow fast Li-ion transport and mitigate or eliminate transition-metal dissolution.
- Use complementary theoretical approaches to further the understanding of electrode structures and electrochemical processes to accelerate the progress of materials development.
- Scale-up, evaluate and verify promising cathode materials using Argonne National Laboratory’s scale-up and cell fabrication facilities.

COLLABORATORS: Brandon R. Long, Joong Sun Park, Eungje Lee, Roy Benedek (and other members of Argonne’s Electrochemical Energy Storage Department). Mali Balsubramanian (APS), V. Dravid (Northwestern University).

Milestones

1. Optimize the capacity and cycling stability of composite cathode structures with a low (~10%) Li_2MnO_3 content. Target capacity = 190-200 mAh/g (baseline electrode). (Sept-15.) **In progress.**
2. Scale up the most promising materials to 1 kg batch size at Argonne’s Materials Engineering Research Facility (MERF). (April-15). **In progress.**
3. Synthesize and characterize unique surface architectures that enable >200 mAh/g at a >1C rate with complementary theoretical studies of surface structures. (Sep-15.) **In progress (see text).**
4. Optimize the capacity and cycling stability of composite cathode structures with a medium (~20%) Li_2MnO_3 content. Target capacity = 200-220 mAh/g (advanced electrode). (Sept-15).

Progress Report

Recent reports have shown that high capacities (~200 mAh/g) and good stability can be obtained from layered-layered (LL) $x\text{Li}_2\text{MnO}_3 \cdot (1-x)\text{LiMO}_2$ ($M=\text{Mn, Ni, Co}$) cathodes at x values less than 0.3. Lowering the Li_2MnO_3 content serves to mitigate structural instabilities brought about by the activation process and the use of excess lithium that resides in the transition metal layers of as-prepared electrodes. Likewise, enhanced stabilization of LL cathode structures at high capacities can be achieved through the integration of a spinel component. These complex, layered-layered-spinel (LLS) structures, of the form $y[x\text{Li}_2\text{MnO}_3 \cdot (1-x)\text{LiMO}_2] \cdot (1-y)\text{LiM}_2\text{O}_4$, have also shown promise for improving first-cycle efficiencies (FCE) as well as the rate performance of LL cathodes. In order to optimize the advantages of the integrated spinel component, it is desirable to integrate spinel chemistries that can accommodate lithium above 3.0 V, thereby enhancing stability and rate capability while minimizing low voltage contributions. $\text{Li}[\text{Co}_2]\text{O}_4$ can accommodate lithium at ~3.4 V and it is expected that $\text{Li}[\text{Co}_{2-x}\text{M}_x]\text{O}_4$ substituted spinels may also allow for lithium insertion within a “tuned” range of voltages. The disadvantage of the spinel strategy lies in the difficulty of synthesizing such complex, multicomponent, and integrated structures. Studies related to a novel synthesis method, utilizing Li_2MnO_3 as a layered template for LL cathodes, have proven the method amenable to the synthesis of LLS structures. Furthermore, this method is versatile because it can be carried out with a variety of starting precursor templates besides Li_2MnO_3 .

The design rationale described above can potentially lead to new directions for fabricating high capacity composite cathode structures. Figure 20(a) shows the first-cycle voltage profiles for lithium cells with $0.1\text{Li}_2\text{MnO}_3 \cdot 0.9\text{LiMn}_{0.4}\text{Ni}_{0.55}\text{Co}_{0.5}\text{O}_2$ electrodes (black) compared with the same material used as a precursor template and treated in an acidic solution in the presence of Co. The Co-treated samples were subsequently annealed at 450°C (red) and 750°C (blue). The acidic solution and subsequent annealing allow for Co ions to be inserted into the Li layers of the LL precursor. The time and temperature of the annealing dictate the concentration of Co ions that remain in the layers of the final product which, strategically, can yield Co-based spinel regions. The first-cycle discharge reveals that annealing at 750°C results in a mostly layered structure, whereas the sample annealed at 450°C shows a clear plateau at ~3.4 V, consistent with regions of a Co-rich spinel. Figure 20(b) shows the first charge and discharge capacities along with FCE's for the profiles in (a). The LLS electrode synthesized at 450°C provides an improved FCE, consistent with previous reports, and capacities equivalent to the starting LL precursor. Future studies will probe the complex structures of these electrodes with the view to optimizing the electrochemical properties of this new class of materials.

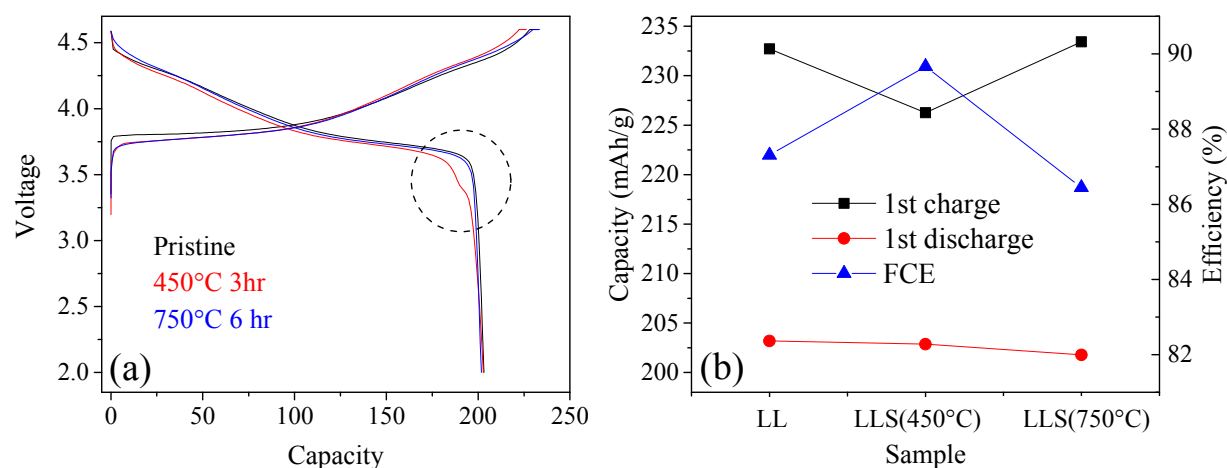


Figure 20: (a) First-cycle charge and discharge profiles (4.6 – 2.0 V, 15 mA/g, half-cells at RT) for $0.1\text{Li}_2\text{MnO}_3 \cdot 0.9\text{LiMn}_{0.4}\text{Ni}_{0.55}\text{Co}_{0.5}\text{O}_2$ (black) and after acid treatment in the presence of Co, followed by annealing at 450°C (red) and 750°C (blue), in order to integrate a Co-based spinel component. (b) First charge (black) and discharge (red) capacities along with FCE's (blue) of the LL and LLS samples shown in (a)

Q2 Patents/Publications/Presentation

1. M. M. Thackeray, J. R. Croy, B. R. Long, J. S. Park, C. S. Johnson, L. Trahey, Z. Yang, Y. Ren, D. J. Miller, J. G. Wen, A. Kinaci, M. K. Y. Chan, S. Kirklin and C. Wolverton, *Designing Advanced High Capacity Electrodes for Lithium Cells*, MRS Meeting, Boston, 30 November - 5 December, 2014 (Invited). (Not disclosed in January Quarterly Report.)
2. M. M. Thackeray, *Looking Back – Looking Forward on the Road to Viable Electrical Energy Storage*, Chemistry Department Seminar, University of Cape Town, South Africa, 12 December 2014 (Invited). (Not disclosed in January Quarterly Report.)
3. M. M. Thackeray, *Electrical Energy Storage: Looking Back – Looking Forward*, International Battery Association Meeting, Waikoloa Village, Hawaii, 5-9 January 2015 (Invited).
4. M. M. Thackeray, *The Road to Viable Electrical Energy Storage: Challenges and Opportunities in an Evolving Lithium Economy*, IV Congress of the Future – The Crossroads of the XXI Century, Santiago, Chile, 15-17 January 2015 (Invited).
5. K. Amine, M. M. Thackeray, J. Warner and M. S. Whittingham, *Fireside Chat: The Future of Lithium Battery Technology*, NAATBatt 2015 Annual Meeting and Conference, Phoenix, Arizona, 16-19 February 2015 (Invited).
6. M. M. Thackeray, B. R. Long, J. R. Croy, J. S. Park, Y. Shin, G. Krumdick, J. G. Wen and D. Miller, *Progress and Challenges in Designing High Capacity Cathodes for Lithium-Ion Cells*, 32nd Annual Battery Seminar & Exhibit, Fort Lauderdale, Florida, 9-12 March 2015 (Invited).

Task 3.6 – High-capacity, High-voltage Cathode Materials for Lithium-ion Batteries (Arumugam Manthiram, University of Texas, Austin)

PROJECT OBJECTIVE: A significant increase in capacity and/or operating voltage is needed to make the lithium-ion technology viable for vehicle applications. This project addresses this issue by focusing on the design and development of cathode materials based on polyanions that have the possibility for reversibly inserting/extracting more than one lithium ion per transition-metal ion and/or operating above 4.3 V. Specifically, high-capacity and/or high-voltage lithium transition-metal phosphate, silicate, and carbonophosphate cathodes are investigated. The major issue with the phosphate and silicate cathodes is the poor electronic and ionic transport, which limits their practical capacity and energy and power densities. To overcome these difficulties, novel microwave-assisted solvothermal, microwave-assisted hydrothermal, and template-assisted synthesis approaches are pursued to realize controlled morphology with smaller particle size and to integrate conductive additives like graphene in a single synthesis step.

PROJECT IMPACT: The critical requirements for the widespread adoption of lithium-ion batteries for vehicle applications are high energy, high power, long cycle life, low cost, and acceptable safety. The currently available cathode materials do not adequately fulfill these requirements. The polyanion cathodes, which are synthesized by novel methods in this project, have the potential to significantly increase the energy and power. More importantly, the covalently bonded polyanion groups can offer excellent thermal stability and enhanced safety. The microwave-assisted synthesis could also lower the manufacturing cost of the cathodes through a significant reduction in reaction time and temperature.

OUT-YEAR GOALS: The overall goal is to enhance the electrochemical performances of high-capacity, high-voltage polyanion cathode systems and to develop a fundamental understanding of their structure-composition-performance relationships. Specifically, the project is focused on enhancing the electrochemical performance of systems such as Li_2MSiO_4 ($\text{M} = \text{Mn, Fe, Co, Ni, and VO}$), $\text{Li}_2\text{MP}_2\text{O}_7$ ($\text{M} = \text{Mn, Fe, Co, Ni, and VO}$), LiMPO_4 ($\text{M} = \text{Co, Ni, and VO}$), $\text{Li}_3\text{V}_2(\text{PO}_4)_3$, $\text{Li}_9\text{V}_3(\text{P}_2\text{O}_7)_3(\text{PO}_4)_2$, $\text{Li}_3\text{M}(\text{CO}_3)(\text{PO}_4)$, and their solid solutions. Advanced structural, chemical, surface, and electrochemical characterizations of the materials synthesized by novel approaches are anticipated to provide in-depth understanding of the factors that control the electrochemical properties of the polyanion cathodes and facilitate design of better-performing cathode materials for vehicle applications. For example, understanding the role of conductive graphene integrated into the polyanion cathodes can help to design better-performing cathodes.

COLLABORATIONS: Collaboration/discussion with Wanli Yang (LBNL), Feng Wang (BNL), and Craig Bridges (ORNL) on structural/chemical characterizations of polyanion cathodes.

Milestones

1. Demonstrate the synthesis of LiVOPO_4 nanoparticles with $> 200 \text{ mAh/g}$ capacity by employing ordered macroporous carbon as a hard-template (Dec-14) **Complete**
2. Demonstrate aliovalent doping with Ti^{4+} in $\text{LiM}_{1-2x}\text{Ti}_x\text{PO}_4$ with enhanced electrochemical properties by the microwave-assisted solvothermal synthesis. (Mar-15) **Complete**
3. Demonstrate the synthesis of α - and/or β - LiVOPO_4 /graphene nanocomposites with $> 200 \text{ mAh/g}$ capacity by the microwave-assisted process. (Jun-15) **Ongoing**
4. Go/No-Go: Stop synthesis attempts if aliovalent doping is not possible or if the doped samples exhibit a capacity of $< 110 \text{ mAh/g}$. Criteria: Demonstrate the extraction of more than one lithium ($> 110 \text{ mAh/g}$) through aliovalent doping in $\text{Li}_2\text{M}_{1-3/2x}\text{V}_x\text{P}_{x/2}\text{P}_2\text{O}_7$ by low-temperature synthesis approaches (Sep-15) **Ongoing**

Progress Report

Our group has previously demonstrated aliovalent substitution of V^{3+} in both $\text{LiFe}_{1-3x/2}\text{V}_x\text{PO}_4$ and $\text{LiMn}_{1-3x/2}\text{V}_x\text{PO}_4$. In both cases, the electronic and ionic conductivities of the materials were enhanced with V^{3+} substitution, resulting in improved electrochemical performances. Furthermore, our group demonstrated the importance of low-temperature synthesis to successfully substitute aliovalent V^{3+} . In this quarter, we attempted the aliovalent substitution of Ti^{4+} for Fe^{2+} in $\text{LiFe}_{1-2x}\text{Ti}_x\text{PO}_4$ with a microwave-assisted solvothermal (MW-ST) synthesis. LiFePO_4 was chosen because it is less sensitive to synthesis conditions than LiMnPO_4 and LiCoPO_4 . Use of various titanium(IV) precursors including TiCl_4 , $\text{Ti(IV)-isopropoxide}$, and $\text{Ti(IV)(SO}_4)_2$ was explored, but all of them hydrolyzed to TiO_2 when exposed to trace amounts of water. Therefore, all syntheses were carried out in tetraethyleneglycol, which was dried well with 4A molecular sieves prior to use, in a microwave at 240 °C along with anhydrous phosphoric acid, lithium hydroxide, and iron oxalate. The use of dry precursors yielded LiFePO_4 crystallizing in the *Cmcm* space group instead of the olivine phase with the *Pnma* space group (Figure 21).

Synthesis of $\text{LiFe}_{1-2x}\text{Ti}_x\text{PO}_4$ (LFTP) with the *Cmcm* space group was attempted with $x = 0.0, 0.025, 0.05, 0.075, 0.10$, and 0.125 . X-ray diffraction (XRD) patterns of the LFTP samples synthesized with the $\text{Ti(SO}_4)_2$ precursor are shown in Figure 21. The only impurity peak appearing at $\sim 32^\circ$ (marked with an arrow in Figure 21) is broad in nature, is independent of titanium content x , and could not be indexed to any known compounds. The LFTP (*Cmcm*) samples show a shift in the peak at 34° to the right, although the shift is not systematic with Ti content. Moreover, the peak position at 34° is known to depend on lithium content, so the shift could not be specifically attributed to variations in lithium content or titanium substitution. Furthermore, the excess lithium in the LFTP samples with higher Ti contents indicates that lithium may be filling Fe vacancies. The LFTP (*Cmcm*) samples were subsequently heated in various inert atmospheres, including 100% Ar, 5% H_2 - 95% Ar, 10% H_2 - 90% Ar, and 100% H_2 , at 450, 475, 500, and 525 °C. The LFTP (*Cmcm*) phase converts fully to the olivine LFTP (*Pnma*) phase at 525 °C and has the least impurity when heated in 10% H_2 - 90% Ar and 100% H_2 . The impurities were indexed to $\text{Fe}_2\text{P}_2\text{O}_7$ and FeP for the samples heated in 10% H_2 - 90% Ar and 100% H_2 , respectively. However, there were no impurity peaks related to titanium oxides. Although no concrete evidence could be obtained for Ti^{4+} substitution, the decreasing experimental Fe/P and increasing Ti/P ratios with increasing Ti content (Table 1) suggest the formation of $\text{LiFe}_{1-2x}\text{Ti}_x\text{PO}_4$ for small values of $x \approx 0.07$, which is about half of the values found by us with the trivalent V^{3+} substitution.

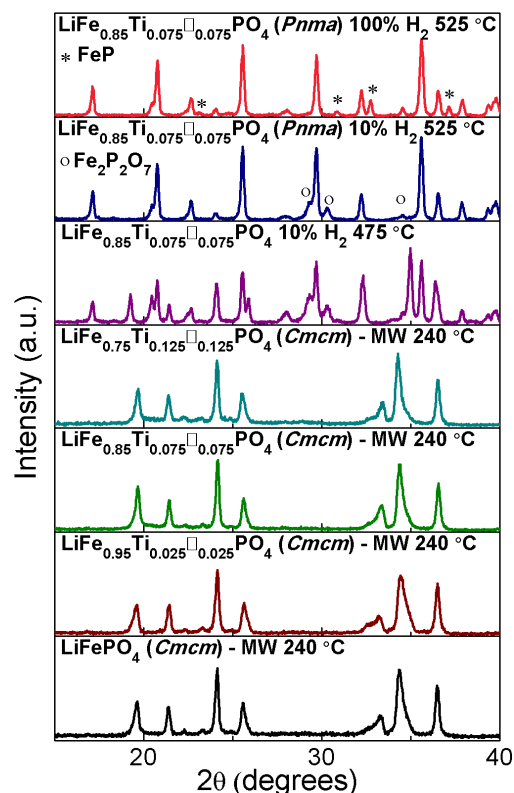


Figure 21: Powder XRD patterns of as-synthesized and post-heated LFTP samples.

Table 1: ICP-OES results for LFTP

Sample	ICP stoichiometry		
	Li/P	Fe/P	Ti/P
LiFePO_4	0.92	0.97	--
$\text{LiFe}_{0.95}\text{Ti}_{0.025}\text{PO}_4$	0.99	0.93	0.014
$\text{LiFe}_{0.90}\text{Ti}_{0.05}\text{PO}_4$	0.93	0.88	0.028
$\text{LiFe}_{0.85}\text{Ti}_{0.075}\text{PO}_4$	0.96	0.84	0.044
$\text{LiFe}_{0.80}\text{Ti}_{0.10}\text{PO}_4$	1.05	0.84	0.064
$\text{LiFe}_{0.75}\text{Ti}_{0.125}\text{PO}_4$	1.08	0.76	0.099

Q2 Patents/Publications/Presentations

Publications:

1. J. C. Knight, P. Nandakumar, and A. Manthiram, “Effect of Ru Substitution on the First Charge-Discharge Cycle of Lithium-rich Layered Oxides,” *Journal of Materials Chemistry A* **3**, 2006-2011 (2015).
2. X. Xiang, J. C. Knight, W. Li, and A. Manthiram, “Tuning the Discharge Capacity and Average Discharge Voltage of Li-rich Layered Oxides through Cation Substitution,” *Journal of Power Sources* (submitted).

Task 3.7 – Lithium-bearing Mixed Polyanion (LBMP) Glasses as Cathode Materials (Jim Kiggans and Andrew Kercher, Oak Ridge National Laboratory)

PROJECT OBJECTIVE: Develop mixed polyanion (MP) glasses as potential cathode materials for lithium ion batteries with superior performance to lithium iron phosphate for use in electric vehicle applications. Modify MP glass compositions to provide higher electrical conductivities, specific capacities, and specific energies than similar crystalline polyanionic materials. Test MP glasses in coin cells for electrochemical performance and cycleability. The final goal is to develop MP glass compositions for cathodes with specific energies up to near 1,000 Wh/kg.

PROJECT IMPACT: The projected performance of MP glass cathode materials addresses the Vehicle Technology Multi-Year Plan goals of higher energy densities, excellent cycle life, and low cost. MP glasses offer the potential of exceptional cathode energy density up to 1,000 Wh/kg, excellent cycle life from a rigid polyanionic framework, and low cost conventional glass processing.

OUT-YEAR GOALS:

MP glass development will focus on compositions with expected multi-valent intercalation reactions within a desirable voltage window and/or expected high-energy glass-state conversion reactions. Polyanion substitution will be further adjusted to improve glass properties to potentially enable multi-valent intercalation reactions and to improve the discharge voltage and cycleability of glass-state conversion reactions. Cathode processing of the most promising mixed polyanion glasses will be refined to obtain desired cycling and rate performance. These optimized glasses will be disseminated to BMR collaborators for further electrochemical testing and validation.

COLLABORATIONS: No collaborations this quarter

Milestones

1. Perform electron microscopy on mixed polyanion glass cathodes at key states of charge. (Dec-14) **Completed 12/04/14**
2. Produce and electrochemically test MP glasses designed to have enhanced ionic diffusivity. (Mar-15) **Completed 3/31/15**
3. Produce and electrochemically test an MP glass designed to have enhanced ionic diffusivity and theoretically capable of a multi-valent intercalation reaction. (Jun-15) **In progress.**
4. Determine the polyanion substitution effect on a series of non-phosphate glasses. (Sep-15) **In progress.**

Progress Report

Cobalt, copper, iron, and nickel-based mixed polyanion (MP) glasses with vanadate have demonstrated high capacity electrochemical reactions. However, in the United States, there is concern about utilizing vanadium-containing materials in transportation applications. Similar to vanadate substitution, molybdate substitution has been reported to dramatically improve the electrical conductivity of iron phosphate glass. Therefore, molybdate was explored as an environmentally friendlier alternative to vanadate in MP glass cathodes. Increasing the molybdate substitution into an iron phosphate glass was shown to improve the intercalation capacity and overall specific capacity (Figure 22). A copper phosphate molybdate glass has been successfully produced for electrochemical testing in the near future to determine the effect of molybdate substitution on other glass systems.

The ionic diffusivity of lithium in a glass cathode material could be a key property affecting the rate, capacity, and hysteresis of intercalation and glass-state conversion reactions. Borate substitution into glasses has been shown to improve the ionic diffusivity in glass systems. Therefore, a series of copper-bearing metaphosphate glasses with different polyanion substitutions was electrochemically tested. Copper phosphate glasses and copper borophosphate glasses had very poor reversibility. The substitution of 50% vanadate into the phosphate glass dramatically improved the voltage and reversibility (Figure 23). The glass with both vanadate and borate substitution did not show significantly improved performance over the glass with only vanadate substitution. Therefore, unfortunately, borate substitution does not appear to provide improved performance in phosphate MP glass cathodes.

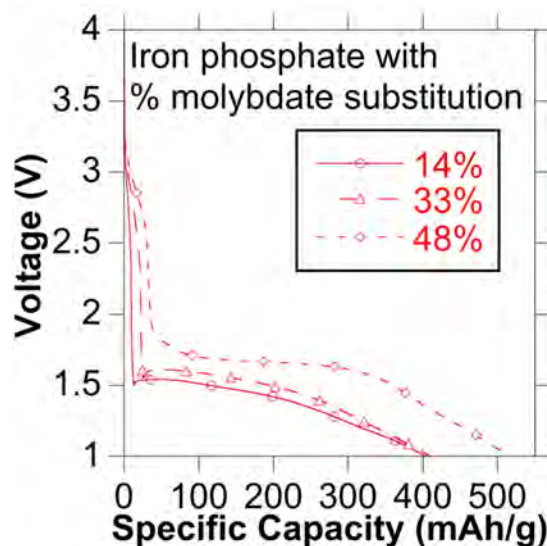


Figure 22: Molybdate substitution can be used as an environmentally friendlier alternative to vanadate substitution for MP glass cathodes.

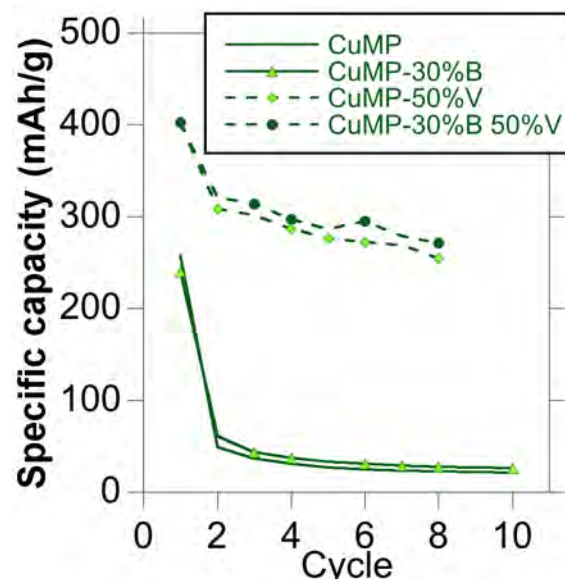


Figure 23: Borate substitution had no significant effect on copper-bearing MP glass cathodes (CuMP = copper metaphosphate, %B = borate substitution, %V = vanadate substitution).

Q2 Patents/Publications/Presentations

None this quarter

Task 3.8 – Design of High Performance, High Energy Cathode Materials (Marca Doeff, Lawrence Berkeley National Laboratory)

PROJECT OBJECTIVE: To develop high energy, high performance cathode materials including composites and coated powders, using spray pyrolysis and other synthesis techniques. The emphasis is on high voltage systems including NMCs designed for higher voltage operation. Experiments are directed towards optimizing the synthesis, improving cycle life, and understanding the behavior of NMCs subjected to high voltage cycling. Particle size and morphology are controlled during spray pyrolysis synthesis by varying residence time, temperature, precursors and other synthetic parameters. By exploiting differences in precursor reactivity, coated materials can be produced, and composites can be prepared by post-processing techniques such as infiltration. These approaches are expected to improve cycling due to reduced side reactions with electrolytes.

PROJECT IMPACT: To increase the energy density of Li-ion batteries, cathode materials with higher voltages and/or higher capacities are required, but safety and cycle life cannot be compromised. In the short term, the most promising materials are based on NMCs modified to undergo high voltage cycling that do not require formation cycles or undergo structural transformations during cycling. Spray pyrolysis synthesis results in high quality materials that can be coated (solid particles) or used as the basis for composites (hollow particles) designed to withstand high voltage cycling.

OUT-YEAR GOALS: The objective is to design high capacity NMC cathodes, which can withstand high voltage cycling without bulk structural transformation. Materials will be synthesized by a simple, low-cost spray pyrolysis method, which has potential for commercialization. This technique produces phase-pure, unagglomerated powders and allows for excellent control over particle morphologies, sizes and distributions. Coated materials will also be produced in either one or two simple steps by exploiting differing precursor reactivities during the spray pyrolysis procedure, or by first preparing hollow spheres of an electroactive material, infiltrating the spheres with precursors of a second phase (e.g., high voltage spinel), and subsequent thermal treatment. The final result is expected to be a high energy density cathode material with good safety and cycling characteristics suitable for use in vehicular applications, which can be made by a low-cost process that is easily scalable.

COLLABORATIONS: TEM has also been used this quarter to characterize NMC materials, work done in collaboration with Dr. Huolin Xin (BNL). Synchrotron and computational efforts are continued in collaboration with Professor M. Asta (UCB), Dr. Dennis Nordlund (SSRL), Dr. Yijin Liu (SSRL), Dr. Tsu-Chien Weng (SSRL) and Dr. Dimosthenis Sokaras (SSRL). Atomic layer deposition was performed in collaboration with Dr. Chunmei Ban (NREL). We are also collaborating with Professor Shirley Meng of UCSD on soft XAS characterization of materials.

Milestones

1. Complete synchrotron X-ray Raman experiments on representative NMC samples (12/31/14) Status: experiments completed, analysis done, paper in preparation.
2. Finish survey of composites made with spray pyrolyzed NMC hollow particles (3/31/15) Status: postponed due to equipment and space issues
3. Go/no go decision on feasibility of coating processes using spray pyrolysis methods or molecular layer deposition (6/30/15) Status: on track
4. Select best-performing coated or composite material based on capacities and high voltage cycling results (9/30/15). Status: on track

Progress Report

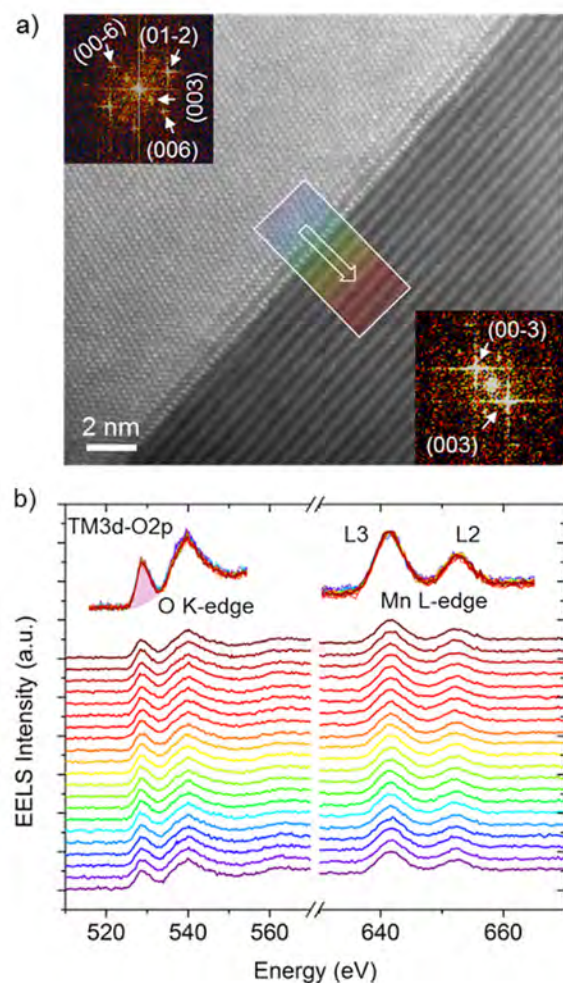


Figure 24: STEM-EELS characterization of a region in the vicinity of a particle-particle interface from spray pyrolysis. (a) STEM image and the corresponding FFT results in the upper left and lower right regions, (b) EELS line scale profile along the marked region in (a), and overlapped curves on the top of the figure demonstrate the nearly identical EELS characteristics at different locations.

scanning was performed across the interfacial region along the pointed direction in the selected area and spectra were recorded every 90 \AA^2 (Figure 24a). There were essentially no changes in the O K-edge EELS or Mn L-edge EELS spectra along the scanning area (Figure 24b). The high TM3d-O2p hybridization intensity is consistent with what was typically reported for NMC materials [Nat Commun 2014, 5, 3529]. Therefore, the spray-pyrolyzed NMC-442 materials exhibit a homogeneous electronic structure across the particle-particle interface, consistent with the R-3m structure.

Spray pyrolysis synthesis of cathode materials was continued this quarter with more syntheses, electrochemical measurements and characterization. In particular, nickel rich NMC (NR-NMC) materials, such as 622 and 811, were targeted. We encountered several challenges in preparing these materials by spray pyrolysis. Different annealing atmospheres, temperature and excess lithium content were examined. The best synthesis conditions are with 10% excess lithium and 800°C , based on performance. The annealing atmosphere plays little role in making 622 materials; no obvious differences were found in materials made under air or oxygen. The resulting performance of these NR-NMC materials was inferior to the NMC 442 materials prepared using the similar protocol. More synthetic parameters need to be tested in order to achieve reasonably high performance of NR-NMC materials.

As for NMC442 materials, spray pyrolyzed materials perform better than the co-precipitated ones. In this quarter, we performed in depth characterization of these NMC442 materials using scanning transmission electron microscopy-electron energy loss spectroscopy (STEM-EELS) and full-field transmission X-ray microscopy to elucidate the materials and electronic structures. The STEM-EELS results are shown in Figure 24. Fast Fourier transform (FFT) results show that both particles can be indexed to the R-3m space group (Figure 24a and insets), although in the brighter particle (left) two domains that are out of phase by π are projected in this image. Mn^{4+} and strong transition metal (TM) 3d-oxygen (O) 2p hybridization states can be used as fingerprints for the R-3m NMC layered structure, because in the possible competing phases (e.g., rock-salt), transition metals are in lower oxidation states (e.g., Mn^{2+}) and the hybridization states are much weaker [Energy Environ. Sci 2014, 7, 3077]. EELS

Q2 Patents/Publications/Presentations

1. “High Voltage Cathode Materials for Lithium Ion Batteries: Freeze-dried $\text{LiMn}_{0.8}\text{Fe}_{0.1}\text{M}_{0.1}\text{PO}_4/\text{C}$ (M=Fe, Co, Ni, Cu) Nanocomposites” Amaia Iturrondobeitia, Aintzane Goñi, Izaskun Gil De Muro, Luis Lezama, Chunjoong Kim, Marca Doeff, Jordi Cabana, and Teofilo Rojo, **Inorg. Chem.**, DOI: 10.1021/ic5028306 (2015).
2. “Transitions from Near-Surface to Interior Redox upon Lithiation in Conversion Electrode Materials”, Kai He, Huolin L. Xin, Kejie Zhao, Xiqian Yu, Dennis Nordlund, Tsu-Chien Weng, Jing Li, Yi Jiang, Christopher A. Cadigan, Ryan M. Richards, Marca M. Doeff, Xiao-Qing Yang, Eric A. Stach, Ju Li, Feng Lin, and Dong Su, **Nano Lett.** DOI: 15, 1437 (2015).
3. “Structural and Chemical Evolution of Amorphous Nickel Iron Complex Hydroxide upon Lithiation/Delithiation” Kai-Yang Niu, Feng Lin, Liang Fang, Dennis Nordlund, Runzhe Tao, Tsu-Chien Weng, Marca Doeff, and Haimei Zheng, **Chem. Mater.**, DOI: 10.1021/cm5041375 (2015).
4. “Overcoming Practical Obstacles to the Use of Garnet LLZO Solid Electrolytes in Lithium Batteries”, Marca M. Doeff, Guoying Chen, and Lei Cheng, 2015 International Battery Association and Pacific Power Symposium Joint Meeting, Waikoloa, HI, Jan. 2015. (Invited talk)

Task 3.9 – Lithium Batteries with Higher Capacity and Voltage (John B. Goodenough, UT Austin)

PROJECT OBJECTIVE:

(a) To increase cell energy density for a given cathode and (b) to allow low-cost rechargeable batteries with cathodes other than insertion compounds.

PROJECT IMPACT:

A solid Na^+ or Li^+ -electrolyte separator would permit use of a Li^0 anode, thus maximizing energy density for a given cathode, and liquid flow-through and air cathodes of high capacity as well as high-voltage solid cathodes given two liquid electrolytes having different windows.

OUT-YEAR-GOALS:

(a) To increase cell energy density for a given cathode and (b) to allow low-cost, high-capacity rechargeable batteries with cathodes other than insertion compounds.

COLLABORATIONS: A. Manthiram, UT Austin and Karim Zaghib, Hydro Quebec.

Milestones

1. Fabricate oxide/polymer composite membrane as a separator in an alkali-ion (Li^+ , Na^+) battery and optimization of pore size, oxide loading, and thickness for blocking anode dendrites with fast alkali-ion transport. (31 March, 2015) **Completed.**
2. Investigate membranes that can block a customized soluble redox couple in a flow-through cathode. (30 June, 2015). **Completed.**
3. Evaluate Li-ion and Na-ion cells with a metallic Li or Na anode, oxide/polymer membrane as separator, and a flow-through liquid cathode. (30 September, 2015).
4. Measure performance of cells with a metallic Li or Na anode, oxide/polymer composite membrane as separator, and an insertion compound as cathode. (31 December, 2015)

Progress Report

Our previous approach to block the redox-molecule (e.g. 6-bromohexyl ferrocene) crossover was accomplished by adopting a highly crosslinked polymer membrane as well as a PEDOT:PSS-coated polypropylene separator between anolyte and catholyte. The approach mainly focused on physical size control of the polymer chain structure. In this term, we have investigated a new membrane with different functional groups to increase chemical interactions between the cathode redox-molecules and polymer backbone chemical structures. The approach was expected to reduce the number of the separator layers, i.e. to remove the PEDOT:PSS separator layer. The previous polymer membrane was fabricated with pentaerythritol tetrakis (3-mercaptopropionate) (*PETT*) and di(ethylene glycol) divinyl ether (*DEGDVE*). We tried to replace DEGDVE with divinyl adipate that has ester groups that can have higher electronic interactions with cathode molecules in the electrolyte.

The new membrane was prepared via thiol-ene polymerization and characterized with FTIR and DSC. In the new polymer, the ester group replaced the ethylene oxide group, which induced an increased carbonyl stretching vibration peak at 1730 cm^{-1} and reduced the C-O-C absorbance around 1100 cm^{-1} as shown in Figure 25. Therefore, the peak intensity ratio of C=O to C-O-C vibrations was reversed by the monomer change. Moreover, ene ($1620\text{--}1680\text{ cm}^{-1}$) and thiol ($2550\text{--}2600\text{ cm}^{-1}$) bands do not appear in the spectra, which indicates complete depletion of monomers during the polymerization.

DSC test was performed to check the glass transition temperature, T_g , and melting point of the polymer membrane. Previous crosslinked polymer between PETT and DEGDVE shows a T_g at $-30.9\text{ }^{\circ}\text{C}$, and the new polymer with the ester groups instead of the ethylene oxides exhibits $-19.9\text{ }^{\circ}\text{C}$ that is well below room temperature. The low T_g values are responsible for the flexible nature of the polymer membranes.

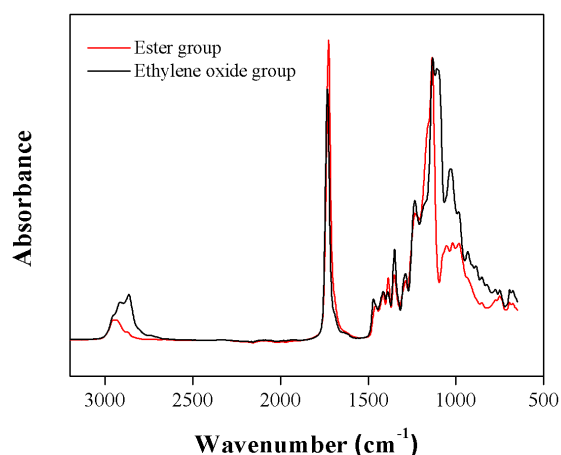


Figure 25: FTIR spectra of the crosslinked polymer membranes made of the tetrathiol crosslinkers and (a) ethylene oxide groups or (b) ester groups.

Q2 Patents/Publications/Presentations

None this quarter

Task 3.10 – Exploiting Co and Ni Spinel in Structurally-Integrated Composite Electrodes (Michael M. Thackeray and Jason R. Croy, Argonne National Laboratory)

PROJECT OBJECTIVE: This is a new project, the goal of which is to stabilize high capacity, composite ‘layered-layered’ electrode structures with lithium-cobalt-oxide and lithium-nickel-oxide spinel components (referred to as LCO-S and LNO-S, respectively), or solid solutions thereof (LCNO-S), which can accommodate lithium at approximately 3.5 V vs. metallic lithium. This approach and the motivation to use LCO-S and LNO-S spinel components, about which relatively little is known, is novel.

PROJECT IMPACT: State-of-the art lithium-ion batteries are currently unable to satisfy the performance goals for plug-in hybrid- (PHEV) and all-electric (EV) vehicles. If successful, this project will impact the advance of energy storage for electrified transportation as well as other applications, such as portable electronic devices and the electrical grid.

APPROACH: Focus on the design and synthesis of new spinel compositions and structures that operate above 3 V and below 4 V and to determine their structural and electrochemical properties through advanced characterization. This information will subsequently be used to select the most promising spinel materials for integration as stabilizers into high capacity composite electrode structures.

OUT-YEAR-GOALS: The electrochemical capacity of most high potential lithium-metal oxide insertion electrodes is generally severely compromised by their structural instability and surface reactivity with the electrolyte at low lithium loadings (i.e., at highly charged states). Although some progress has been made by cation substitution and structural modification, the practical capacity of these electrodes is still restricted to approximately 160-170 mAh/g. This project proposes a new structural and compositional approach with the goal of producing electrode materials that can provide 200-220 mAh/g without significant structural or voltage decay for 500 cycles. If successful, the materials processing technology will be transferred to Argonne’s Materials Engineering and Research Facility (MERF) for scale up and further evaluation.

COLLABORATIONS: Eungje Lee, Brandon R. Long and Joong Sun Park (CSE, ANL), Mali Balasubramanian (APS, ANL), V. Dravid and C. Wolverton (Northwestern University)

Milestones

1. Synthesize and optimize LCO-S, LNO-S and LCNO-S spinel compositions and structures and determine their structural and electrochemical properties (Sep-15). **In progress - see text.**
2. Devise synthesis techniques to embed the most promising spinel compositions into layered structures (Sep-15).
3. Determine the impact of embedding LCO-S or LNO-S components on the electrochemical properties and cycling stability of composite ‘layered-spinel’ or ‘layered-layered-spinel’ structures (Sep-15).
4. Use complementary theoretical approaches to further the understanding of the structural and electrochemical properties of LCO-S, LNO-S and LCNO-S electrodes and protective surface layers (Sep-15).

Progress Report

This project builds on previous reports that have indicated that (1) it is possible to synthesize a lithiated cobalt oxide spinel ($\text{Li}_2[\text{Co}_2]\text{O}_4$) by a ‘low-temperature’ (LT, $\sim 400^\circ\text{C}$) solid-state synthesis method, and (2) the electrochemical performance of LT- LiCoO_2 electrodes can be markedly enhanced by 10% Ni substitution (i.e., LT- $\text{LiCo}_{0.9}\text{Ni}_{0.1}\text{O}_2$). In this exploratory work, given the stability and wide compositional range of Li-Mn-O spinel structures, the effects of manganese substitution on the electrochemical properties of LT- LiCoO_2 and LT- $\text{LiCo}_{0.9}\text{Ni}_{0.1}\text{O}_2$ electrodes were investigated.

First, compounds in the LT- $\text{LiCo}_{1-y}\text{Mn}_y\text{O}_2$ ($0 \leq y \leq 1.0$) system were fabricated and analyzed. High-resolution synchrotron XRD data of the end member LT- LiMnO_2 ($y=1$) indicated the presence of a spinel phase, but also a broad peak at $\sim 22^\circ 2\theta$, characteristic of LiMn_6 cation ordering in Li_2MnO_3 . The low-temperature synthesis and overlap of the spinel peaks with Li_2MnO_3 strongly suggests that the LT- LiMnO_2 product has a composite structure, $\text{Li}_2\text{MnO}_3 \bullet \text{Li}_4\text{Mn}_5\text{O}_{12}$, in which the Li:Mn ratio is 1:1 as it is in LiMnO_2 . Figure 26 shows the structural relationship of the manganese (magenta) sublattices between (a) LiMn_2O_4 spinel (for convenience) and (b) Li_2MnO_3 . For LT- $\text{LiCo}_{1-y}\text{Mn}_y\text{O}_2$ ($0.25 \leq y \leq 0.75$) compositions, synchrotron HR-XRD data have shown that it is difficult to incorporate cobalt into a ‘layered-spinel’ $\text{Li}_2\text{MnO}_3 \bullet \text{Li}_4\text{Mn}_5\text{O}_{12}$ composite structure, as evident from an impurity phase that was detected and tentatively attributed to Co_3O_4 .

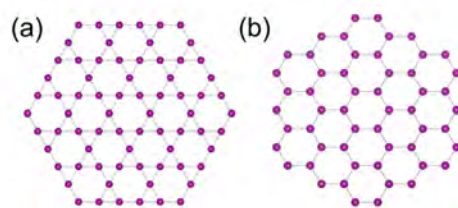


Figure 26: Mn arrangements in (a) (111) plane of LiMn_2O_4 and (b) (001) plane of Li_2MnO_3 .

Second, the effects of Mn substitution on the structure and electrochemistry of LT- $\text{LiCo}_{0.9}\text{Ni}_{0.1}\text{O}_2$ electrodes were studied. Pure LT- $\text{LiCo}_{1-y}\text{Ni}_{0.1}\text{Mn}_y\text{O}_2$ samples ($y=0, 0.1, 0.2$) were prepared without any noticeable impurity phases after extended periods (~ 7 days) of low-temperature firing of the precursor materials (Figure 27(a)). A comparison of the electrochemistry of lithium cells with LT- $\text{LiCo}_{0.9}\text{Ni}_{0.1}\text{O}_2$ ($y=0$) and LT- $\text{LiCo}_{0.9-y}\text{Ni}_{0.1}\text{Mn}_y\text{O}_2$ ($y=0.1, 0.2$) electrodes is provided in Figure 27 (b) and (c), respectively. It appears that Mn substitution has a negative effect on the capacity of LT- $\text{LiCo}_{0.9-y}\text{Ni}_{0.1}\text{Mn}_y\text{O}_2$ electrodes. When cycled between 3.9 and 2.5 V, the initial discharge capacity decreases with increasing Mn substitution from 120 mAh/g ($y=0$) to 100 mAh/g for $y=0.1$, and to 80 mAh/g for $y=0.2$ (Figure 27b). Increasing the upper cut-off voltage to 4.2 V yields slightly higher capacities, but significantly reduces the cycling stability of the electrodes (Figure 27b, inset).

Efforts to improve the electrochemical stability of lithiated spinel LT- $\text{LiCo}_{1-x}\text{Ni}_x\text{O}_2$ electrodes, which offer an attractive ~ 3.5 V vs. lithium metal, by compositional control, are continuing.

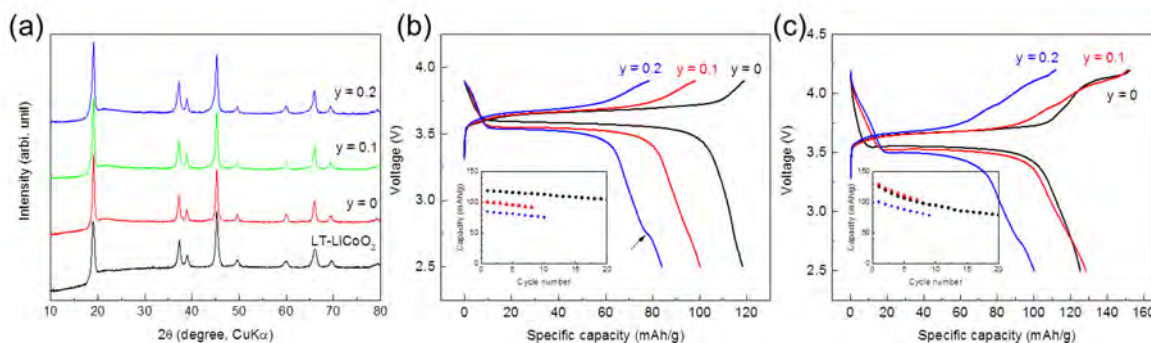


Figure 27: (a) XRD patterns of LT- LiCoO_2 and LT- $\text{LiCo}_{0.9-y}\text{Ni}_{0.1}\text{Mn}_y\text{O}_2$ samples ($y = 0, 0.1$, and 0.2). Initial voltage profiles of Li/LT- $\text{LiCo}_{0.9-y}\text{Ni}_{0.1}\text{Mn}_y\text{O}_2$ ($y = 0, 0.1$, and 0.2) cells charged to upper cut-off voltages of (b) 3.9 V and (c) 4.2 V at a rate of 15 mA/g. Capacity vs. cycle number plots are provided as insets in (b) and (c).

Q2 Patents/Publications/Presentations

None – this is a new project.

TASK 4 – ELECTROLYTES FOR HIGH VOLTAGE HIGH ENERGY LITHIUM-ION BATTERIES

Summary and Highlights

The current lithium-ion electrolyte technology is based on LiPF_6 solutions in organic carbonate mixtures with one or more functional additives. Lithium-ion battery chemistries with energy density of 175~250 Wh/Kg are currently the most promising choice. To further increase the energy density, the most efficient way is to raise either the voltage and/or the capacity of the positive materials. Several high energy materials including high-capacity composite cathode $x\text{Li}_2\text{MnO}_3 \bullet (1-x)\text{LiMO}_2$ and high-voltage cathode materials such as $\text{LiNi}_{0.5}\text{Mn}_{1.5}\text{O}_4$ (4.8 V) and LiCoPO_4 (5.1 V) have been developed. However, their increased operating voltage during the activation and charging poses great challenges to the conventional electrolytes, whose organic carbonate-based components tend to oxidatively decompose at the threshold beyond 4.5 V vs Li^+/Li .

Other candidate positive materials for PHEV application that have potential of providing high capacity are the layered Ni-rich NCM materials. When charged to a voltage higher than 4.5 V, they can deliver a much higher capacity. For example, $\text{LiNi}_{0.8}\text{Co}_{0.1}\text{Mn}_{0.1}\text{O}_2$ (NCM 811) only utilizes 50% of its theoretical capacity of 275 mAh/g when operating in a voltage window of 4.2 V-3.0 V. Operating voltage higher than 4.4 V would significantly increase the capacity to 220 mAh/g; however, the cell cycle life becomes significantly shortened mainly due to the interfacial reactivity of the charged cathode with the conventional electrolyte. The oxidative voltage instability of the conventional electrolyte essentially prevents the practicality to access the extra capacities of these materials.

To address the above challenges, new electrolytes that have substantially high voltage tolerance at high temperature with improved safety are needed urgently. Organic compounds with low HOMO (highest occupied molecular orbital) energy level are suitable candidates for high voltage application. Alternative approach to address the electrolyte challenges is to mitigate the surface reactivity of high voltage cathodes by developing cathode passivating additives. Like the indispensable role of SEI on the carbonaceous anodes, cathode electrolyte interphase (CEI) formation additives could kinetically suppress the thermodynamic reaction of the delithiated cathode and electrolyte, thus significantly improving the cycle life and calendar life of the high energy density lithium-ion battery.

An ideal electrolyte for high voltage high energy cathodes also requires high compatibility with anode materials (graphite or silicon). New anode SEI formation additives tailored for the new high voltage electrolyte are equally critical for the high energy lithium-ion battery system. Such an electrolyte should have the following properties: high stability against 4.5-5.0 V charging state, particularly with cathodes exhibiting high surface oxygen activity; high compatibility with a strongly reducing anode under high voltage charging; high Li salt solubility (>1.0 M) and ionic conductivity ($> 6 \times 10^{-3}$ S/cm @ room temperature); non-flammability (no flash point) for improved safety and excellent low temperature performance (-30°C).

Task 4.1 – Fluorinated Electrolyte for 5-V Li-ion Chemistry (Zhengcheng Zhang, Argonne National Laboratory)

PROJECT OBJECTIVE: The objective of this project is to develop a new advanced electrolyte system with outstanding stability at high voltage and high temperature and improved safety characteristic for an electrochemical couple consisting of the high voltage $\text{LiNi}_{0.5}\text{Mn}_{1.5}\text{O}_4$ (LNMO) cathode and graphite anode. The specific objectives of this proposal are the design, synthesis and evaluation of (1) non-flammable high voltage solvents to render intrinsic voltage and thermal stability in the entire electrochemical window of the high-voltage cathode materials, and (2) electrolyte additives to enhance the formation of a compact and robust solid electrolyte interphase (SEI) on the surface of the high voltage cathode. A third objective is to gain fundamental understanding of the interaction between electrolyte and high voltage electrode materials, the dependence of SEI functionality on electrolyte composition, and the effect of high temperature on the full Li-ion cells using the advanced electrolyte system.

PROJECT IMPACT: This innovative fluorinated electrolyte is intrinsically more stable in electrochemical oxidation due to the fluorine substitution; therefore it would be also applicable to cathode chemistries based on TM oxides other than LNMO. The results of this project can be further applied to a wide spectrum of high-energy battery systems oriented for PHEVs that operate at high potentials, such as LiMPO_4 ($\text{M}=\text{Co}, \text{Ni}, \text{Mn}$), or battery systems that require a high-voltage activation process, such as the high-capacity Li-Mn-rich $x\text{Li}_2\text{MnO}_3 \cdot (1-x)\text{Li}[\text{Ni}_x\text{Mn}_y\text{Co}_z]\text{O}_2$. This electrolyte innovation will push the U.S. supply base of batteries and battery materials past the technological and cost advantages of foreign competitors, thereby increasing economic value to the USA. ANL's new fluorinated electrolyte material will enable the demand for more PHEVs and EVs, which directly transforms to much less gasoline consumption and less pollutant emissions.

OUT-YEAR-GOALS: The goal of this project is to deliver a new fluorinated electrolyte system with outstanding stability at high voltage and high temperature with improved safety characteristic for an electrochemical couple consisting of 5-V Ni-Mn spinel $\text{LiNi}_{0.5}\text{Mn}_{1.5}\text{O}_4$ (LNMO) cathode and graphite anode. The specific objectives of this proposal are the design, synthesis, and evaluation of (1) non-flammable high voltage fluorinated solvents to attain intrinsic voltage stability in the entire electrochemical window of the high-voltage cathode material and (2) effective electrolyte additives that form a compact and robust solid-electrolyte interphase (SEI) on the surfaces of the high voltage cathode and graphitic anode.

COLLABORATIONS: Dr. Kang Xu, U.S. Army Research Laboratory; Dr. Xiao-Qing Yang, Brookhaven National Laboratory; Dr. Brett Lucht, University of Rhode Island; Dr. Andrew Jansen and Dr. Gregory Krumdick, Argonne National Laboratory.

Milestones

1. Complete theoretical calculation of electrolyte solvents; Validate the electrochemical properties of the available fluorinated solvents by CV and leakage current experiment. (March-14) **Complete.**
2. Synthesize and characterize the Gen-1 electrolyte. (June-14) **Complete.**
3. Evaluate the LNMO/graphite cell performance of Gen-1 F-electrolyte. (Sep-14) **Complete.**
4. Design and build interim cells and baseline pouch cells. (Jan.-15) **On-going.**
5. Synthesize and evaluate Gen-2 F-electrolyte based on TF-PC. (Mar.-15) **Complete.**
6. Develop optimized F-electrolyte containing multinary F-solvents. (Jun.-15) **On Track.**
7. Design and build final cells. (sep.-15) **On Track.**

Progress Report

This quarter, considerable efforts have been expended to understand the issue associated with long term cycling performance at elevated temperature and methods to address the issue. First we investigated the thermal stability of the FEC-based electrolyte and provided insight of Li^+ solvation in the mixed fluorinated carbonate solvents by NMR spectroscopy. Figure 28 illustrates the thermal decomposition of FEC solvent at the presence of LiPF_6 at 50 °C. Thermal treatment of FEC solvent or FEC + LiTFSI causes no decomposition of the solvent, however when FEC and LiPF_6 coexist, discoloration and solidification occurred (center tube in Figure 28a). ^1H (Figure 28b), ^{19}F (Figure 28c) and ^{31}P (not shown) NMR analysis concluded that FEC suffers from elimination of HF catalyzed by the Lewis base PF_5 or POF_3 originating from the thermal decomposition or hydrolysis of LiPF_6 salt. The thermal decomposition pathway of the FEC- LiPF_6 is proposed in Figure 28d. The polymerization of vinylene carbonate, the decomposition product of FEC, will lead to the depletion of FEC solvent and ultimately jeopardize the cell performance at high temperature.

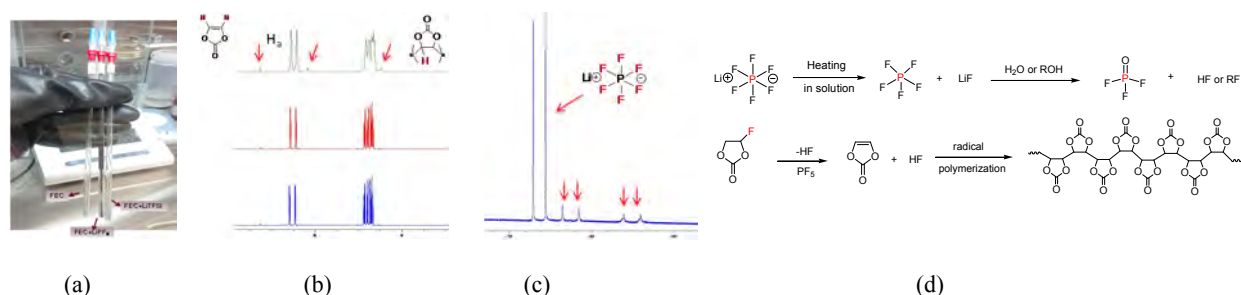


Figure 28: (a) Thermal decomposition of FEC- LiPF_6 ; (b) ^1H -NMR of 0.5 M LiPF_6 in FEC (top), 0.5 M LiTFSI in FEC (center) and FEC (bottom) after 5-day thermal treatment at 50°C; (c) ^{19}F -NMR of 0.5 M LiPF_6 in FEC after 5-day thermal treatment at 50°C; (d) proposed pathway of FEC thermal decomposition catalyzed by Lewis base PF_5 .

From the organic chemistry standpoint, the strong electron-withdrawing F- group renders the adjacent H atom more labile and more reactive. By switching from -F to $-\text{CF}_3$, it stabilizes the new solvent TF-PC and shows significant thermal stability when dissolved with LiPF_6 salt as evidenced from the ^1H , ^{19}F , ^{31}P NMR data (not shown). Next we have formulated a new electrolyte based on TF-PC (TFPC-FMC- LiPF_6 +Additive). Surprisingly, this new electrolyte is thermally stable, but shows high oxidation stability when tested in LNMO/Li cells (Figure 29a, Figure 29b) compared with Gen 2. Moreover, TF-PC, as a main electrolyte solvent, can passivate the graphite surface forming a protective SEI layer on the surface of graphite anode (Figure 29c) and enables the LNMO/Graphite cells as shown in Figure 29d.

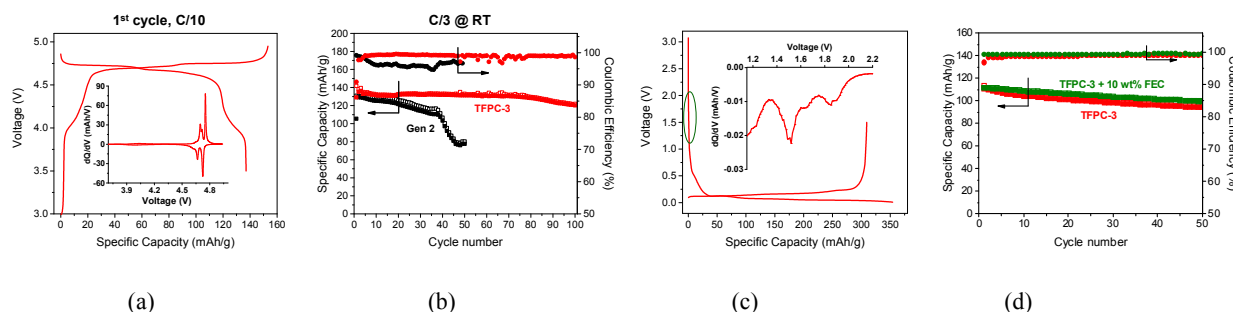


Figure 29: (a) 1st cycle voltage profiles and (b) cycling data of LNMO/Li cell with 1.0 M LiPF_6 TFPC-FEMC (5/5) electrolyte; (c) 1st lithiation and delithiation profiles of graphite/Li cell with 1.0 M LiPF_6 TFPC-FEMC (5/5) electrolyte; (d) cycling performance of LNMO/graphite full cell with 1.0 M LiPF_6 TFPC-FEMC (5/5) electrolyte.

In the next quarter, we will optimize the new TFPC electrolyte by developing tailored additives to further stabilize the anode surface. We will also seek to understand the solvation difference between the TFPC electrolyte and nonfluorinated electrolyte using 2D DOSY NMR spectroscopy.

TASK 5 – DIAGNOSTICS

Summary and Highlights

In order to meet the goals of Vehicle Technology Office's (VTO's) Multi Year Program Plan (MYPP) and develop lower-cost, abuse-tolerant batteries with higher energy density, higher power, better low-temperature operation and longer lifetimes suitable for the next-generation of HEVs, PHEVs and EVs, there is a strong need to identify and understand structure-property-electrochemical performance relationships in materials, life-limiting and performance-limiting processes, and various failure modes to guide battery development activities and scale-up efforts. In the pursuit of batteries with high energy density, high cell operating voltages and demanding cycling requirements lead to unprecedented chemical and mechanical instabilities in cell components. Successful implementation of newer materials such as Si anode and high voltage cathodes also requires better understanding of fundamental processes, especially those at the solid/electrolyte interface of both anode and cathode.

The Battery Materials Diagnostics Research Task 5 takes on these challenges by combining model system, *ex situ*, *in situ* and *operando* approaches with an array of the start-of-the-art analytical and computational tools. Four subtasks are tackling the chemical processes and reactions at the electrode/electrolyte interface. Researchers at LBNL use *in situ* and *ex situ* vibrational spectroscopy, far- and near-field scanning probe spectroscopy and laser-induced breakdown spectroscopy (LIBS) to understand the composition, structure, and formation/degradation mechanisms of the solid electrolyte interface at Si anode and high voltage cathodes. UCSD combines scanning transmission electron microscopy (STEM)/electron energy loss spectroscopy (EELS), X-ray photoelectron spectroscopy (XPS) and *ab initio* computation for surface and interface characterization and identification of instability causes at both electrodes. At Cambridge, nuclear magnetic resonance (NMR) is being used to identify major SEI components, their spatial proximity and how they change with cycling. Subtasks at BNL and PNNL focus on the understanding of fading mechanisms in electrode materials, with the help of synchrotron based X-ray techniques (diffraction and hard/soft X-ray absorption) at BNL and high-resolution transmission electron microscopy (HRTEM) and spectroscopy techniques at PNNL. At LBNL, model systems of electrode materials with well-defined physical attributes are being developed and used for advanced diagnostic and mechanistic studies at both bulk and single-crystal levels. These controlled studies remove the ambiguity in correlating material's physical properties and reaction mechanisms to its performance and stability which is critical for further optimization. The final subtask takes advantage of the user facilities at ANL that brings together X-ray and neutron diffraction, X-ray absorption, emission and scattering, HRTEM, Raman spectroscopy and theory to look into the structural, electrochemical and chemical mechanisms in the complex electrode/electrolyte systems. The diagnostics team not only produces a wealth of knowledge that is key to the development of the next-generation batteries, it also advances analytical techniques and instrumentation that have a far-reaching effect on material and device development in a variety of other related fields.

The highlights for this quarter are as follows:

1. Chen's group reported transition metal reduction on the surface of pristine Li- and Mn-rich layered oxides and demonstrated its dependence on particle morphology.
2. Wang's group visualized the effect of thin coating on the lithiation kinetics of Si anode using *in situ* transmission electron microscopy on alucone and Al₂O₃ coated Si nanowires.
3. Kostecki's group validated the positive effect of alucone coating on Si anode with improved cycling performance and reduced the interfacial resistance.

Task 5.1 – Design and Synthesis of Advanced High-Energy Cathode Materials (Guoying Chen, Lawrence Berkeley National Laboratory)

PROJECT OBJECTIVE: The successful development of next-generation electrode materials requires particle-level knowledge of the relationships between materials' specific physical properties and reaction mechanisms to their performance and stability. This single-crystal-based project was developed specifically for this purpose and it has the following objectives: 1) obtain new insights into electrode materials by utilizing state-of-the-art analytical techniques that are mostly inapplicable to conventional, aggregated secondary particles, 2) gain fundamental understanding of structural, chemical and morphological instabilities during Li extraction/insertion and prolonged cycling, 3) establish and control the interfacial chemistry between the cathode and electrolyte at high operating voltages, 4) determine transport limitations at both particle and electrode levels, and 5) develop next-generation electrode materials based on rational design as opposed to more conventional empirical approaches.

PROJECT IMPACT: This project will reveal performance-limiting physical properties, phase-transition mechanisms, parasitic reactions, and transport processes based on the advanced diagnostic studies of well-formed single crystals. The findings will establish rational, non-empirical design methods that will improve the commercial viability of next-generation $\text{Li}_{1+x}\text{M}_{1-x}\text{O}_2$ (M=Mn, Ni and Co) and spinel $\text{LiNi}_x\text{Mn}_{2-x}\text{O}_4$ cathode materials.

APPROACH: Prepare crystal samples of Li-rich layered oxides and high-voltage Ni/Mn spinels with well-defined physical attributes. Perform advanced diagnostic and mechanistic studies at both bulk and single-crystal levels. Global properties and performance of the samples will be established from the bulk analyses, while the single-crystal based studies will utilize time- and spatial-resolved analytical techniques to probe material's redox transformation and failure mechanisms.

OUT-YEAR GOALS: This project aims to determine performance- and stability-limiting fundamental properties and processes in high-energy cathode materials and outline mitigating approaches. Improved electrode materials will be designed and synthesized.

COLLABORATIONS: Drs. R. Kostecki, M. Doeff, K. Persson, V. Zorba, T. Tylliszczak and Z. Liu (LBNL), Prof. C. Grey (Cambridge), Prof. B. Lucht (URI), and Prof. Y.-M. Chiang (MIT).

Milestones

1. Characterize Ni/Mn spinel solid solutions and determine the impact of phase transformation and phase boundary on rate capability (Dec-14) **Completed**
2. Complete the investigation on crystal-plane specific reactivity between Li-rich layered oxides and the electrolyte. Determine morphology effect in side reactions (Mar-15) **Completed**
3. Develop new techniques to characterize reactions and processes at the cathode-electrolyte interface. Evaluate the effect of surface compositions and modifications on side reactions and interface stability (Jun-15) **On schedule**
4. Go/No-Go: Continue the approach of using synthesis conditions to vary surface composition if significant structural and performance differences are observed (Sep-15) **On schedule**

Progress Report

During this quarter, the effect of particle morphology, particularly surface area and surface facet, on the surface layer of Li- and Mn-rich layered oxides and its evolution during charge/discharge was investigated. By varying heating temperature, time, precursors, and reaction flux in the molten-salt synthesis, phase-pure $\text{Li}_{1.2}\text{Mn}_{0.13}\text{Mn}_{0.54}\text{Co}_{0.13}\text{O}_2$ crystals were synthesized in six different morphologies: plate, needle, large polyhedron (L-Poly), small polyhedron (S-Poly), box and octahedron (Figure 30). All samples were micron-sized crystals with a similar surface area of about $0.4 \text{ m}^2/\text{g}$, except that the S-Poly sample had a smaller particle size with 10x more surface area.

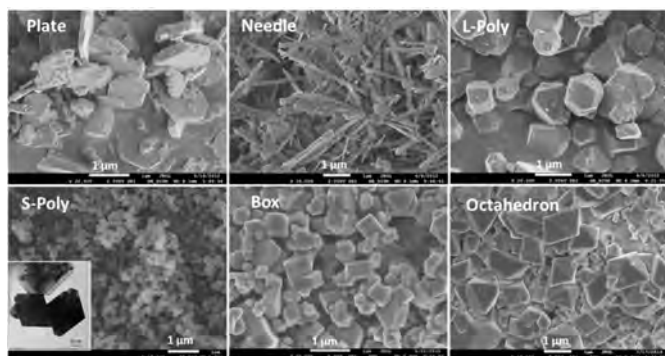


Figure 30: SEM images of $\text{Li}_{1.2}\text{Ni}_{0.13}\text{Mn}_{0.54}\text{Co}_{0.13}\text{O}_2$ crystals.

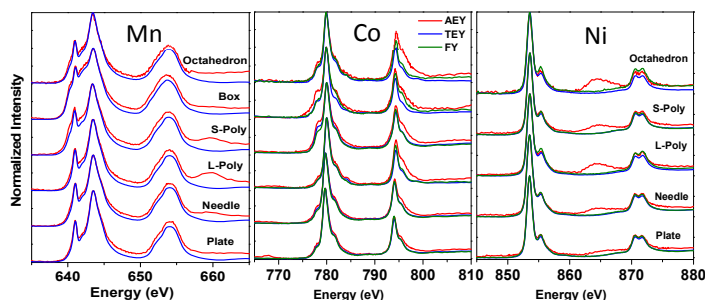


Figure 31: Soft XAS spectra of Mn, Co and Ni *L*-edges collected in AEY, TEY and FY modes on pristine $\text{Li}_{1.2}\text{Ni}_{0.13}\text{Mn}_{0.54}\text{Co}_{0.13}\text{O}_2$ crystals.

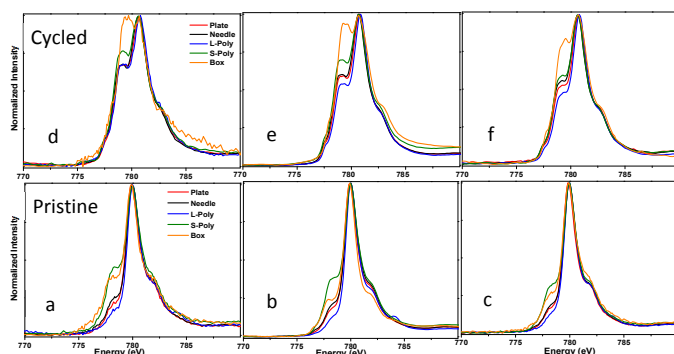


Figure 32: Soft XAS spectra of Co *L*-edge collected in AEY (a and d), TEY (b and e) and FY (c and f) modes on pristine (bottom) and cycled (top) $\text{Li}_{1.2}\text{Ni}_{0.13}\text{Mn}_{0.54}\text{Co}_{0.13}\text{O}_2$ composite electrodes.

FY suggests that Co reduction progressed from the surface to the bulk. Furthermore, the extent of cycling-induced reduction is particle surface dependent. The most reduction occurred on the box sample and least on L-Poly, consistent with what was observed on the initial Co reduction on the pristine oxides.

The synthesized $\text{Li}_{1.2}\text{Mn}_{0.13}\text{Mn}_{0.54}\text{Co}_{0.13}\text{O}_2$ crystal samples were carefully evaluated by soft X-ray absorption spectroscopy (XAS) carried out at beamline 10-1 at SSRL. XAS is a technique capable of depth-resolved probing of transition metal (TM) oxidation state by using three detection modes: Auger electron yield (AEY) that probes the top surface of 1-2 nm, total electron yield (TEY) that probes the depth of 2 to 5 nm, and fluorescence yield (FY) that collects signal from the bulk with a penetration depth of about 50 nm. Figure 31 shows the Mn, Co and Ni *L*-edge spectra collected on the pristine crystals. The FY XAS spectra confirm that the oxidation states of Mn, Co and Ni in the bulk were 4+, 3+ and 2+, respectively. While Ni remains 2+ in the entire particle, Mn and Co were reduced from the bulk to the top surface layer of a few nm, as suggested by the intensity increase in the peaks around 640 and 780 eV in the Mn and Co AEY spectra, respectively. The thickness of this reduced surface layer is morphology dependent, with the least reduction found on plate and L-Poly samples and the most found on the S-Poly and box samples. Figure 32 compares the Co *L*-edge spectra collected on the pristine and cycled composite electrodes containing $\text{Li}_{1.2}\text{Mn}_{0.13}\text{Mn}_{0.54}\text{Co}_{0.13}\text{O}_2$ crystals, a PVDF binder and carbon. The cycled electrode was recovered from a half cell that was charged and discharged in a 1 M LiPF_6 in EC-DEC (1:1) electrolyte for 45 cycles (2-4.6 V). Cycling promoted further Co reduction in all samples as the content of reduced Co increased with cycling. The monotonous increase in oxidation state from AEY, TEY to

Patents/Publications/Presentations

1. L. Cheng, W. Chen, M. Kunz, K. Persson, N. Tamura, G. Chen, and M. M. Doeff, “Interrelationships among Grain Size, Surface Composition, Air Stability and Interfacial Resistance of Al-substituted $\text{Li}_7\text{La}_3\text{Zr}_2\text{O}_{12}$ Solid Electrolytes,” submitted to *ACS Applied Materials & Interfaces*, (2015).
2. L. Cheng, W. Chen, M. Kunz, K. Persson, N. Tamura, G. Chen, and M. M. Doeff, “Effect of Surface Microstructure on Electrochemical Performance of Garnet Solid Electrolytes,” *ACS Applied Materials & Interfaces*, **7** (3), 2073 (2015).
3. S. Kuppan, A. Jarry, R. Kostecki, and G. Chen, “A study of room-temperature $\text{Li}_x\text{Mn}_{1.5}\text{Ni}_{0.5}\text{O}_4$ solid solutions” *Scientific Reports*, doi:10.1038/srep08027 (2015).
4. J. S. Park, L. Cheng, V. Zorba, A. Mehta, J. Cabana, G. Chen, M. M. Doeff, T. J. Richardson, J. H. Park, J.-W. Son, W.-S. Hong, “Effects of Crystallinity and Impurities on the Electrical Conductivity of Li-La-Zr-O Thin Films” *Thin Solid Films*, **576**, 55 (2015).

Task 5.2 – Interfacial Processes – Diagnostics (Robert Kostecki, Lawrence Berkeley National Laboratory)

PROJECT OBJECTIVE: The main objective of this task is to obtain detailed insight into the dynamic behavior of molecules, atoms, and electrons at electrode/electrolyte interfaces of intermetallic anodes (Si) and high voltage Ni/Mn-based materials at a spatial resolution that corresponds to the size of basic chemical or structural building blocks. The aim of these studies is to unveil the structure and reactivity at hidden or buried interfaces and interphases that determine battery performance and failure modes. To accomplish these goals, novel far- and near-field optical multifunctional probes must be developed and deployed *in situ*. The proposed work constitutes an integral part of the concerted effort within the BMR Program and it attempts to establish clear connections between diagnostics, theory/modelling, materials synthesis, and cell development efforts.

PROJECT IMPACT: This project provides better understanding of the underlying principles that govern the function and operation of battery materials, interfaces and interphases, which is inextricably linked with successful implementation of high energy density materials such as Si and high voltage cathodes in Li-ion cells for PHEVs and EVs. This task also involves the development and application of novel innovative experimental methodologies to study and understand the basic function and mechanism of operation of materials, composite electrodes, and Li-ion battery systems for PHEV and EV applications.

APPROACH: Design and employ novel and sophisticated *in situ* analytical methods to address the key problems of the BMR baseline chemistries. Experimental strategies combine imaging with spectroscopy aimed at probing electrodes at an atom, molecular, or nanoparticulate level to unveil structure and reactivity at hidden or buried interfaces and determine electrode performance and failure modes in baseline Li_xSi -anodes and high-voltage LMNO cathodes. The proposed methodologies include *in situ* and *ex situ* Raman, FTIR and LIBS far- and near-field spectroscopy/microscopy, scanning probe microscopy (SPM), spectroscopic ellipsometry, electron microscopy (SEM, HRTEM), and standard electrochemical techniques and model single particle and/or monocrystal model electrodes to probe and characterize bulk and surface processes in Si anodes, and high-energy cathodes.

OUT-YEAR GOALS: The main goal is to gain insight into the mechanism of surface phenomena on thin-film and monocrystal Sn and Si intermetallic anodes and evaluate their impact on the electrode long-term electrochemical behavior. Comprehensive fundamental study of the early stages of SEI layer formation on polycrystalline and single crystal face Sn and Si electrodes will be carried out. *In situ* and *ex situ* far- and near-field scanning probe spectroscopy and LIBS will be employed to detect and monitor surface phenomena at the intermetallic anodes and high-voltage (>4.3V) model and composite cathodes.

COLLABORATIONS: Vincent Battaglia, Ban Chunmei, Vassilia Zorba, Bryan D. McCloskey

Milestones

1. Determine the mechanism of formation of the metal complexes species that are produced at high-energy Li-ion cathodes (Dec-14) **Status: completed**
2. Resolve SEI layer chemistry of coated Si single crystal and thin film anodes (collaboration with Chunmei Ban). (Mar-15) **Status: completed**
3. Determine the mechanism of SEI layer poisoning by Ni and Mn coordination compounds (collaboration with the Bryan D. McCloskey). (Jun-15) **Status: on schedule**
4. Go/No-Go: Demonstrate feasibility of *in situ* near-field and LIBS techniques at Li-ion electrodes (collaboration with Vassilia Zorba). **Criteria:** Stop development of near-field and LIBS techniques, if the experiments fail to deliver adequate sensitivity. (Sep-15) **Status: on schedule**

Progress Report

The effect of aluminium alkoxide polymer (alucone) coating on SEI formed on Si anode and its impact on the Li-ion system's long term stability was investigated. 100 nm Si thin films were deposited on copper foil by magnetron sputtering deposition and used as a model electrode for interfacial evaluation. The thin film electrodes were coated with a 8 nm alucone layer by molecular layer deposition. The sample was annealed in Ar at 200°C for 12 hours, assembled in coin cells filled with 1 M LiPF₆, EC/DEC (1:2) electrolyte, and cycled galvanostatically at C/10 for 3 cycles and at 1C for 47 cycles.

The positive impact of the alucone coating on the cyclability of the Si thin film was confirmed (Figure 33). Alucone coating improved the cycling performance of Si thin film and reduced the interfacial resistance.

These effects originate from the variation in SEI composition. While the SEI on the non-coated sample consists mainly of inorganic compounds (LiF, Li₂O/Li₂CO₃), the alucone coating produces improved, ROCO₂Li-enriched SEI. These results are consistent with the literature reports on the behavior of alucone-coated Si composite anodes and they support the general “coating” strategy, indicating that coating of the silicon surface can partially reduce its interfacial instability by changing the nature and/or kinetics of surface reactions. Further advances were also made in near-field IR spectroscopy and imaging. Figure 34(a) shows the conclusive identification of Li₂C₂O₄ in the surface film on Si (111) swept to 1 V in 1 M LiPF₆ + 2% LiBOB in EC:DMC 1:2, by comparison to a reference ATR-FTIR spectrum. Figure 34 shows a near-field image at 1412 cm⁻¹, associated with ROCO₂Li (see Figure 33) of the surface film on Si (111) swept to 1.5 V in the same

electrolyte. This image was taken in an N₂-purged enclosure, so the SEI has not been altered by exposure to air or water. Together, these data demonstrate that near-field techniques can be used to both map and identify functional chemical compounds in the real SEI layer. This completes our efforts toward milestone “2”. Further investigations of the mechanism of SEI poisoning by the fluorescent compounds formed on high voltage Ni/Mn-based materials (milestone 3) and developments of *ex situ* and *in situ* LIBS and near-field IR techniques to identify the SEI components function (milestone 4) are currently underway.

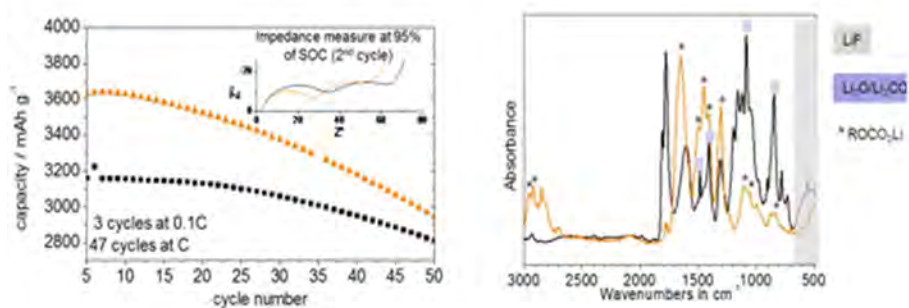


Figure 33: SEI layer forms after 50 cycles on 100 nm Si thin film (coated 8 nm Alucone/non coated) in 1M LiPF₆ EC:DEC [1:2] and corresponding impedance spectra

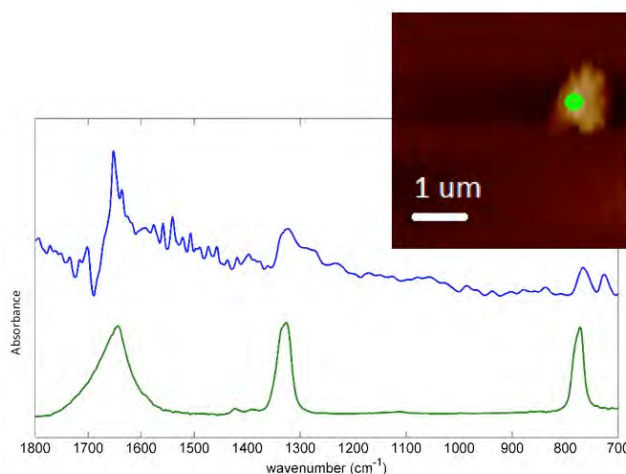


Figure 34: (a) Near-field IR (top) spectrum of particle in Si surface film compared to ATR-FTIR spectrum of Li₂C₂O₄. Inset: AFM topography with particle marked.

Patents/Publications/Presentations

1. Maurice Ayache, Simon Franz Lux, and Robert Kostecki, “IR Near-Field Study of the Solid Electrolyte Interphase on a Tin Electrode”, *J. Phys. Chem. Lett.*, 2015, 6, pp 1126–1129 (2015) DOI: 10.1021/acs.jpcclett.5b00263
2. Angélique Jarry, Sébastien Gottis, Young-Sang Yu, Josep Roque-Rosell, Chunjoong Kim, Jordi Cabana, John Kerr, and Robert Kostecki, “The Formation Mechanism of Fluorescent Metal Complexes at the $\text{Li}_x\text{Ni}_{0.5}\text{Mn}_{1.5}\text{O}_4\text{-}\delta/\text{Carbonate Ester Electrolyte Interface}$ ”, *J. Am. Chem. Soc.*, 2015 DOI: 10.1021/ja5116698
3. Ulrike S. Vogl, Simon F. Lux, Ethan J. Crumlin, Zhi Liu, Lydia Terborg, Martin Winter and Robert Kostecki, “The mechanism of SEI formation on a single crystal Si(100) electrode”, *Journal of Electrochemical Society*, 62 (4) A603-A607 (2015); DOI:10.1149/2.0391504jes
4. Wong, Dominica; Vitale, Alessandra; Devaux, Didier; Taylor, Austria; Pandya, Ashish; Hallinan, Daniel; Thelen, Jacob; Mecham, Sue; Lux, Simon; Lapidès, Alexander; Resnick, Paul; Meyer, Thomas; Kostecki, Robert; Balsara, Nitash; DeSimone, Joseph, “Phase Behavior and Electrochemical Characterization of Blends of Perfluoropolyether, Poly(ethylene glycol) and a Lithium Salt”, *Chemistry of Materials*, 2015, 27 (2), pp 597–603; DOI: 10.1021/cm504228a
5. Vogl, Ulrike; Das, Prodip K.; Weber, Adam; Winter, Martin; Kostecki, Robert; Lux, Simon, “The mechanism of interactions between CMC binder and Si single crystal facets”, *Langumir*, 2014, 30 (34), pp 10299–10307
6. Saravanan Kuppan, Angelique Jarry, Robert Kostecki, and Guoying Chen, “Thermal Behavior of Chemically-Delithiated $\text{Li}_x\text{Mn}_{1.5}\text{Ni}_{0.5}\text{O}_4$ ($0 \leq x < 1$) and the Isolation of Room-Temperature Solid Solutions”, *Scientific Reports*, **5**, 8027 (2015). doi:10.1038/srep08027
7. Lei Cheng, Ethan Crumlin, Wei Chen, Ruimin Qiao, Huaming Hou, Simon Franz Lux, Vassilia Zorba, Richard Russo, Robert Kostecki, Kristin Persson, Wanli Yang, Jordi Cabana, Thomas Richardson, Guoying Chen, and Marca Doeff, “Origin of High Electrolyte-Electrode Interfacial Resistances in Lithium Cells Containing Garnet Type Solid Electrolytes”, *Advanced Materials, Phys. Chem. Chem. Phys.*, 2014, 16, 18294-18300 DOI:10.1039
8. Robert Kostecki, “Battery Characterization and Diagnostics Across Length and Time Scales”, 10th China-U.S. Electric Vehicle and Battery Technology Workshop Beijing P.R.China, March 29-30, 2015
9. Robert Kostecki, Maurice Ayache, Simon Lux, Ivan Lucas, “Near-field optical imaging of the SEI layer on a Sn anode”, 249th ACS National Meeting & Exposition March 22-26, 2015, Denver, CO, USA
10. Robert Kostecki, Maurice Ayache, Angelique Jarry, Ivan Lucas, “Chemical Imaging of Interfaces and Interphases in Li-ion Anodes”, International Battery Association (IBA) and Pacific Power Source Symposium, January 5-9, 2015, Waikoloa Village, Hawaii, USA

Task 5.3 – Advanced *in situ* Diagnostic Techniques for Battery Materials (Xiao-Qing Yang and Xiqian Yu, Brookhaven National Laboratory)

PROJECT OBJECTIVE: The primary objective of this project is to develop new, advanced *in situ* material characterization techniques and to apply these techniques to support the development of new cathode and anode materials for the next generation of lithium-ion batteries (LIBs) for plug-in hybrid electric vehicles (PHEV). In order to meet the challenges of powering the PHEV, LIBs with high energy and power density, low cost, good abuse tolerance, and long calendar and cycle life must be developed.

PROJECT IMPACT: In the Multi Year Program Plan (MYPP) of Vehicle Technology Office (VTO), the battery goals were described as: “Specifically, lower-cost, abuse-tolerant batteries with higher energy density, higher power, better low-temperature operation, and longer lifetimes are needed for the development of the next-generation of HEVs, PHEVs, and EVs.” The knowledge learned from diagnostic studies through this project will help US industries develop new materials and processes for a new generation of lithium-ion batteries in their efforts to reach these VTO goals.

APPROACH: This project will use the combined synchrotron based *in situ* X-ray techniques (x-ray diffraction and hard and soft x-ray absorption) with other imaging and spectroscopic tools such as high resolution transmission electron microscopy (HRTEM), mass spectroscopy (MS) to study the mechanisms governing the performance of electrode materials and provide guidance for new material and new technology development regarding Li-ion battery systems.

OUT-YEAR GOALS: For the high voltage spinel $\text{LiMn}_{1.5}\text{Ni}_{0.5}\text{O}_4$, the high voltage charge and discharge cycling is a serious challenge due to the electrolyte oxidation decomposition. The studies on the improvement of the thermal stability are quite important for the better safety characteristics. For the high energy density $\text{Li}(\text{NiMnCo})\text{O}_2$ composite materials, the problem of poor rate capability during charge and discharge and performance degradation during charge-discharge cycling are issues which need to be addressed.

COLLABORATIONS: The BNL team works closely with the material synthesis groups at ANL (Drs. Thackeray and Amine) due to the high energy composite; UT Austin for the high voltage spinel; and PNNL for the Si-based anode materials. Such interaction between the diagnostic team at BNL and synthesis groups of these other BMR members helps catalyze innovative design and synthesis of advanced cathode and anode materials. We also collaborate with industrial partners at General Motor, Duracell, and Johnson Controls to obtain feedback information from battery end users.

Milestones

1. Complete the thermal stability studies of a series of blended LiMn_2O_4 (LMO) - $\text{LiNi}_{1/3}\text{Co}_{1/3}\text{Mn}_{1/3}\text{O}_2$ (NCM) cathode materials with different weight ratios using *in situ* time-resolved x-ray diffraction (XRD) and mass spectroscopy techniques in the temperature range of 25°C to 580°C (Dec-14).
Completed
2. Complete the *in situ* XRD studies of the structural evolution of $\text{Li}_{2-x}\text{MoO}_3$ ($0 \leq x \leq 2$) high energy density cathode material during charge-discharge cycling between 2.0 and 4.8 V. (Mar-15)
Completed
3. Complete the x-ray absorption near edge structure (XANES) and extended x-ray absorption fine structure (EXAFS) studies at Mo K-edge of Li_2MoO_3 at different charge-discharge states. (Jun-15)
In progress
4. Complete the preliminary studies of elemental distribution of Fe substituted high voltage spinel cathode materials using transmission x-ray microscopy (TXM). (Sep-15) **In progress**

Progress Report

During the 2nd quarter of FY2015, the second milestones for FY2015 had been completed.

During the 2nd quarter of FY2015, BNL has been focused on the studies of a new cathode material, lithium molybdenum trioxide (Li_2MoO_3). Through a systematic study, a new “unit-cell-breathing” mechanism is introduced based on both crystal and electronic structural changes of transition metal oxide cathode materials during charge-discharge: For widely used LiMO_2 ($\text{M} = \text{Co}, \text{Ni}, \text{Mn}$), lattice parameters, a and b contracts during charge. However, for Li_2MoO_3 , such changes are in opposite directions. Metal-metal bonding is used to explain such “abnormal” behavior and a generalized hypothesis is developed. The expansion of M-M bond becomes the controlling factor for $a(b)$ evolution during charge, in contrast to the shrinking M-O as controlling factor in “normal” materials. The cation mixing caused by migration of Mo ions at higher oxidation state provides the benefits of reducing the c expansion range in early stage of charging and suppressing the structure collapse at high voltage charge. These results open a new strategy for designing and engineering layered cathode materials for high energy density lithium-ion batteries. The *in situ* X-ray diffraction patterns of Li_2MoO_3 upon the first charge are shown in Figure 35. The patterns for fully charged and pristine Li_2MoO_3 are plotted in Figure 35a and Figure 35c, respectively. All the peaks can be indexed by a layered structure with the space group R-3m, except for one strong peak at 38.5° , which is from the Al current collector. To demonstrate the phase transition clearly, the contour plots of peak intensity and position for several main peaks as a function of capacity during charge are presented in Figure 35b. It should be noted that the (003), (107) and (108) peaks mainly reflect the evolution along c axis, while the (110) and (101) peaks reflect the evolution along a (and b) axis. The initial charge curves are shown on the right side in Figure 35d. In the region of $0 < x < 0.5$, with a voltage slope from 3.0 to 3.6 V, all of these peaks shifted to the lower angles, indicating a solid solution reaction with decreasing d-spacing for Phase I. In the region of $0.5 < x < 1.0$, a new phase (Phase II) started to form and grow at the expense of Phase I. The new phase has the same layered structure as Phase I but larger unit cell with increased lattice parameters in both a (b) and c , migrated Mo ions into the original Li layers, as the number of Li ions decreasing. (Structure schematics of Phase I and Phase II are shown in Figure 35.)

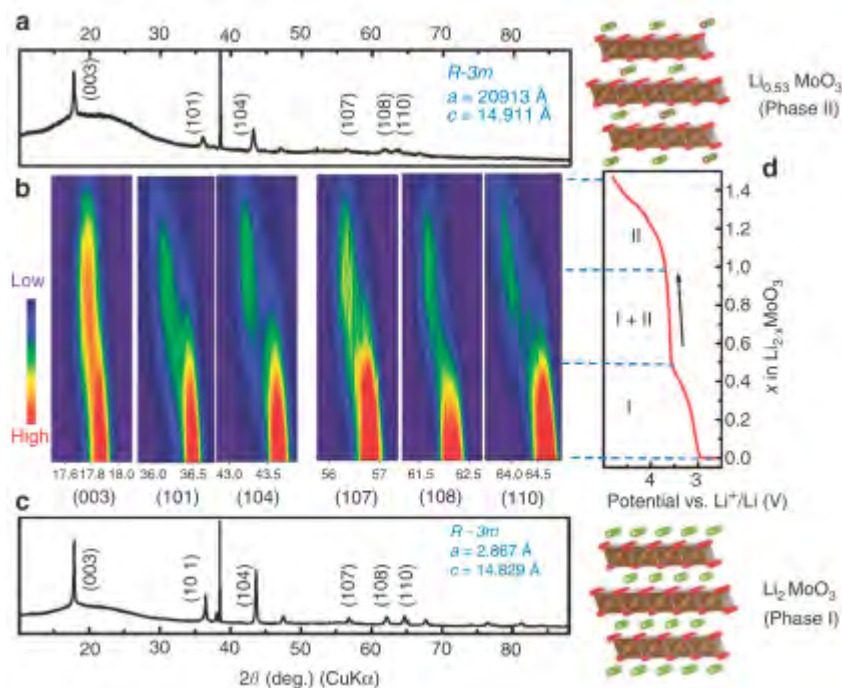


Figure 35: *In situ* X-ray diffraction (XRD) of Li_2MoO_3 during the first charge. (a) The XRD pattern of the Li_2MoO_3 electrode right after charging to 4.8 V. (b) Contour plot of diffraction peak evolution of (003), (101), (104), (107), (108) and (110) during delithiation. (c) The XRD pattern of the Li_2MoO_3 electrode before charge. (d) Charge curve at a current density of 10 mA g^{-1} from open circuit voltage (OCV) to 4.8 V during XRD data collection.

Patents/Publications/Presentations

1. Linjing Zhang, Ning Li, Borong Wu, Hongliang Xu, Lei Wang, Xiao-Qing Yang, and Feng Wu, “Sphere-Shaped Hierarchical Cathode with Enhanced Growth of Nanocrystal Planes for High-Rate and Cycling-Stable Li-Ion Batteries”, *Nano Lett.*, 2015, 15 (1), pp 656–661
2. Enyuan Hu, Seong Min Bak, Sanjaya D. Senanayake, Xiao-Qing Yang, Kyung-Wan Nam, Lulu Zhang, Minhua Shao, “Thermal stability in the blended lithium manganese oxide – Lithium nickel cobalt manganese oxide cathode materials: An *in situ* time-resolved X-Ray diffraction and mass spectroscopy study”, *Journal of Power Sources*, Volume 277, 1 March 2015, Pages 193–197
3. Kai He, Huolin L. Xin, Kejie Zhao, Xiqian Yu, Dennis Nordlund, Tsu-Chien Weng, Jing Li, Yi Jiang, Christopher A. Cadigan, Ryan M. Richards, Marca M. Doeff, Xiao-Qing Yang, Eric A. Stach, Ju Li, Feng Lin, and Dong Su, “Transitions from Near-Surface to Interior Redox upon Lithiation in Conversion Electrode Materials” *Nano Lett.*, 2015, 15 (2), pp 1437–1444
4. Mingxiang Lin, Liubin Ben, Yang Sun, Hao Wang, Zhenzhong Yang, Lin Gu, Xiqian Yu, Xiao-Qing Yang, Haoifei Zhao, Richeng Yu, Michel Armand, and Xuejie Huang, “Insight into the Atomic Structure of High-Voltage Spinel $\text{LiNi}_{0.5}\text{Mn}_{1.5}\text{O}_4$ Cathode Material in the First Cycle”, *Chem. Mater.*, 2015, 27 (1), pp 292–303
5. Xiqian Yu, Yongning Zhou, Enyuan Hu, Seongmin Bak, **Xiao-Qing Yang**, Hung Sui Lee, Jun Ma, Zhaoxiang Wang, Hong Li, Xuejie Huang, Liquan Chen, Kyung-Wan Nam, Yijin Liu, Huilin Pan, Jie Xiao, and Jun Liu “Using Synchrotron Based X-ray Diffraction and Absorption and TXM to Study the New Electrode Materials for Next Generation of Batteries”, presented at the International Battery Association (IBA) and Pacific Power Source Symposium Joint Meeting 2015, January 5, 2015, Hilton Waikoloa Village, Hawaii, USA, as **the IBA2015 Research Award Speech, Invite**

Task 5.4 – NMR and Pulse Field Gradient Studies of SEI and Electrode Structure (Clare Grey, Cambridge University)

PROJECT OBJECTIVE: The formation of a stable surface electrode interphase (SEI) is critical to the long-term performance of a battery, since the continued growth of the SEI on cycling/aging results in capacity fade (due to Li consumption) and reduced rate performance due to increased interfacial resistance. Although arguably a (largely) solved problem with graphitic anodes/lower voltage cathodes, this is not the case for newer, much higher capacity anodes such as silicon, which suffer from large volume expansions on lithiation, and for cathodes operating above 4.3 V. Thus it is essential to identify how to design a stable SEI. The objectives are to identify major SEI components, and their spatial proximity, and how they change with cycling. SEI formation on Si vs. graphite and high voltage cathodes will be contrasted. Li⁺ diffusivity in particles and composite electrodes will be correlated with rate. The SEI study will be complemented by investigations of local structural changes of high voltage/high capacity electrodes on cycling.

PROJECT IMPACT: The first impact of this project will be an improved, molecular based understanding of the surface passivation (SEI) layers that form on electrode materials, which are critical to the operation of the battery. Second, we will provide direct evidence for how additives to the electrolyte modify the SEI. Third, we will provide insight to guide and optimize the design of more stable SEIs on electrodes beyond LiCoO₂/graphite.

OUT-YEAR GOALS: The goals of this project are to identify the major components of the SEI as a function of state of charge and cycle number for different forms of silicon. We will determine how the surface oxide coating affects the SEI structure and establish how the SEI on Si differs from that on graphite and high voltage cathodes. We will determine how the additives that have been shown to improve SEI stability affect the SEI structure and explore the effect of different additives that react directly with exposed fresh silicon surfaces on SEI structure. Via this program, we will develop new NMR-based methods for identifying different components in the SEI and their spatial proximities within the SEI, which will be broadly applicable to the study of SEI formation on a much wider range of electrodes. These studies will be complemented by other studies of electrode bulk and surface structure to develop a fuller model with which to describe how these electrodes function.

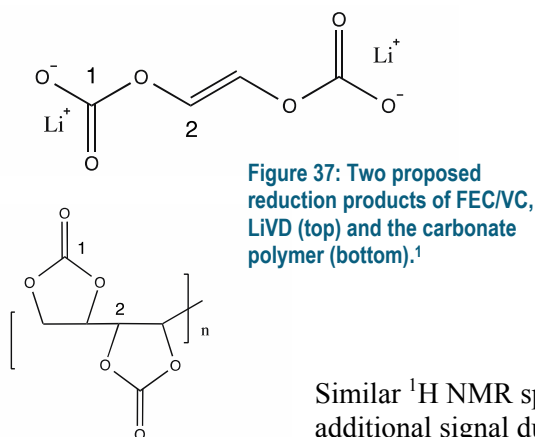
COLLABORATIONS: B. Lucht (Rhode Island); E. McCord, W. Holstein (DuPont); J. Cabana, (UIC); G. Chen, K. Persson (LBNL); S. Whittingham (Binghamton); P. Bruce (St. Andrews), R. Seshadri, A. Van der Ven (UCSB), S. Hoffman, A. Morris (U. Cam), N. Brandon (Imperial), P. Shearing (UCL).

Milestones

Quarter	Milestones/Deliverables Description and Due Date	Go/No-Go Description and Due Date
Q1	Complete initial Si SEI work and submit for publication. Paper under preparation. Complete 4V spinel work (<i>in situ</i> NMR) and submit for publication (12/31/14) Complete; paper under preparation.	
Q2	Identify differences in Si SEI after one and multiple cycles. ¹H NMR complete	
Q3	Identify major organic components on the SEIs formed on high surface area carbons by NMR.	
Q4	Complete initial carbon-SEI interfacial studies	Determine whether NMR has the sensitivity to probe organics on the cathode side in paramagnetic systems.

Progress Report

In a collaborative project with Prof. B. Lucht (U. Rhode Island) we have explored the products formed on reducing the electrolyte additives, fluoroethylene carbonate (FEC) and vinylene carbonate (VC), both additives having been shown to reduce the initial irreversible capacity loss, particularly on silicon anodes. These additives are believed to improve the stability of the solid electrolyte interphase (SEI) by forming a series of organic species, possibly cross-linking with solvent molecules such as ethylene carbonate. As a first step towards characterising the FEC/VC decomposition products in the SEI, we have examined chemically reduced species, formed with the reducing agent lithium naphthalenide, by using multinuclear NMR spectroscopy. ^{19}F NMR spectroscopy of reduced FEC, shows the expected resonance from LiF (Figure 36). No other signals from fluorinated products are seen. By contrast, the ^1H NMR spectra show resonances from ether CH_2O protons and saturated carbons in addition to a higher frequency signal at 6.1 ppm. While it was initially tempting to assign this to an unsaturated product such as lithium vinylene dicarbonate (LiVD) (Figure 37), a spectrum acquired from a sample prepared using the deuterated Li naphthalenide did not contain this resonance, indicating that the signal arises from lithium naphthalenide trapped in the solid reduction product. The ^{13}C NMR spectra of the same compounds confirmed this assignment and no signals that could be assigned to LiVD or any another products containing unsaturated $\text{C}=\text{C}$ double bonds were observed.



Similar ^1H NMR spectra were observed from reduced VC, except that an additional signal due to formate was observed. A number of different signals were observed in the ^{13}C NMR spectra of FEC and VC, which could be assigned to the species such as those expected from the polymer shown in Figure 37, but also to carbonate species including Li_2CO_3 and $(\text{LiOCO}_2\text{CH}_2)_2$.

A comprehensive NMR study of the SEI that forms on silicon following the first cycle has now been completed. Anodes were prepared without any binder (so as to remove the complication of the ^{13}C signal from the binder) and were then cycled using ^{13}C -enriched electrolytes. Assignments of the resulting ^{13}C spectra were performed with the help of two-dimensional NMR studies and by calculating the shifts with DFT methods.

¹Ouatani, El, L.; Dedryvere, R.; Siret, C.; Biensan, P.; Reynaud, S.; Iratçabal, P.; Gonbeau, D. *J. Electrochem. Soc.* **2014**, *156*, A103.

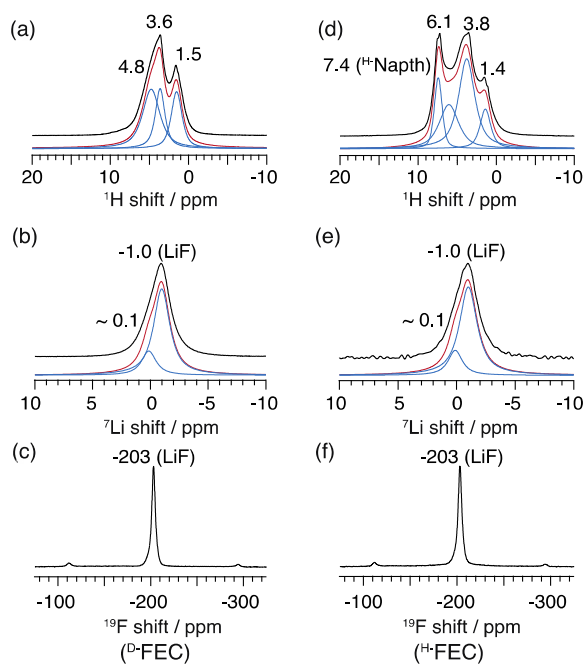


Figure 36: ^1H , ^7Li and ^{19}F MAS NMR spectra of reduced protonated (H-FEC) and deuterated (D-FEC).

Task 5.5 – Optimization of Ion Transport in High-Energy Composite Cathodes (Shirley Meng, UC San Diego)

PROJECT OBJECTIVE: This project aims to probe and control the atomic-level kinetic processes that govern the performance limitations (rate capability and voltage stability) in a class of high energy composite electrodes. A systematic study with powerful suite of analytical tools (including atomic resolution scanning transmission electron microscopy (a-STEM) & Electron energy loss spectroscopy (EELS), X-ray photoelectron spectroscopy (XPS) and first principles (FP) computation) will be used to pin down the mechanism and determine the optimum bulk compositions and surface characteristics for high rate and long life. Moreover, to help the synthesis efforts to produce the materials at large scale with consistently good performance. It is also aimed to extend the suite of surface-sensitive tools to diagnose the silicon anodes types.

PROJECT IMPACT: If successful, this research will provide a major breakthrough in commercial applications of the class of high energy density cathode material for lithium ion batteries. Additionally, it will provide an in-depth understanding of the role of surface modifications and bulk substitution in the high voltage composite materials. The diagnostic tools developed here can also be leveraged to study a wide variety of cathode and anode materials for rechargeable batteries.

APPROACH: Unique approach that combines STEM/EELS, XPS and *Ab initio* computation as quantities diagnostic tools for surface and interface characterization and to enable quick identification of causes of surface instability (or stability) in various types of electrode materials including both high voltage cathodes and low voltage anodes.

OUT-YEAR GOALS: The goal is to control and optimize Li ion transport, TM migration and oxygen activity in the high-energy composite cathodes and to optimize electrode/electrolyte interface in silicon anodes so that their power performance and cycle life can be significantly improved.

COLLABORATIONS:

- Michael Sailor (UCSD) – porous silicon and carbonization of silicon based anodes.
- Keith Stevenson (UT Austin) – XPS and TOF-SIMS
- Nancy Dudney and Juchuan Li (Oak Ridge National Lab) – silicon thin film fabrication
- Chunmei Ban (National Renewable Energy Laboratory – Molecular Layer Deposition

Milestones

1. Identify ways to extend the STEM/EELS and XPS techniques for anode materials, such as silicon anode. (09/30/14) **On Track (STEM/EELS operational in Jan 2015)**
2. Identify at least two high voltage cathode materials that deliver 200mAh/g reversible capacity when charged to high voltages (12/31/14) **Complete**
3. Obtain the optimum surface coating and substitution compositions in lithium rich layered oxides when charged up to 4.8V (or 5.0 V) (3/31/15) **Complete**
4. Identify the appropriate SEI characteristics and microstructure for improving first cycle irreversible capacity of silicon anode. (Improve to 85-95%) (6/30/15) **On Track**
5. Identify the mechanisms of ALD and MLD coated silicon anode for their improved chemical stability upon long cycling. (9/30/15) **On Track**

Progress Report

Investigate the effects of substitution on oxygen vacancy formation energy in Li-excess material

First principles computation was applied to investigate the effects of cations substitution on the oxygen vacancy formation energy in high energy density $0.5\text{Li}_{4/3}\text{Mn}_{2/3}\text{O}_2\cdot 0.5\text{LiNi}_{1/2}\text{Mn}_{1/2}\text{O}_2$ cathode material. Figure 38(a) shows the cation ordering in the transition metal layer: Li ions (in red color), Mn ions (in green color), and Ni ions (in blue color), there are two different Li sites; one is surrounded by six Mn-ions, the other is surrounded by five Mn ions and one Ni-ion. Since Ni-ions contribute to the reversible capacity, we substitute one of Mn-ions with different cations. From our previous study, as Li is extracted from the structure, the oxygen vacancy formation energy decreased drastically. Figure 38(b) shows the oxygen vacancy formation energy as a function of different substitution elements. It can be seen that elements #9 and #10 enhanced the oxygen stability in the lattice.

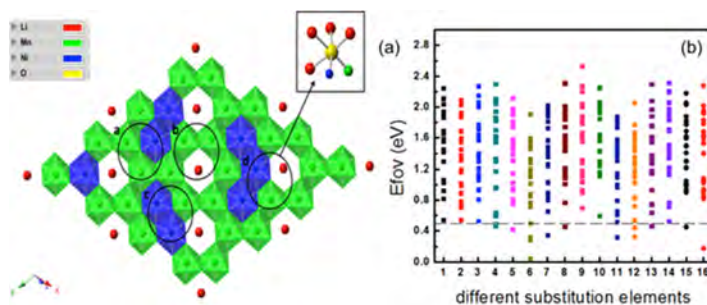


Figure 38: (a) cation ordering in transition metal layer: $0.5\text{Li}_{4/3}\text{Mn}_{2/3}\text{O}_2\cdot 0.5\text{LiNi}_{1/2}\text{Mn}_{1/2}\text{O}_2$. (b) oxygen vacancy formation energy of $\text{Li}_{8/12}\text{Ni}_{3/12}\text{Mn}_{6/12}\text{M}_{1/12}\text{O}_2$ at different configurations. #1 is the model without substitution.

Effect of FEC additive on the electrochemistry and surface chemistry on a-Si thin film electrodes

Applying previously developed anoxic and anhydrous analytical characterization techniques such as XPS and TOF-SIMS, one can understand how inclusion of FEC in the electrolyte affects SEI structure and evolution. We attempt to reconcile these differing accounts of the reduction mechanism of FEC of silicon electrodes. As previously demonstrated, XPS has shown the fast production of LiF during the first lithiation when cycling with the FEC-containing electrolyte (45:45:10 (wt%) EC:DEC:FEC) versus with the traditional electrolyte (1:1 (wt%) ethylene carbonate (EC):diethylene carbonate (DEC)). Figure 39 presents the DC-sputtered silicon electrodes in the same two electrolyte mixtures that underwent the following TOF-SIMS analysis: (1) a single lithiation event; (2) one complete lithiation and delithiation cycle and; (3) 100 cycles. With the TOF-SIMS depth profiling shows subtle changes in the chemical composition and structure between the SEI resulting from the two electrolytes (Figure 39). After the

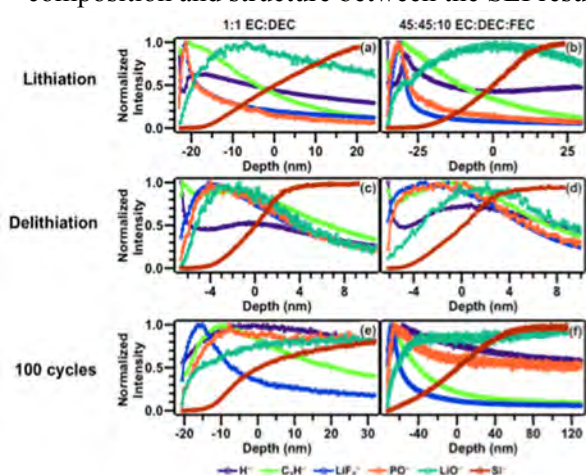


Figure 39: A relative composition of the 10nm outer SEI after 100 cycles. The layer is adjacent to and in contact with the electrolyte 1:1 EC:DEC and 45:45:10 EC:DEC:FEC when cycled.

initial lithiation, the electrode cycled in FEC containing electrolyte had a thicker SEI compared to the SEI produced by the traditional electrolyte. The LiF signal (LiF_2^-) in the FEC containing electrolyte was greater than in the SEI from traditional electrolyte, which correlated well with the XPS results. After 100 cycles, the LiF layer increased thicker for the electrode cycled in the FEC containing electrolyte compared to that for the electrode cycled in the traditional electrolyte. These results indicate that rather than producing a new subset of fluorocarbon/organic species proposed in the literature, FEC undergoes a ring opening reduction mechanism. The subtle chemical changes throughout electrochemical cycling in both electrolytes are expressed in the TOF-SIMS measurement of lithium fluoride / inorganic species (Figure 39).

Patents/Publications/Presentations

1. T. A. Yersak, J. Shin, Z. Wang, D. Estrada, J. Whiteley, S-H Lee, M. J. Sailor, and Y. S. Meng, “Preparation of Mesoporous Si@PAN Electrodes for Li-Ion Batteries via the *In situ* Polymerization of PAN”, ECS Electrochemistry Letters, 2015, 4 (3), A33
2. K.J. Shroder, J. Alvarado, T.A Yersak, J. Li, N. Dudney, L. Webb, Y.S Meng, K.J Stevenson “The Effect of Fluoroethylene Carbonate as an Additive on the Solid Electrolyte Interphase on Silicon Lithium-ion Electrodes” **Submitted**

Task 5.6 – Analysis of Film Formation Chemistry on Silicon Anodes by Advanced *In situ* and *Operando* Vibrational Spectroscopy (Gabor Somorjai, UC Berkeley and Phil Ross, Lawrence Berkeley National Laboratory)

PROJECT OBJECTIVE: Understand the composition, structure, and formation/degradation mechanisms of the solid electrolyte interface (SEI) on the surfaces of Si anodes during charge/discharge cycles by applying advanced *in situ* vibrational spectroscopies. Determine how the properties of the SEI contribute to failure of Si anodes in Li-ion batteries in vehicular applications. Use this understanding to develop electrolyte additives and/or surface modification methods to improve Si anode capacity loss and cycling behavior.

PROJECT IMPACT: A high capacity alternative to graphitic carbon anodes is Si, which stores 3.75 Li per Si versus 1 Li per 6 C yielding a theoretical capacity of 4,008 mAh/g versus 372 mAh/g for C. But Si anodes suffer from large first cycle irreversible capacity loss and continued parasitic capacity loss upon cycling leading to battery failure. Electrolyte additives and/or surface modification developed from new understanding of failure modes will be applied to reduce irreversible capacity loss, improve long term stability and cyclability of Si anodes for vehicular applications.

APPROACH: Model Si anode materials including single crystals, e-beam deposited polycrystalline films, and nanostructures are studied using baseline electrolyte and promising electrolyte variations. A combination of *in situ* and *operando* Fourier Transform Infrared (FTIR), Sum Frequency Generation (SFG), and UV-Raman vibrational spectroscopies are used to directly monitor the composition and structure of electrolyte reduction compounds formed on the Si anodes. Pre-natal and post-mortem chemical composition is identified using X-ray photoelectron spectroscopy. The Si films and nanostructures are imaged using scanning electron microscopies.

OUT-YEAR GOALS: Extend the study of interfacial processes with advanced vibrational spectroscopies to high voltage oxide cathode materials. The particular oxide to study will be chosen based on materials of interest at that time and availability of the material in a form suitable for these studies, e.g. sufficiently large crystals or sufficiently smooth/reflective thin films. The effect of electrolyte composition, electrolyte additives, and surface coatings will be determined and new strategies for improving cycle life developed.

COLLABORATIONS: Chunmei Ban (NREL): Functionalization of Si by Atomic Layer Deposition (ALD): Effect of functionalization on electrolyte reduction

Gao Liu (LBNL): Surface electrochemistry of electrolyte additives on model Si electrodes

Milestones

1. Develop method to attach Si nanostructures to the electrode substrate used in our spectroelectrochemical cell (Sep-14) **Completed**
2. Determine the oxidation and reduction potentials and products of at least one electrolyte additive provided by Gao Liu's group. (Mar-14) **Completed**
3. Determine role of the Si nanostructure on the SEI formation structure and properties (Sep-14) **Completed**
4. Go/No-Go: Feasibility of surface functionalization to improve SEI structure and properties. Criteria: Functionalize a model Si anode surface and determine how SEI formation is changed. (Sep-15) **On schedule**

Progress Report

In Q2, an *in situ* ATR-FTIR cell was used to analyze the chemistry of the electrolyte reduction at the surface of a p-type Si (100) single crystal electrode (Boron-doped). This design minimized the absorption from the bulk electrolyte and enabled us to analyze near-surface regions precisely. This cell was applied to compare the reduction chemistry on Si surface, with that on Au and Sn surfaces obtained earlier by thin-layer electrochemical ATR-FTIR spectroscopy. Synthesized reference compound spectra, which has been proven very helpful in identification of reaction products in previous study, were also utilized in this work.

Figure 40 shows the first negative scan segment and corresponding *in situ* FTIR spectra from the near surface region. By comparing with the spectrum of synthesized compound, three strong peaks observed above the electrolyte features were attributed to diethyl 2,5 dioxohexane dicarboxylate (DEDOHC). The amount of DEDOHC was time-potential-depth dependent. It has been suggested in our recent publication that the formation of DEDOHC is originated from DEC reacting with oxygen species on the Sn. In comparison with noble electrode materials, e.g., Au, this reaction may be catalyzed by the oxide functional groups found on Si or Sn electrodes. Thus, the electrolyte decomposition exhibits clear surface dependence, which has important implications for silicon electrode modification and electrolyte recipe selection.

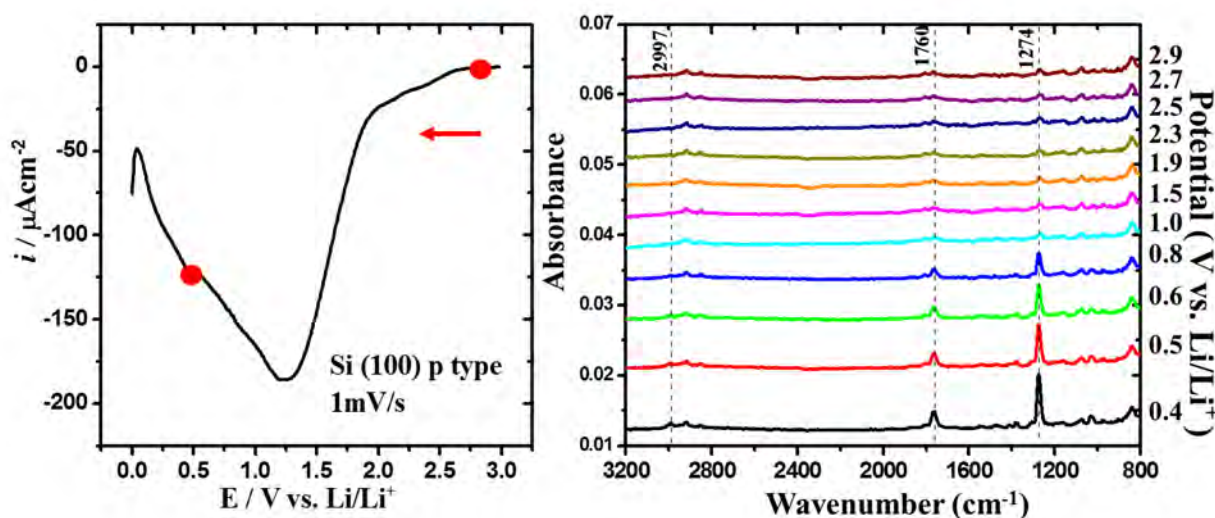


Figure 40: First negative scan segment and *in situ* ATR-FTIR spectra of Si electrode obtained after applying a potential from open circuit potential (OCP) to 0.4 V. *In situ* CV scan speed is 1mV/s, ATR-FTIR incident angle is 60 degree, electrolyte is EC/DEC/LiPF₆ (1:2 v/v)

Patents/Publications/Presentations

1. Feifei Shi, Philip N. Ross, Hui Zhao, Gao Liu, Gabor A. Somorjai, and Kyriakos Komvopoulos “A Catalytic Path for Electrolyte Reduction in Lithium-ion Cells Revealed by *in situ* Attenuated Total Reflection-Fourier Transform Infrared Spectroscopy”, J. Am. Chem. Soc. 2015, 137, 3181–3184

Task 5.7 – Microscopy Investigation on the Fading Mechanism of Electrode Materials (Chongmin Wang, Pacific Northwest National Laboratory)

PROJECT OBJECTIVE: The objective of this work is to use *ex situ*, *in situ* and *operando* high-resolution transmission electron microscopy (TEM) and spectroscopy to probe the fading mechanism of electrode materials. The focus of the work will be on using *in situ* TEM under real battery operating conditions to probe the structural evolution of electrodes and interfaces between the electrode and electrolyte and correlate this structural and chemical evolution with battery performance. The following three questions will be addressed:

- How do the structure and chemistry of electrode materials evolve at a dimension ranging from atomic-scale to meso-scale during the charge and discharge cycles?
- What is the correlation of the structural and chemical change to the fading and failure of lithium (Li)-ion batteries?
- How does the interface evolve between the electrode and the electrolyte and their dependence on the chemistry of electrolytes?

PROJECT IMPACT: Most previous microscopic investigations on solid-electrolyte interphase (SEI) layer formation and morphology evolution on electrodes are either *ex situ* studies or used low-vapor-pressure electrolytes so they cannot reveal the details of the dynamic information under practical conditions. We have developed new *operando* characterization tools to characterize SEI formation and electrode/ electrolyte interaction using practical electrolyte that are critical for making new breakthroughs in this field. The success of this work will increase the energy density of Li-ion batteries and accelerate market acceptance of electrical vehicles (EV), especially for plug-in hybrid electrical vehicles (PHEV) required by the *EV Everywhere* Grand Challenge proposed by DOE/EERE.

APPROACH: Extend and enhance the unique *ex situ* and *in situ* TEM methods for probing the structure of Li-ion batteries, especially for developing a biasing liquid electrochemical cell that uses a real electrolyte in a nano-battery configuration. Use various microscopic techniques, including *ex situ*, *in situ*, and especially the *operando* TEM system, to study the fading mechanism of electrode materials in batteries. This project will be closely integrated with other research and development efforts on high-capacity cathode and anode projects in the BMR Program to 1) discover the origins of voltage and capacity fading in high-capacity layered cathodes and 2) provide guidance for overcoming barriers to long cycle stability of silicon (Si)-based anode materials.

OUT-YEAR-GOALS:

- Extended the *in situ* TEM capability for energy storage technology beyond Li ions, such as Li-S, Li-air, Li-metal, sodium ions, and multi-valence ions
- Multi-scale (i.e., ranging from atomic scale to meso-scale) *in situ* TEM investigation of failure mechanisms for energy-storage materials and devices (both cathode and anode)
- Integration of the *in situ* TEM capability with other microscopy and spectroscopy methods to study energy-storage materials, such as *in situ* SEM, *in situ* SIMS, and *in situ* x-ray diffraction
- Atomic-level *in situ* TEM and scanning transmission electron microscopy (STEM) imaging to help develop a fundamental understanding of electrochemical energy-storage processes and kinetics of both cathodes and anode

COLLABORATIONS: Currently, we are collaborating with the following PIs:

Dr. Chunmei Ban (NREL); Dr. Gao Liu (LBNL); Dr. Khalil Amine (ANL); Professor Yi Cui (Stanford); Dr. Jason Zhang (PNNL); Dr. Jun Liu (PNNL); Dr. Guoying Chen (LBNL). Dr. Xingcheng Xiao (GM).

Milestones

1. Establish the methodology that enables reliably positioning of a nanowire on the chip to assembly the closed liquid cell. Complete the *in situ* TEM study of the behavior of native oxide layer during lithiation and delithiation (12/31/2014). **Completed.**
2. Complete quantitative measurement of coating layer and SEI layer thickness as a function of cycle number on a Si anode in a liquid cell with a practical electrolyte (03/31/2015). **Completed**
3. Complete the *operando* TEM study of cathode materials with/without coating layer and the SEI layer formation (9/30/2015). **Ongoing.**

Progress Report

It was known that nanostructured Si coated with carbon or other functional materials can lead to significantly improved cyclability. However, the underlying mechanism and comparative performance of different coatings remain poorly understood. Using *in situ* transmission electron microscopy (TEM) through a nanoscale half-cell battery, in combination with chemo-mechanical simulation, the effect of thin (~ 5 nm) alucone and Al_2O_3 coatings on the lithiation kinetics of Si nanowires (SiNWs) was investigated. It was observed that the alucone coating leads to a “V-shaped” lithiation front of the SiNWs, while the Al_2O_3 coating yields an “H-shaped” lithiation front. These observations indicate that the difference between the Li surface diffusivity and bulk diffusivity of the coatings dictates lithiation induced morphological evolution in the nanowires. The experiments also indicate that the reaction rate in the coating layer can be the limiting step for lithiation and therefore critically influences the rate performance of the battery (Figure 41).

It should be pointed out that the electrode/electrolyte interface in the current open-cell configuration is different from that in real battery. For the case of a real battery, the Si NWs are fully immersed in the liquid electrolyte, forming a conformal coating and therefore Li ion can diffuse in from all directions. Therefore, the “V-shape” lithiation profile observed for alucone coated Si NWs may be absent in real battery. For the *in situ* open-cell, the Li source is in contact with one end of the Si NW, which appears to be distinctively

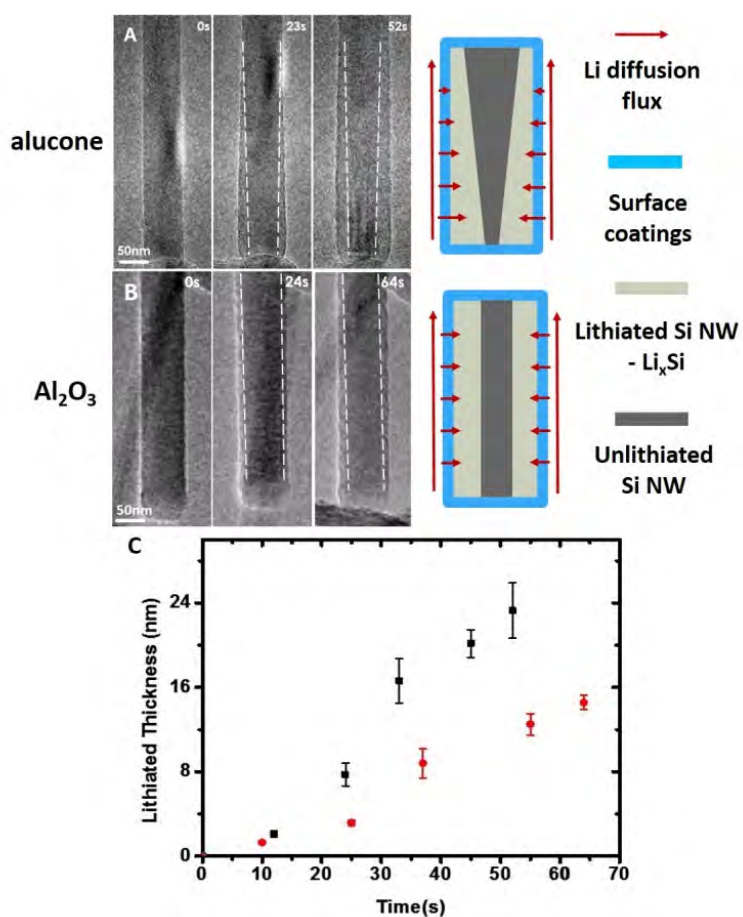


Figure 41: A) and B) Time-resolved TEM images show the development of lithiation profiles of the alucone and Al_2O_3 coated SiNWs and schematics of the Li diffusion paths through the SiNWs that dictate the lithiation behavior; C) Average lithiation thickness vs. time for the alucone (black square) and Al_2O_3 (red dot) coated SiNWs.

different from the real situation, but it is just this open-cell configuration that uniquely offers the opportunity of probing the effect of the coating layer on Li ion diffusion. Therefore, the intrinsic structural change (core-shell mode) and the effect of coatings on the lithiation kinetics of Si NWs are well presented for real battery.

Further, the failure mechanism of the Al_2O_3 coated SiNWs was also explored. The studies shed light on the design of high capacity, high rate and long cycle life Li-ion batteries. The asymmetric lithiation kinetics in the Al_2O_3 coated SiNWs results in asymmetric pulverization of the SiNW. The surface coating effect on the lithiation behavior of SiNWs revealed here provides insights on the surface structural and chemical modifications of Si nanostructured anodes for enhanced battery performance.

Patents/Publications/Presentations

1. Pengfei Yan, Liang Xiao, Jianming Zheng, Yungang Zhou, Yang He, Xiaotao Zu, Scott X. Mao, Jie Xiao, Fei Gao, Ji-Guang Zhang, and Chong-Min Wang, “Probing the Degradation Mechanism of Li_2MnO_3 Cathode for Li-Ion Batteries”, *Chem. Mater.* 2015, 27, 975–982.
2. Ping Lu, Pengfei Yan, Eric Romero, Erik David Spoerke, Ji-Guang Zhang, and Chong-Min Wang, “Observation of Electron-Beam-Induced Phase Evolution Mimicking the Effect of the Charge–Discharge Cycle in Li-Rich Layered Cathode Materials Used for Li Ion Batteries”, *Chem. Mater.* 2015, 27, 1375–1380.
3. Pengfei Yan, Jiguang Zhang, Chongmin Wang, “Direct correlation of electrochemical properties with structural and chemical evolution of electrode materials in rechargeable batteries”, Presented at ACS 2015 Spring Meeting, Denver, April, 2015.

Task 5.8 – Energy Storage Materials Research using DOE’s User Facilities and Beyond (Michael M. Thackeray and Jason R. Croy, Argonne National Laboratory)

PROJECT OBJECTIVE: The primary objective of this project is to explore the fundamental, atomic-scale processes that are most relevant to the challenges of next-generation, energy-storage technologies. A deeper understanding of these systems will rely on novel and challenging experiments that are only possible through unique facilities and resources. The goal of this project is to capitalize on a broad range of facilities to advance the field through cutting-edge science, collaborations, and multi-disciplinary efforts.

PROJECT IMPACT: This project is being implemented to capitalize on and exploit DOE’s user facilities and other accessible national and international facilities (including skilled/trained personnel) in order to produce knowledge to advance energy-storage technologies. Specifically, furthering the understanding of structure-electrochemical property relationships and degradation mechanisms will contribute significantly to meeting the near- to long-term goals of EV and PHEV battery technologies.

APPROACH: A wide array of unique capabilities including X-ray and neutron diffraction, X-ray absorption, emission and scattering, high resolution transmission electron microscopy, Raman spectroscopy, and theory will be brought together to focus on challenging experimental problems. Combined, these resources promise an unparalleled look into the structural, electrochemical and chemical mechanisms at play in novel, complex electrode/electrolyte systems being explored at Argonne National Laboratory.

OUT-YEAR-GOALS:

- Gain new, fundamental insights into complex structures and degradation mechanisms of composite cathode materials from novel, probing experiments carried out at user facilities and beyond.
- Investigate structure-property relationships that will provide insight into the design of improved cathode materials.
- Use the knowledge and understanding gained from this project to develop and scale up advanced cathode materials in practical lithium-ion prototype cells,

COLLABORATORS: Jason R. Croy, Mahalingam Balasubramanian, Joong Sun Park, Brandon R. Long, Bill David, Thomas Wood, Vinayak Dravid, HackSung Kim

Milestones

1. Evaluation of lithium-ion battery electrodes using DOE’s User Facilities at Argonne (APS, EMC and ALCF) and facilities elsewhere, e.g., neutron spallation sources at SNS (Oak Ridge). Other facilities include the neutron facility ISIS, Rutherford Laboratory (UK) and the NUANCE characterization center (Northwestern University). (Sep-15). **In progress.**
2. Evaluation of Li_2MnO_3 end member and composite $\text{Li}_2\text{MnO}_3 \bullet (1-x)\text{LiMO}_2$ ($M = \text{Mn, Ni, Co}$) structures by combined neutron/X-ray diffraction. (Sep-15). **In progress.**
3. Evaluation of transition metal migration in lithium-metal-oxide insertion electrodes. (Sep-15). **In progress.**
4. Analysis, interpretation, and dissemination of collected data for publication and presentation. (Sep-15). **In progress.**

Progress Report

Complex, integrated ‘layered-layered-spinel’ $y[x\text{Li}_2\text{MnO}_3 \cdot (1-x)\text{LiMO}_2] \cdot (1-y)\text{LiM}_2\text{O}_4$ ($M=\text{Mn, Ni, Co}$) structures have shown promise as high performance lithium-ion cathodes. In order to better understand the properties and, therefore, the design of such structures, a comprehensive study of end-member and ‘composite’ materials is being undertaken. An important component of these structures is the end-member Li_2MnO_3 . Capable of providing capacity and stability, integration of Li_2MnO_3 -like domains plays a key role in the electrochemical performance of these electrodes; understanding the complexity of Li_2MnO_3 -integrated structures and, in particular, the atomic arrangement of the transition metal ions within these structures is of critical importance. One difficulty in modeling these structures results from stacking fault disorder that can occur along the c-axis of the monoclinic ($C2/m$) structure in either pure or integrated Li_2MnO_3 materials. This report focuses on recent structural refinements of Li_2MnO_3 conducted in collaboration with Professor Bill David and Dr. Thomas Wood at the Rutherford Laboratory/Oxford University, UK.

Figure 42(b) shows a zoomed image of the “superstructure” peaks (red=calculated from standard Rietveld analysis, black=HRXRD data) that appear in Li_2MnO_3 as a result of LiMn_6 ordering throughout the mixed Li/Mn planes. The diffuse background, above the model curve, is a result of faulted stacking along the c-axis. Figure 42(a) shows the case of ideal $C2/m$ stacking where the variations in this stacking, which are responsible for the diffuse background, must be accurately modeled to describe real materials. It is clear from Figure 42(b) that standard methods do not describe the faulted stacking. Figure 42(c) shows the results of a DIFFaX model where the background and the superstructure peaks have been fitted (brown=model, blue=HRXRD data). (Note: DIFFaX is software that calculates diffraction intensities expected from crystals containing planar defects such as stacking faults. The program uses a recursion algorithm by exploiting the recurring patterns found in randomized stacking sequences. This calculates the average interference function from each layer type, which in turn leads to smooth calculated diffraction patterns.) As shown in Figure 42(c), the diffuse background and peak intensities above the background are described well by the DIFFaX model. An important implication of these results is the possibility of modeling “domain” geometries within composite structures and relating that information to electrochemical performance. For example, the current model indicates that ~25% of the layers within the sample have pure $C2/m$ stacking (Figure 42(a)). Studies are currently underway to apply the same methodology to model more complex composite electrode structures, the results of which will be described in a future report.

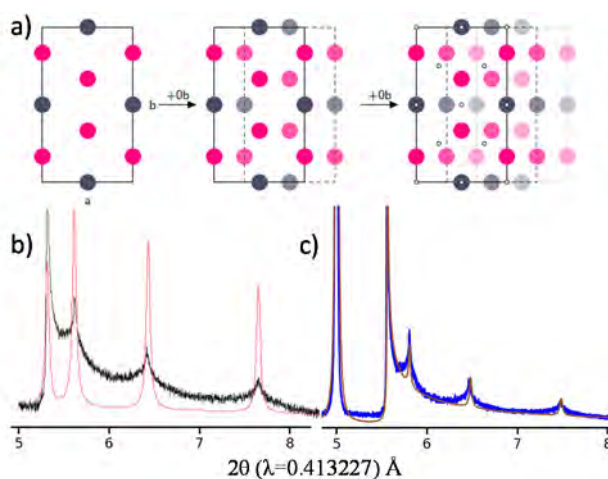


Figure 42: (a) Model of pure $C2/m$ stacking in Li_2MnO_3 (grey=Li, pink=Mn). (b) HRXRD data of Li_2MnO_3 made at 850°C (black) along with standard Rietveld analysis (red). (c) HRXRD data of the 850°C Li_2MnO_3 (blue) and the DIFFaX model including stacking faults (brown).

Patents/Publications/Presentations

1. M. M. Thackeray, B. R. Long, J. R. Croy, J. S. Park, Y. Shin, G. Krumdick, J. G. Wen and D. Miller, *Progress and Challenges in Designing High Capacity Cathodes for Lithium-Ion Cells*, 32nd Annual Battery Seminar & Exhibit, Fort Lauderdale, Florida, 9-12 March 2015 (Invited).

TASK 6 – MODELING ADVANCED ELECTRODE MATERIALS

Summary and Highlights

Achieving the performance, life, and cost targets outlined in the *EV Everywhere* Grand Challenge will require moving to next generation chemistries, such as higher capacity Li-ion intercalation cathodes, silicon and other alloy-based anodes, lithium metal anodes, sulfur cathodes, and Na-ion systems. However, numerous problems plague the development of these systems, from material level challenges in ensuring reversibility to electrode level issues in accommodating volume changes, to cell-level challenges in preventing cross talk between the electrodes. In this task, a mathematical perspective is applied to these challenges in order to provide an understanding of the underlying phenomenon and to suggest solutions that can be implemented by the material synthesis and electrode architecture groups.

The effort spans multiple length scales from *ab initio* methods to continuum-scale techniques. Models are combined with experiments and extensive collaborations are established with experimental groups to ensure that the predictions match reality. Efforts are also focused on obtaining the parameters needed for the models either from lower length scale methods or from experiments. Projects also emphasize pushing the boundaries of the modeling techniques used to ensure that the task stays at the cutting edge.

In the area of intercalation cathodes, the effort is focused on understanding the working principles of the high Ni layered materials with the aim of understanding structural changes and associated changes in transport properties. In addition, focus is paid to the assembling of porous electrodes with particles to predict the conduction behavior and developing tools to measure electronic conduction. The dynamic particle packing model shows remarkable agreements with experiments on predicting the structure of the electrode.

In the area of silicon anodes, the effort is in trying to understand the interfacial instability and to suggest ways to improve the cycleability of the system. In addition, effort is focused on designing artificial SEI layers that can accommodate the volume change, and in understanding the ideal properties for a binder to accommodate the volume change without delamination. The reactivity of alucone coatings has been understood using these models, whereby the film was seen to become conductive as lithium occupies sites in the coating. In addition, the mechanical effects of core-shell silicon anodes have been studied and a critical shell thickness identified.

In the area of sulfur cathodes, the focus is on developing better models for the chemistry with the aim of describing the precipitation reactions accurately. Efforts are focused on performing the necessary experiments to obtain a physical picture of the phase transformations in the system and in measuring the relevant thermodynamic, transport, and kinetic properties. In addition, changes in the morphology of the electrode are described and tested experimentally. Cells that incorporate a single ion conducting ceramic with small electrolyte volume have been fabricated and tested in the lab.

Calculations are also performed that look at understanding the nature of Na insertion into lattices with the aim of identifying new materials for this class of batteries.

Finally, microstructure models are an area of focus to ensure that the predictions move away from average techniques to more sophisticated descriptions of processes inside electrodes. Efforts are focused on understanding conduction within the electrode and also on simulating the full electrode that describe the intricate physics inside the battery electrode. These efforts are combined with tomography information as input into the models.

Task 6.1 – Electrode Materials Design and Failure Prediction (Venkat Srinivasan, Lawrence Berkeley National Laboratory)

PROJECT OBJECTIVE: The goal of this project is to use continuum-level mathematical models along with controlled experiments on model cells to (i) understand the performance and failure models associated with next-generation battery materials, and (ii) design battery materials and electrodes to alleviate these challenges. The focus of the research will be on the Li-S battery chemistry and on microscale modeling of electrodes. The initial work on the Li-S system will be on developing a mathematical model for the chemistry along with obtaining the necessary experimental data, using a single ion conductor (SIC) as a protective layer to prevent polysulfide migration to the Li anode. The initial work on microscale modeling will use the well-understood $\text{Li}(\text{NiMnCo})_{1/3}\text{O}_2$ (NMC) electrode to establish a baseline for modeling next-generation electrodes.

PROJECT IMPACT: Li-S cells promise to increase the energy density and decrease the cost of batteries compared to the state-of-the-art. If the performance and cycling challenges can be alleviated, these systems hold the promise for meeting the EV-Everywhere targets.

OUT-YEAR-GOALS: At the end of this project, a mathematical model will be developed that can address the power and cycling performance of next-generation battery systems. The present focus is on microscale modeling of electrodes and Li-S cells, although the project will adapt to newer systems, if appropriate. The models will serve as a guide for better design of materials, such as in the kinetics and solubility needed to decrease the morphological changes in sulfur cells and increase the power performance.

COLLABORATIONS: None this quarter.

Milestones

1. Develop a model of a Li-S cell incorporating concentration solution framework (Due on 12/31/14). **Status: Complete**
2. Develop a custom Li-S electrochemical cell with small ($\sim 200\ \mu\text{m}$) catholyte layer incorporating a SIC. (Due on 3/31/15) Stop custom cell development if unable to prevent SIC damage during cell assembly. **Status: Go**
3. Use custom cell to perform rate experiments (Due on 6/30/15). If unsuccessful in developing custom cell, develop cell without SIC and measure shuttle current. **Status: In progress**
4. Compare microscale and macroscale simulation results and experimental data to determine the importance of microstructural detail (Due on 9/30/15). **Status: In progress**

Progress Report

Custom Li-S cell with small catholyte layer: An electrochemical cell was fabricated according to the novel Li-S cell design developed in Q1. In the design, the single-ion conductor (SIC) is intended to be permanently mounted within the cell with epoxy. However, as the SIC is not inexpensive and the cell performance was not yet known to be satisfactory, trial electrochemical tests were run using the cell without including the SIC. Figure 43 shows cycling data for one of these tests, involving a lithium metal anode, a cathode consisting of elemental sulfur, poly(3,4-ethylenedioxythiophene) (PEDOT), and conductive additive on an aluminum foil current collector, and an electrolyte solution consisting of 1M bis(trifluoromethane) sulfonimide lithium (LiTFSI) in 1:1 dioxolane (DOL) / dimethoxyethane (DME) with 1% LiNO₃. These tests showed a large ohmic drop, although preliminary tests with a graphite electrode have suggested that this is not a consequence of the cell design. Experience with this assembling this cell prototype suggested slight design modifications to further reduce electrolyte solution volumes, and a second cell was fabricated based on the modified design. Assembling the revised cell with a SIC left the fragile SIC intact. The catholyte layer is guaranteed to be thinner (and likely significantly thinner) than 140 μm , smaller than the 200 μm target. These achievements complete the Q2 milestone, making the decision to use the new custom cell to perform rate experiments in Q3 a “go.”

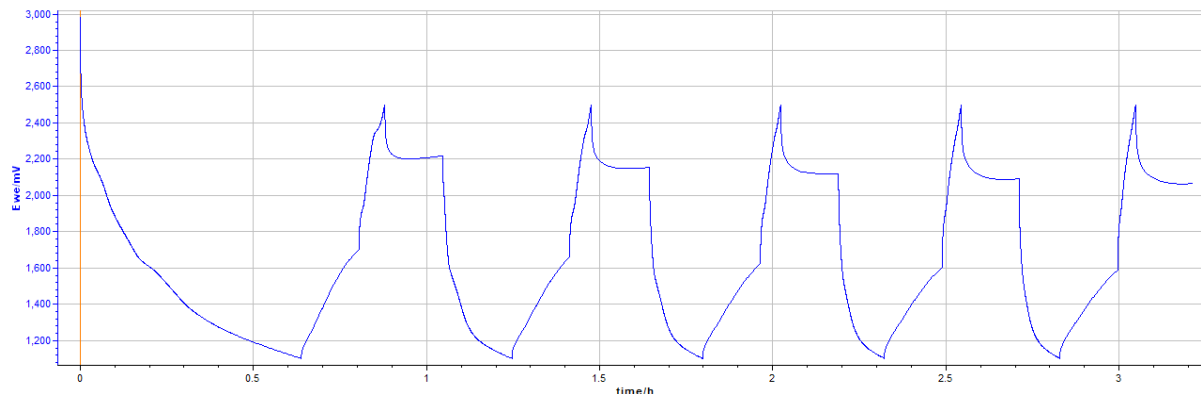


Figure 43: Trial cycling data from Li-S cell.

Microscale simulation: Progress toward the Q4 milestone has continued. The workflow for obtaining X-ray tomography images of NMC porous electrodes (generated at the Advanced Light Source at LBNL) and processing the data into simulation domains has been refined further to provide higher image quality and faster and more reliable surface mesh repairs.

Q2 Patents/Publications/Presentations

Publication

1. K. Higa and V. Srinivasan, “Stress and Strain in Silicon Electrode Models”, *Journal of the Electrochemical Society*, **162**, 6, A1111 (2015)

Task 6.2 – Predicting and Understanding Novel Electrode Materials from First-Principles (Kristin Persson, Lawrence Berkeley National Laboratory)

PROJECT OBJECTIVE: The aim of the Project is model and predict novel electrode materials from first-principles focusing on 1) understanding the atomistic interactions behind the behavior and performance of the high-capacity lithium excess and related composite cathode materials and 2) predict new materials using the recently developed Materials Project high-throughput computational capabilities at LBNL. More materials and new capabilities will be added to the Materials Project Lithium Battery Explorer App (www.materialsproject.org/apps/battery_explorer/).

PROJECT IMPACT: The project will result in a fundamental-level understanding of the atomistic mechanisms underlying the behavior and performance of the Li-excess as well as related composite cathode materials. The models of the composite materials will result in prediction of voltage profiles and structural stability – the ultimate goal being to suggest improvements based on the fundamental understanding that will increase the life and safety of these materials. The Materials Project aspect of the work will result in improved data and electrode properties being calculated to aid predictions of new materials for target chemistries relevant for ongoing BMR experimental research.

OUT-YEAR GOALS: During year 1-2, the bulk phase diagram will be established – including bulk defect phases in layered Li_2MnO_3 , layered LiMO_2 ($M = \text{Co}, \text{Ni}, \text{and Mn}$) and LiMn_2O_4 spinel to map out the stable defect intermediate phases as a function of possible transition metal rearrangements. Modeling of defect materials (mainly Li_2MnO_3) under stress/strain will be undertaken to simulate effect of composite nano-domains. The composite voltage profiles as function of structural change and Li content will be obtained. In year 2-4, the project will focus on obtaining Li activation barriers for the most favorable TM migration paths as a function of Li content as well as electronic DOS as a function of Li content for the most stable defect structures identified in year 1-2. Furthermore, stable crystal facets of the layered and spinel phases will be explored, as a function of O_2 release from surface and oxygen chemical potential. Within the Materials Project, hundreds of novel Li intercalation materials will be calculated and made available.

COLLABORATIONS: Gerbrand Ceder (MIT), Clare Grey (U Cambridge, UK). Mike Thackarey (ANL), Guoying Chen (LBNL).

Milestones

1. Mn mobilities as a function of Li content in layered Li_xMnO_3 and related defect spinel and layered phases (3/31/15) **Done**
2. Surface facets calculated and validated for Li_2MnO_3 (3/31/15) **Delayed**
3. Calculate stable crystal facets. Determine whether facet stabilization is possible through morphology tuning. (6/30/15) **Delayed**
4. Go/No-Go: Stop this approach if facet stabilization can not be achieved. (6/30/15)
5. Li mobilities as a function of Li content in layered Li_xMnO_3 and related defect spinel and layered phases (9/30/15) **Ongoing**

Progress Report

The project has experienced some delay due to change in staffing as of August 2014. A new post-doc was hired in November and arrived early 2015.

To meet our goals for 2015, we have continued to perform first-principle calculation to understanding Li diffusion mechanisms – particularly related to the Li content, and the impact of Mn migration into the Li layer. Our computations verify that the layered Li_xMnO_3 structure is unstable when 50% of Li-ion removed ($x < 1.0$). Moreover, we have calculated all possible configurations for a given Li-concentration assuming a coherent interface between delithiated and lithiated structures as well as fully relaxed structures. For low Li-ion distributions ($x < 1.25$) the most stable structures show significant difference in terms of structural distortions and volume changes corresponding to different Li orderings. On the other hand, at high Li-concentration ($x > 1.5$), the Li-ion distributions are close to identical to each other indicating a continuous structural evolution and solid-solution behavior. Throughout these computational results, we are able to catch a glimpse of the driving force for structural distortion in the delithiation process.

To elucidate the kinetic limitations in this system, we have investigated different delithiation mechanisms in the high Li content regime ($x > 1.0$). The single vacancy, di-vacancy mechanism as well as Li migration barriers for different Li concentrations have been calculated, mapping out the barriers as a function of different local environments. Migration of Li from the Mn layer into the Li layer is observed, but sluggish. Furthermore, our preliminary calculations indicate that the migrating Li ion in the Li layer experiences significant interactions with its first nearest neighbors. In the absence of di-vacancy migration, this is evidenced by the distortion of the octahedral cages of the two occupied Li nearest neighbors to open the space for Li-ion migration (Figure 44). Going forward, these calculations will be used as a basis for a kinetic Monte Carlo investigation of Li diffusivity as a function of Li concentration and Mn defect formation.

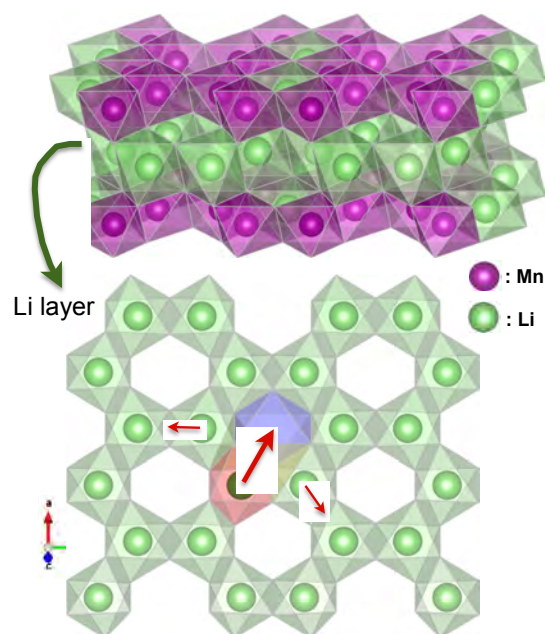


Figure 44: Lithium-ion migration in delithiated Li-layer, showing the interaction of the nearest Li neighbor distortions as the migrating Li moves.

Q2 Patents/Publications/Presentations

None this quarter.

Task 6.3 – First Principles Calculations of Existing and Novel Electrode Materials (Gerbrand Ceder, MIT)

PROJECT OBJECTIVE: Identify the structure of layered cathodes that leads to high capacity. Clarify the role of the initial structure as well as structural changes upon first charge and discharge. Give insight into the role of Li-excess and develop methods to predict ion migration in layered cathodes upon cycling and during overcharge. Develop predictive modeling of oxygen charge transfer and oxygen loss. Give insight into the factors that control the capacity and rate of Na-intercalation electrodes, as well as Na-vacancy ordering. Develop very high capacity layered cathodes with high structural stability (> 250 mAh/g).

PROJECT IMPACT: The project will lead to insight in how Li excess materials work and ultimately to higher capacity cathode materials for Li-ion batteries. The project will help in the design of high capacity cathode materials that are tolerant to transition metal migration.

OUT-YEAR GOALS: Higher capacity Li-ion cathode materials, and novel chemistries for higher energy density storage devices. Guide the field in the search for higher energy density Li-ion materials..

COLLABORATIONS: Persson (LBNL), Grey (Cambridge U).

Milestones

1. Demonstrate capability to accurately predict oxygen redox activity in cathode materials by comparing calculations to spectroscopic data. (Dec-31) **Completed**
2. Develop model for effect of Li-excess in $\text{Li}(\text{Li},\text{Ni},\text{Sb})\text{O}_2$. **Ongoing**
3. Develop model for Na-vacancy ordering in Na-intercalation compounds (March 31). **Completed**
4. Identify at least one other disordered material with high reversible capacity. **Ongoing**

Progress Report

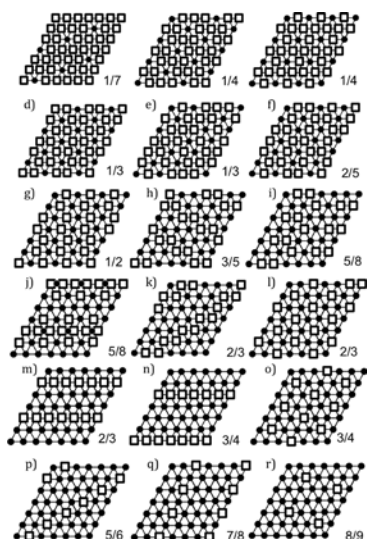


Figure 45: All Na-vacancy orderings that occur in the Na_xMO_2 systems with seven different choices of M.

phases appearing as ground states in all Na_xMO_2 systems, and investigate the effect of ordering interactions between adjacent layers. We calculated a total of approximately 500 possible Na-vacancy orderings for each transition metal system (see Figure 46).

From these, any ordering occurring as a ground state in any of the systems was collected and grouped into a collection of 18 low-energy ordering types.

We are currently investigating how some of the phase transformations in the materials can be prevented so that very high rate systems can be developed.

Current state of the art Na-ion battery cathodes are selected from the broad chemical space of layered first row transition metal (TM) oxides. Unlike their lithium-ion counterparts, seven first row layered TM oxides can intercalate Na ions reversibly, unlike in lithium systems where among the single metal systems only LiCoO_2 and LiNiO_2 can exchange lithium reversibly. In contrast to Li-systems, the voltage curves of Na-systems indicate significant and numerous reversible phase transformations during electrochemical cycling. These transformations are not yet fully understood, but arise from Na-ion vacancy ordering and metal oxide slab glide and can significantly affect rate capability (see Figure 45). Hence, in this study, we investigated the nature of Na-vacancy ordering transformations within the O3 lattice framework. We generate predicted electrochemical voltage curves for each of the Na-ion intercalating layered single TM oxides using a high-throughput framework of density functional theory (DFT) calculations. We determine a set of vacancy ordered

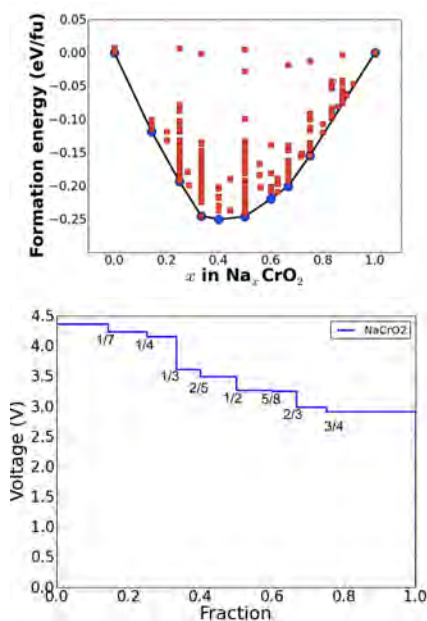


Figure 46: Convex energy hull of the ground states of the Na_xCrO_2 systems showing that a large number of ordered structures can occur, explaining the stepped voltage curve of this material.

Task 6.4 – First Principles Modeling of SEI Formation on Bare and Surface/Additive Modified Silicon Anode (Perla Balbuena, Texas A&M University)

PROJECT OBJECTIVE: This project aims to develop fundamental understanding of the molecular processes that lead to the formation of a solid electrolyte interphase (SEI) layer due to electrolyte decomposition on Si anodes, and to use such new knowledge in a rational selection of additives and/or coatings. The focus is on SEI layer formation and evolution during cycling and subsequent effects on capacity fade through two concatenated problems: 1) SEI layers formed on lithiated Si surfaces, and 2) SEI layers formed on coated surfaces. Key issues that this project addresses include the dynamic evolution of the system and electron transfer through solid-liquid interfaces.

PROJECT IMPACT: Finding the correspondence between electrolyte molecular properties and SEI formation mechanism, structure, and properties will allow the identification of new/improved additives. Studies of SEI layer formation on modified surfaces will allow the identification of effective coatings able to overcome the intrinsic deficiencies of SEI layers on bare surfaces.

APPROACH: Investigating the SEI layer formed on modified Si surfaces involves analysis of the interfacial structure and properties of specific coating(s) deposited over the Si anode surface, characterization of the corresponding surface properties before and after lithiation, especially how such modified surfaces may interact with electrolyte systems (solvent/salt/additive), and what SEI layer structure, composition, and properties may result from such interaction. This study will allow identification of effective additives and coatings able to overcome the intrinsic deficiencies of SEI layers on bare surfaces. Once the SEI layer is formed on bare or modified surfaces, it is exposed to cycling effects that influence its overall structure (including the anode), chemical, and mechanical stability.

OUT-YEAR GOALS: Elucidating SEI nucleation and electron transfer mechanisms leading to growth processes using a molecular level approach will help establish their relationship with capacity fading, which will lead to revisiting additive and/or coating design.

COLLABORATIONS: Work with Chunmei Ban, (NREL, BMR) consists in modelling the deposition-reaction of alucon coating on Si surfaces and their reactivity. Work with B. Lucht (URI, BMR) relates to finding the best additives for optimum SEI formation on Si anodes. Reduction of solvents and additives on Si surfaces were studied in collaboration with K. Leung and S. Rempe, from Sandia National Labs. Collaborations with Prof. Jorge Seminario (TAMU) on electron transfer reactions, and Dr. Partha Mukherjee (TAMU) focusing on the development of a multi-scale model to describe the SEI growth on Si anodes.

Milestones

1. Identification of lithiation and SEI formation mechanisms through alucon coatings on Si surfaces. (Q1) **Completed**
2. Clarify role of additives (VC, FEC) vs. electrolyte without additive on SEI properties. (Q2). **Completed**
3. Characterization of SEI mosaic formation from building blocks. (Q3) **In progress**
4. Go/No-Go: Prediction of irreversible capacity loss and electron transfer mechanisms through the SEI layer. (Q4) **In progress**.

Progress Report

Lithiation and reactivity of coated silicon surfaces. a) DFT calculations were used to study the growth mechanism and structure of the MLD alucone coating for Si particles. A compact alucone film was found to be formed by thermodynamically favorable reactions between tri-methyl aluminum and the silanol groups of the surface and posterior reaction with glycerol. A dense and conformal coating is enabled by numerous cross-links connected by Al-O bonds. First principles analyses illustrated the molecular mechanisms of lithium irreversible binding in the alucone coating. Al was found in three coordination modes and these functional structures are the basis for Li binding with values ranging -2.63 to -3.30 eV. Considering these strong Li-O interactions, the lithiation of the film involving these most favorable sites may be considered irreversible. In agreement with experimental results from Ban's group (NREL), the irreversible lithiation process modifies the electronic and ionic transport properties and the reactivity of the alucone coating. Once the Li atoms occupy all the favorable coating sites, the film becomes electronically conductive, and EC molecules easily decompose on its surface following similar electron transfer mechanisms as detected previously on lithiated silicon anodes. A manuscript has been submitted for publication. b) DFT studies of an amorphous SiO₂ film with hydroxylated surfaces revealed lithiation mechanisms. A model amorphous SiO₂ film was built reproducing the main surface properties: Si ring size distribution, silanol type distribution, and total number of silanol groups per unit surface area, in comparison with experimental values. Breaking of the SiO bond by simultaneous reaction with two Li atoms causing partial reduction of the involved Si atoms was found to be the most favorable lithiation pathway. A lithiation protocol was followed to characterize lithiation at each step by computing the formation energies. It was found that the film becomes saturated at a Li/Si ratio of 3.48 and that the lowest energy configuration usually corresponds to a displaced Si atom bonded to at least one hydroxyl group, thus revealing the role of the hydroxyl groups on lithiation. Si atoms are displaced from their tetrahedral positions as they are partially reduced, and starting from a Li/Si ratio of ~1.85, some Si atoms lose all the Si-O bonds and form Si-Si bonds. Further analysis indicated that breaking of SiO bonds becomes less favorable at high degrees of lithiation and is accompanied by SiSi bond formation and nucleation of Li₆O complexes stabilized by Si atoms. A manuscript has been submitted for publication.

Role of additives. DFT and AIMD analyses showed that the successful FEC and VC additives yield similar decomposition products derived from the radical anion VC⁻ [Martinez de la Hoz and Balbuena, PCCP, 16., 17091, (2014)]. The main dimer products Li₂EDC and Li₂VDC are both susceptible to nucleophilic attack by the surface or by other radical species thus transferring electrons and resulting in SEI growth. However, competition between polymerization vs. aggregation reactions of the initial radical anion products influence the stability of the SEI layer formed. A manuscript is under preparation.

Construction of Li_xSi_y films coated with stretched model SEI. Using DFT-based *ab initio* molecular dynamics (AIMD) simulated-annealing techniques, an amorphous LiSi (a-LiSi) slab was built coated with amorphous LiF_z coatings film on each side. This LiF_x-coated LiSi is transformed into Li_xF_y, x>y, by gradually increasing the Li content, using a procedure derived from Chevrier and Dahn [JES 156:A454 (2009)]. As more Li is inserted, the simulation cell is manually expanded in all spatial dimensions before geometry relaxation is applied. This ensures that the volumetric expansion is not artificially constrained by the finite thickness of the Li_xSi_y slab; otherwise the stiff LiF_z coating will dominate the mechanical properties. With this procedure, lithiated silicon interfaces coated with stretched model SEI (e.g., LiF₂) films due to volumetric expansion are built. The effect of stretching the surface films on SEI regeneration and healing, under approximately constant voltage conditions, will be examined in the future.

Dielectric properties of EC and PC. As a prerequisite to evaluating ionic transport at the interface of SEI blocks and the electrolyte solution, the dielectric properties of EC and PC has been evaluated using classical MD simulations in a wide range of temperatures and compared to experimental values.

Patents/Publications/Presentations

1. J. M. Martinez de la Hoz, F. A. Soto, and P. B. Balbuena, “Effect of the electrolyte composition on SEI reactions at Si anodes of Li-ion batteries,” *J. Phys. Chem. C*, in press, DOI: 10.1021/acs.jpcc.5b01228.
2. J. M. Martinez de la Hoz and P. B. Balbuena, “Reduction Mechanisms of Additives on Si Anodes of Li-Ion Batteries,” *Phys. Chem. Chem. Phys.*, 16, 17091-17098 (2014).

Task 6.5 – A Combined Experimental and Modeling Approach for the Design of High Current Efficiency Si Electrodes (Xingcheng Xiao, General Motors and Yue Qi, Michigan State University)

PROJECT OBJECTIVE: The use of high capacity Si-based electrode has been hampered by its mechanical degradation due to the large volume expansion/contraction during cycling. Nanostructured Si can effectively avoid Si cracking/fracture. Unfortunately, the high surface-to-volume ratio in nanostructures leads to an unacceptable amounts of solid-electrolyte interphase (SEI) formation and growth, thereby low current/coulombic efficiency and short life. Based on mechanics models we demonstrate that the artificial SEI coating can be mechanically stable despite the volume change in Si, if the material properties, thickness of the SEI, and the size/shape of Si are optimized. Therefore, the objective of this project is to develop an integrated modeling and experimental approach to understand, design, and make coated Si anode structures with high current efficiency and stability.

PROJECT IMPACT: The validated model will ultimately be used to guide the synthesis of surface coatings and the optimization of Si size/geometry that can mitigate SEI breakdown. The optimized structures will eventually enable a negative electrode with a 10x improvement in capacity (compared to graphite) while providing a >99.99% coulombic efficiency, which could significantly improve the energy/power density of current LIB.

OUT-YEAR GOALS: The out year goal is to develop a well validated mechanics model that directly import material properties either measured from experiments or computed from atomic simulations. The predicted SEI-induced stress evolution and other critical phenomena will be validated against *in situ* experiments in a simplified thin-film system. This comparison will also allow fundamental understanding of the mechanical and chemical stability of artificial SEI in electrochemical environments and the correlation between the coulombic efficiency and the dynamic process of SEI evolution. Thus the size and geometry of coated Si nanostructures can be optimized in order to mitigate SEI breakdown, thus providing a high current efficiency.

COLLABORATIONS: LBNL, PNNL, NREL.

Milestones

1. Identify SEI failure mode by using combined *in situ* electrochemical experiments and modeling techniques developed in 2014 (12/31/14) (**Identified some failure modes, continue comparing individual SEI components**)
2. Reveal detailed SEI failure mode by using MD simulations with ReaxFF for Li-Si-Al-O-C system to model the deformation of SEI on a Si as it undergoes large strain. (3/31/15) (**completed**)
3. Correlate and determine the desirable material properties for stable SEI, by applying the continuum model and experimental nanomechanics. Establish the material property design methodology for stabilizing SEI on Si. (6/30/15)
4. Make Go/No-Go decision on whether to select oxide, fluoridated, or carbon artificial SEI chemistry based on comparisons of their mechanical stability and transport properties. (9/30/15)

Progress Report

Investigated the impact of surface coating on the cycle stability of coated Si system.

Both Al_2O_3 and SiO_2 shells expand upon lithiation since the volume increases as lithiation occurs. In the meantime, the swelling lithiated Si core imposes stress on the shell and stretches them, which make the shells thinner. In other words, shell thickness is governed by volume expansion due to lithiation at the initial stage of time, while mechanical stretching effect controls the shell thickness during the later stage of time. For the 7.5\AA Al_2O_3 shell, these two competing effects reach dynamic equilibrium and stable shell thickness of 11\AA is obtained after 5 ps. Li/Si and Li/Al ratios which are responsible for volume expansion depend on the shell thickness and the stretching effect is more pronounced when the coating is thin and the lithiated shell is soft (see Figure 47).

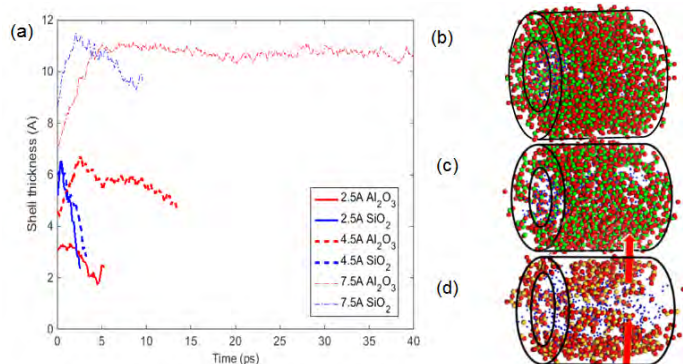


Figure 47: Shell failure mechanisms. (a) Shell thickness with time (b) example of mechanically intact shell: 7.5\AA Al_2O_3 (c) example of cracked shell: 4.5\AA Al_2O_3 , 7.5\AA SiO_2 (d) example of broken shell: 2.5\AA Al_2O_3 , 2.5\AA SiO_2 , and 4.5\AA SiO_2 (Si: yellow, O: red, Al: green).

Established a mathematical model to describe the isotope exchange experiments in LiF. The model was built based on the assumption that Li ion vacancy was the dominant defect in LiF (Figure 48) coated on Si electrode. The results show that the rate of isotope exchange in LiF is slow compared with that in Li_2CO_3 coatings on Si electrode. Furthermore, this model provides a way to compare our atomic-scale computational results with the experimental measurements (e.g., XPS).

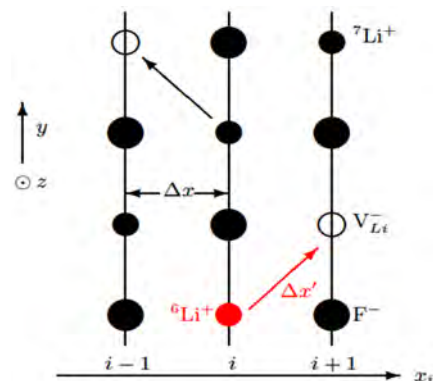


Figure 48: Schematic picture of the 1-D model for LiF (001) plane. Mechanical stability of yolk-shell structure.

Established a design map toward the mechanical stability of the yolk-shell structure with Si yolk in a C shell. It is found that a thick C shell could prevent lithiation in Si core after contact due to the confining compressive stress in response to the lithiation induced volume expansion, while a thin C shell could not resist the volume expansion and lead to the shell fracture. For optimal design, it will be important to determine the optimal design parameters such as the size of the Si yolk and the thickness of C shell. Our model predicts a critical condition for the transition between incomplete lithiation of Si core and through-thickness fracture of C shell, as shown in Figure 49.

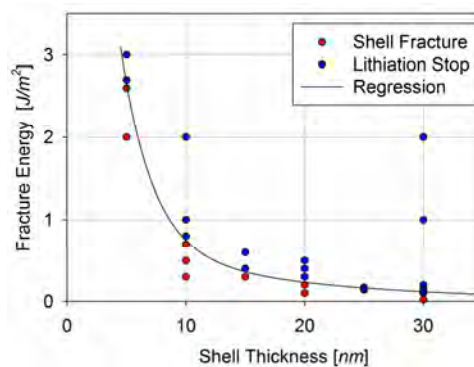


Figure 49: Critical shell thickness from the finite element simulations of lithiation in a Si-C yolk-shell structure.

Patents/Publications/Presentations

Publications

1. Pan, Jie; Zhang, Qinglin; Li, Juchuan; Beck, Matthew; Xiao, Xingcheng; Cheng, Yang-Tse, Stress Effect on the Li Transport in Nanostructured Amorphous Si Electrodes for Li-ion Batteries, Nano Energy, Volume 13, April 2015, Pages 192–199
2. Xiaolei Wang, Ge Li, Fathy M Hassan, Xingcheng Xiao,* and Zhongwei Chen,* Building sponge-like robust architectures of CNT–graphene–Si composites with enhanced rate and cycling performance for lithium-ion batteries, Journal of Materials Chemistry A, 2015, 3, 3962 – 3967

Invited Talks

1. Xingcheng Xiao “Towards high cycle efficiency of high energy lithium ion batteries” American Chemistry Society, Denver, CO. March, 23, 2015
2. Yue Qi, “Predicting the transport properties of the solid electrolyte interphase (SEI) in Li-ion batteries”. MRS 2015 Spring Meeting, San Francisco, CA. April, 02, 2015.

Task 6.6 – Predicting Microstructure and Performance for Optimal Cell Fabrication (Dean Wheeler and Brian Mazzeo, Brigham Young University)

PROJECT OBJECTIVE: This work uses microstructural modeling coupled with extensive experimental validation and diagnostics to understand and optimize fabrication processes for composite particle-based electrodes. The first main outcome will be revolutionary methods to assess electronic and ionic conductivities of porous electrodes attached to current collectors, including heterogeneities and anisotropic effects. The second main outcome is a particle-dynamics model parameterized with fundamental physical properties that can predict electrode morphology and transport pathways resulting from particular fabrication steps. These two outcomes will enable the third, which is an understanding of the effects of processing conditions on microscopic and macroscopic properties of electrodes.

PROJECT IMPACT: This work will result in new diagnostic tools for rapidly and conveniently interrogating electronic and ionic pathways in porous electrodes. A new mesoscale 3D microstructure prediction model, validated by experimental structures and electrode-performance metrics, will be developed. The model will enable virtual exploration of process improvements that currently can only be explored empirically.

OUT-YEAR GOALS: This project was initiated April 2013 and concludes March 2017. Goals by fiscal year are as follows.

- 2013: Fabricate first-generation micro-four-line probe and complete associated computer model.
- 2014: Assess conductivity variability in electrodes; characterize microstructures of multiple electrodes.
- 2015: Fabricate first-gen ionic conductivity probe, N-line probe, and dynamic particle packing (DPP) model.
- 2016: Fabricate second-gen N-line probe and DPP model; assess effect of processing variables.
- 2017: Use conductivity predictions in full electrochemical model; evaluate effect of innovative processing conditions.

COLLABORATIONS: Bryant Polzin (ANL) and Karim Zaghbi (Hydro-Québec) provided battery materials. Transfer of our technology to A123 to improve their electrode production process is in process. There are ongoing collaborations with Simon Thiele (IMTEK, University of Freiburg) and Mårten Behm (KTH, Sweden)

Milestones

1. Develop localized ionic conductivity probe and demonstrate method by testing two candidate electrode materials (Dec-14). **Complete**
2. Use dynamic particle-packing (DPP) model to predict electrode morphology of Toda 523 material (Mar-15). **Complete**
3. Develop fabrication process of micro-N-line probe and demonstrate method by testing two candidate electrode materials (Jun-15). **Ongoing**
4. Go/No-Go: Discontinue dynamic particle-packing (DPP) model if predictions are not suitable match to real electrode materials (Sep-15). **Ongoing**

Progress Report

Milestone 1 (Complete)

The first milestone of FY2015 was previously partially delayed, but is now complete. The milestone was to adapt the micro-four-line probe (μ 4LP) apparatus to measure local effective ionic conductivity of thin-film battery electrodes. Six electrode films, two separators, and five probe designs were tested (see Figure 50). Initial proof-of-concept experiments were completed, but showed large uncertainties in the measurements, namely $\pm 40\%$ from expected ionic tortuosity results. Thus, although the milestone is completed, the method is judged not to be of satisfactory reliability in its current state. In parallel with other efforts, work will continue on the ionic probe to obtain a more robust design and method.

Milestone 2 (Complete)

Under development for over one year, the dynamic particle packing (DPP) model is intended to predict liquid-slurry and dried-film properties from a simple set of input parameters, enabling electrode fabrication process optimization. The model imitates interactions between discrete mesoscale domains containing carbon, binder, solvent, and active materials (see Figure 51). The model was initially tested and validated by comparing to structures and other physical properties of cathode films made from Toda 523 active material, chosen for its spheroidal shapes. At present the simulations have shown remarkable agreement with the following experimental properties measured at BYU: shear-dependent slurry viscosity, volume change upon film drying, solid film elasticity, and solid microstructure (see Figure 52). Efforts to validate the model will continue with Go/No-Go Milestone 4.

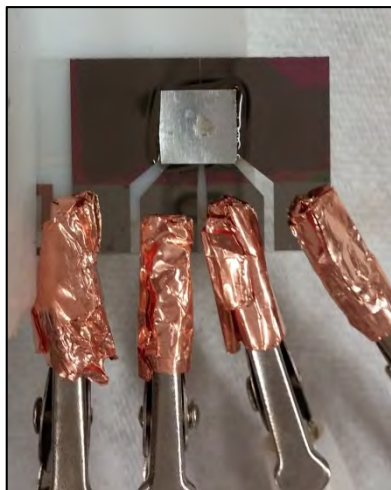


Figure 50: (left) Micro-four-line-probe with electrode film sample on top. Sampling area for ionic conductivity is $70 \times 500 \mu\text{m}$.

Figure 51: (right) The DPP model uses superpositions of spheres to represent active material (blue) and carbon/binder/solvent domains (green).

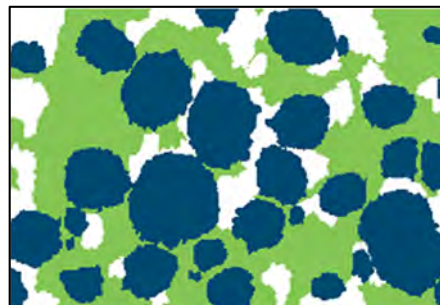
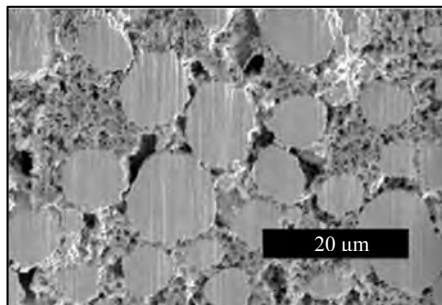
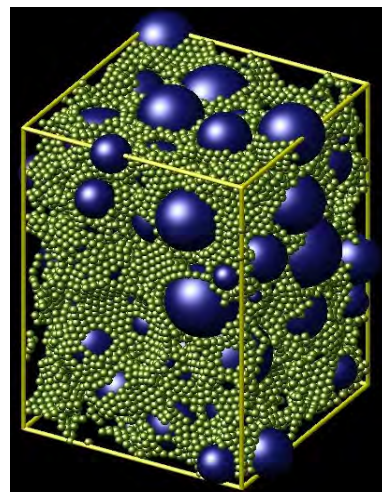


Figure 52: Simulated cross section of cathode (left) compared to experimental results. The SEM/FIB image (center) is segmented (right) using computer tools developed at BYU.

Q2 Patents/Publications/Presentations

Publications

1. C.W. Monroe, D.R. Wheeler, and J. Newman, “Nonequilibrium linear response theory: Application to Onsager-Stefan-Maxwell diffusion,” *Indust. Eng. Chem. Res.*, published online (2015).

Publications Under Review

1. B.J. Lanterman, A.A. Riet, N.S. Gates, J.D. Flygare, A.D. Cutler, J.E. Vogel, D.R. Wheeler, and B.A. Mazzeo, “Micro-four-line probe to measure electronic conductivity and contact resistance of thin-film battery electrodes,” *J. Electrochem. Soc.*, submitted (2015).
2. J.D. Flygare, A.A. Riet, B.A. Mazzeo, and D.R. Wheeler, “Mathematical model of four-line probe to determine conductive properties of thin-film battery electrodes,” *J. Electrochem. Soc.*, submitted (2015).

Product Delivery

1. Two electronic conductivity probes and the associated computer code were sold to A123 this quarter for their use in improving the quality of their electrode fabrication process.

TASK 7 – METALLIC LITHIUM AND SOLID ELECTROLYTES

Summary and Highlights

The use of a metallic lithium anode is required for advanced battery chemistries like Li-air and Li-S in order to realize dramatic improvements in energy density, vehicle range, cost economy and safety. However, the use of metallic Li with liquid and polymer electrolytes has been so far limited due to parasitic SEI reactions and dendrite formation. Adding excess lithium to compensate for such losses effectively negates the high energy density for lithium in the first place. For a long lifetime and safe anode, it is essential that no lithium capacity is lost to either physical isolation from roughening, dendrites or delamination processes, or to chemical isolation from side reactions. The key risk and current limitation for this technology is the gradual loss of lithium over the cycle life of the battery.

To date there are no examples of battery materials and architectures that realize such highly efficient cycling of metallic lithium anodes for a lifetime of 1,000 cycles due to degradation of the Li-electrolyte interface. A much deeper analysis of the degradation processes is needed, so that materials can be engineered to fulfill the target level of performance for EV, namely 1,000 cycles and a 15 year lifetime, with adequate pulse power. Projecting the performance required in terms of just the Li anode, this requires a high rate of lithium deposition and stripping reactions, specifically about 40µm Li per cycle, with pulse rates up to 10 and 20 nm/s charge and discharge, respectively. This is a conservative estimate, yet daunting in the total mass and rate of material transport. While such cycling has been achieved for state-of-the-art batteries using *molten* Na in Na-S and zebra cells, solid Na and Li anodes are proving more difficult.

The efficient and safe use of metallic lithium for rechargeable batteries is then a great challenge, one that has eluded R&D efforts for many years. The Battery Materials Research Task 7, takes a broad look at this challenge for both solid state batteries and batteries continuing to use liquid electrolytes. Four of the projects are new endeavors; two are ongoing. For the liquid electrolyte batteries, PNNL researchers are examining the use of cesium salts and organic additives to the typical organic carbonate electrolytes to impede dendrite formation at both the lithium and graphite anodes. If successful, this is the simplest approach to implement. At Stanford, novel coatings of carbon and boron nitride with a 3D structure are applied to the lithium surface and appear to suppress roughening and lengthen cycle life. A relatively new family of solid electrolytes with a garnet crystal structure show superionic conductivity and good electrochemical stability. Four programs chose this family of solid electrolytes for investigation. Aspects of the processing of this ceramic garnet electrolyte are addressed at the University of Maryland and at the University of Michigan with attention to effect of flaws and composition. Computational models will complement their experiments to better understand interfaces and reduce the electrode area specific resistance (ASR). At Oak Ridge National Laboratory, composite electrolytes composed of ceramic and polymer phases are being investigated, anticipating that the mixed phase structures may provide additional means to adjust the mechanical and transport properties. The last project takes on the challenge to used nanoindentation methods to measure the mechanical properties of the solid electrolyte, the lithium metal anode, and the interface of an active electrode. Each of these projects involve a collaborative team of experts with the skills needed to address the challenging materials studies of this dynamic electrochemical system.

Task 7.1 – Mechanical Properties at the Protected Lithium Interface (Nancy Dudney, ORNL; Erik Herbert, UTK; Jeff Sakamoto UM)

PROJECT OBJECTIVE: This project will develop the understanding of the Li metal-solid electrolyte interface through state of the art mechanical nanoindentation methods coupled with solid electrolyte fabrication and electrochemical cycling. Our goal is to provide critical information that will enable transformative insights into the complex coupling between the microstructure, its defects and the mechanical behavior of Li metal anodes.

PROJECT IMPACT: Instability and/or high resistance at the interface of lithium metal with various solid electrolytes limit the use of the metallic anode for batteries with high energy density batteries, such as Li-air and Li-S. The critical impact of this endeavor will be a much deeper analysis of the degradation, so that materials can be engineered to fulfill the target level of performance for EV batteries, namely 1,000 cycles and 15 year lifetime, with adequate pulse power.

APPROACH: Mechanical property studies through state of the art nanoindentation techniques will be used to probe the surface properties of the solid electrolyte and the changes to the lithium that result from prolonged electrodeposition and dissolution at the interface. An understanding of the degradation processes will guide future electrolyte and anode designs for robust performance. In the first year, the team will address the two critical and poorly understood aspects of the protected Li metal anode assembly: (1) the mechanical properties of the solid electrolyte, and (2) the morphology of the cycled Li metal.

OUT-YEAR GOALS: Work will progress toward study of the electrode assembly during electrochemical cycling of the anode. We hope to capture the formation and annealing of vacancies and other defects in the lithium and correlate this with the properties of the solid electrolyte and the interface.

COLLABORATIONS: This project funds work at Oak Ridge National Laboratory, University of Tennessee at Knoxville, and University of Michigan. Asma Sharafi (UM Ph. D. student), Dr. Robert Schmidt (UM) also contribute to the project. Steve Visco (PolyPlus) will serve as a technical advisor.

Milestones

1. Four nano-indentation maps showing grain boundary regions of the crystalline LLZO and the glass ceramic material from Ohara (Q1) **(complete)**
2. Two or three indentation studies with as-fabricated, air reacted and polished surfaces (Q2) **(complete)**
3. Demonstrate capability to transfer and then map viscoelastic properties of Li films and rolled lithium foils in vacuum system of SEM (Q3) **(on schedule for glove box studies)**
4. Determine elastic properties of battery grade lithium from different sources and preparation, comparing to values from the reference literature (Q4)

Progress Report

Last quarter we reported nanoindentation maps of Al-doped LLZO pellet which had been cycled to failure. Although quite dense and single phase by XRD, darkened regions were visible which are believed to be the shorted. Statistically, these areas have higher elastic modulus (E) and hardness (H) than the white areas.

During this quarter sample preparation was varied to assess the importance of the surface condition (milestone 2). A new polishing approach gives a mirror finish and a better resolution of nanoindentation mapping. Preliminary results suggests there is also a change in the distribution of damage (visible darkening) upon cycling, compared to the earlier dry sanding process. For indentation mapping, the samples were protected with mineral oil. Left overnight, there was clearly some degradation in the

surface visible in the microscope, although significant air reaction was not expected. The surface finish is clearly important and needs to be considered along with the composition and other processing variables.

Nanoindentation mapping was completed for 8 additional samples, including: our ceramic LLZO samples, Ohara's glass ceramic LATP, and Ohara's sintered ceramic (milestone 1). The latter were examined with only minor cleaning of the surface. The difference in the elastic modulus for the glass ceramic (black) and sintered (red) LATP electrolytes is shown in

Figure 53 (2 samples each and 100 points per sample). The difference is striking. The glass ceramic is much more uniform and slightly harder on average than the tape cast sintered body. For comparison, we show the sintered LLZO sample (blue) has a slightly higher modulus and similar distribution as the Ohara ceramic. A series of LLZO with Ta doping of 0.25 to 1.5 mol% were also tested. One composition with Ta 0.5 mol% appears to be an outlier. This is shown in the Table 2 and Figure 54.

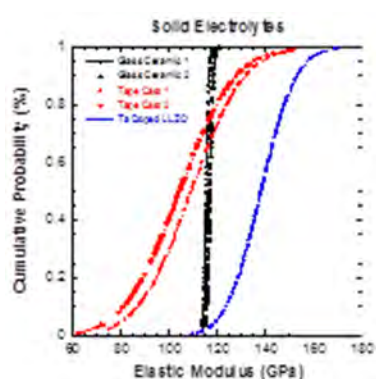


Figure 53: Elastic modulus for the glass ceramic (black) and sintered (red) LATP electrolytes

Table 2: Results of testing LLZO with Ta doping of 0.25 to 1.5 mol%

No.	Ta (mol%)	Elastic modulus (GPa)	Hardness (GPa)
1	0.5	105 ± 12	3.9 ± 1.0
2	0.75	141 ± 15	8.3 ± 1.6
3	1.5	137 ± 12	8.0 ± 1.5
4	0.25	138 ± 11	7.6 ± 1.3

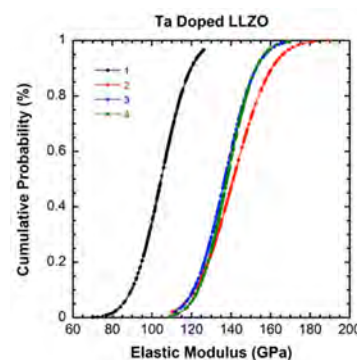


Figure 54: Plots of testing LLZO with Ta doping of 0.25 to 1.5 mol%.

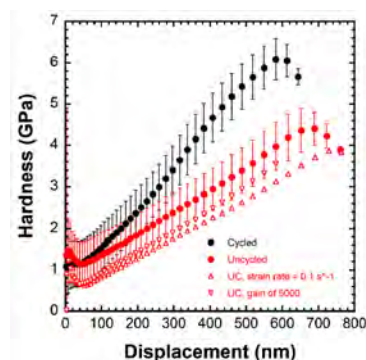


Figure 55: Change in mechanical properties with Li cycling

Most interesting is the change in mechanical properties with Li cycling. Preliminary data indicates the hardness increases after cycling. This is consistent with trends reported last quarter. For results shown in the Figure 55, a 0.27Al doped LLZO pellet was mapped before (red) and after cycling at high current density cycling (black). The depth dependence is under investigation, but seems to hold for a range of measurement parameters.

Studies of the Li metal are underway with measurements conducted in the glove box (milestone 3).

Patents/Publications/Presentations

None this quarter.

Task 7.2 – Solid Electrolytes for Solid-State and Lithium-Sulfur Batteries (Jeff Sakamoto, University of Michigan)

PROJECT OBJECTIVES: *Enable advanced Li-ion solid-state and lithium-sulfur EV batteries using LLZO solid-electrolyte membrane technology.* Owing to its combination of fast ion conductivity, stability, and high elastic modulus, LLZO exhibits promise as an advanced solid-state electrolyte. To demonstrate relevance in EV battery technology, several objectives must be met. First, LLZO membranes must withstand current densities approaching $\sim 1 \text{ mA/cm}^2$ (commensurate with EV battery charging and discharging rates). Second, low area specific resistance (ASR) between Li and LLZO must be achieved to achieve cell impedance comparable to conventional Li-ion technology ($\sim 10 \text{ Ohms/cm}^2$). Third, low ASR and stability between LLZO and sulfur cathodes must be demonstrated.

PROJECT IMPACT: The expected outcomes will: (i) enable Li metal protection, (ii) augment DOE's access to fast ion conductors and/or hybrid electrolytes, (iii) mitigate Li-polysulfide dissolution and deleterious passivation of Li metal anodes, and (iv) prevent dendrite formation. Demonstrating these aspects could enable the development of Li-S batteries with unprecedented end-of-life, cell-level performance: $\geq 500 \text{ Wh/kg}$, $\geq 1080 \text{ Wh/l}$, ≥ 1000 cycles, lasting ≥ 15 years.

APPROACH: Our effort will focus on the promising new electrolyte known as LLZO ($\text{Li}_7\text{La}_3\text{Zr}_2\text{O}_{12}$). LLZO is the first bulk-scale ceramic electrolyte to simultaneously exhibit the favorable combination of high conductivity ($\sim 1 \text{ mS/cm}$ at 298K), high shear modulus (61 GPa) to suppress Li dendrite penetration, and apparent electrochemical stability (0-6V vs Li/Li^+). While these attributes are encouraging, additional R&D is needed to demonstrate that LLZO can tolerate current densities in excess of 1 mA/cm^2 , thereby establishing its relevance for PHEV/EV applications. We hypothesize that defects and the polycrystalline nature of realistic LLZO membranes can limit the critical current density. However, the relative importance of the many possible defect types (porosity, grain boundaries, interfaces, surface & bulk impurities), and the mechanisms by which they impact current density, have not been identified. Using our experience with the synthesis and processing of LLZO (Sakamoto and Wolfenstine), combined with sophisticated materials characterization (Nanda), we will precisely control atomic and microstructural defects and correlate their concentration with the critical current density. These data will inform multi-scale computation models (Siegel and Monroe) which will isolate and quantify the role(s) that each defect plays in controlling the current density. By bridging the knowledge gap between composition, structure, and performance we will determine if LLZO can achieve the current densities required for vehicle applications.

COLLABORATIONS: Don Siegel (UM atomistic modeling), Chuck Monroe (UM, continuum scale modeling), Jagjit Nanda (ORNL sulfur chemical and electrochemical spectroscopy), Jeff Wolfenstine (ARL atomic force microscopy of Li-LLZO interfaces).

Milestones

1. **M1.1 Milestone (to be completed Q2):** Demonstrate ability to vary porosity from 1 to 15 volume %. Correlate critical current density with scale and volume of porosity. **On-going.**
2. **M1.2 Milestone (to be completed Q3):** Establish baseline atomistic and continuum theory to predict the maximum critical current density based on pore size and volume. Fabricate ceramic-polymer composite sheets with 20-60 vol% ceramic to determine the composition dependence of the conductivity as the structure. **On-going.**

Progress Report

M1.1 Milestone (to be completed Q3): Demonstrate ability to vary porosity from 1 to 15 volume%. Correlate critical current density with scale and volume of porosity.

University of Michigan

The Sakamoto group demonstrated the ability to control the porosity between 1 and 20 % in cubic LLZO pellets (Figure 56). Materials and mechanical behavior characterization is complete on these pellets. The electrochemical characterization and critical current density will be measured in the next quarter. 97% relative density cycled and un-cycled LLZO pellets were also sent to ARL for atomic force microscopy measurements.

M1.2 Milestone (to be completed Q4): Establish baseline atomistic and continuum theory to predict the maximum critical current density based on pore size and volume.

The Siegel and Monroe groups continue interaction with the Sakamoto group to integrate the experiments from Milestone 1.1 with atomistic and continuum scale theory. The goal is to demonstrate a correlation between critical current density and porosity. Establishing the model entailed the following activities conducted in the current reporting period.

Re-scoping

Discussions are underway with ORNL to re-scope the Sulfur-cathode related tasks. The task plan will be updated in the next quarter.

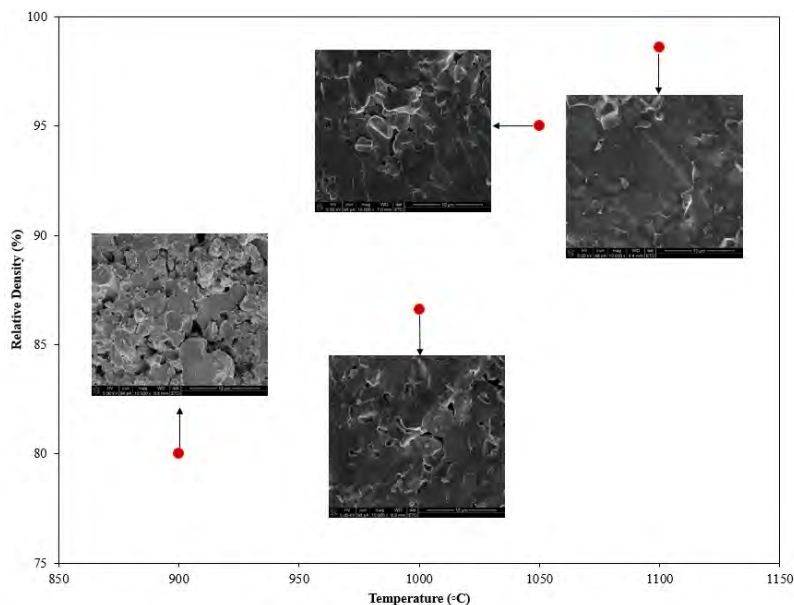


Figure 56: Secondary electron SEM images of LLZO fracture surfaces RIHP'ed between 900 and 1100 C (10,000 X).

Patents/Publications/Presentations

1. None.

Task 7.3 – Composite Electrolytes to Stabilize Metallic Lithium Anodes (Nancy Dudney and Sergiy Kalnaus, Oak Ridge National Laboratory)

PROJECT OBJECTIVE: Prepare composites of representative polymer and ceramic electrolyte materials to achieve thin membranes which have the unique combination of electrochemical and mechanical properties required to stabilize the metallic lithium anode while providing for good power performance and long cycle life. Understand the lithium-ion transport at the interface between polymer and ceramic solid electrolytes which is critical to the effective conductivity of the composite membrane. Identify key features of the composite composition, architecture and fabrication that optimize the performance. Fabricate thin electrolyte membranes to use with a thin metallic lithium anode that provide good power performance and long cycle life.

PROJECT IMPACT: A stable lithium anode is critical to achieve high energy density with required safety, lifetime and cycling efficiency. This study will identify the key design strategies that should be used to prepare composite electrolytes to meet the challenging combination of physical, chemical and manufacturing requirements to protect and stabilize the lithium metal anode for advanced batteries. By utilizing well-characterized and controlled component phases, the design rules developed for the composite structures will be generally applicable toward the substitution of alternative and improved solid electrolyte component phases as they become available. Success in this program will enable these specific DOE technical targets: 500-700Wh/kg, 3,000-5,000 deep discharge cycles, robust operation.

APPROACH: This program seeks to develop practical solid electrolytes that will provide stable and long-lived protection for the lithium metal anode. Current electrolytes all have serious challenges when used alone: oxide ceramics are brittle, sulfide ceramics are air sensitive, polymers are too resistive and soft, and many electrolytes react with lithium. Composites provide a clear route to address these issues. This program does not seek discovery of new electrolytes, rather the goal is to study combinations of current well known electrolytes. The program emphasizes the investigation of polymer-ceramic interfaces formed as bilayers and as simple composite mixtures where the effects of the interface properties can be readily isolated. In general, the ceramic phase is several orders of magnitude more conductive than the polymer electrolyte, and interfaces can contribute an additional source of resistance. Using finite element simulations as a guide, composites with promising compositions and architectures are fabricated and evaluated for lithium transport properties using AC impedance and DC cycling with lithium in symmetric or half cells. General design rules will be determined that can be widely applied to other combinations of solid electrolytes.

OUT-YEAR GOAL: Use advanced manufacturing processes where the architecture of the composite membrane can be developed and tailored to maximize performance and cost-effective manufacturing.

COLLABORATIONS: Electrolytes currently under investigation include a garnet electrolyte from Jeff Sakamoto (Michigan State University) and a block styrene copolymer from Nitash Balsara (U.C. Berkeley). Staff at Corning Corporation will serve as our industrial consultant.

Milestones

1. Q1: Compare the vapor absorption (rate and equilibrium) of small molecules in a single phase polymer and a corresponding ceramic/polymer composite electrolyte. **(Complete)**
2. Q2: Compare Li cycling, contacting Li with a buried Ni tab versus a surface metal contact. **(Complete)**
3. Q3: By generating a database with at least 5 compositions, determine if the presence of trace solvent molecules that enhance the ionic conductivity are also detrimental to the stability and cycleability of a lithium metal electrode, and if the effect can be altered by adding an overlayer film. **(SMART, ongoing)**
4. Q4: Demonstrate a practical processing route to a thin, dense membrane 100 μ m x 50cm². **(not started)**

Progress Report

Work this quarter continued to address quantitative analysis of the reaction of small organic solvent molecules with the polymer electrolyte and polymer-ceramic electrolyte composite (SMART milestone) with attention to the vapor pressure, the total amount of solvent available, and the exposure time. A comparison of the DMC and H₂O effect on conductivity for a 40vol% ceramic composite is shown in Figure 57. These are two of several additives under investigation and those most likely to be present as contaminants. The trends support the assumption that all the available water (or DMC) is adsorbed in the composite with the overnight exposure, but this is still being confirmed. To realize a dramatic increase in the ionic conductivity requires a surprising amount of the solvents. Also all of the samples show a stable conductivity after assembly of the conductivity test cell. Both of these observations suggest that ~15 minute exposure to contaminants in our standard glove box may not be the critical effect that so dramatically enhanced the ionic conductivity shown in earlier reports. Indeed careful analysis (mass spec, FTIR, XPS) of gas samples taken from our standard glove box versus our volatile-free glove box have so far failed to identify a specific contaminant. Regarding stability of the electrolytes with lithium metal (SMART milestone), to date all the polymer only samples are nominally stable with Li, while all the ceramic composites are not. Future work will use an alternate and/or lower ceramic powder loading in the composite to reveal the effect of the molecular additives on the Li stability.

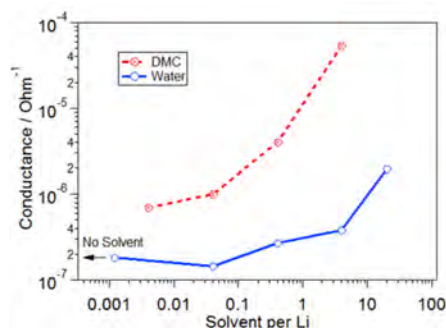


Figure 57: Effect of solvents on conductivity of composite electrolyte

To separate the effect of solvent contaminants to the bulk versus interface conductivities, trilayer polymer/ceramic/polymer “composites” were fabricated. The EIS of the trilayer is compared to a polymer-only sample to confirm assignment of the ceramic-polymer interface impedance. The samples were measured as prepared in the volatile-free glove box and then after solvent vapor exposure, as for the dispersed composites above. Figure 58 shows one representative result, before and after DMC exposure giving up to 1DMC:Li. Dispersion of polymer layer and the interface are seen, while that of ceramic (~200 ohms) occurs outside the frequency range at 25°C. Both the bulk and interface resistances are reduced by the DMC treatment. Improved (crack-free) samples are providing better component resolution for future reports.

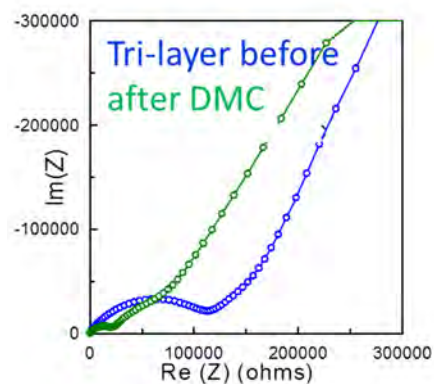


Figure 58: Effect of DMC on ceramics/polymer interface resistance

Our belief that the contact resistance to lithium might be better with a buried metal contact (milestone 2) has proven to be wrong. An excellent contact is achieved by pressing a polished stainless pellet to the Li, even when the lithium surface has become dull and gray. Forming a buried contact on an electrolyte pellet or sheet is tedious and easily damaged. This will be checked again with after more extensive Li cycling, during which defects and reaction products may accumulate at the contacts.

Patents/Publications/Presentations

None this quarter.

Task 7.4 – Overcoming Interfacial Impedance in Solid-State Batteries (Eric Wachsman, University of Maryland, College Park)

PROJECT OBJECTIVE: Develop a multifaceted and integrated (experimental and computational) approach to solve the key issue in solid-state Li-ion batteries (SSLiBs), interfacial impedance, with a focus on Garnet-based solid-state electrolytes (SSEs), the knowledge of which can be applied to other SSE chemistries. The focus is to develop methods to decrease the impedance across interfaces with the solid electrolyte, and ultimately demonstrate a high power/energy density battery employing the best of these methods.

PROJECT IMPACT: Garnet electrolytes have shown great promises for safer and higher energy density batteries due to their stability to both high voltage cathodes and Li metal anodes, as well as their inherent non-flammability. The success of the proposed research can lead to dramatic progress in the development of SSLiBs based on Garnet electrolytes. With regard to the fundamental science, our methodology by combining computations and experiments can lead to an understanding of the thermodynamics, kinetics and structural stability and evolution of SSLiBs with the Garnet electrolytes. Due to the ceramic nature of Garnet electrolyte, being brittle and hard, Garnet electrolyte particles intrinsically lead to poor contacts among themselves or with electrode materials. A fundamental understanding at the nanoscale and through computations, especially with interface layers, can guide improvements to their design and eventually help lead to the commercial use of such technologies.

APPROACH: SSLiB interfaces are typically planar resulting in high impedance due to low specific surface area, and attempts to make 3D high surface area interfaces can also result in high impedance due to poor contact at the electrode-electrolyte interfaces that hinder ion transport or degrade due to expansion/contraction with voltage cycling. We will experimentally and computationally determine the interfacial structure-impedance relationship in SSLiBs to obtain fundamental insight into design parameters to overcome this issue. Furthermore, we will investigate interfacial modification (layers between SSE and electrode) to see if we can extend these structure-property relationships to higher performance.

COLLABORATIONS: We are in collaboration with Dr. Venkataraman Thangadurai on garnet synthesis. We will collaborate with Dr. Leonid A. Bendersky and Dr. Howard Wang at NIST to use Neutron scattering to investigate the lithium profile across the bilayer interface with different charge-discharge rates.

Milestones

1. Determine frequency dependence of garnet and electrode impedances – **Complete.**
2. Develop computation models for garnet based interfaces – **in progress.**
3. Identify gel or PFPE based electrolyte with a stable voltage window (0V-4.2 V) – **in progress.**

Progress Report

Electrochemical impedance (EIS) of LLCZN electrolyte, LFMO cathode, and laminated LLCZN-LFMO pellets were measured. The characteristic frequency response of LLCZN and LFMO were observed to be in the MHz frequency range. The room temperature total lithium-ion conductivity of LLCZN electrolyte and LFMO cathode pellets were both $\sim 2 \times 10^{-4}$ S/cm. Figure 59 shows the typical Nyquist plot of laminated LLCZN/LFMO pellets. The huge arc at low (kHz) frequency region corresponds to the significant interfacial impedance between laminated LLCZN electrolyte and LFMO cathode. This is caused by rough interfacial contact and sluggish conduction across the solid-solid interface. The high frequency (inserted curve) electrochemical response represents the sum of LLCZN electrolyte and LFMO cathode contributions. Effect of pellet thickness on bulk and interfacial resistance is also shown in Figure 59, with thicker pellets exhibiting higher bulk and interfacial resistances. These results demonstrate the ability to use the EIS frequency response to separate out garnet, electrode, and interfacial impedances (Milestone 1).

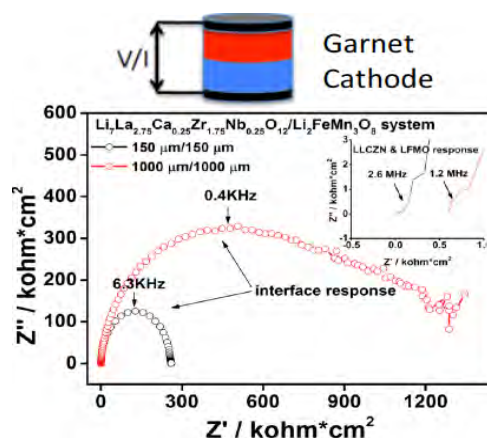


Figure 59: EIS of laminated LLCZN/LFMO.

The first interfacial layer (PFPE-DMC) was synthesized by the following steps: dissolve Fluorolink D10 and triethylamine in 1,1,1,3,3-pentafluorobutane at 0 °C under stirring and N₂ atmosphere, followed by dropping a solution of methyl chloroformate in 1,1,1,3,3-pentafluorobutane; keep at 25 °C and stir for 12 h; filter and wash the organic with water and brine; evaporate the filtrate under reduced pressure to give product PFPE-DMC. Subsequently dissolve

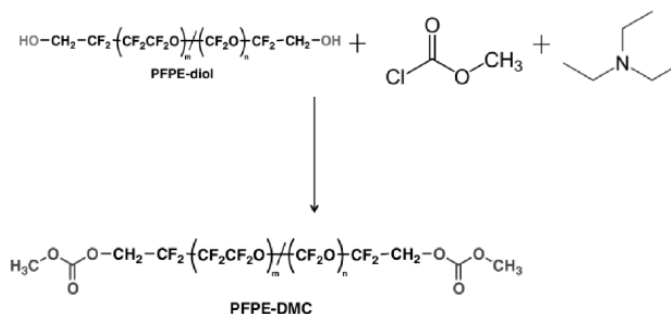


Figure 60: Synthesis method for PFPE-DMC.

Lithium bis(Trifluoromethanesulfonyl)Imide in PFPE-DMC, to make interlayer between solid garnet and cathode materials. The PFPE-DMC electrolytes will be vacuum-filled in the garnet membrane.

First principle models were constructed to evaluate the structure and energetics of the solid-solid interfaces in all-solid-state batteries. We found that Li metals have a very weak interfacial binding with Li₂CO₃, which are found on the garnet surfaces, and Li metal binds strongly with oxides materials, such as alumina. The weak interface binding may lead to forming interfacial gaps and intervals, thus a low contact area and a high interfacial resistance.

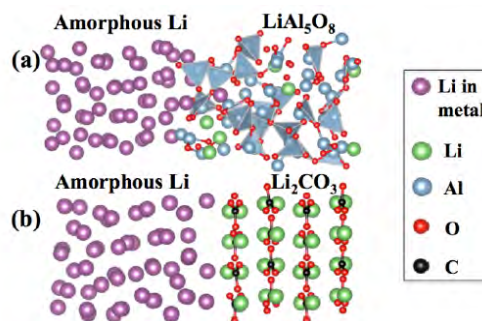


Figure 61: Li|LiAl₅O₈ and Li|Li₂CO₃ interface configurations.

Patents/Publications/Presentations

Presentations

1. Yifei Mo, “Challenges of Solid Electrolyte Materials in All-Solid-State Li-ion Batteries: Insights from First-Principles Calculations”, Materials Research Society, San Francisco, April 6-10, 2015

Task 7.5 – Nanoscale Interfacial Engineering for Stable Lithium Metal Anodes (Yi Cui, Stanford University)

PROJECT OBJECTIVE:

This study aims to render lithium metal anode with high capacity and reliability by developing chemically and mechanically stable interfacial layers between lithium metal and electrolytes, which is essential to couple with sulfur cathode for high-energy lithium-sulfur batteries. With the nanoscale interfacial engineering approach, various kinds of advanced thin films will be introduced to overcome the issues related to dendritic growth, reactive surface and virtually “infinite” volume expansion of lithium metal anode.

PROJECT IMPACT: The cycling life and stability of lithium metal anode will be dramatically increased. The success of this project, together with breakthroughs of sulfur cathode, will significantly increase the specific capacity of lithium batteries and decrease the cost as well, therefore stimulating the popularity of electric vehicles.

OUT-YEAR GOALS: Along with suppressing dendrite growth, the cycle life, Coulombic efficiency as well as the current density of lithium metal anode will be greatly improved (No dendrite growth for current density up to 3.0 mA/cm², with Coulombic efficiency >99.5%) by choosing the appropriate interfacial nanomaterial.

Milestones

1. Fabrication of interconnected carbon hollow spheres with various sizes (3/31/2015) **Completed**
2. Synthesis of layered hexagonal boron nitride and graphene with different thicknesses and defect levels (3/31/2015) **Completed**
3. Demonstrate the improved cycling life and Coulombic efficiency of lithium metal anode with nanoscale interfacial engineering (9/30/2015) **on going**
4. Demonstrate the improved cycling performance of lithium metal anode with different current density and areal capacity (9/30/2015) **on going**

Progress Report

Based on our progress achieved in last quarter, especially with hexagonal boron nitride, we demonstrated the concept of a full battery with traditional lithium cobalt oxide as the cathode and an empty copper foil as the anode. As shown in Figure 62, the copper foil covered with h-BN interfacial layer exhibits better capacity retention when the full cell is discharged from 4.2V. Though the performance is not yet ready for practical use, the successful cycling of empty anode in real scenario is still promising.

In order to optimize the performance of h-BN for stable interfacial layer of lithium metal, we tuned the growth condition of h-BN at different growth temperatures. The samples were thereafter tested at stimulated cycling condition for lithium metal plating and stripping, with total capacity of 1.0 mAh/cm² at current density of 2.0 mA/cm². As shown in Figure 63, the stability of lithium metal anode correlated positively with growth temperature of h-BN, which means better crystallinity is necessary for stable interfacial layer. However, we also found that h-BN grown at only 600°C could achieve comparable performance if the copper

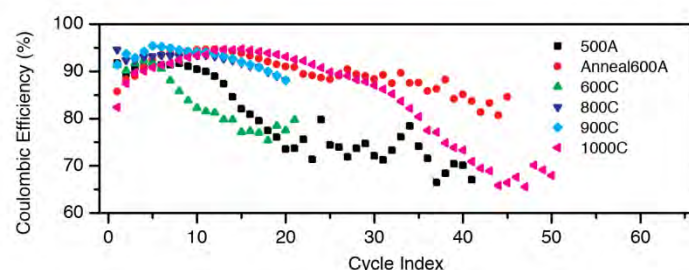


Figure 63: Stimulated lithium metal cycling test on h-BN synthesized at different temperatures. Tests were carried out with fixed lithium metal capacity of 1.0 mAh/cm² at 2.0mA/cm². The sample synthesized at 600°C on preannealed copper foil demonstrated best performance.

substrate was annealed in advance. This discovery enabled a more economic way for the synthesis of h-BN.

The proper selection of electrolyte was also found to determine the performance of interfacial layer. Comparing with traditional ethylene carbonate (EC) and diethylene carbonate (DEC) with no

additive, ether based electrolyte such as dimethoxyethane (DME) and 1,3-dioxolane (DOL), which are compatible with lithium-sulfur chemistry, shows better cycling performance with fixed lithium capacity of 1.0 mAh/cm² and current density of 0.5 mA/cm² exhibit pretty high stability, as shown in Figure 64.

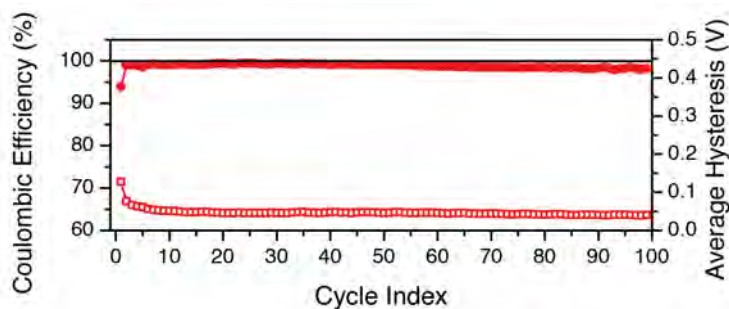


Figure 64: h-BN as interfacial layer for lithium metal cycled in ether electrolyte with LiNO₃ as additive. Stable cycling with Coulombic efficiency above 98% was achieved for more than 100 cycles, with the voltage hysteresis stable at minimum level.

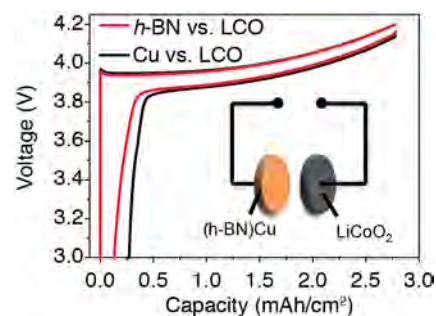


Figure 62: Conceptual Demonstration of a full cell with empty anode. The copper foil with h-BN protection exhibited better capacity retention at full cell condition.

Task 7.6 – Lithium Dendrite Suppression for Lithium-Ion Batteries (Wu Xu and Ji-Guang Zhang, Pacific Northwest National Laboratory)

PROJECT OBJECTIVE:

The objective of this project is to prevent lithium (Li) dendrite formation on Li-metal anode used in Li-metal batteries and to prevent its formation on carbon anodes used in Li-ion batteries during extreme charge conditions such as overcharge, fast charge and charge at low temperatures. We will further explore various factors that affect the morphology of Li deposition, especially at high current density conditions. These factors include solvent-cation reaction, Li-ion additive cation interaction, etc. The long-term stability of these additives also will be investigated. Novel additives will be combined with common electrolytes used in state-of-the-art Li-ion batteries to prevent Li dendrite growth in these batteries, especially when operated under extreme conditions.

PROJECT IMPACT:

Li metal is an ideal anode material for rechargeable batteries. Unfortunately, uncontrollable dendritic Li growth and limited Coulombic efficiency during Li deposition/stripping inherent in these batteries have prevented their practical applications. This work will explore the new electrolyte additives that can lead to dendrite-free Li deposition with high Coulombic efficiency. The success of this work will increase energy density of Li and Li-ion batteries and accelerate market acceptance of electrical vehicles (EV), especially for plug-in hybrid electrical vehicles (PHEV) required by the *EV Everywhere* Grand Challenge proposed by DOE/EERE.

OUT-YEAR-GOALS:

- The long term goal of the proposed work is to enable Li and Li-ion batteries with a >120 Wh/kg (for PHEVs), 1,000 deep-discharge cycles, 10-year calendar life, improved abuse tolerance, and less than 20% capacity fade over a 10-year period.

COLLABORATIONS:

- Bryant Polzin (ANL) – NCA, NMC and graphite electrodes
- Chongmin Wang (PNNL) – Characterization by TEM/SEM
- Kang Xu (ARL) – ESI-MS studies on cation-solvent interactions in electrolytes

Milestones

1. Develop electrolytes to suppress Li dendrite growth on Li metal and graphite anode and to maintain Li Coulombic efficiency over 98% (12/31/2014). **Completed**
2. Protect graphite electrode in PC-EC-based carbonate electrolytes with electrolyte additives.(3/31/2015). **Completed**
3. Demonstrate over 300 cycles for 4-V Li-metal batteries without internal short circuiting, through optimized electrolyte formulation. (6/30/2015). **Ongoing**
4. Achieve over 500 cycles for 4-V Li-metal batteries without internal short circuiting, through optimized electrolyte formulation (9/30/2015). **Ongoing**

Progress Report

In this quarter, several electrolyte additives have been investigated to suppress Li dendrite formation on graphite anode during extreme charging conditions. The studies on the protection of graphite anode in PC-EC-based carbonate electrolytes revealed several interesting findings, as summarized below.

After the graphite|NCA full-cells with two electrolytes (E1Cs and E1FEC) were tested for 100 cycles at 60°C and C/3 rate, the graphite anodes were analyzed after cleaning. The graphite from E1Cs (which contain CsPF₆) showed much cleaner surface (Figure 65a) and had a very uniform and thin (ca. 1.5 nm) SEI layer (Figure 65c), nearly the same thickness as the SEI generated at 0.3 V during the first charge (1 nm) indicating almost no change to the SEI layer. However, the graphite tested in E1FEC electrolyte shows a large amount of particles (Figure 65b) on the sample surface. The SEI layer was uneven and thick ranging from 11 to 28 nm (Figure 65d), indicating a significant increase in this SEI layer. These results demonstrated that electrolyte with CsPF₆ additive lead to thinner and higher quality SEI film on graphite as compared to the conventional SEI film-formation additives on enhancing the compatibility between the graphite anode and PC-based nonaqueous electrolytes.

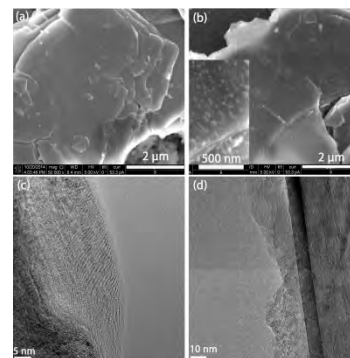


Figure 65: SEM (a, b) and TEM (c, d) images of graphite anodes from the graphite|NCA full cells with E1Cs (a, c) or E1FEC (b, d).

The structures of the solvates in the electrolyte E1Cs and other reference electrolytes and solvents were analyzed by ¹⁷O NMR and ESI-MS. The ¹⁷O NMR results (Figure 66A) and revealed that Cs⁺ caused much less chemical shift ($\delta = 1.1$ ppm) to C=O on the carbonate solvents than Li⁺ did ($\delta = 11.6$ ppm), indicating Cs⁺ has weaker coordination or less

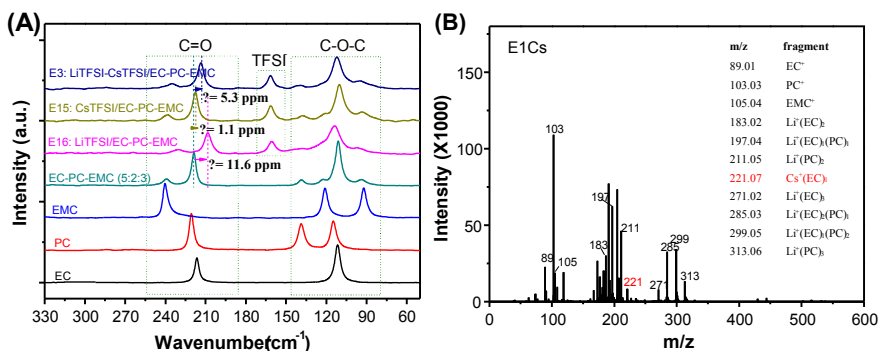


Figure 66: (A) ¹⁷O NMR spectra of various solvents and electrolytes. (B) ESI-MS results of electrolyte E1Cs.

solvation number with cyclic carbonate solvents. The ESI-MS results of the E1Cs electrolyte (Figure 66B) showed the strong peak at m/z of 221 demonstrating the existence of Cs⁺-(EC)₁; however, no Cs⁺-(PC)₁ peak at m/z 235 is detected.

By using the density functional theory (DFT) calculations, we obtained the binding energies and molecular energies of Li⁺-(sol)_n and Cs⁺-(sol)_m solvates (where 1 ≤ n, m ≤ 4). Both Cs⁺-(EC)₁ and Cs⁺-(EC)₂ had much lower LUMO energies than Li⁺-(EC)_a(PC)_b where 0 ≤ a, b ≤ 4 and a + b = 3 or 4, indicating Cs⁺-(EC)₁ and Cs⁺-(EC)₂ are easily reduced prior to the reduction of Li⁺-(sol)_n solvates. Therefore, Cs⁺-(EC)_m (m = 1-2) are preferentially reduced to form a stable SEI film prior to PC decomposition and graphite exfoliation. This is the main reason that the graphite structure is well protected and further reductive decomposition of solvents is suppressed.

Patents/Publications/Presentations

1. W. Xu, J.-G. Zhang, "Lithium dendrite prevention for lithium-ion batteries", *Presentation at 2015 BMR Program Review Meeting*, LBNL, CA, January 21, 2015.

TASK 8 – LITHIUM SULFUR BATTERIES

Summary and Highlights

Advances in Li-ion technology thus far have been stymied by challenges facing the development of high reversible capacity cathodes and stable anodes. Hence, there is a critical need for the development of alternate battery technologies with superior energy densities and cycling capabilities. Lithium-sulfur (Li-S) batteries in this regard have been flagged as the next flagship technology holding much promise due to the attractive theoretical specific energy densities of 2,567 Wh/kg. Moreover, realization of the high theoretical specific capacity of 1,675 mAh/g corresponding to the formation of Li_2S utilizing earth-abundant sulfur renders the system highly promising compared to other hitherto available cathode systems. Current research focus has thus shifted towards the development of lithium sulfur (Li-S) batteries. The system, however, suffers from major drawbacks as elucidated below.

1. Limited inherent electronic conductivity of sulfur and sulfur compound based cathodes.
2. Volumetric expansion and contraction of both the sulfur cathode and lithium anode.
3. Soluble polysulfide formation/dissolution and sluggish kinetics of subsequent conversion of polysulfides to Li_2S resulting in poor cycling life.
4. Particle fracture and delamination as a result of the repeated volumetric expansion and contraction.
5. Irreversible loss of lithium at the sulfur cathode, resulting in poor columbic efficiency.
6. High diffusivity of polysulfides in the electrolyte, resulting in plating at the anode and consequent loss of driving force i.e. drop in cell voltage.

The above major issues cause sulfur loss from the cathode leading to mechanical disintegration. Additionally, surface passivation of anode and cathode systems results in a decrease in the overall specific capacity and columbic efficiency (CE) upon cycling. As a result, the battery becomes inactive within the first few charge-discharge cycles. Achievement of stable high capacity in Li-S batteries requires execution of fundamental studies to understand the degradation mechanisms in conjunction with engineered solutions. Task 8 of the Battery Materials Research (BMR) program addresses both aspects with execution of esoteric fundamental *in situ* X-ray spectroscopy (XAS) and *in situ* electron paramagnetic resonance (EPR) studies juxtaposed with applied research comprising use of suitable additives, coatings, and exploring composite morphologies. Both ANL and LBNL use X-ray based techniques to study phase evolution and loss of CE in SeS_x during lithiation/delithiation, while understanding polysulfide formation in sulfur and polysulfides (PSL) in oligomeric polyethylene oxide (PEO) solvent, respectively. Work from PNNL, UPitt and Stanford demonstrates high areal capacity electrodes in excess of $2\text{mAh}/\text{cm}^2$. Following loading studies reported in Q1, PNNL has performed *in situ* EPR to study reaction pathways mediated by sulfur radical formation. Coating/encapsulation approaches adopted by UPitt and Stanford comprise flexible sulfur wire (FSW) electrodes coated with Li-ion conductors, and TiS_2 encapsulation of Li_2S in the latter, both ensuring polysulfide retention at sulfur cathodes. BNL work has focused on benchmarking of pouch cell testing by optimization of voltage window and study of additives such as LiI and LiNO_3 . *Ab-initio* studies at Stanford and UPitt involving calculation of binding energies and reaction pathways respectively, augment the experimental results. *Ab-initio* molecular dynamics (AIMD) simulations performed at TAMU reveal multiple details regarding electrolyte decomposition reactions and the role of soluble polysulfides (PS) on such reactions. Using Kinetic Monte-Carlo (KMC) simulations, electrode morphology evolution and mesostructured transport interaction studies were also executed. Each of these projects has a collaborative team of experts with the required skill set needed to address the *EV everywhere* challenge of 350 Wh/kg and 750Wh/l, and cycle life of at least 1000 cycles.

Task 8.1 – New Lamination and Doping Concepts for Enhanced Li – S Battery Performance (Prashant N. Kumta, University of Pittsburgh)

PROJECT OBJECTIVE: To successfully demonstrate generation of novel sulfur cathodes for Li-S batteries meeting the targeted gravimetric energy densities ≥ 350 Wh/kg and ≥ 750 Wh/l with a cost target \$125/kWh and cycle life of at least 1,000 cycles for meeting the *EV everywhere* blueprint. The proposed approach will yield sulfur cathodes with specific capacity $\geq 1,400$ mAh/g, at ≥ 2.2 V generating ~ 460 Wh/kg energy density higher than the target. Full cells meeting the required deliverables will also be made.

PROJECT IMPACT: Identification of new laminated Sulfur cathode based systems displaying higher gravimetric and volumetric energy densities than conventional lithium-ion batteries will likely result in new commercial battery systems that are more robust, capable of delivering better energy and power densities and will be more lightweight than current Li-ion battery packs. New lithium-ion conductor (LIC)-coated sulfur cathodes based strategies and configurations will also lead to more compact battery designs for the same energy and power density specifications as current Li-ion systems.

Commercialization of these new S cathode based Li-ion battery packs will basically represent a major hallmark contribution from the DOE-VTO Program.

OUT-YEAR GOALS: This is a multi-year project comprising of three major phases to be successfully completed in three years. Phase – 1 (Year 1): Synthesis, Characterization and Scale up of suitable LIC matrix materials and multilayer composite sulfur cathodes. This phase is currently ongoing. Phase – 2 (Year 2): Development of LIC coated sulfur nanoparticles, scale up of high capacity engineered LIC coated multilayer composite electrodes and doping strategies for improving electronic conductivity of sulfur. Phase-3 (Year 3): Advanced high energy density, high rate, extremely cyclable cell development.

COLLABORATIONS: The project will involve collaboration with following members with the corresponding expertise:

- Dr. Moni Datta (University of Pittsburgh) for expertise on experimental generation of nanoscale composites; Dr. Oleg Velikokhatnyi (University of Pittsburgh) for expertise on density functional theory and first principles studies; Dr. Spandan Maiti (University of Pittsburgh) for expertise on mechanical stability and computational multi-scale modeling; Dr. A. Manivannan (NETL) for expertise on x-ray photoelectron spectroscopy (XPS) for surface characterization; Dr. D. Krishnan Achary (University of Pittsburgh) for expertise on solid-state nuclear magnetic resonance (MAS-NMR) characterization.

Milestones

1. Demonstrate synthesis of finely dispersed nanoparticles of sulfur (December 2014) – **Completed**
2. Develop novel lithium-ion conducting membrane systems using *ab-initio* methods displaying impermeability to sulfur diffusion (December 2014) – **Completed**
3. Demonstrate capabilities for generation of novel sulfur 1-D, 2-D and 3-D morphologies exhibiting superior stability and capacity (June 2015) – **On-going**
4. Novel encapsulation and sheathing techniques and exploration of unique architectures and generation of 3-D composites displaying superior Li-ion conduction, reversible capacity and stability (June 2015) – **On-going**
5. Go/No-Go (October 2015) decision based on the ability to demonstrate improvement in cycling upon use of the LIC coating. – **On-course**

Progress Report

Following early work demonstrating significant improvement in capacity and stability of sulfur cathodes by using a thin layer of lithium-ion conductor (LIC) material on sulfur nanoparticles, work in the second quarter involved identification of strategies to further improve the stability by tailoring the morphology of

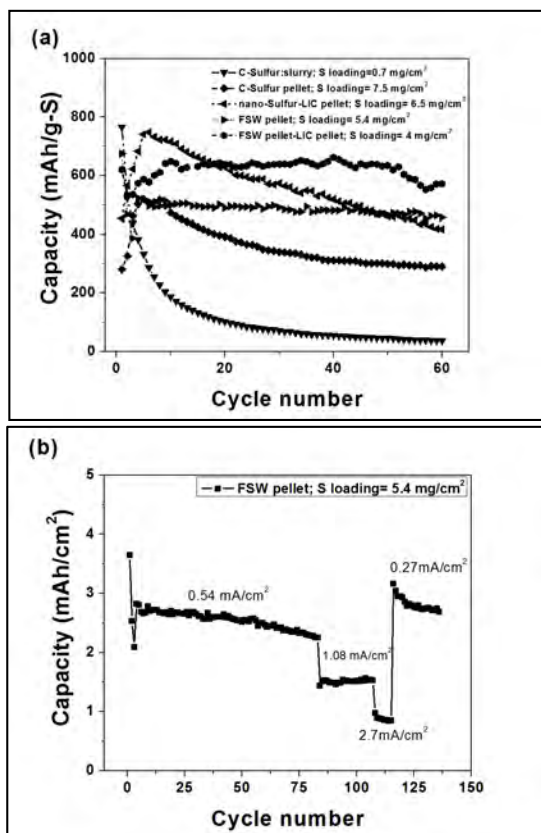


Figure 67: Comparison of cycling behavior of various FSW materials and LIC coated materials.

sulfur. Towards this end, flexible sulfur wires (FSWs) were generated using a straightforward polymer-handling method reported in Q1. The synthesis method allows for a polymer-sulfur wire morphology wherein the polymer not only acts as a structural template but helps improve cycling characteristics by aiding in polysulfide retention. Figure 67a shows the cycling behavior of various sulfur electrodes including commercial sulfur, slurry cast (C-Sulfur:slurry) and pellet-pressed (C-Sulfur pellet); nano-sulfur pellet-pressed with an LIC layer (nano-Sulfur-LIC pellet); FSWs with (FSW pellet-LIC) and without (FSW pellet) an LIC layer. The FSW pellet demonstrates superior stability and minimal capacity fade over ~75 cycles as seen in Figure 67b. The FSW pellet demonstrates an initial capacity of ~700 mAh/g which stabilizes to ~450-500 mAh/g over the first 5 cycles. Studies are on to understand this stabilization behavior which is a feature of the FSW materials. This 1st cycle irreversible loss behavior however is circumvented by the use of a thin LIC coating on the FSW as seen in Figure 67a wherein the FSW-LIC pellet maintains a stable capacity of ~650 mAh/g over 60 cycles. Electrochemical impedance analysis is ongoing to understand the improved stability and lack of 1st cycle irreversible loss in the FSW-LIC pellet material as compared to the FSW-pellet material. Optimization of

the LIC thickness and nature of the LIC coating material is an important component of subsequent studies in tandem with optimization of polymer composition to improve FSW rate capability and initial capacity will be reported in the quarterly reports to follow. No change in FY 15 key goals and expected outcomes are anticipated. As a part of the *ab-initio* studies during Q2 period the ionic conductivity of undoped Li_4SiO_4 has been studied from first principles. Using nudged elastic band method various Li-ion migration pathways have been considered and corresponding activation barriers E_a have been calculated. Corresponding results shown on Figure 68 indicate that the pathway (0-2) requires the lowest activation energy (~1 eV) for the Li-ion migration from the central position (0) to the Li-vacancy (2). All other pathways demonstrate higher activation barriers (up to 2.2 eV). Introduction of dopants, such as B, Al, Mg, Ca, or F could create Li-ion vacancies as well as

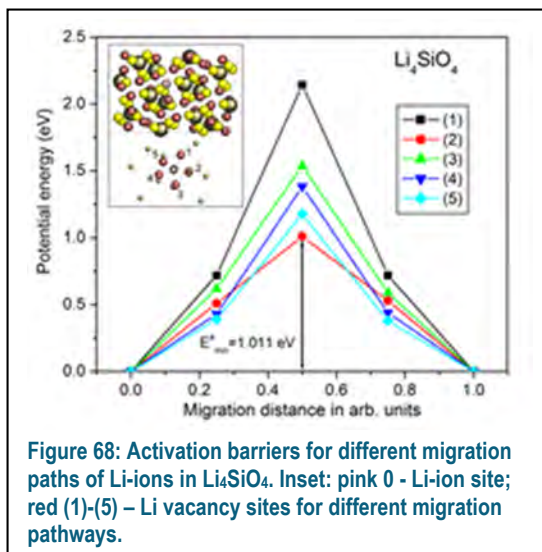


Figure 68: Activation barriers for different migration paths of Li-ions in Li_4SiO_4 . Inset: pink 0 - Li-ion site; red (1)-(5) - Li vacancy sites for different migration pathways.

decrease the activation barriers for the ionic migration, thus improving the overall ionic mobility. A systematic study of effects of various dopants on ionic migration in lithium orthosilicate is planned to be conducted in the close future.

Q2 Patents/Publications/Presentations

1. P. J. Hanumantha, B. Gattu, et al., Journal of The Electrochemical Society, 2014, 161, A1173-A1180.
2. P.J. Hanumantha, B. Gattu, P.M. Shanthi, P.N. Kumta, Provosional Patent, 2015, Application number: 62132014.

Task 8.2 – Simulations and X-ray Spectroscopy of Li-S Chemistry (Nitash Balsara, Lawrence Berkeley National Laboratory)

PROJECT OBJECTIVE: Lithium-sulfur cells are attractive targets for energy storage applications as their theoretical specific energy of 2,600 Wh/kg is much greater than the theoretical specific energy of current lithium-ion batteries. Unfortunately, the cycle-life of lithium-sulfur cells is limited due to migration of species generated at the sulfur cathode. These species, collectively known as polysulfides, can transform spontaneously, depending on the environment, and it has thus proven difficult to determine the nature of redox reactions that occur at the sulfur electrode. The objective of this project is to use X-ray spectroscopy to track species formation and consumption during charge-discharge reactions in a lithium-sulfur cell. Molecular simulations will be used to obtain X-ray spectroscopy signatures of different polysulfide species, and to determine reaction pathways and diffusion in the sulfur cathode. The long-term objective of this project is to use the mechanistic information to build high specific energy lithium-sulfur cells.

PROJECT IMPACT: Enabling rechargeable lithium-sulfur cells has the potential to change the landscape of rechargeable batteries for large-scale applications beyond personal electronics due to: (1) high specific energy, (2) simplicity and low cost of cathode (the most expensive component of current lithium-ion batteries), and (3) earth abundance of sulfur. The proposed diagnostic approach also has significant potential impact as it represents a new path for determining the species that form during charge-discharge reactions in a battery electrode

OUT-YEAR GOALS: Year 1 Goals: Simulations of sulfur and polysulfides (PSL) in oligomeric polyethylene oxide (PEO) solvent. Prediction of X-ray spectroscopy signatures of PSL/PEO mixtures. Measurement of X-ray spectroscopy signatures PSL/PEO mixtures. Year 2 Goals: Use comparisons between theory and experiment to refine simulation parameters. Determine speciation in PSL/PEO mixtures without resorting to adhoc assumptions. Year 3 Goals: Build an all-solid lithium-sulfur cell that enables measurement of X-ray spectra *in situ*. Conduct simulations of reduction of sulfur cathode. Year 4 Goals: Use comparisons between theory and experiment to determine the mechanism of sulfur reduction and Li₂S oxidation in all-solid lithium-sulfur cell. Use this information to build lithium-sulfur cells with improved life-time.

COLLABORATIONS:

Tsu-Chien Weng, Dimosthenis Sokaras and Dennis Nordlund, Stanford Synchrotron Radiation Lightsource, SLAC National Accelerator Laboratory, Stanford, California 94720, USA.

Milestones

1. Extend theoretical calculations of XAS to finite polysulfide concentrations. (12/1/14) **Completed**
2. Experimental study of the effect of polysulfide concentration on XAS spectra. (2/15/15) **On schedule**
3. Quantitative comparison of experimental and theoretical XAS spectra. (5/20/15) **On schedule**
4. Build and test cell for *in situ* XAS analysis. (8/23/15) **On schedule**

Progress Report

Milestones (1) has been completed.

Milestone (2) is underway. Experimental spectra of polysulfide species at various concentrations will be compared to analogous theoretical systems. Additionally, the experimental spectra/temperature effects on experimental polysulfide solution composition will also be compared to theoretical results.

Milestone (3) is underway. XAS spectra of three Li-S cells discharged to 2.25V, 2.00V and 1.50V were previously obtained and shown in the Q1 2015 report. The experimental XAS were interpreted using theoretical spectra for various lithium polysulfide species. These species were fit to the experimental spectra through linear combinations using least-square regression and the compositions are shown below. The theoretical work reveals that lithium polysulfide radical species are present in the electrolyte after initial discharge and decrease in presence as time moves on. XAS gives us the ability to distinguish different polysulfide radical species. Shown below are the fittings of the experimental spectra with theoretical spectra, along with the composition breakdown at each voltage.

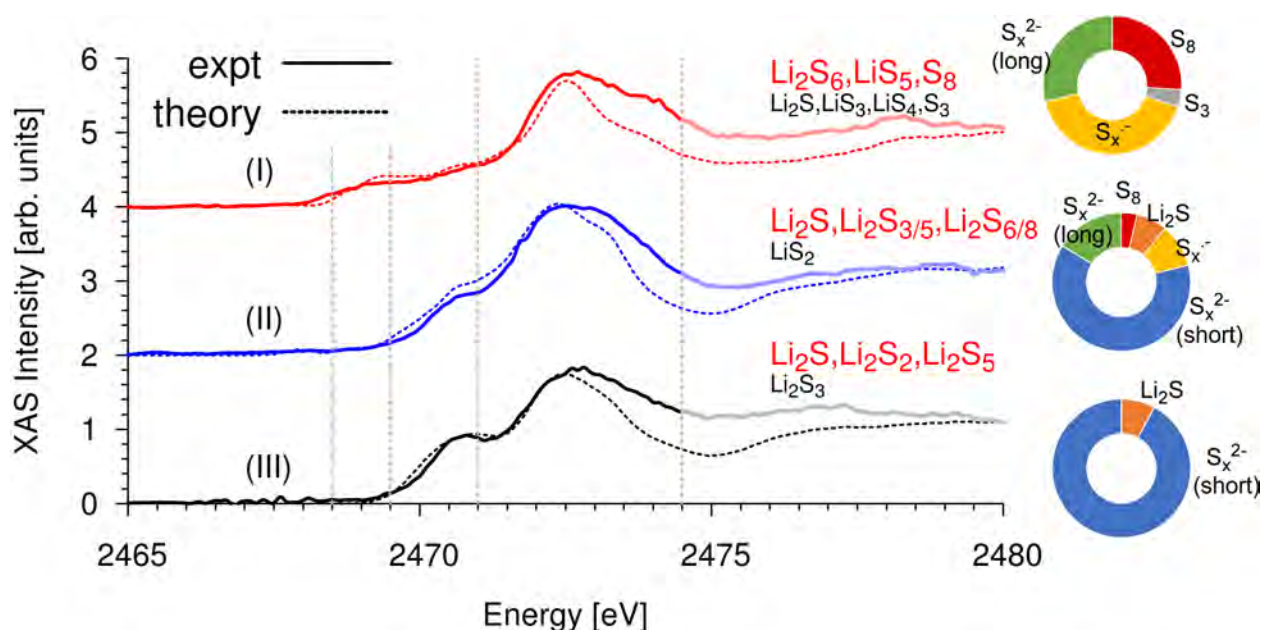


Figure 69: Comparison of the best fit spectra from theory (dashed lines) compared to experiments (solid lines) for each of the three voltages (spectrum I – 2.25V, spectrum II – 2.02 V, spectrum III – 1.50 V). The isolated species used to obtain the best fit are also indicated: the major components are in red, while the minor components are in black. *Right insets:* Relative ratios types of sulfur species (S_8 (red), Li_2S (orange), neutrals: S_3 (grey), radicals (yellow) and dianions) that constitute each best fit spectra from theory. We separately consider short (S_2^{2-} to S_2^{5-} , blue) and long ($S_6^{2-}/S_7^{2-}/S_8^{2-}$, green) polysulfide dianions.

Milestone (4) is underway. Numerous Li-S pouch cells adapted for *in situ* soft X-ray XAS have been designed and tested. Heating stages for XAS at beamlines 9.3.1 of ALS and 4-3 of SSRL have also been built and tested with Li-S cells and are ready for use. Now we await beam time to perform *in situ* studies of Li-S chemistry.

Q2 Patents/Publications/Presentations

Presentations

1. Kevin Wujcik, American Physical Society March Meeting, San Antonio, TX, “X-ray absorption spectroscopy of lithium sulfur battery reaction intermediates,” March 6, 2015
2. Tod Pascal, American Physical Society March Meeting, San Antonio, TX, “X-ray absorption spectroscopy as a probe of dissolved polysulfides in lithium sulfur batteries,” March 6, 2015
3. Nitash Balsara, “X-ray Absorption Spectroscopy of Lithium Sulfur Battery Reaction Intermediates”, Symposium on Energy Storage, National Meeting of the American Chemical Society, Denver, Colorado, March 24, 2015
4. Nitash Balsara, American Physical Society March Meeting, San Antonio, TX, “Segmental Interactions between Polymers and Small Molecules in Batteries and Biofuel Purification”, March 2, 2015

Publications

1. “X-ray spectroscopy as a probe for lithium polysulfide radicals”, Tod A Pascal, CD Pemmaraju and David Prendergast, Phys. Chem. Chem. Phys. 2015, 17, 7743-7753

Task 8.3 – Novel Chemistry: Lithium Selenium and Selenium Sulfur Couple (Khalil Amine, Argonne National Laboratory)

PROJECT OBJECTIVE: The objective of this project is to develop a novel SeS_x cathode material for rechargeable lithium batteries with high energy density, long life along with low cost and high safety.

PROJECT IMPACT: Developing a new battery chemistry that is promising to support the goal of PHEV and EV applications.

OUT-YEAR GOALS: When this new cathode is optimized, the following results can be achieved:

- A cell with nominal voltage of 2 V and energy density of 600 Wh/kg;
- A battery capable of operating for 500 cycles with low capacity fade.

COLLABORATIONS: Prof. Chunsheng Wang of University of Maryland
Dr. Yang Ren and Dr. Chengjun Sun of APS at ANL

Milestones

The following are the milestones for each Quarter during FY15:

1. Investigate the phase stability of SeS_x .
2. Confine Se, SeS in different carbon matrix including porous organic polymer to suppress the dissolution of lithium polysulfides and polyselenide.
3. Understand the specific interaction between S (and Se) with porous substrate and their dissolution in different solvents.
4. Develop new capsulation strategy to further suppress the dissolution of lithium polysulfides or polyselenide.

Progress Report

In situ X-ray diffraction (XRD) and X-ray absorption spectroscopy (XAS) were applied to track the Se phase change, oxidation states, and phase distribution during electrochemical cycling. The *in situ* XRD patterns and the cycling profile are shown in Figure 70a and Figure 70b, respectively. In Figure 70a, the very strong peaks at $2\theta = 2.74^\circ$, 3.16° , 4.47° , 2.57° , and 3.65° are due to the Al current collector and the Li anode.

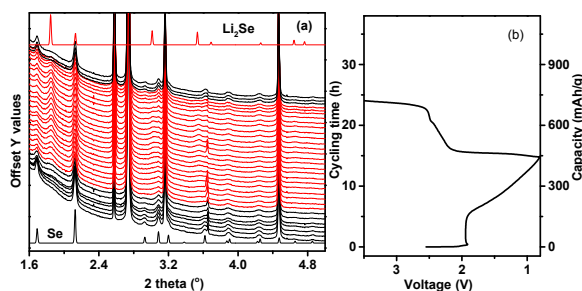


Figure 70: *In situ* high-energy XRD characterization of Li-Se cell in GenII electrolyte cycled between 0.8 and 3.5 V with a charging rate of 30 mA/g: (a) XRD pattern of the cell during cycling and the reference material Se and Li₂Se and (b) voltage profile.

We focus here on the Se characteristic peaks at 1.69 and 2.13° and the Li₂Se peak at 1.85° to monitor the phase transition. With discharging, the intensity of the Se peak keeps decreasing; Li₂Se starts to appear at 1.86 V and keeps increasing to the end of discharge. The discharge capacity is 445 mAh/g at the charging rate of 30 mA/g. A small amount of Se remains by the end of discharge. The XRD patterns proved that Se is partially reduced into Li₂Se by the end of discharge, and then Li₂Se is oxidized into Se at the end of charge without any intermediate phases formed during cycling.

Although XRD is a powerful technique in determining the crystalline phase change, it alone may not be conclusive in determining the phase change in a battery system, considering the complexity of a battery system including both solid and liquid phases. Therefore, we selected *in situ* X-ray absorption near edge structure (XANES) spectroscopy to monitor the oxidation state changes during cell cycling, which can provide reliable information on all phases.

We carried out *in situ* X-ray near edge absorption spectroscopy (XANES) measurements on a pouch cell made with Gen-II electrolyte and cycled at a rate of 110 mA/g. The Gen-II electrolyte was a solution of 1.2M LiPF₆ in mixture solvent of ethylene carbonate (EC) and ethyl methyl carbonate (EMC) with a mass ratio of 3:7. The selenium K-edge absorption, at 12,658 eV, arises from the transition of Se 1s core electrons to the unoccupied 4p states. The Se K-edge of Li₂Se shifts to a higher energy (to 12,660 eV). The abnormal shifts of the Li₂Se Se-edge toward higher energy could be explained by the reduced screening effect (see Figure 71). The linear combination analysis of *in situ* XANES data shows that there were still substantial amount of Li₂Se left after the initial charge to 3.5 V vs. Li⁺/Li, leading to low initial columbic efficiency.

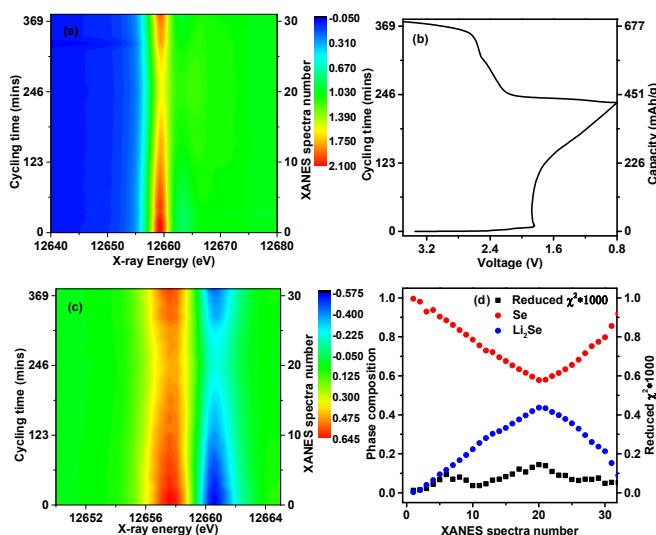


Figure 71: *In situ* XANES measurement for Li-Se pouch cell in GenII electrolyte: (a) normalized XANES spectra of the cycling cell, (b) voltage profile, (c) derivative of normalized XANES spectra, and (d) linear combination fitting of residue values and corresponding phase compositions in different state of charge/discharge.

In order to identify the root of the low initial columbic efficiency, a similar experiment was carried out using an ether-based electrolyte (see Figure 72). A much better reversibility was achieved by using ether-based electrolyte. This implies that the selection of the solvent can also have significant impact on the charge/discharge mechanism of Li-Se batteries. New strategies to immobilize lithium polyselenides to further improve the overall performance will be explored in the coming quarter. Also, the experiment to prove that no dissolution takes place when using carbonate based electrolyte will also be carried out.

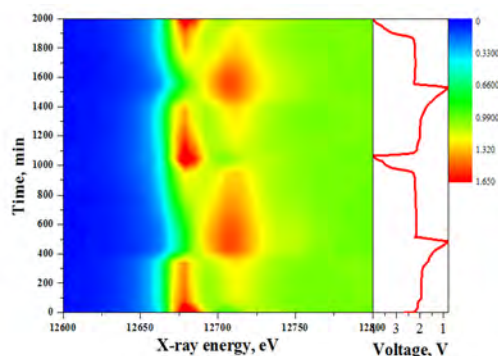


Figure 72: *In situ* XANES measurement for Li-Se cell using an ether-based electrolyte.

Task 8.4 – Multi-Functional Cathode Additives (MFCA) for Li-S Battery Technology (Hong Gan, Brookhaven National Laboratory and Co-PI Esther Takeuchi, Brookhaven National Laboratory and Stony Brook University)

PROJECT OBJECTIVE: Develop a low cost battery technology for PEV application utilizing Li-S electrochemical system by incorporating multifunctional cathode additives (MFCA), consistent with the long-term goals of DOE *EV Everywhere* Blueprint.

PROJECT IMPACT: The Li-S battery system has gained significant interest due to its low material cost potential (35% cathode cost reduction over Li-ion) and its attractive 2.8x (volumetric) to 6.4x (gravimetric) higher theoretical energy density compared to conventional Li-ion benchmark systems. Commercialization of this technology requires overcoming several technical challenges. This effort will focus on improving the cathode energy density, power capability and cycling stability by introducing multifunctional cathode additives (MFCA). The primary deliverable of this project is to identify and characterize the best MFCA for Li-S cell technology development.

APPROACH: Transition metal sulfides are evaluated as cathode additives in Sulfur cathodes due to their high electronic conductivity and chemical compatibility with the Sulfur cell system. Electrochemically active additives will also be selected for this investigation to further improve the energy density of the Sulfur cell system. In the first year, the team will evaluate the transition metal sulfide cathode cells and Sulfur cathode cells individually to establish the baseline. Then the interaction between transition metal sulfide additives and the Sulfur electrode will be investigated. In parallel, commercially unavailable selected additives will be synthesized for electrochemical cell interaction studies.

OUT-YEAR GOALS: This is a multi-year project comprised of two major phases to be successfully completed in three years. Phase 1 includes cathode and MFCA investigation, and Phase 2 will include cell component interaction studies and full cell optimization. The work scope for year 1 will focus on the cathode and cathode additive studies. The proof of concept and feasibility studies will be completed for the Multi Functional Cathode Additives. By year-end, multiple types of additives will be identified and prepared, including the synthesis of the non-commercially available additives. The electrochemical testing of all selected MFCA will be initiated.

COLLABORATIONS: Amy Marschilok (SBU), Kenneth Takeuchi (SBU), Dong Su (BNL) and Can Erdonmez (BNL).

Milestones

1. Baseline Li/MFCA cell demonstration with selected transition metal sulfides. (Q1) (**Complete**)
2. Baseline Li/S cell demonstration with Sulfur and/or Li₂S cathode. (Q2) (**Complete**)
3. Li/Sulfur-MFCA concept cell demonstration for cathode-MFCA interaction. (Q3) (**Initiated**)
4. Synthesis of selected non-commercial MFCA. (Q4) (**Initiated**)

Progress Report

Benchmark Li-Sulfur Coin Cells: For this task, Li-Sulfur coin cells are tested using either Sulfur or Lithium Sulfide (Li_2S) as the starting cathode. Several factors, such as electrode processing conditions, electrolyte additives, and testing conditions, are studied. As benchmark, Sulfur cathode, carbon black and PVDF binder are used without any special treatment.

Figure 73 shows the Li/Sulfur coin cell 1st cycle voltage profile under a C/10 rate between 1.0V to 3.0V. Two typical Li/Sulfur cell discharge voltage plateaus at $\sim 2.3\text{V}$ and $\sim 2.1\text{V}$ are observed. Up to 847 mAh/g Sulfur capacity was delivered, which is $\sim 50\%$ of the theoretical capacity ($\sim 46\%$ to 1.8V cut off). The Coulombic efficiency is improved from $\sim 60\%$ to above 90% by using LiNO_3 additive in the electrolyte. Regardless of the presence of LiNO_3 additive, the cells showed similar capacity fade rate during cycling test (Figure 74). The results are consistent with literature-reported observation (Nature Communications|4:1481|DOI:10.1038/ncomms2513; *J. Phys. Chem. C* 2011, 115, 15703–15709).

Figure 75 presents the activation of coin cells using Li_2S as cathode. Without electrolyte additives, the Li_2S cathode cannot be activated when charging to 3.6V. Around 15% of cell theoretical capacity can be achieved when LiNO_3 is present in the electrolyte. However, when LiI additive was used, up to 57% (669 mAh/g Li_2S) of theoretical capacity can be obtained at C/40 activation cycle between 1.8V to 3.2V. Figure 76 shows the C/10 cycling test results of Li/ Li_2S coin cells containing LiNO_3 and LiI additives. Over 20 cycles, the capacity dropped to below 50% of the 2nd cycle that is also consistent with literature-reported observation (*J. Phys. Chem. Lett.* 2014, 5, 915-918).

During this period, we have established the coin cell capability in testing the benchmark Sulfur cells either with Sulfur or with Li_2S as cathode starting material. Over 50% of cathode utilization has been achieved for both systems. LiNO_3 additive is beneficial to maintain high Coulombic efficiency during cell cycling, while LiI is needed to activate coin cells with Li_2S as starting cathode. The interaction between these electrolyte additives and the Multi-Functional Cathode Additives (MFCA) needs to be considered in future MFCA studies.

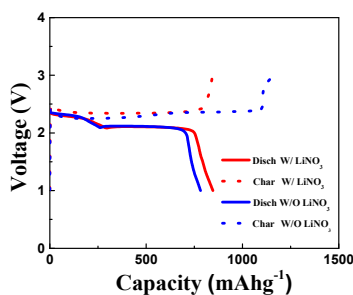


Figure 73: Li/Sulfur Cycling Voltage Profiles

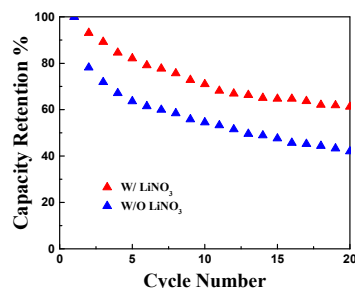
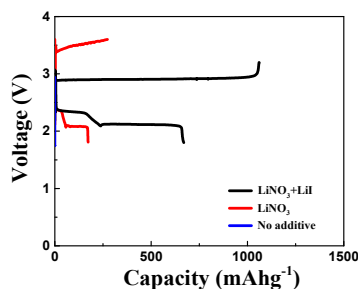
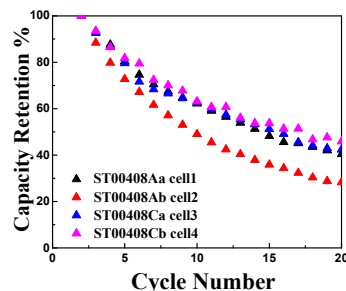


Figure 74: Li/Sulfur Cell Cycling Test

Figure 75: Li/ Li_2S Cycling Voltage ProfilesFigure 76: Li/ Li_2S Cell Cycling Test

Patents/Publications/Presentations

None this quarter.

Task 8.5 – Development of High-Energy Lithium-Sulfur Batteries (Jie Xiao and Jun Liu, Pacific Northwest National Laboratory)

PROJECT OBJECTIVE:

The objective of this project is to develop high-energy, low-cost lithium sulfur (Li-S) batteries with long lifespan. All proposed work will employ thick sulfur cathode (≥ 2 mAh/cm² of sulfur) at a relevant scale for practical applications. The diffusion process of soluble polysulfide out of the thick cathode will be revisited to investigate the cell failure mechanism at different cycling. Alternative anode will be explored to address the lithium anode issue. The fundamental reaction mechanism of polysulfide under the electrical field will be explored by applying advanced characterization techniques to accelerate the development of Li-S battery technology.

PROJECT IMPACT:

The theoretical specific energy of Li-S batteries is $\sim 2,300$ Wh/kg, which is almost three times higher than that of state-of-art Li-ion batteries. The major challenge for Li-S batteries is polysulfide shuttle reactions, which initiate a series of chain reactions that significantly shorten the battery life. The proposed work will design novel approaches to enable Li-S battery technology and accelerate market acceptance of long-range electrical vehicles (EV) required by the *EV Everywhere* Grand Challenge proposed by DOE/EERE.

OUT-YEAR-GOALS:

- Fabricate Li-S pouch cells with thick electrodes to understand sulfur chemistry/electrochemistry in the environments similar to the real application.
- Leverage the Li-metal protection project funded by DOE and PNNL's advanced characterization facilities to accelerate the development of Li-S battery technology.
- Develop Li-S batteries with a specific energy of 400 Wh/kg at cell level, 1,000 deep-discharge cycles, improved abuse tolerance, and less than 20% capacity fade over a 10-year period to accelerate commercialization of electrical vehicles.

COLLABORATIONS:

- Dr. Xiao-Qing Yang (LBNL) – *In situ* characterization
- Dr. Bryant Polzin (ANL) – Electrode fabrication
- Dr. Xingcheng Xiao (GM) – materials testing

Milestones

1. Optimization of sulfur loading to reach 3-4 mAh/cm² areal specific capacity on the cathode (12/31/2014). **Complete**
2. Complete the investigation on the fundamental reaction mechanism of Li-S batteries (3/31/2015). **Complete**
3. Identify alternative anode to stabilize the interface reactions on the anode side (6/30/2014). **On going**
4. Demonstrate the stable cycling of sulfur batteries (2-4 mAh/cm²) with less than 20% degradation for 200 cycles. (9/30/2015). **On going**

Progress Report

The Q2 milestone was completed in this quarter. The fundamental reaction mechanism of Li-S cells was systematically investigated by using *in situ* electron paramagnetic resonance (EPR) technique. The key findings from the mechanistic study of polysulfides are summarized below:

1. Sulfur radicals were periodically generated and never completely disappeared during cycling. These radicals functioned as reaction media to facilitate the electrochemical processes.
2. The reaction pathway was very different between the discharge and charge processes of Li-S cells.
3. The reason why alkyl carbonate-based electrolyte was incompatible with Li-S cells was identified.

A specifically designed *in situ* EPR cell is shown in Figure 77a. The detected EPR resonance signals were assigned to S_3^{*-} radicals, which showed periodic changes with changing potentials (time) in Figure 77b. S_3^{*-} was identified throughout the whole cycling, indicating the temporal equilibrium among different polysulfides (Figure 77c), instead of producing a single polysulfide component at each different potential. The equilibria between S_6^{2-} and S_3^{*-} always existed and shifted continuously at different potentials. S_6^{2-} preferred to stay at relatively high potential (> 2.1 V), while S_3^{*-} was the preferred form at low potentials (≤ 2.1 V). The chemical and electrochemical reactions in the Li-S cell drove each other to move forward via using sulfur radicals as the media. Completely different discharge-charge reaction pathways were proposed (Figure 77c), which well explained the mismatch of discharge and charge curves regardless of the current densities.

In addition, the identification of sulfur radicals also explained why traditional alkyl carbonate-based electrolyte such as ethylene carbonate (EC) and dimethyl carbonate (DMC) cannot be used in Li-S batteries. This was because S_3^{*-} easily reacted with the alkyl carbonates through nucleophilic attack and converted the discharge products into the inactive byproducts. Similar phenomenon was also found in Li-O₂ batteries, in which O_2^{*-} was generated.

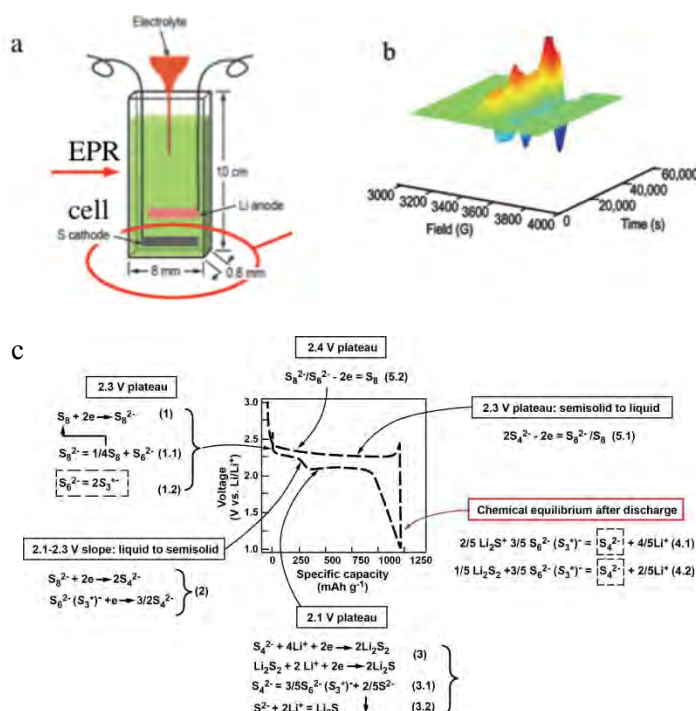


Figure 77: a) *In situ* EPR cell for Li-S batteries. b) 3D plot of EPR spectra in a functioning Li-S cell vs. time during cyclic voltammetry (CV) scan at 0.2 mV/s between 1-3 V. c) Proposed discharge-charge reaction mechanisms for Li-S batteries.

Q2 Patents/Publications/Presentations

1. Q. Wang, J. Zheng, E. Walter, H. Pan, D. Lv, P. Zuo, H. Chen, Z. D. Deng, B. Y. Liaw, X. Yu, X.-Q. Yang, J.-G. Zhang, J. Liu and J. Xiao “Direct Observation of Sulfur Radicals as Reaction Media in Lithium Sulfur Batteries”, *J. Electrochem. Soc.*, **2015**, 162, A474-A478.
2. D. Lv, J. Zheng, Q. Li, X. Xie, S. Ferrara, Z. Nie, L. B. Mehdi, N. D. Browning, J.-G. Zhang, G. L. Graff, J. Liu and J. Xiao, “High Energy Density Lithium–Sulfur Batteries: Challenges of Thick Sulfur Cathodes”, *Adv. Energy Mater.*, **2015**, DOI: 10.1002/aenm.201402290.

Task 8.6 – Nanostructured Design of Sulfur Cathodes for High Energy Lithium-Sulfur Batteries (Yi Cui, Stanford University)

PROJECT OBJECTIVE: The charge capacity limitations of conventional transition metal oxide cathodes are overcome by designing optimized nano-architected sulfur cathodes.

This study aims to enable sulfur cathodes with high capacity and long cycle life by developing sulfur cathodes from the perspective of nanostructured materials design, which will be used to combine with lithium metal anodes to generate high-energy lithium-sulfur batteries. Novel sulfur nanostructures as well as multifunctional coatings will be designed and fabricated to overcome the issues related to volume expansion, polysulfide dissolution and insulating nature of sulfur.

PROJECT IMPACT: The capacity and the cycling stability of sulfur cathode will be dramatically increased. This project's success will make lithium-sulfur batteries practicable to power electric vehicles and decrease the high cost of batteries.

OUT-YEAR GOALS: The cycle life, capacity retention as well as the capacity loading of sulfur cathodes will be greatly improved (200 cycles with 80% capacity retention, $>0.3 \text{ mAh/cm}^2$ capacity loading) by optimizing material design, synthesis and electrode assembly.

COLLABORATIONS:

- BMR program PI's
- SLAC: *In situ* X-ray, Dr. Michael Toney.
- Stanford: Prof. Nix, mechanics; Prof. Bao, materials.

Milestones

1. Demonstrate synthesis to generate monodisperse sulfur nanoparticles with/without hollow space (Oct-13) **Completed**
2. Develop surface coating with one type of polymers and one type of inorganic materials (Jan-14) **Completed**
3. Develop surface coating with several types of polymers; understand amphiphilic interaction of sulfur and sulfide species (Apr-14) **Completed**
4. Demonstrate sulfur cathodes with 200 cycles with 80% capacity retention and 0.3 mAh/cm^2 capacity loading (July-14) **Completed**
5. Demonstrate Li_2S cathodes capped by layered metal disulfides (Dec-14) **Completed**

Progress Report

Previously, we designed high-performance lithium sulfide (Li_2S) cathodes based on encapsulation using titanium disulfide (TiS_2). TiS_2 possesses a combination of high electronic conductivity ($\sim 10^3 \text{ S/cm}$) and polar Ti–S groups which can potentially interact strongly with $\text{Li}_2\text{S}/\text{Li}_2\text{S}_n$ species. Based on this work, we further demonstrated the generality of using 2D layered transition metal disulfides as encapsulation materials for Li_2S cathodes. We synthesized $\text{Li}_2\text{S}@ZrS_2$ and $\text{Li}_2\text{S}@VS_2$ core-shell structures (Figure 78a,b) using the same reaction mechanism: $\text{MCl}_4 + 2\text{Li}_2\text{S} \rightarrow \text{MS}_2 + 4\text{LiCl}$ ($\text{M} = \text{Ti}, \text{Zr}$ and V). The conductivities of the $\text{Li}_2\text{S}@ZrS_2$ and $\text{Li}_2\text{S}@VS_2$ structures were measured to be 4.0×10^{-9} and $3.8 \times 10^{-9} \text{ S cm}^{-1}$ respectively, which are about 4 orders of magnitude higher than those of bare Li_2S ($10^{-13} \text{ S cm}^{-1}$). The results of *ab initio* simulations also show strong binding of Li_2S to ZrS_2 and VS_2 , with calculated binding energies of 2.70 and 2.94 eV, respectively (Figure 78c,d), which are about 9 to 10 times higher than that between Li_2S and carbon-based graphene (0.29 eV). Working electrodes on aluminum foil were prepared for the $\text{Li}_2\text{S}@ZrS_2$ and $\text{Li}_2\text{S}@VS_2$ structures and the cells were subject to galvanostatic cycling. Using $\sim 1 \text{ mg}_{\text{Li}_2\text{S}} \text{ cm}^{-2}$, the $\text{Li}_2\text{S}@ZrS_2$ and $\text{Li}_2\text{S}@VS_2$ cathodes exhibited high initial specific capacities of 777 and $747 \text{ mAh g}^{-1}_{\text{Li}_2\text{S}}$ respectively at 0.2C, with capacity retentions of 85% and 86%, respectively, after 100 cycles (Figure 78e), both of which are much higher than in the case of bare Li_2S cathodes (66% after 100 cycles). Both the $\text{Li}_2\text{S}@ZrS_2$ and $\text{Li}_2\text{S}@VS_2$ cathodes were also subject to cycling under high mass loading conditions. Using $4.8 \text{ mg}_{\text{Li}_2\text{S}} \text{ cm}^{-2}$ for the $\text{Li}_2\text{S}@ZrS_2$ cathodes and current densities of 0.1, 0.3 and 0.6 mA cm^{-2} , we achieve areal capacities of 2.7, 2.0 and 1.7 mAh cm^{-2} respectively (Figure 78f). The areal capacities attained are similarly high in the case of $\text{Li}_2\text{S}@VS_2$ cathodes containing $5.0 \text{ mg}_{\text{Li}_2\text{S}} \text{ cm}^{-2}$: 2.7, 1.9 and 1.6 mAh cm^{-2} respectively at the above-mentioned current densities (Figure 78f).

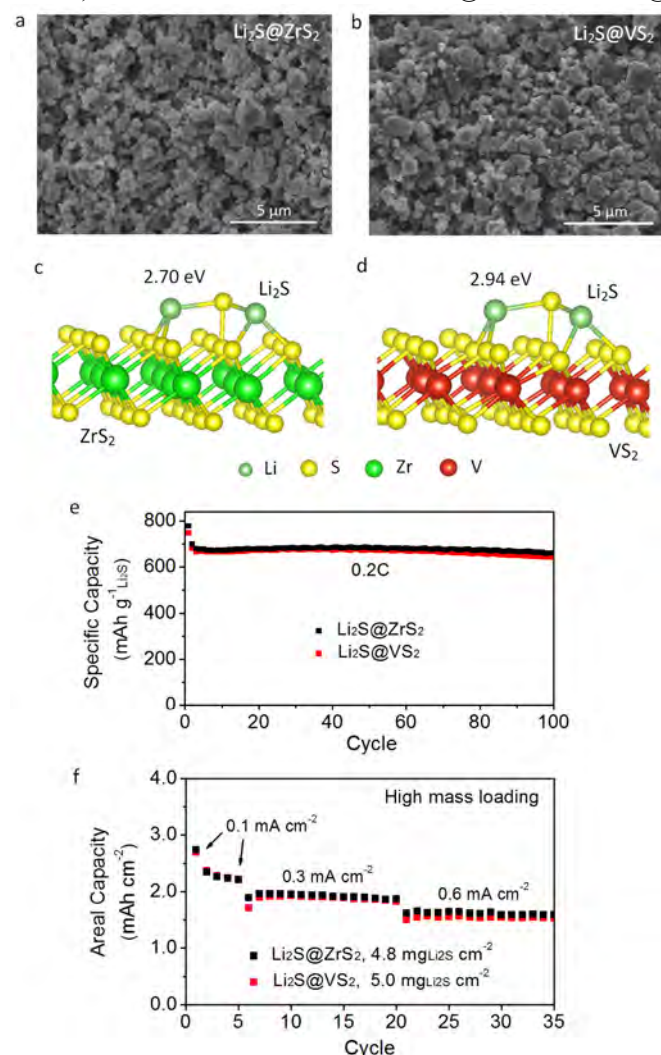


Figure 78: (a,b) SEM images of (a) $\text{Li}_2\text{S}@ZrS_2$ and (b) $\text{Li}_2\text{S}@VS_2$ structures. (c,d) *Ab initio* simulations showing the most stable binding configuration of Li_2S with a single layer of (c) ZrS_2 and (d) VS_2 with calculated binding energies of 2.70 and 2.94 eV respectively. (e) Specific capacity of $\text{Li}_2\text{S}@ZrS_2$ and $\text{Li}_2\text{S}@VS_2$ cathodes cycled at 0.2C ($1\text{C} = 1,166 \text{ mA g}^{-1}_{\text{Li}_2\text{S}}$). (f) Areal capacity of $\text{Li}_2\text{S}@ZrS_2$ and $\text{Li}_2\text{S}@VS_2$ cathodes with high mass loading cycled from 0.1 to 0.6 mA cm^{-2} .

Patents/Publications/Presentations

1. Z. W. Seh, J. H. Yu, W. Li, P. C. Hsu, H. Wang, Y. Sun, H. Yao, Q. Zhang, Y. Cui, "Two-Dimensional Layered Transition Metal Disulphides for Effective Encapsulation of High-Capacity Lithium Sulphide Cathodes." *Nature Communications* **2014**, 5: 5017.

Task 8.7 – Addressing Internal “Shuttle” Effect: Electrolyte Design and Cathode Morphology Evolution in Li-S Batteries (Perla Balbuena, Texas A&M University)

PROJECT OBJECTIVE: The objective of this project is to overcome the lithium-metal anode deterioration issues through advanced Li-anode protection/stabilization strategies including (i) *in situ* chemical formation of a protective passivation layer and (ii) alleviation of the “aggressiveness” of the environment at the anode by minimizing the polysulfide shuttle with advanced cathode structure design.

PROJECT IMPACT: Through formulation of alternative electrolyte chemistries and design, fabrication, and test of improved cathode architectures, it is expected that this project will deliver Li/S cells operating for 500 cycles at efficiency greater than 80%.

APPROACH: A mesoscale model including different realizations of electrode mesoporous structures generated based on a stochastic reconstruction method will allow virtual screening of the cathode microstructural features and the corresponding effects on electronic/ionic conductivity and morphological evolution. Interfacial reactions at the anode due to the presence of polysulfide species will be characterized with *ab initio* methods. For the cathode interfacial reactions, data and detailed structural and energetic information obtained from atomistic-level studies will be used in a mesoscopic-level analysis. A novel sonochemical fabrication method is expected to generate controlled cathode mesoporous structures that will be tested along with new electrolyte formulations based on the knowledge gained from the mesoscale and atomistic modeling efforts.

OUT-YEAR GOALS: By determining reasons for successes or failures of specific electrolyte chemistries, and assessing relative effects of composite cathode microstructure and internal shuttle chemistry vs. that of electrolyte chemistry on cell performance, expected results are: 1) Develop an improved understanding of the Li/S chemistry and ways to control it; 2) Develop electrolyte formulations able to stabilize the Li anode; 3) Develop new composite cathode microstructures with enhanced cathode performance; 4) Develop a Li/S cell operating for 500 cycles at an efficiency > 80%.

COLLABORATIONS: This is a collaborative project combining first-principles modelling (Perla Balbuena, Texas A&M University), mesoscopic level modelling (Partha Mukherjee, Texas A&M University), and synthesis, fabrication, and test of Li/S materials and cells (Vilas Pol, Purdue University).

Milestones

1. Synthesis of the C/S cathode hybrid materials: Develop lab-scale Li-S composite.(Dec-14)
Completed- Perform advanced characterization- **Completed** (Mar-15)
2. Determination of the structure of the PS/Li Interface: Characterization of thermodynamics of nucleation and growth of PS deposits on the Li surface. (Mar-15) **Completed**
3. Determination of the chemistry of the C/S composite cathode: Characterize dissolution, reduction, and lithiation of S in the composite cathode microstructure. (Jun-15) **In progress**
4. Study of electrode morphology evolution and mesostructure transport interaction: Study cathode mesostructure impact on product formation and deposition. Go/No-Go: Comparative analysis of the mesoscale model and experimental characterization. (Sep-15) **In progress.**

Progress Report

Reactions at the anode surface: *Ab initio* molecular dynamics (AIMD) simulations revealed multiple details regarding electrolyte decomposition reactions and the role of soluble polysulfides (PS) on such reactions. Simulations were done with 1M solution of LiTFSI in various pure solvents (ethylene carbonate (EC), DME, 1,3-dioxolane (DOL), and 1,1,2,2-Tetrafluoroethyl 2,2,3,3-tetrafluoropropyl ether (D2) and their mixtures (DME/DOL, EC/DME, DOL/D2) on Li(100) and Li (110) surfaces. Rapid decomposition of the salt and EC solvent was observed; the other solvents remained intact during the

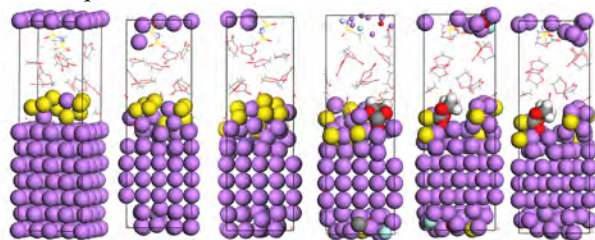


Figure 79: Time evolution of the Li (100) surface in contact with an electrolyte solution containing 1M solution of Li_2S_8 . Color code: Li is purple, S yellow, O red, C gray, H white.

timeframe of the simulation (20 ps), indicating their relatively higher stability. The presence of 1M concentration of Li_2S_8 caused numerous changes to the SEI reactions characterized in absence of PS.

When the PS molecule is close to the surface it decomposes in successive stages (Figure 79: first 3 images) finally forming a Li_2S surface film that significantly slows down the decomposition of the salt and solvents. The decomposition of a reactive solvent (EC) tested over such film (Figure 79: last 3 images) determined that the reaction mechanism

and products are very different from those in absence of the Li_2S film. Figure 79 illustrates the sequence of events where the PS molecule successively decomposes forming a Li_2S film. The carbonyl C of EC becomes bonded to one of the S atoms while the O atoms closely interact with Li atoms, thus inducing the EC opening. The product remains strongly adsorbed on the surface, becoming one of the SEI nucleation seeds, however, of a very different composition due to the presence of the S atoms.

Experimental characterization of the produced carbon-sulfur composite: Although the capacity was initially high for the 60% S and 40 % C composite reported earlier, due to reduced conductivity it was observed to fade during cycling. Therefore, synthesis conditions were optimized to produce a sulfur-carbon composite, where the weight of sulfur is 27.89 wt%. This composition was confirmed via thermogravimetric analysis (TGA) under inert atmosphere. X-Ray powder diffraction (XRD) is performed to confirm the orthorhombic crystal structure of the sulfur inserted in a carbon “hotel” cavity. Scanning electron microscopy (SEM) and energy-dispersive X-ray spectroscopy (EDS) is under investigation to demonstrate the mono-dispersity of nanosulfur in the carbon-sulfur composite. That will also clarify whether most of the sulfur is loaded in the cavities and not outside the carbon “hotel” cavities. The electrochemical performance is under investigation using a newly prepared electrolyte composed of 1 M solution of LiTFSI in organic solvent of equal parts DOL/D2. Initial results show lower capacities and slight fading with cycling. It could be due to insufficient drying of solvent that could have some water content leading to poor electrochemical performance. Thus further work is continued to optimize solvents (DOL and D2) via drying in dried molecular sieves followed by addition of 1 M solution of LiTFSI salt and electrochemical testing of newly developed C/S composite with ~30% S content.

Electrode morphology evolution and mesostructured transport interaction: A mesoscale coarse-grained model accompanied by Kinetic Monte Carlo (KMC) algorithm was developed to predict the growth rate of Li_2S film on the cathode. The effects of reactant concentrations and geometric properties of cathode microstructure (porosity and specific surface area) are being systematically investigated. Introducing the growth rate into 3D virtual cathode reconstruction, the microstructure evolution caused by Li_2S precipitation and corresponding electrochemical properties are predicted. Both the porosity and specific surface area of cathode tend to decrease as the Li_2S thickness increases. The porosity is predominant in determining the growth rate of Li_2S during discharge. The ionic conductivity decreases as the Li_2S thickness increases as a consequence of the porosity changes.

Patents/Publications/Presentations

1. Z. Liu, D. Hubble, P. B. Balbuena, and P. P. Mukherjee, “Adsorption of Insoluble Polysulfides Li_2S_x ($x = 1, 2$) on Li_2S Surfaces,” *Phys. Chem. Chem. Phys.*, 17, 9032-9039, (2015).

TASK 9 – LI-AIR BATTERIES

Summary and Highlights

High-density energy storage systems are critical for electric vehicles (EV) required by the *EV Everywhere* Grand Challenge proposed by DOE/EERE. Conventional Li-ion batteries still cannot fully satisfy their increasing needs because of limited energy density, high cost, and safety concerns. As an alternative, the rechargeable Li-O₂ battery has the potential to be used for long range EVs. The practical energy density of a Li-O₂ battery is expected to be ~ 800 Wh kg⁻¹. The advantages of Li-O₂ batteries come from their open structure; that is, they can absorb the active cathode material (oxygen) from the surrounding environment instead of carrying it within the batteries. However, the open structure of Li-O₂ batteries also leads to several disadvantages. The energy density of Li-O₂ batteries will be much lower if oxygen has to be provided by an onboard container. Although significant progress has been made in recent years on the fundamental properties of Li-O₂ batteries, the research in this field is still at an early stage and many barriers have to be overcome before practical applications. The main barriers in this field include:

1. Instability of electrolytes – Superoxide species generated during discharge or O₂ reduction process is highly reactive with electrolyte and other components in the battery. Electrolyte decomposition during charge or O₂ evolution process is also significant due to high over-potentials.
2. Instability of air electrode (dominated by carbonaceous materials) and other battery components (such as separators and binders) during charge/discharge processes in an oxygen-rich environment.
3. Limited cycleability of the battery associated with instability of the electrolyte and other components of the batteries.
4. Low energy efficiency associated with large over-potential and poor cyclability of Li-O₂ batteries.
5. Low power rate capability due to electrode blocking by the reaction products.
6. Absence of a low-cost, high efficiency oxygen supply system (such as oxygen selective membrane).

The main goal of the Battery Materials Research Task 9 is to provide a better understanding on the fundamental reaction mechanisms of Li-O₂ batteries and identify the required components (especially electrolytes and electrodes) for stable operation of Li-O₂ batteries. PNNL researchers will investigate stable electrolytes and oxygen evolution reaction (OER) catalysts to reduce the charging overvoltage of Li-O₂ batteries and improve their cycling stability. New electrolytes will be combined with stable air electrodes to ensure their stability during Li-O₂ reaction. Considering the difficulties in maintain the stability of conventional liquid electrolyte, Liox team will explore the use of a nonvolatile, inorganic molten salt comprising nitrate anions and operating Li-O₂ cells at elevated temperature (>80 °C). It is expected that these Li-O₂ cells will have a long cycle life, low over potential, and improved robustness under ambient air compared to current Li-air batteries. At Argonne National Laboratory, new cathode materials and electrolytes for lithium-air batteries will be developed for Li-O₂ batteries with long cycle life, high capacity, and high efficiency. State-of-the-art characterization techniques and computational methodologies will be used to understand the charge and discharge chemistries. UMass/BNL team will investigate the root causes of the major obstacles of the air cathode in the Li-air batteries. Special attention will be paid to the optimization of high surface carbon material used in the gas diffusion electrode, catalysts, electrolyte, and additives stable in Li-air system and with capability to dissolve Li oxide and peroxide. Success of this project will establish a solid foundation for further development of Li-O₂ batteries towards their practical applications for long range EVs. The fundamental understanding and breakthrough in Li-O₂ batteries may also provide insight on improving the performance of Li-S batteries and other energy storage systems based on chemical conversion processes.

Task 9.1 – Rechargeable Lithium-Air Batteries (Ji-Guang Zhang and Wu Xu, PNNL)

PROJECT OBJECTIVE:

The objective of this work is to develop stable electrolyte and oxygen evolution reaction (OER) catalysts to reduce the charging overvoltage of lithium (Li)-air batteries and improve the cycling stability of rechargeable Li-air batteries. New catalysts will be synthesized to improve the capacity and cycling stability of Li-O₂ batteries. New electrolytes will be investigated to ensure their oxygen-stability during Li-O₂ reaction.

PROJECT IMPACT:

Li-air batteries have a theoretical specific energy that is more than five times of state of the art Li-ion batteries and are potential candidates for use in next-generation, long-range electric vehicles (EV). Unfortunately, the poor cycling stability and low Coulombic efficiency of Li-air batteries have prevented their practical application so far. This work will explore a new electrolyte and electrode that could lead to long cyclability and high Coulombic efficiencies in Li-air batteries that can be used in the next generation EVs required by the *EV Everywhere* Grand Challenge proposed by DOE/EERE.

OUT-YEAR-GOALS:

- The long-term goal of the proposed work is to enable rechargeable Li-air batteries with a specific energy of 800 Wh/kg at cell level, 1,000 deep-discharge cycles, improved abuse tolerance, and less than 20% capacity fade over a 10-year period to accelerate commercialization of long-range EVs.

COLLABORATIONS:

- Yangchuan (Chad) Xing (University of Missouri) – Metal oxide coated glassy carbon electrode.
- Chunmei Ben (NREL) – Metal oxide coated glassy carbon electrode

Milestones

1. Synthesize and characterize the modified glyme solvent and the dual transition metal oxide catalyst (12/31/2014). **Completed**
2. Improve the stability of solvent using conventional carbon air electrode (3/31/2015). **In progress**
3. Identify the solvent to be stable for at least 50 cycles on modified air electrode. (6/30/2015). **Completed.**
4. Integrate the new electrolyte and modified air electrode to assemble Li-O₂ batteries with at least 120 cycles stable operation (9/30/2015). **In progress**

Progress Report

In this quarter, nano-structured ZnCo_2O_4 (ZCO) has been used as a catalyst in Li-O_2 batteries. ZCO was synthesized on the surface of single walled carbon nanotubes (SWCNTs). The obtained ZCO/ SWCNTs composites were confirmed by x-ray and SEM as shown in Figure 80a-Figure 80d. ZCO/ SWCNTs were then coated on porous carbon paper to form ZCO-based air electrode (Figure 80e-Figure 80h) and tested in coin cell type Li-O_2 batteries with the electrolyte of 1 M LiTf in tetraglyme. Two cycling protocols – the full discharge/charge protocol and the capacity-limited protocol were used. The results were compared with the sole SWCNTs based air electrode as discussed below.

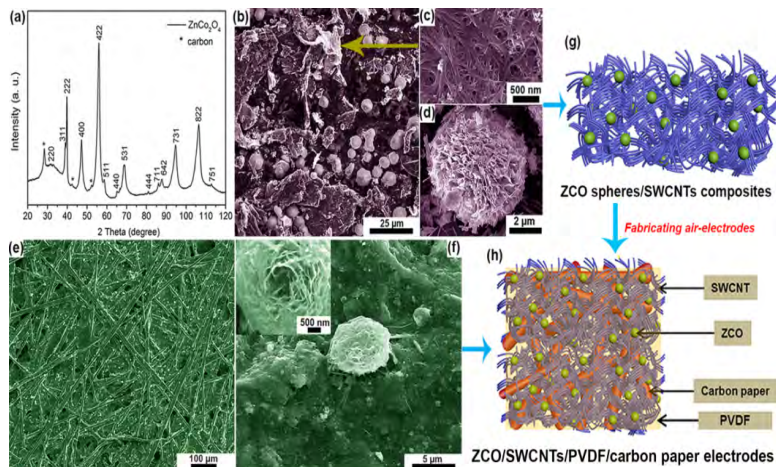


Figure 80: (a) XRD pattern of ZCO/SWCNTs composite powders. (b-d) Typical SEM images of ZCO/SWCNTs composite powders. (e,f) SEM images of the as-prepared ZCO-based electrodes by coating ZCO/SWCNTs/PVDF on carbon paper. (g,h) Schematic illustration of the synthesized ZCO/SWCNTs composites and the fabricated ZCO/SWCNT/PVDF/carbon paper air-electrodes.

When the ZCO-based Li-O_2 cells were cycled using the full discharge/charge protocol, the first discharge capacity of ZCO/ SWCNTs ($2,750 \text{ mAh g}^{-1}$ based on the total weight of ZCO and SWCNTs in the air electrode, or $3,667 \text{ mAh g}^{-1}$ based on the weight of SWCNTs) was far more than those of SWCNTs ($2,000 \text{ mAh g}^{-1}$ - SWCNTs) due to the enhanced ORR activity by ZCO catalyst. When cycled under capacity limitation of 800 mAh g^{-1} at 0.1 mA cm^{-2} , the discharge/charge voltage profiles of ZCO/SWCNTs were more stable than the SWCNTs electrodes (Figure 81a-Figure 81b). The ZCO/SWCNTs dramatically reduced the charge overpotential by 0.54 V (Figure 81c), demonstrating the efficient catalytic effect of ZCO on the reduction of over-potential of OER process in Li-O_2 batteries. The ZCO/SWCNTs electrode also remained almost the same discharge/charge capacities for 50 cycles and leads to very stable cycling performance at constant capacity of 800 mAh g^{-1} -ZCO/SWCNTs. However, the sole SWCNTs electrode resulted in a sharp capacity drop after 25th cycle (Figure 81d). ZCO/SWCNTs electrodes exhibited much better cycling stability than SWCNTs electrodes. The mechanism behind this improved performance will be further investigated.

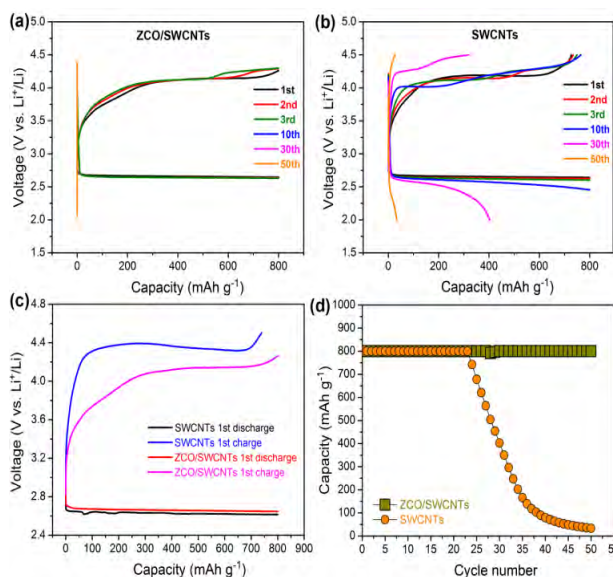


Figure 81: (a-c) Voltage profiles of selected cycles for ZCO/SWCNTs (a), SWCNTs (b) electrodes at a current density of 0.1 mA cm^{-2} . (c-d) 1st cycle voltage profile and cycling performance.

Patents/Publications/Presentations

1. ZnCo_2O_4 Catalyzed Single Walled Carbon Nanotubes as Air Electrode for Rechargeable Lithium-Oxygen Batteries, Bin Liu, Wu Xu, Pengfei Yan, Priyanka Bhattacharya, Ruiguo Cao, Mark E. Bowden, Mark H. Engelhard, Chongmin Wang, Ji-Guang Zhang, submitted for publication.

Task 9.2 – Efficient Rechargeable Li/O₂ Batteries Utilizing Stable Inorganic Molten Salt Electrolytes (Vincent Giordani, Liox)

PROJECT OBJECTIVE: The objective of this project is to develop high specific energy, rechargeable Li-air batteries having lower overpotential and improved robustness under ambient air compared to current Li-air batteries. The technical approach involves replacing traditional organic and aqueous electrolytes with nonvolatile, inorganic molten salt comprising nitrate anions and operating the cell at elevated temperature (>80 °C). The research methodology includes powerful *in situ* spectroscopic techniques coupled to electrochemical measurements (e.g. electrochemical mass spectrometry) designed to provide quantitative information about the nature of chemical and electrochemical reactions occurring in the air electrode.

PROJECT IMPACT: If successful, this project will solve particularly intractable problems relating to air electrode efficiency, stability and tolerance to the ambient environment. Furthermore, these solutions may translate into reduced complexity in the design of a Li-air stack and system, which in turn may improve prospects for use of Li-air batteries in EVs. Additionally, the project will provide materials and technical concepts relevant for the development of other medium temperature molten salt Li battery systems of high specific energy, which may also have attractive features for EVs.

OUT-YEAR-GOALS: The long term goal of this project is to develop Li-air batteries comprising inorganic molten salt electrolytes and protected Li anodes which demonstrate high (>500 Wh/kg) specific energy and efficient cycleability in ambient air. By the end of the project it is anticipated that problems hindering the use of both the Li anode and air electrode will be overcome due to materials advances and strategies enabled within the intermediate (>80 °C) operating temperature range of the system under development.

COLLABORATIONS:

- Bryan McCloskey (LBNL): Analysis of air electrode and electrolyte
- Julia Greer (Caltech): Design of air electrode materials and structures

Milestones

1. Demonstrate eutectic compositions having eutectic points below 120 °C. (Dec. 14) **Complete**
2. Measure ionic conductivity and Li⁺ transference number in eutectic compositions. (Dec. 14) **Complete**
3. Measure diffusion coefficients and solubilities of O₂, Li₂O₂ and Li₂O. (Mar. 15) **Complete**
4. Synthesize oxidation-resistant carbons. (Mar. 15) **Complete**
5. Go/No-Go: Demonstrate suitability of analytical approach for elevated temperature molten salt metal-O₂ cells. Criteria: Quantify Li₂O₂ yield, e⁻/O₂ and OER/ORR ratios for baseline carbon air electrodes. (Jun. 15) **Complete**
6. Quantify Li₂O₂ yield, e⁻/O₂ and OER/ORR ratios for oxidation-resistant carbon air electrodes. (Jun. 15) **Ongoing**
7. Measure diffusion coefficients and solubilities of H₂O, CO₂, LiOH and Li₂CO₃. (Sept. 15) **Ongoing**
8. Synthesize metals and metal alloys of high air electrode stability and/or catalytic activity. (Sept. 15) **Ongoing**

Progress Report

Q2 Milestones 1 and 2 consist of measuring diffusion coefficients and solubilities of O_2 , Li_2O_2 and Li_2O ; as well as preparing and characterizing oxidation-resistant carbon materials for the O_2 electrode.

Levich/Cottrell analysis at a Pt rotating disk electrode ($A=0.196\text{ cm}^2$) was used to determine solubility and diffusivity of active species such as lithium peroxide, oxide and molecular oxygen. Electrochemical measurements were performed inside an Argon-filled glovebox designed for experiments involving oxygen (see Figure 82). Typically, excess amount of Li_2O_2 , or Li_2O , were added to carefully dried $LiNO_3$ - KNO_3 eutectic heated up to $150\text{ }^\circ\text{C}$ inside a PTFE beaker. Once saturation of Li salts was reached, the Levich/Cottrell analysis was performed (see Table 3).

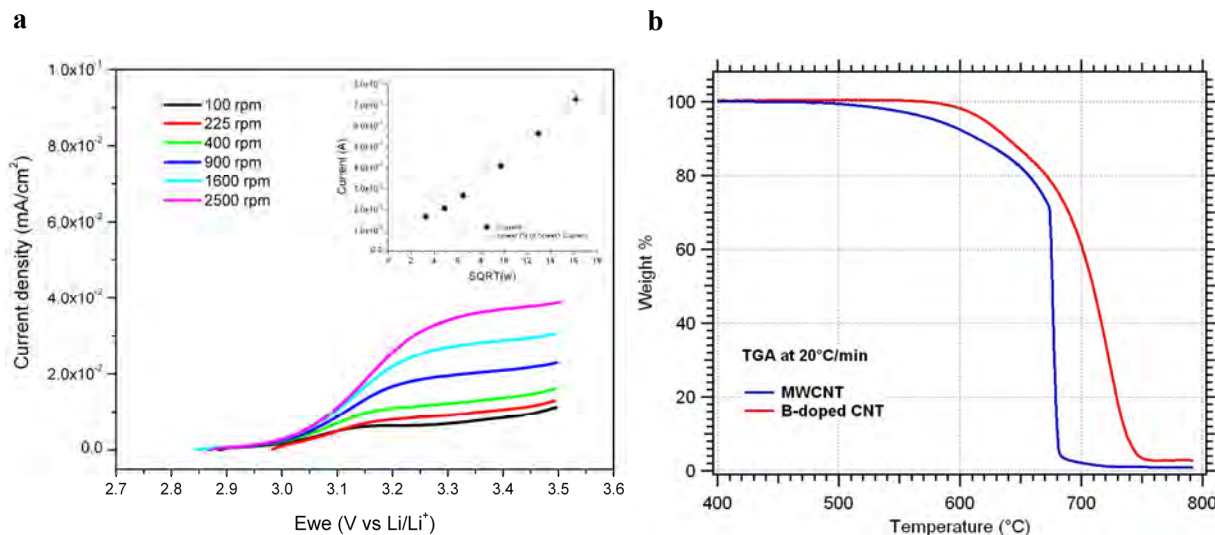


Figure 82: a) Electrochemistry of Li_2O in $LiNO_3$ - KNO_3 eutectic at $150\text{ }^\circ\text{C}$, at a Pt RDE (CE: Pt wire, RE: Li rod): Linear sweep voltammograms recorded at 5 mV/s at various electrode rotation rates, with Levich plot inset. b) Synthesis of oxidation-resistant carbons: TGA analysis of newly synthesized MWCNT and B-doped CNT (under O_2 , $20\text{ }^\circ\text{C}/\text{min}$).

Table 3: Concentrations and Diffusion coefficients for Li_2O_2 , Li_2O in $LiNO_3$ - KNO_3 eutectic, obtained by Levich/Cottrell method; and O_2 in $NaNO_3$ - KNO_3 eutectic at $150\text{ }^\circ\text{C}$.

	Li_2O_2	Li_2O	O_2 in $(Na,K)NO_3$
Solubility (mM)	0.414	0.044	0.0013
Diffusivity (cm^2/s)	$6.63 \cdot 10^{-9}$	$4.25 \cdot 10^{-6}$	$1.37 \cdot 10^{-4}$

Boron-doped carbon nanotubes (B-doped CNT) were synthesized and their oxidative stability assessed by TGA-MS analysis under oxygen. O_2 electrodes were also prepared using newly synthesized carbon and compared to our baseline carbon material, Super P amorphous carbon black. XRD analysis of our new carbon cathode following discharge under O_2 revealed the presence of Li_2CO_3 at the surface, similar to a cell employing Super P. An array of carbon materials with different degree/type of doping have been prepared and tested in Li - O_2 cells. Results indicate sustained formation of Li_2CO_3 and therefore focus is on non-carbon containing cathode materials.

Patents/Publications/Presentations

Patents:

1. PCT Application No. WO2015021451 “Rechargeable Batteries Employing Catalyzed Molten Nitrate Positive Electrodes”

Presentations:

1. Poster Presentation by Dylan Tozier at The Nanomaterials for Applications in Energy Technology Gordon Research Conference in Ventura, CA (February 2015)
2. Oral Presentation by Vincent Giordani at Materials Research Society conference in San Francisco, CA (April 2015)
3. Oral Presentation by Dan Addison at Next Generation Batteries 2015 conference in San Diego, CA (April 2015)

Task 9.3 – Li-Air Batteries (Khalil Amine, ANL)

PROJECT OBJECTIVE:

- Develop new cathode materials and electrolytes for lithium-air batteries for long cycle life, high capacity, and high efficiency.
- Use state-of-the-art characterization techniques to understand the charge and discharge chemistries.
- Use state-of-the-art computational methodologies to understand and design new materials and electrolytes for Li-air batteries.

PROJECT IMPACT:

- New electrolytes that are stable and increase cycle life
- New cathode materials that increase cycle life and reduce overpotentials
- Increased cycle life

OUT-YEAR-GOALS:

The out-year goals of this work is to find catalysts that promote discharge product morphologies that reduce charge potentials and find electrolytes for long cycle life through testing and design.

Milestones

The following are the milestones for each Quarter during FY15:

1. Characterize the stability of the LiO_2 component of the activated carbon cathode using Raman techniques. Use DFT calculations to model the stability of the LiO_2 component of the activated carbon cathode to explain the Raman results. (12/31/2014) **Completed**
2. Investigate the role of impurities in the performance of activated carbon and how they can promote the formation and stability of LiO_2 and reduce charge overpotentials. Use DFT calculations to help understand how the impurities affect morphologies. (3/31/2015) **Completed**
3. Investigate addition of metal nanoparticle catalysts to high surface area carbons such as reduced graphene oxides to promote growth of morphologies with higher LiO_2 contents to reduce charge overpotentials. Use DFT calculations to model the nanoparticle catalysts. (6/30/2015) **Ongoing**
4. Use one of the metal catalyst/carbon systems with good performance to start investigations of how electrolytes can be used to improve the performance (cycle life) of the Li-air battery. Use DFT calculations to help design new electrolytes for the Li-air batteries. (9/30/2015) **Ongoing**

Progress Report

During the cycling of Li-O₂ batteries, the discharge process gives rise to dynamically evolving agglomerates composed of lithium-oxygen nanostructures; however, little is known about their composition. We have continued our study of a Li-O₂ battery based on an activated carbon cathode that indicate interfacial effects involving the electrolyte can suppress disproportionation of a LiO₂ component in the discharge product. The stability of the discharge product was then probed by investigating the dependence of the charge potential and Raman intensity of the superoxide peak with time.

Characterization of the discharge product by both high intensity XRD and TEM measurements reveals that there is a LiO₂ component along with Li₂O₂ in the product. The stability of the discharge product from the AC-based Li-O₂ cell was further investigated by varying the interface conditions of the discharge product and characterizing the subsequent effect on the disproportionation process with time.

Six different conditions were investigated with the resulting charge curves given in Figure 83. The Raman intensity of the superoxide peak was checked over the same six different conditions and the results are given in Figure 84. The results indicate that the LiO₂ component can be stable for possibly up to days when an electrolyte is left on the surface of the discharged cathode. The results are explained by DFT calculations that find the disproportionation process to be slower at an electrolyte/ LiO₂ interface shown in Figure 85 compared to a vacuum/ LiO₂ interface. The combined experimental and theoretical results provide new insight into how interfacial effects can stabilize LiO₂, which may play an important role in the charge and discharge chemistries of a Li-O₂ battery.

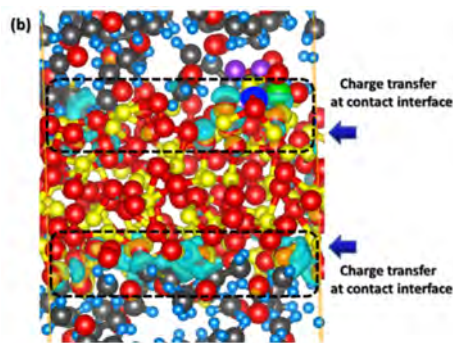


Figure 85: Charge transfer (light blue) at the LiO₂ slab/electrolyte interface from a charge density plot during a particular snapshot of a AIMD trajectory. This may be the reason for suppression of the disproportionation.

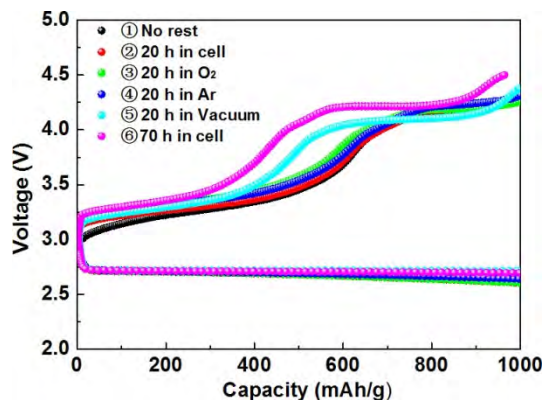


Figure 83: Galvanostatic discharge/charge curves of cells under the six different conditions. The discharged capacity is 1000 mAh/g, and the discharge/charge current density is 0.2 and 0.1 mA/cm², respectively.

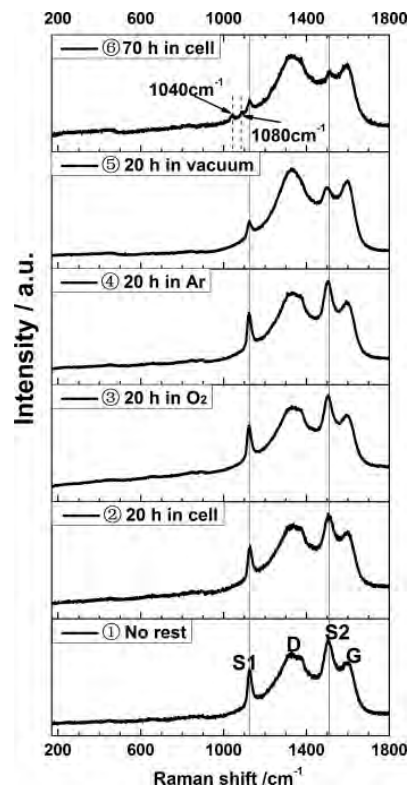


Figure 84: Raman spectra of the toroids on the surface of the discharged AC cathode for the six different conditions described in the text. The values of the peaks (in cm⁻¹) are: 1123 (S1), 1505 (S2), 1340 (D), 1600 (G).

Patents/Publications/Presentations

1. Interfacial Effects on Lithium Superoxide Disproportionation in Li-O₂ Batteries, D. Zhai, K. C. Lau, H.-H. Wang, J. Wen, D. J. Miller, J. Lu, F. Kang, B. Li, W. Yang, J. Gao, E. Indacochea, L. A. Curtiss, and K. Amine, *Nano Lett.*, 2015, 15 (2), pp 1041–1046 DOI: 10.1021/nl503943z

Task 9.4 – Overcome the Obstacles for the Rechargeable Li-air Batteries (Deyang Qu, University of Massachusetts, Boston and Xiao-Qing Yang, Brookhaven National Laboratory)

PROJECT OBJECTIVE: The primary objective is to investigate the root causes of the major obstacles in the air cathode of Li-air batteries, which impede the realization of high energy, high power, long cycle life Li-air batteries, and understand the mechanisms of such barriers and eventually overcome them obstacles. In this objective, special attentions will be paid to the investigation of high surface carbon material use in the gas diffusion electrode (GDE), establishment of 2-phase interface on the GDE, catalysts, electrolyte and additives stable in Li-air system and with capability to dissolve Li oxide and peroxide. The electrolyte investigation and development closely collaborates with Brookhaven National Laboratory. The secondary objectives is the engineering design of a Li-air battery with high energy, high rate, long cycle life and high round-trip efficiency, special attention will be paid to Li-air flow cell.

PROJECT IMPACT: Li-air chemistry represents the highest energy density among chemical energy systems. The successful implementation of the technology in electric vehicles would not only reduce the cost of electrochemical energy storage system but also provide long driving distance per charge by significantly increase the energy density. The attributes would enable cost-effective market entry of electric vehicles for US automakers.

OUT-YEAR GOALS: The specific research in the project year will be focused on the fundamental mechanisms of oxygen reduction in non-aqueous electrolytes and the re-oxidization of the soluble boron-peroxide complex, multiple boron complexes will be synthesized at BNL and tested at UMB. The impact of carbon surface structure on the O₂ reduction will be investigated. The unique flow-cell design will be further optimized by means of the inclusion of boron additives.

INDUSTRY COLLABORTOR: The University of Massachusetts, Boston and BNL team maintains close collaboration with Johnson Controls' scientists and engineers. The collaboration enables the team to validate the outcomes of fundamental research in pilot scale cells. This team has been closely working with top scientists on new material synthesis at ANL, LBNL, and PNNL, with US industrial collaborators at General Motor, Duracell, and Johnson Control; as well as international collaborators in Japan and South Korea. These collaborations will be strengthened and expanded to give this project a vision on both today's state of art technology and tomorrow' technology under development and the feed-back from the material designer and synthesizers at upstream, as well as from the industrial end users at downstream.

Milestones

1. Complete the studies of the impact of carbon surface structure on the O₂ reduction. (Dec. 14) **Completed**
2. Complete the kinetics studies of catalytic disproportionation of superoxide (determination of reaction order and reaction constant). (March 15) **completed**
3. Complete the test of the Li-air flow cell. (June 15). **In progress**
4. Complete *in situ* electrochemical study for the oxygen reduction in various boron additives. (September 14). **In progress**

Progress Report

In the 2nd quarter of FY2015, progress toward milestones has been made. Firstly, the solvent effects on the oxygen reduction and evolution in non-aqueous electrolyte with Li salts have been investigated. In Q1, it was reported that strong Lewis acid can catalyze fast disproportionation of superoxide ions which is the product of the oxygen reduction in non-aqueous electrolyte. Li^+ is a Lewis acid and proven to catalyze superoxide disproportionation. The Lewis acidity of Li^+ can be substantially altered by the solvation of different solvent. Therefore, the solvent could have significant impacts on the oxygen reduction and evolution in the electrolyte containing Li ion. In this quarter, a reliable analytical method based on HPLC MS was developed and tested to determine the solvation number of solvents to Li cation. The interaction between the solvents and the solvated Li^+ was also evaluated. Figure 86 shows the distribution of various solvents in the solvation shell of Li cation (left) and example of the relative strength of integration between solvent molecules and Li ion in the solvation shell (right).

In addition, the impact of the additive of strong boron based Lewis acid was further investigated. As shown in Figure 87, the catalytic effect of boron containing Lewis acid is clearly shown. The 1-e oxygen

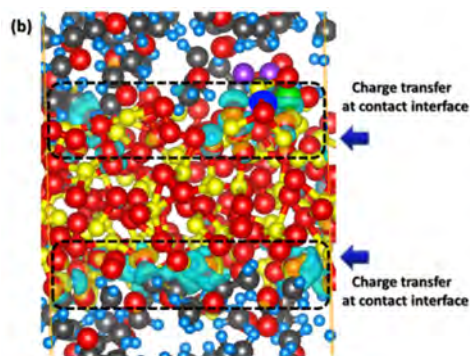


Figure 86: Distribution of DMSO in the Li^+ solvation adducts obtained from ESI-MS spectra of 5mM LiBF_4 DMSO and other solvents (1:1) mixture (left); The CID spectra of $\{\text{DMSO}+\text{Li}+\text{DMSO}^{\text{d6}}\}^+$ obtained at collision voltage= 20V, and the scheme of CID procedure (right).

reduction ($\text{O}_2 + \text{e}^- \rightarrow \text{O}_2^{\cdot-}$) and the subsequent second electrode reduction ($\text{O}_2^{\cdot-} + \text{e}^- \rightarrow \text{O}_2^{2-}$) can be observed. The phenomena can only be seen at medium concentration of the Lewis acid. This result can be attributed to the combination effects of fast superoxide disproportionation and the stabilization of $\text{B}-\text{O}_2^{2-}$ complex.

Table 4 lists the reaction rate constant for the chemical reaction between PC and superoxide ion, superoxide disproportionation reaction rate constants catalyzed by both Li ion and borate complex.

Table 4: Reaction rate constants calculated from table 3. Initial concentration for $\text{O}_2^{\cdot-}$ was 0.01 M.

	Concentration (M)	STD	R	$k' (\text{s}^{-1})$	$k (\text{s}^{-1}\text{M}^{-1})$
PC	0.08	6.87×10^{-5}	0.998	0.003	0.037
Li ion	0.2	3.78×10^{-4}	0.960	0.004	0.02
TPFPB	0.009	1.59×10^{-4}	0.997	0.006	0.67

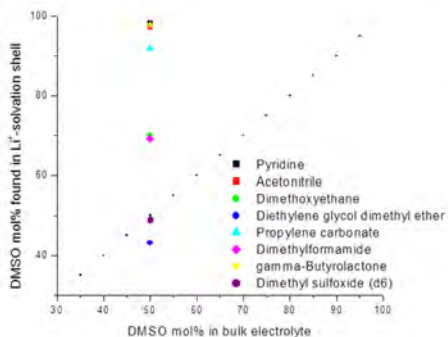


Figure 87: Cyclic voltammetry oxygen reduction in acetonitrile with various concentration of borate.

Patents/Publications/Presentations

None in this quarter.

TASK 10 – NA-ION BATTERIES

Summary and Highlights

In order to meet the challenges of powering the PHEV, next generation of rechargeable battery systems with higher energy and power density, lower cost, better safety characteristics, and longer calendar and cycle life (beyond lithium-ion batteries, which represent today's state-of-art technology), need to be developed. Recently, Na—ion battery systems have attracted more and more attention due to the more abundant and less expensive nature of Na resource. The issue is not insufficient lithium on a global scale, but what fraction can be used and still be economically effective. Most untapped lithium reserves occur in remote or politically sensitive areas. Scale-up will require a long lead time, involve heavy capital investment in mining, and may require the extraction and processing of lower quality resources, which could drive extraction costs higher. Currently, high costs remain a critical barrier to the widespread scale-up of battery energy storage. Recent computational studies on voltage, stability and diffusion barrier of Na-ion and Li-ion materials indicate that Na-ion systems can be competitive with Li-ion systems.

The primary barriers and limitations of current state of art of Na-ion systems are as follows:

1. Building a sodium battery requires redesigning battery technology to accommodate the chemical reactivity and larger size of sodium ions.
2. Lithium batteries pack more energy than sodium batteries per unit mass. Therefore, for sodium batteries to reach energy densities similar to lithium ones, the positive electrodes in the sodium battery need to hold more ions.
3. Since Na-ion batteries are an emerging technology, new materials to enable Na electrochemistry and the discovery of new redox couples, and the diagnostic studies of these new materials and redox couples are quite important.
4. In sodium electrochemical systems, the greatest technical hurdles to overcome are the lack of high-performance electrode and electrolyte materials that are easy to synthesize, safe, non-toxic, with long calendar and cycling life and low cost.
5. Furthermore, fundamental scientific questions need to be further elucidated, including (1) the difference in transport and kinetic behaviors between Na and Li in analogous electrodes; (2) Na insertion/extraction mechanism; (3) solid electrolyte interphase (SEI) layer on the electrodes from different electrolyte systems; and (4) charge transfer in the electrolyte–electrode interface and Na⁺ ion transport through the SEI layer.

This task will use the synchrotron based *in situ* x-ray techniques and other diagnostic tools to evaluate new materials and redox couples, to explore fundamental understanding of the mechanisms governing the performance of these materials and provide guidance for new material developments. This task will also be focused on developing advanced diagnostic characterization techniques to investigate these issues, providing solutions and guidance for the problems. The synchrotron based *in situ* X-ray techniques (x-ray diffraction and hard and soft x-ray absorption) will be combined with other imaging and spectroscopic tools such as high resolution transmission electron microscopy (HRTEM), mass spectroscopy (MS), and transmission x-ray microscopy (TXM)

Task 10.1 – Exploratory Studies of Novel Sodium-Ion Battery Systems (Xiao-Qing Yang and Xiqian Yu, Brookhaven National Laboratory)

PROJECT OBJECTIVE: The primary objective of this project is to develop new advanced *in situ* material characterization techniques and to apply them to explore the potentials, challenges, and feasibility of new rechargeable battery systems beyond the lithium-ion batteries (LIBs), namely the sodium-ion battery systems for plug-in hybrid electric vehicles (PHEV). In order to meet the challenges of powering the PHEV, new rechargeable battery systems with high energy and power density, low cost, good abuse tolerance, and long calendar and cycle life need to be developed. This project will use the synchrotron based *in situ* x-ray diagnostic tools developed at BNL to evaluate the new materials and redox couples, to explore in fundamental understanding of the mechanisms governing the performance of these materials.

PROJECT IMPACT: In the Multi Year Program Plan (MYPP) of the Vehicle Technology Office (VTO), the goals for battery were described as: “Specifically, lower-cost, abuse-tolerant batteries with higher energy density, higher power, better low-temperature operation, and longer lifetimes are needed for the development of the next-generation of HEVs, PHEVs, and EVs.” If this project is successfully carried out, the knowledge learned from diagnostic studies and collaborations with US industries and international research institutions through this project will help them develop new materials and processes for new generation of rechargeable battery systems beyond lithium-ion batteries, such as Na-ion battery systems in their efforts to reach these VTO goals.

APPROACH. This project uses the synchrotron based *in situ* x-ray diagnostic tools developed at BNL to evaluate the new materials and redox couples to enable a fundamental understanding of the mechanisms governing the performance of these materials and provide guidance for new material and new technology development regarding Na-ion battery systems.

OUT-YEAR GOALS: Complete the *in situ* x-ray diffraction and absorption studies of sodium iron ferrocyanide (Prussian Blue Analogous) as cathode materials for Na-ion batteries during charge-discharge cycling.

COLLABORATIONS: BNL team has been closely working with top scientists on new material synthesis at ANL, LBNL, and PNNL, with US industrial collaborators at General Motor, Duracell, and Johnson Control; as well as international collaborators in Japan and South Korea. These collaborations will be strengthened and expanded to give this project a vision on both today’s state of art technology and tomorrow’ technology under development and the feed-back from the material designer and synthesizers at upstream, as well as from the industrial end users downstream.

Milestones

1. Complete the particle size effects on kinetic properties of $\text{Li}_4\text{Ti}_5\text{O}_{12}$ as anode materials for Na-ion batteries using synchrotron based *in situ* x-ray diffraction (Dec-14) **Completed**
2. Complete the *in situ* x-ray diffraction studies of sodium iron ferrocyanide (Prussian Blue Analogous) as cathode materials for Na-ion batteries during charge-discharge cycling (Mar-15),) **Completed**
3. Complete the *in situ* x-ray diffraction studies of NaCrO_2 during electrochemical chemical de-sodiation. NaCrO_2 is considered as a potential cathode material for Na-ion batteries. (Jun-15) **In progress**
4. Complete the x-ray absorption studies of NaCrO_2 at different sodiation levels.. (Sep-15) **In progress**

Progress Report

In the 2nd quarter of FY2015, the second milestones for FY2015 had been completed.

In the 2nd quarter of FY2015, BNL has been focused on the studies of a new cathode material for sodium-ion batteries. This new material, the sodium iron ferrocyanide with high Na concentration is a Prussian blue analogues with Na concentration as high as 1.63 per formula. The Na-rich sodium iron ferrocyanide demonstrates a high specific capacity of 160 mAh g^{-1} and 90% capacity retention after 200 cycles. The Na intercalation/deintercalation mechanism is systematically studied by *in situ* Raman, X-ray diffraction and X-ray absorption spectroscopy analysis. The Na-rich sodium iron ferrocyanide has great potentials as cathode materials for practical applications. In the 2nd quarter of FY2015, the Na intercalation/deintercalation mechanism of Prussian blue analogues, such as $\text{Na}_{1.63}\text{Fe}_{1.89}(\text{CN})_6$ [NaFe(1.63)] electrode during first charge/discharge process was studied using *in situ* synchrotron based XRD technique. The structure changes are monitored by the shift of the major diffraction peaks (Figure 88). The peak intensities of the initial rhombohedral phase gradually decreased while the new peaks of the final cubic phase emerged during the early stage of Na extraction (i.e. charging). The peaks representing the cubic phase monotonically shifted towards high two-theta angle positions upon further charging up to 3.3V, suggesting Na^+ extraction through a solid-solution reaction during the first half of charging. Only small structural changes were observed in the high voltage charging region ($>3.5\text{V}$) although more than 70 mAh g^{-1} capacity was delivered. Some part of it could be due to the electrolyte decomposition. The phase transitions proceeded in a reverse manner when Na ions were re-inserted. The initial rhombohedral structure was restored at the end of discharge at 2.0V. This result suggests the highly reversible structural changes during the Na^+ extraction/insertion process, which is responsible for its superior cycling stability.

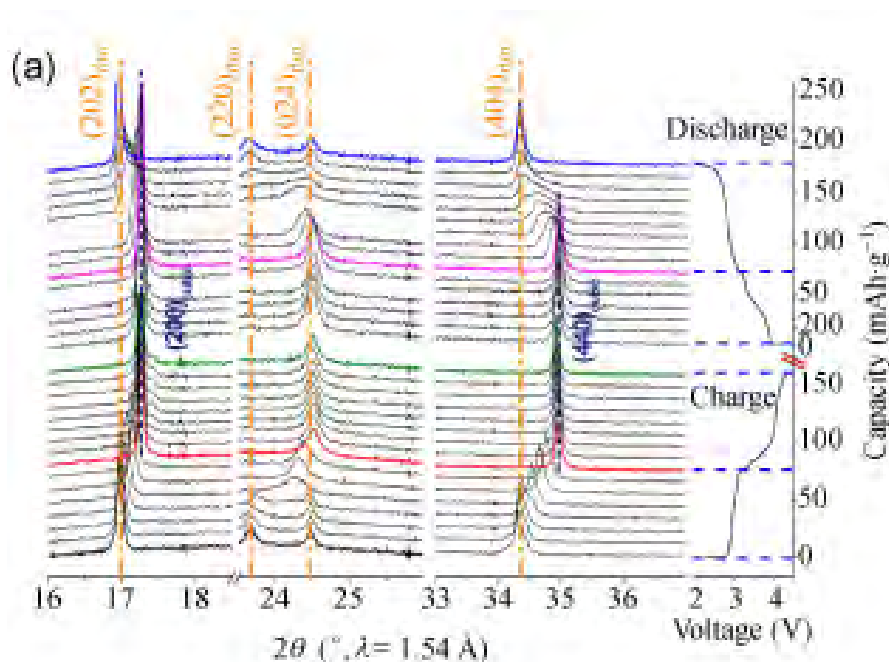


Figure 88: *In situ* XRD patterns of NaFe(1.63) electrode collected during first charge and discharge. The major diffraction peaks selected from the full XRD patterns are plotted to clearly show the phase transitions between the pristine rhombohedral and cubic phases. The charge and discharge curves are shown on the right column respectively.

Patents/Publications/Presentations

1. Jie Song, Long Wang, Yuhao Lu, Jue Liu, Bingkun Guo, Penghao Xiao, Jong-Jan Lee, Xiao-Qing Yang, Graeme Henkelman, and John B. Goodenough, “Removal of Interstitial H₂O in Hexacyanometallates for a Superior Cathode of a Sodium-Ion Battery”, *J. Am. Chem. Soc.*, 2015, 137 (7), pp 2658–2664, DOI: 10.1021/ja512383b, Publication Date (Web): February 13, 2015.
2. Ji-Li Yue, Yong-Ning Zhou, Si-Qi Shi, Zulipiya Shadike, Xuan-Qi Huang, Jun Luo, Zhen-Zhong Yang, Hong Li, Lin Gu, Xiao-Qing Yang, Zheng-Wen Fu, “Discrete Li-occupation versus pseudo-continuous Na-occupation and their relationship with structural change behaviors in Fe₂(MoO₄)₃”, *Scientific Reports* 5, Article number: 8810 doi:10.1038/srep08810, Published 06 March 2015.